

Targeting Solid Tumors

Advances in treatment strategies for glioma and colorectal cancer

Winan van Houdt

Targeting Solid Tumors

Advances in treatment strategies for glioma and colorectal cancer

Thesis, Utrecht University, The Netherlands

Proefschrift, Universiteit Utrecht, Nederland

The work described in this thesis was supported by The Netherlands Organisation for Scientific Research (ZonMW, AGIKO grant number 920-03-382)

Copyright ©

W.J. van Houdt, 2011

ISBN:

978-94-6108-176-6

Cover:

W.J. van Houdt, Nicole Nijhuis - Gildeprint Drukkerijen

Layout and printed by:

Gildeprint Drukkerijen, Enschede

Publication of this thesis was financially supported by: J.E. Jurriaanse Stichting, Abbott Nederland, Amgen BV, Baxter, Chipsoft, Chirurgisch Fonds UMC Utrecht, Covidien Nederland BV, Eurotec BV, Glaxo Smith Kline, Hoogland Medical BV, Novartis Oncology, Nycomed, Merck Sharp & Dome BV, Olympus Nederland BV, PQR BV, Roche Nederland BV, Sanofi Aventis, Sigma Medical

Targeting Solid Tumors

Advances in treatment strategies for glioma and colorectal cancer

Het gericht behandelen van tumoren

Nieuwe ontwikkelingen in behandelstrategieën
voor gliomen en colon carcinomen
(met een samenvatting in het Nederlands)

PROEFSCHRIFT

ter verkrijging van de graad van doctor aan de Universiteit Utrecht
op gezag van de rector magnificus, prof.dr. G.J. van der Zwaan,
ingevolge het besluit van het college voor promoties in het
openbaar te verdedigen op

dinsdag 14 juni 2011 des middags te 2.30 uur

door

Willem Johanan van Houdt

geboren op 24 april 1977 te Assen

Promotor: Prof. dr. I.H.M. Borel Rinkes

Co-promotor: Dr. O. Kranenburg

voor Marijke
voor Charlotte en Hugo

Contents

Chapter 1:	General introduction and outline of the thesis	9
Targeting solid tumors with viral gene therapy		
Chapter 2:	Gene delivery into malignant glioma by infectivity-enhanced adenovirus: in vivo versus in vitro models. <i>Neuro Oncology, 2007 Jul;9(3):280-90.</i>	21
Chapter 3:	The human survivin promoter: a novel transcriptional targeting strategy for treatment of glioma. <i>Journal of Neurosurgery, 2006 Apr;104(4):583-92</i>	41
Chapter 4:	Transient infection of freshly isolated human colorectal tumor cells by reovirus T3D intermediate subviral particles. <i>Cancer Gene Therapy, 2008 May;15(5):284-92.</i>	59
Targeting the EGFR-RAS-ERK pathway in colorectal cancer		
Chapter 5:	Oncogenic KRAS desensitizes colorectal tumor cells to EGFR inhibition and activation. <i>Neoplasia, 2010 Jun;12(6):443-52</i>	75
Chapter 6:	Oncogenic K-ras activates p38 to maintain colorectal cancer cell proliferation during MEK inhibition. <i>Cellular Oncology, 2010 Jan 1;32(4):245-57</i>	97
Targeting colon cancer stem cells		
Chapter 7:	Differentiated Human Colorectal Cancer Cells Protect Tumor-Initiating Cells From Irinotecan. <i>Gastroenterology, 2011 March 31 (epub ahead of print)</i>	115
Chapter 8:	Proteome differences between colon cancer stem cells and differentiated tumor cells identifies BIRC6 as a potential therapeutic target. <i>Submitted.</i>	145
Chapter 9:	General Discussion	165

Chapter 10: Summary in Dutch – Nederlandse samenvatting	175
Chapter 11: Acknowledgements – Dankwoord; Curriculum vitae auctoris List of publications;	183
Chapter 12: Color figures	193

Review committee

Prof. dr. P.J. van Diest
Department of Pathology
University Medical Center Utrecht

Prof. dr. R. van Hillegersberg
Department of Surgery
University Medical Center Utrecht

Prof. dr. C.M.F. Dirven
Department of Neurosurgery
Erasmus Medical Center Rotterdam

Prof. dr. R.C. Hoeben
Department of Molecular Cell Biology
Leiden University Medical Center

Prof. dr. P.D. Siersema
Department of Gastroenterology
University Medical Center Utrecht

1

General Introduction

Curative treatment of most solid tumors includes surgical interference. However, the incidence of local recurrence or distant micrometastases is significantly lower when patients are treated with systemic or locally administered chemo- or targeted therapy. In the last decade, many novel targeting strategies have been developed for several tumor types. This thesis aims to identify promising targeting strategies for glioma and colorectal carcinoma and reveals resistance mechanisms for these new promising strategies.

Glioma

In adults, malignant glioma is the most common primary brain tumor which comprises about 60% of all primary brain tumors, including benign tumors¹. Gliomas are tumors deriving from glia cells, which are astrocytes, oligodendrocytes and ependymal cells. Glia cells are supporting cells for neurons and are found throughout the central nervous system in both grey and white matter. Depending on the cell-of-origin, malignant gliomas include astrocytomas, oligodendrogliomas and ependymomas. The most frequently found malignant gliomas are astrocytomas. Although the nomenclature can be confusing, the most widely used classification of astrocytoma is based on division into low-grade astrocytoma, anaplastic astrocytoma and glioblastoma multiforme¹⁻³. This classification is based on histological features, in which grade 1 and 2 are both low grade astrocytoma, grade 3 is anaplastic astrocytoma and glioblastoma multiforme is grade 4. Low grade tumors are growing slowly, but may become very large over time and tend to progress into high grade tumors. At the time of diagnosis, ~50% of all glioma are glioblastoma multiforme^{4,5}. Glioma seldomly metastasize systemically. However, local invasiveness is an important characteristic of this tumor type, contributing to poor prognosis. Glioblastoma multiforme is a devastating disease, since the 5 year survival is only 2-3%, whereas prognosis of low grade glioma is around 30%^{1,3,6}. The treatment of choice for high grade glioma is surgery, combined with radiotherapy⁷. Adjuvant treatment with systemic chemotherapy does not influence median survival, although in recent studies temozolomide treatment increased the median survival from 12,1 to 14.6 months^{8,9}. Since prognosis of malignant glioma remains poor, the development of new treatment strategies is urgent. This explains the high attention for viral gene therapy in the context of malignant glioma. Malignant gliomas are attractive targets for local gene therapy because of their biological behaviour: local invasiveness, but absent distant micrometastases¹⁰⁻¹².

Colorectal cancer

Colorectal carcinoma remains one of the most common causes of cancer-related death. Nearly one million new patients worldwide are diagnosed each year. Death from this disease is usually associated with the formation of liver metastases^{13,14}. Liver metastases will develop in approximately 50% of all colorectal cancer patients. Treatment of colorectal cancer normally includes surgery and, depending on the stage of the disease, chemotherapy and/or radiotherapy. Until recently, curative resection of liver metastases was restricted to only a small minority of patients. All other patients received palliative chemotherapy with a median survival of only 6-12

months¹⁵. However, in the last decade important progress has been made in the field of treatment of colorectal liver metastases. This progress includes more effective neo-adjuvant and adjuvant chemo- and targeted therapies and new surgical strategies for safer hepatic resection. These developments have increased the resectability rate of patients with colorectal liver metastases to almost 30% and led to increased survival rates¹⁶. Furthermore, radiofrequency ablation (RFA) is a novel alternative treatment option for patients with irresectable colorectal metastases confined to the liver.^{17,18}

In approximately 35-40% of all sporadic colorectal carcinomas, activating mutations in the *KRAS* oncogene are observed¹⁹⁻²¹. These mutations are acquired at the early pre-malignant stages of colorectal tumor formation. However, additional mutations are essential for tumorigenesis, most frequently in the tumor suppressor gene *APC*^{22,23}. The *KRAS* oncogene encodes the small membrane bound guanine nucleotide binding protein KRAS, a member of the Ras protein family²⁴. Approximately 30% of all human cancer types contain a point mutation in one of the RAS genes (*HRAS*, *KRAS*, *NRAS*)²⁵. In colorectal cancer patients, *KRAS* is by far the most frequently mutated isoform. *KRAS* is localized at the inner face of the plasma membrane, where it mediates downstream signaling by growth factor receptors like EGFR. *KRAS* activity is regulated by cycling between inactive GDP-bound and active GTP-bound forms²⁴. Activating mutations lead to a continuously active GTP-bound state which leads to growth factor independent signaling. *KRAS* activates a number of signal transduction pathways, among which the RAF/MEK/ERK pathway, the PI3K/AKT pathway and the RAC pathway²⁶. Mutations in the *KRAS* oncogene lead to constitutive activation of these pathways, resulting in uncontrolled growth, proliferation, invasion and apoptosis resistance^{26,27}.

Targeting Solid tumors with Viral Gene therapy

Since approximately 20 years, gene therapy has been developed as a new treatment modality for several diseases. The principle of gene therapy is the delivery of therapeutic genes to cells with damaged or absent genes that can cause a broad spectrum of genetic diseases^{28,29}. In the case of cancer gene therapy, originally the 'therapeutic' gene was an apoptotic gene responsible for cell killing like the HSV-TK gene, delivered by a replication incompetent viral vector^{28,30}. However, when starting this thesis interest in cancer gene therapy was shifted to replication competent oncolytic viruses without carrying a 'therapeutic' gene. The most widely used viral vectors are the adenovirus, retroviruses, the herpes simplex virus and the adeno-associated virus (AAV).³⁰ In addition, The Reovirus type 3 Dearing strain was used as an oncolytic agent in specific types of cancer, among which colorectal cancer^{31,32}. In the context of glioma, adenoviral vectors are widely applied in pre-clinical and clinical studies^{5,10}.

The therapeutic mechanism of these replicating viral vectors is based on their ability to replicate. Once a virus enters a host cell, the virus employs its host RNA machinery for viral replication. The newly produced virus particles escape the host cells by causing cell lysis. The new viruses infect neighboring cells and replicate again, resulting in cell death and viral spread throughout multi layered tissue^{33,34}. However, this process may also be toxic to normal tissues. Therefore, several

targeting strategies are developed in order to maximize the therapeutic ('oncolytic') effect on tumor cells and simultaneously prevent toxic effects to normal cells.

Targeting strategies for viral vectors can be divided into two major categories: transductional targeting and transcriptional targeting. Transductional targeting of an adenoviral vector implies redirecting the virus from its natural receptor to an alternative binding site. Transcriptional targeting strategies restrict viral replication to cancer cells only, causing cell death in tumor cells but not in normal cells. The primary receptor for adenovirus binding is the coxsackievirus and adenovirus receptor (CAR). CAR is expressed on most human tissues, but is often downregulated on cancer cells like glioma cells^{35, 36}. In an attempt to overcome this limitation, there have been significant efforts to retarget adenoviridae away from CAR to an alternative receptor. Although preferably this alternative receptor is upregulated in tumor cells, the major goal is to overcome CAR deficiency and enhance vector delivery into tumor cells³⁷⁻³⁹. To retarget the adenoviral vector, the binding site of the adenovirus needs to be modified. Normally, the fiber knob of the viral capsid binds to CAR. In order to retarget the virus to alternative binding sites, the whole fiber or the fiber knob can be replaced or modified. In this thesis, strategies investigated for use in glioma include insertion of a poly-lysine (pK7) or an RGD4C (RGD) motif into the C-terminal end of the adenovirus serotype 5 fiber gene, the HI loop of the fiber knob, or both.^{40, 41} Another CAR-independent approach employed display of a xeno-fiber knob on human adenovirus capsid fiber⁴². These genetic approaches to alter vector tropism all proved highly efficient in cancer cells grown in monolayer.

Transcriptional targeting of adenoviral vectors is achieved by genetic alterations of the viral genome resulting in selective transcription of the viral genome in tumor cells. This can be achieved by placing the expression of essential viral genes under the control of specific promoters that are highly active in cancer cells^{43, 44}. Good candidates are tumor specific promoters or tissue specific promoters, although tissue specific promoters are more associated with local side effects. Adenoviral vectors targeted in this manner are called conditionally replicating adenoviral vectors (CRAds)⁴⁵.

A less commonly used viral vector for gene therapy is the reovirus. Reoviruses are commonly found in the human respiratory and gastrointestinal tracts. However, they are not associated with any known human diseases and thus are considered to be benign^{32, 46}. Recent studies on the molecular basis of host cell permissiveness to reovirus have revealed that infection of KRAS mutated (cancer) cells result in drastic enhancement of reovirus infection of these cells.^{31, 47, 48} Therefore, reoviral vectors are of much interest in the treatment of colorectal cancer harboring KRAS mutations.

Targeting the EGFR-RAS-ERK pathway in colorectal cancer.

In the context of treatment of colorectal cancer and colorectal livermetastases, many targeted therapeutics have been developed and tested in pre-clinical and clinical settings. Most widely applied in the clinical setting is combination treatment with Bevacizumab⁴⁹⁻⁵¹. Bevacizumab is a

monoclonal antibody directed against vascular endothelial growth factor (VEGF). It has improved the response rate and survival of patients with metastatic colorectal cancer when combined with standard 5-FU based chemotherapy regimens.^{52, 53}.

Another monoclonal antibody, Cetuximab, has also proven to be effective in patients with colorectal cancer. Cetuximab, and the related antibody Panitumumab, specifically block the epidermal growth factor receptor (EGFR). EGFR activates downstream signaling pathways, among which the RAS-MEK-ERK pathway and the PI3K-Akt pathway. The EGFR is frequently overexpressed in human colorectal tumors when compared to normal intestinal tissue, and this is associated with increased metastatic potential and poor prognosis⁵⁴⁻⁵⁶. Not only the extracellular domain of EGFR was targeted with monoclonal antibodies, several small molecules like gefitinib and erlotinib have been successfully developed targeting the intracellular tyrosine kinase domain of EGFR.⁵⁷ Cetuximab therapy combined with conventional chemotherapy is very effective in about 10-20% of all treated patient⁵⁸⁻⁶¹. However, colorectal tumors with activating mutations in the *KRAS* oncogene are strongly associated with a lack of response to EGFR targeted therapy^{62, 63}. This might be due to the constitutive signaling of pathways downstream of RAS, resulting in EGFR independent signaling. However, this hypothesis was never proven and also other resistance mechanisms might play a roll.

Many efforts have been directed to develop specific inhibitors of the *KRAS* oncogene, but so far these efforts have remained unsuccessful^{26, 27}. Therefore, the search for alternative targets in pathways downstream Ras has intensified. Most efforts have focused on the classical Ras-activated RAF/MEK/ERK pathway. In particular RAF and MEK have served as targets for the development of novel anti-cancer drugs⁶⁴⁻⁶⁶. It has been well established that MEK inhibitors are especially effective in cancer cells with an activating mutation in the *BRAF* oncogene. In cancer cells with activating mutations in the *KRAS* oncogene however, response levels to MEK inhibitors varies greatly⁶⁷⁻⁷⁰. In colon cancer patients, the majority of tumors display elevated levels of phosphorylated ERK and MEK when compared to normal mucosa^{71, 72}. Nevertheless, suppression of ERK phosphorylation in human tumors by MEK inhibitors does not correlate with impressive anti-tumor responses^{73, 74}. This suggests that the growth of tumor cells driven by the *KRAS* oncogene does not rely on MEK/ERK signaling.

Targeting colon cancer stem cells

Most cells in colorectal tumors are differentiated and do not display an intrinsic ability to generate new tumors. The bulk of differentiated tumor cells are generated by a small population of undifferentiated tumor cells that selectively display tumor-initiating capacity.⁷⁵ These cells are mostly referred to as cancer stem cells. In accordance with stem cells in normal tissue, the cancer stem cell is a cell within a tumor that is able to self-renew and to produce the heterogeneous lineages of cancer cells that comprise the tumor⁷⁶⁻⁸⁰. Cancer stem cells (CSC) – or tumor initiating cells – not only have the capacity to initiate tumors, but they may also be responsible for tumor recurrence after chemotherapy or radiotherapy treatment^{81, 82}. For specific tumor types, it has

indeed been proven that cancer stem cells display resistance against chemotherapy. However, the underlying resistance mechanisms have to be unraveled and may vary from drug to drug^{81, 83-85}. The observed resistance of CSC against conventional chemotherapy has major implications for the development of novel anti-cancer therapeutics. While conventional strategies focused on the bulk of the tumor, CSC-directed therapeutics may be required in addition if curative systemic treatment is to be achieved. To study the properties of cancer stem cells it is essential to establish proper experimental culture systems directly derived from human colorectal tumors. Massive efforts have been made to identify specific cancer stem cell markers for their isolation and characterization. For colorectal cancer, several candidate markers have been suggested, such as prominin-1 (CD133)^{79, 80}, CD44 in combination with the epithelial cell adhesion molecule (EpCAM)^{86, 87}, and ALDH1⁸⁸. Although the recently discovered small intestine and colon stem cell marker LGR5 has shown to be very specific for normal intestinal stem cells in mice, no reliable method has been described yet to utilize this marker in human colorectal cancer⁸⁹. Crucial pathways for maintaining stemness in colorectal cancers are only partly uncovered. Therefore, the development of reliable cancer stem cell models, with material directly derived from patients, is crucial for identifying stemness pathways and CSC markers. These cultures, can then be used to study the resistance mechanisms in cancer stem cells and the pathways on which they depend. This area is of great interest given that virtually all chemotherapy-treated cancer patients show either intrinsic or acquired resistance to conventional chemotherapy.

Outline of the thesis

In this thesis, we aim to evaluate several novel anti-cancer therapeutics and their limitations, to understand their mechanism of action and the mechanisms of resistance. Specifically, we explore the therapeutic effects of oncolytic viral vectors on glioma and colorectal cancer. Furthermore, we evaluate EGFR and MEK targeting in *KRAS* mutated colorectal cancer cells. Finally, we explore strategies to target colorectal cancer stem cells.

In the first three chapters, this thesis focuses on oncolytic viral vectors. In the context of glioma, genetically modified adenoviral vectors were evaluated. In **chapters 2 and 3**, infectivity and cell killing properties of transductional and transcriptional targeted adenoviral vectors is evaluated on glioma cell lines and freshly derived glioma tissue from patients. **Chapter 4** describes efforts to overcome infectivity limitations observed in reovirus treatment of primary colorectal cancer samples.

Chapters 5 and 6 determined how the *KRAS* oncogene affects colorectal tumor cell responses to EGFR and MEK targeted therapy. In **chapter 5**, the mechanisms underlying resistance to EGFR-targeted therapy are examined in colorectal cancer cells harboring *KRAS* mutations. In **chapter 6**, the sensitivity of *KRAS* mutated colorectal cancer cell lines to MEK targeted therapy is evaluated.

In the ensuing chapters we focus on colorectal cancer stem cells. We developed a novel model for culturing colorectal cancer stem cells from freshly resected colorectal tumors or liver metastases. We identify two different mechanisms of resistance of cancer stem cells to common chemotherapeutic drugs. In **chapter 7**, we show that CSC and differentiated tumor cells display functional cooperation to resist irinotecan treatment. In **chapter 8**, we used proteomics to identify a CSC-intrinsic factor that contributes to oxaliplatin and cisplatin resistance.

References

1. Surawicz,T.S., Davis,F., Freels,S., Laws,E.R., Jr., & Menck,H.R. Brain tumor survival: results from the National Cancer Data Base. *J. Neurooncol.* 40, 151-160 (1998).
2. Wrensch,M., Minn,Y., Chew,T., Bondy,M., & Berger,M.S. Epidemiology of primary brain tumors: current concepts and review of the literature. *Neuro. Oncol.* 4, 278-299 (2002).
3. Davis,F.G., McCarthy,B.J., & Berger,M.S. Centralized databases available for describing primary brain tumor incidence, survival, and treatment: Central Brain Tumor Registry of the United States; Surveillance, Epidemiology, and End Results; and National Cancer Data Base. *Neuro. Oncol.* 1, 205-211 (1999).
4. Hill,C.I., Nixon,C.S., Ruehmeier,J.L., & Wolf,L.M. Brain tumors. *Phys. Ther.* 82, 496-502 (2002).
5. Alemany,R. et al. Gene therapy for gliomas: molecular targets, adenoviral vectors, and oncolytic adenoviruses. *Exp. Cell Res.* 252, 1-12 (1999).
6. Davis,F.G. & McCarthy,B.J. Epidemiology of brain tumors. *Curr. Opin. Neurol.* 13, 635-640 (2000).
7. Brown,P.D. et al. A prospective study of quality of life in adults with newly diagnosed high-grade gliomas: the impact of the extent of resection on quality of life and survival. *Neurosurgery* 57, 495-504 (2005).
8. Stupp,R. et al. Radiotherapy plus concomitant and adjuvant temozolomide for glioblastoma. *N. Engl. J. Med.* 352, 987-996 (2005).
9. Athanassiou,H. et al. Randomized phase II study of temozolomide and radiotherapy compared with radiotherapy alone in newly diagnosed glioblastoma multiforme. *J. Clin. Oncol.* 23, 2372-2377 (2005).
10. Dirven,C.M. et al. Oncolytic adenoviruses for treatment of brain tumours. *Expert. Opin. Biol. Ther.* 2, 943-952 (2002).
11. Lamfers,M.L. et al. Potential of the conditionally replicative adenovirus Ad5-Delta24RGD in the treatment of malignant gliomas and its enhanced effect with radiotherapy. *Cancer Res.* 62, 5736-5742 (2002).
12. Jiang,H., Gomez-Manzano,C., Lang,F.F., Alemany,R., & Fueyo,J. Oncolytic adenovirus: preclinical and clinical studies in patients with human malignant gliomas. *Curr. Gene Ther.* 9, 422-427 (2009).
13. Boyle,P. & Leon,M.E. Epidemiology of colorectal cancer. *Br. Med. Bull.* 64, 1-25 (2002).
14. Steele,G., Jr. & Ravikumar,T.S. Resection of hepatic metastases from colorectal cancer. Biologic perspective. *Ann. Surg.* 210, 127-138 (1989).
15. Thirion,P. et al. Modulation of fluorouracil by leucovorin in patients with advanced colorectal cancer: an updated meta-analysis. *J. Clin. Oncol.* 22, 3766-3775 (2004).
16. Choti,M.A. et al. Trends in long-term survival following liver resection for hepatic colorectal metastases. *Ann. Surg.* 235, 759-766 (2002).
17. Abdalla,E.K. et al. Recurrence and outcomes following hepatic resection, radiofrequency ablation, and combined resection/ablation for colorectal liver metastases. *Ann. Surg.* 239, 818-825 (2004).
18. Stang,A., Fischbach,R., Teichmann,W., Bokemeyer,C., & Braumann,D. A systematic review on the clinical benefit and role of radiofrequency ablation as treatment of colorectal liver metastases. *Eur. J. Cancer* 45, 1748-1756 (2009).
19. Andreyev,H.J. et al. Kirsten ras mutations in patients with colorectal cancer: the 'RASCAL II' study. *Br. J. Cancer* 85, 692-696 (2001).
20. Andreyev,H.J., Norman,A.R., Cunningham,D., Oates,J.R., & Clarke,P.A. Kirsten ras mutations in patients with colorectal cancer: the multicenter "RASCAL" study. *J. Natl. Cancer Inst.* 90, 675-684 (1998).
21. Samowitz,W.S. et al. Relationship of Ki-ras mutations in colon cancers to tumor location, stage, and survival: a population-based study. *Cancer Epidemiol. Biomarkers Prev.* 9, 1193-1197 (2000).
22. Fodde,R., Smits,R., Hofland,N., Kielman,M., & Meera,K.P. Mechanisms of APC-driven tumorigenesis: lessons from mouse models. *Cytogenet. Cell Genet.* 86, 105-111 (1999).
23. Janssen,K.P. et al. APC and oncogenic KRAS are synergistic in enhancing Wnt signaling in intestinal tumor formation and progression. *Gastroenterology* 131, 1096-1109 (2006).
24. Malumbres,M. & Barbacid,M. RAS oncogenes: the first 30 years. *Nat. Rev. Cancer* 3, 459-465 (2003).
25. Bos,J.L. ras oncogenes in human cancer: a review. *Cancer Res.* 49, 4682-4689 (1989).
26. Downward,J. Targeting RAS signalling pathways in cancer therapy. *Nat. Rev. Cancer* 3, 11-22 (2003).
27. Friday,B. & Adjei,A. KRAS as a target for cancer therapy. *Biochim.Biophys.Acta, Reviews on Cancer in press.* 2005. Ref Type: Generic

28. Dobbstein,M. Viruses in therapy--royal road or dead end? *Virus Res.* 92, 219-221 (2003).
29. Stribley,J.M., Rehman,K.S., Niu,H., & Christman,G.M. Gene therapy and reproductive medicine. *Fertil. Steril.* 77, 645-657 (2002).
30. Thomas,C.E., Ehrhardt,A., & Kay,M.A. Progress and problems with the use of viral vectors for gene therapy. *Nat. Rev. Genet.* 4, 346-358 (2003).
31. Coffey,M.C., Strong,J.E., Forsyth,P.A., & Lee,P.W. Reovirus therapy of tumors with activated Ras pathway. *Science* 282, 1332-1334 (1998).
32. Norman,K.L. & Lee,P.W. Reovirus as a novel oncolytic agent. *J. Clin. Invest* 105, 1035-1038 (2000).
33. Curiel,D.T. & Rancourt,C. Conditionally replicative adenoviruses for cancer therapy. *Adv. Drug Deliv. Rev.* 27, 67-81 (1997).
34. Douglas,J.T., Kim,M., Sumerel,L.A., Carey,D.E., & Curiel,D.T. Efficient oncolysis by a replicating adenovirus (ad) in vivo is critically dependent on tumor expression of primary ad receptors. *Cancer Res.* 61, 813-817 (2001).
35. Douglas,J.T., Kim,M., Sumerel,L.A., Carey,D.E., & Curiel,D.T. Efficient oncolysis by a replicating adenovirus (ad) in vivo is critically dependent on tumor expression of primary ad receptors. *Cancer Res.* 61, 813-817 (2001).
36. Okegawa,T. et al. The mechanism of the growth-inhibitory effect of coxsackie and adenovirus receptor (CAR) on human bladder cancer: a functional analysis of car protein structure. *Cancer Res.* 61, 6592-6600 (2001).
37. Haviv,Y.S. et al. Adenoviral gene therapy for renal cancer requires retargeting to alternative cellular receptors. *Cancer Res.* 62, 4273-4281 (2002).
38. Kanerva,A. et al. Targeting adenovirus to the serotype 3 receptor increases gene transfer efficiency to ovarian cancer cells. *Clin. Cancer Res.* 8, 275-280 (2002).
39. Seki,T. et al. Fiber shaft extension in combination with HI loop ligands augments infectivity for CAR-negative tumor targets but does not enhance hepatotropism in vivo. *Gene Ther.* 9, 1101-1108 (2002).
40. Seki,T. et al. Fiber shaft extension in combination with HI loop ligands augments infectivity for CAR-negative tumor targets but does not enhance hepatotropism in vivo. *Gene Ther.* 9, 1101-1108 (2002).
41. Wu,H. et al. Double modification of adenovirus fiber with RGD and polylysine motifs improves coxsackievirus-adenovirus receptor-independent gene transfer efficiency. *Hum. Gene Ther.* 13, 1647-1653 (2002).
42. Glasgow,J.N. et al. An adenovirus vector with a chimeric fiber derived from canine adenovirus type 2 displays novel tropism. *Virology* 324, 103-116 (2004).
43. Haviv,Y.S. & Curiel,D.T. Conditional gene targeting for cancer gene therapy. *Adv. Drug Deliv. Rev.* 53, 135-154 (2001).
44. Haviv,Y.S. & Blackwell,J. Transcriptional regulation in cancer gene therapy. *Isr. Med. Assoc. J.* 3, 517-522 (2001).
45. Suzuki,K. et al. A conditionally replicative adenovirus with enhanced infectivity shows improved oncolytic potency. *Clin. Cancer Res.* 7, 120-126 (2001).
46. Tyler,K.L., Clarke,P., Debiasi,R.L., Kominsky,D., & Poggioli,G.J. Reoviruses and the host cell. *Trends Microbiol.* 9, 560-564 (2001).
47. Strong,J.E., Coffey,M.C., Tang,D., Sabinin,P., & Lee,P.W. The molecular basis of viral oncolysis: usurpation of the Ras signaling pathway by reovirus. *EMBO J.* 17, 3351-3362 (1998).
48. Smakman,N., van den Wollenberg,D.J., Borel,R., I, Hoeben,R.C., & Kranenburg,O. Sensitization to apoptosis underlies KrasD12-dependent oncolysis of murine C26 colorectal carcinoma cells by reovirus T3D. *J. Virol.* 79, 14981-14985 (2005).
49. Hurwitz,H. & Kabbinavar,F. Bevacizumab combined with standard fluoropyrimidine-based chemotherapy regimens to treat colorectal cancer. *Oncology* 69 Suppl 3, 17-24 (2005).
50. Cassidy,J. et al. Effect of bevacizumab in older patients with metastatic colorectal cancer: pooled analysis of four randomized studies. *J. Cancer Res. Clin. Oncol.* 136, 737-743 (2010).
51. Kabbinavar,F., Irl,C., Zurlo,A., & Hurwitz,H. Bevacizumab improves the overall and progression-free survival of patients with metastatic colorectal cancer treated with 5-fluorouracil-based regimens irrespective of baseline risk. *Oncology* 75, 215-223 (2008).
52. Kabbinavar,F.F., Hurwitz,H.I., Yi,J., Sarkar,S., & Rosen,O. Addition of bevacizumab to fluorouracil-based first-line treatment of metastatic colorectal cancer: pooled analysis of cohorts of older patients from two randomized clinical trials. *J. Clin. Oncol.* 27, 199-205 (2009).

53. Kabbinavar,F.F. et al. Health-related quality of life impact of bevacizumab when combined with irinotecan, 5-fluorouracil, and leucovorin or 5-fluorouracil and leucovorin for metastatic colorectal cancer. *Oncologist*. 13, 1021-1029 (2008).
54. Radinsky,R. et al. Level and function of epidermal growth factor receptor predict the metastatic potential of human colon carcinoma cells. *Clin. Cancer Res.* 1, 19-31 (1995).
55. O'Dwyer,P.J. & Benson,A.B., III Epidermal growth factor receptor-targeted therapy in colorectal cancer. *Semin. Oncol.* 29, 10-17 (2002).
56. Nicholson,R.I., Gee,J.M., & Harper,M.E. EGFR and cancer prognosis. *Eur. J. Cancer* 37 Suppl 4, S9-15 (2001).
57. Quintela-Fandino,M. et al. Phase I combination of sorafenib and erlotinib therapy in solid tumors: safety, pharmacokinetic, and pharmacodynamic evaluation from an expansion cohort. *Mol. Cancer Ther.* 9, 751-760 (2010).
58. Amado,R.G. et al. Wild-type KRAS is required for panitumumab efficacy in patients with metastatic colorectal cancer. *J. Clin. Oncol.* 26, 1626-1634 (2008).
59. Bokemeyer,C. et al. Fluorouracil, leucovorin, and oxaliplatin with and without cetuximab in the first-line treatment of metastatic colorectal cancer. *J. Clin. Oncol.* 27, 663-671 (2009).
60. De,R.W. et al. KRAS wild-type state predicts survival and is associated to early radiological response in metastatic colorectal cancer treated with cetuximab. *Ann. Oncol.* 19, 508-515 (2008).
61. Van,C.E. et al. Cetuximab and chemotherapy as initial treatment for metastatic colorectal cancer. *N. Engl. J. Med.* 360, 1408-1417 (2009).
62. Allegra,C.J. et al. American Society of Clinical Oncology provisional clinical opinion: testing for KRAS gene mutations in patients with metastatic colorectal carcinoma to predict response to anti-epidermal growth factor receptor monoclonal antibody therapy. *J. Clin. Oncol.* 27, 2091-2096 (2009).
63. Linardou,H. et al. Assessment of somatic k-RAS mutations as a mechanism associated with resistance to EGFR-targeted agents: a systematic review and meta-analysis of studies in advanced non-small-cell lung cancer and metastatic colorectal cancer. *Lancet Oncol.* 9, 962-972 (2008).
64. Friday,B.B. & Adjei,A.A. Advances in targeting the Ras/Raf/MEK/Erk mitogen-activated protein kinase cascade with MEK inhibitors for cancer therapy. *Clin. Cancer Res.* 14, 342-346 (2008).
65. Roberts,P.J. & Der,C.J. Targeting the Raf-MEK-ERK mitogen-activated protein kinase cascade for the treatment of cancer. *Oncogene* 26, 3291-3310 (2007).
66. Sebolt-Leopold,J.S., Herrera,R., & Ohren,J.F. The mitogen-activated protein kinase pathway for molecular-targeted cancer treatment. *Recent Results Cancer Res.* 172, 155-167 (2007).
67. Solit,D.B. et al. BRAF mutation predicts sensitivity to MEK inhibition. *Nature* 439, 358-362 (2006).
68. Davies,B.R. et al. AZD6244 (ARRY-142886), a potent inhibitor of mitogen-activated protein kinase/extracellular signal-regulated kinase kinase 1/2 kinases: mechanism of action in vivo, pharmacokinetic/pharmacodynamic relationship, and potential for combination in preclinical models. *Mol. Cancer Ther.* 6, 2209-2219 (2007).
69. Pohl,G. et al. Inactivation of the mitogen-activated protein kinase pathway as a potential target-based therapy in ovarian serous tumors with KRAS or BRAF mutations. *Cancer Res.* 65, 1994-2000 (2005).
70. Wang,Y. et al. A role for K-ras in conferring resistance to the MEK inhibitor, CI-1040. *Neoplasia*. 7, 336-347 (2005).
71. Hoshino,R. et al. Constitutive activation of the 41-/43-kDa mitogen-activated protein kinase signaling pathway in human tumors. *Oncogene* 18, 813-822 (1999).
72. Lee,S.H. et al. Colorectal tumors frequently express phosphorylated mitogen-activated protein kinase. *APMIS* 112, 233-238 (2004).
73. Adjei,A.A. et al. Phase I pharmacokinetic and pharmacodynamic study of the oral, small-molecule mitogen-activated protein kinase kinase 1/2 inhibitor AZD6244 (ARRY-142886) in patients with advanced cancers. *J. Clin. Oncol.* 26, 2139-2146 (2008).
74. Rinehart,J. et al. Multicenter phase II study of the oral MEK inhibitor, CI-1040, in patients with advanced non-small-cell lung, breast, colon, and pancreatic cancer. *J. Clin. Oncol.* 22, 4456-4462 (2004).
75. Rich,J.N. & Bao,S. Chemotherapy and cancer stem cells. *Cell Stem Cell* 1, 353-355 (2007).
76. Clarke,M.F. et al. Cancer stem cells--perspectives on current status and future directions: AACR Workshop on cancer stem cells. *Cancer Res.* 66, 9339-9344 (2006).

77. Hamburger,A.W. & Salmon,S.E. Primary bioassay of human tumor stem cells. *Science* 197, 461-463 (1977).
78. Akashi,K., Reya,T., ma-Weiszhausz,D., & Weissman,I.L. Lymphoid precursors. *Curr. Opin. Immunol.* 12, 144-150 (2000).
79. O'Brien,C.A., Pollett,A., Gallinger,S., & Dick,J.E. A human colon cancer cell capable of initiating tumour growth in immunodeficient mice. *Nature* 445, 106-110 (2007).
80. Ricci-Vitiani,L. et al. Identification and expansion of human colon-cancer-initiating cells. *Nature* 445, 111-115 (2007).
81. Dean,M., Fojo,T., & Bates,S. Tumour stem cells and drug resistance. *Nat. Rev. Cancer* 5, 275-284 (2005).
82. Donnenberg,V.S. & Donnenberg,A.D. Multiple drug resistance in cancer revisited: the cancer stem cell hypothesis. *J. Clin. Pharmacol.* 45, 872-877 (2005).
83. Hermann,P.C. et al. Distinct populations of cancer stem cells determine tumor growth and metastatic activity in human pancreatic cancer. *Cell Stem Cell* 1, 313-323 (2007).
84. Liu,G. et al. Analysis of gene expression and chemoresistance of CD133+ cancer stem cells in glioblastoma. *Mol. Cancer* 5, 67 (2006).
85. Dean,M. ABC transporters, drug resistance, and cancer stem cells. *J. Mammary. Gland. Biol. Neoplasia.* 14, 3-9 (2009).
86. Dalerba,P. et al. Phenotypic characterization of human colorectal cancer stem cells. *Proc. Natl. Acad. Sci. U. S. A* 104, 10158-10163 (2007).
87. Huang,E.H. et al. Aldehyde dehydrogenase 1 is a marker for normal and malignant human colonic stem cells (SC) and tracks SC overpopulation during colon tumorigenesis. *Cancer Res.* 69, 3382-3389 (2009).
88. Dylla,S.J. et al. Colorectal cancer stem cells are enriched in xenogeneic tumors following chemotherapy. *PLoS. ONE.* 3, e2428 (2008).
89. Barker,N. et al. Identification of stem cells in small intestine and colon by marker gene *Lgr5*. *Nature* 449, 1003-1007 (2007).

2

Gene delivery into malignant glioma by infectivity-enhanced adenovirus: In vivo vs. in vitro models

Winan J. Van Houdt, Hongju Wu, Joel N. Glasgow,
Martine L. Lamfers, Clemens M. Dirven, G. Yancey Gillespie,
David T. Curiel, and Yosef S. Haviv

Neuro Oncology, 2007 Jul;9(3):280-90

Abstract

Adenoviral vectors (Ad) demonstrate several attributes of potential utility for glioma gene therapy. Although Ad infection is limited *in vitro* by low expression levels of the Coxsackie-adenoviral receptor (CAR), *in vivo* studies have shown the efficacy of Ad as gene delivery vectors. To evaluate the *in vivo* utility of CAR-independent, infectivity-enhanced Ad, we employed genetically modified Ad vectors in several experimental models of human gliomas. We used three capsid-modified Ad vectors: 1) a chimeric Ad with a human Ad backbone and a fiber knob of a canine Ad, 2) an Ad vector with a polylysine motif incorporated into the fiber gene, and 3) a double-modified Ad incorporating both an RGD4C peptide and the polylysine motif. These three modified Ads target the putative membrane receptor(s) of the canine Ad, heparin sulfate proteoglycans (HSPGs), and both integrins and HSPGs, respectively. Our *in vitro* studies indicated that these retargeting strategies all enhanced CAR-independent infectivity in both established and primary low-passage glioma cells. Enhancement of *in vitro* gene delivery by the capsid-modified vectors correlated inversely with the levels of cellular CAR expression. However, *in vivo* in orthotopic human glioma xenografts, infectivity of the capsid-modified Ads was not superior to the unmodified Ad. Although genetic strategies to circumvent CAR deficiency in glioma cells could reproducibly expand the cellular entry mechanisms of Ad vectors in cultured and primary glioma cells, these approaches were insufficient to confer *in vivo* significant infectivity enhancement over unmodified Ad. Other factors, probably the extracellular matrix, stromal cells, and the three-dimensional tumor architecture, clearly play important roles *in vivo* and interfere with Ad-based gene delivery into glioma tumors.

Introduction

Currently available therapeutic modalities for high-grade malignant gliomas often fail to improve patient prognosis. Standard therapy is limited by a low therapeutic index¹ and by the cross-resistance between chemotherapeutic drugs². Within this context, gene therapy is a promising therapeutic strategy for malignant gliomas, potentially offering both tumor targeting and novel cell-killing mechanisms. Recombinant adenoviruses (Ad)² appear promising as gene therapy vectors for glioma, on the merit of their ability to infect both dividing and quiescent tumor cells, genome plasticity, mild pathogenicity in humans, and safety shown in gene therapy clinical trials for glioma³⁻⁶. While the efficiency of Ad-based gene delivery into glioma cells may depend on the expression levels of the Coxsackie-adenoviral receptor (CAR), the primary Ad receptor⁷⁻¹⁰, other reports have found that capsid-unmodified Ad is a highly efficient vector in the context of glioma¹¹⁻¹³. Another factor confounding the use of Ad for glioma involves the dose of vector inoculum, which can be potentially toxic to neighboring brain cells¹⁴. Clearly, both CAR-dependent and CAR-independent glioma cell infection by Ad vectors need to be further explored. In this study, we evaluated the utility of CAR-independent genetic retargeting of Ad in glioma models. Genetic retargeting is generally superior to antibody-conjugated Ad in respect to easier administration and the potential for tropism modification in the progeny of conditionally replicative Ad viruses¹⁵.

Genetic modification of Ad capsid for CAR-independent infection may involve either replacement of the entire Ad fiber or the fiber knob, or the insertion of heterologous ligands into the fiber knob of Ad5¹⁶⁻²⁰. Recent genetic approaches developed by our group for CAR-independent Ad infection include insertion of a polysine (Pk7) motif or an RGD4C (RGD) motif into the C-terminal end of the Ad5 fiber gene or the HI loop of the fiber knob, respectively, or both. Another CAR-independent approach employed display of a xeno-fiber knob on human Ad capsid fiber. These genetic approaches to alter vector tropism all proved highly efficient in cancer cells grown in monolayer cultures. In this study, we investigated whether the utility of tropism modification of Ad vectors attained *in vitro* is maintained in solid glioma tumor xenografts. This issue is critical for cancer gene therapy endeavors because tumor components may impose several levels of blockage on vector distribution and gene delivery. In addition to cancer cells, tumors consist of stroma comprising reactive fibroblasts and extracellular matrix, basement membranes, abnormal blood vessels, necrotic regions, and infiltrating cells of the immune system. Standard cancer therapy may further accentuate necrosis, apoptosis, and fibrosis within the tumor, thereby potentially confounding the potential distribution of viral vectors. Our results indicate that while tropism-modified Ad vectors could dramatically enhance infectivity in low-CAR glioma cells *in vitro*, Ad capsid modification was not the sole determinant of *in vivo* gene delivery in glioma xenografts.

Methods

Glioma Cells

Both established and primary human malignant glioma cell lines were used in this study. The glioma cell lines U-118MG and M59K were purchased from the American Type Culture Collection

(ATCC, Manassas, VA, USA). D-65MG, U-251MG, U-87MG, and D-54MG cells were provided by Dr. Darell D. Bigner (Duke University Medical Center, Durham, NC, USA). U87 cells were cultured with MEM (Mediatech, Herndon, VA, USA) with 15% fetal bovine serum (FBS; HyClone, Logan, UT, USA), 2 Mm L-glutamine, penicillin (100 IU/ml), streptomycin (100 µg/ml), and amphotericin B (2.5 µg/ml) (Mediatech). U251, U118, M59K, D65, and D54 cells were cultured in Dulbecco's modified Eagle's medium/F12 50:50 with 7–10% FBS, L-glutamine, and antibiotics as above. All cells were cultured at 37°C in a 5% CO₂ humidified atmosphere. The primary glioma cells VU-15, VU-28, VU-78, and VU-84 were obtained and used before the eighth passage, as previously described (Lamfers et al, 2002). Primary malignant glioma cells were cultured in Dulbecco's modified Eagle's medium (Mediatech) with 10% FBS, L-glutamine, and antibiotics as above.

Adenoviral Vectors

All Ad vectors used in this study were replication deficient (E1 deleted) and based on the serotype-5 Ad genome. The construction of Ad5, Ad5.Pk7, Ad5.RGD, and Ad5.RGD.Pk7 has been described previously (Wu, et al 2002). Ad5 is an untargeted Ad vector, used as an isogenic control for Ad5.Pk7, Ad5.RGD, and Ad5.RGD.Pk7. Ad5.Pk7 and Ad5.RGD differ from Ad5 by the respective insertion of a polylysine (Pk7) or an RGD4C motif into the C-terminal end of the Ad5 fiber gene or the HI loop of the fiber knob. Ad5.RGD.Pk7 contains an RGD4C (RGD) motif in the HI loop of the fiber knob in addition to the Pk7 motif at the C-terminal end. These Ad vectors all include two identical bicistronic reporter gene cassettes, i.e., the firefly luciferase and the green fluorescent protein (GFP), each driven by a separate cytomegalovirus (CMV) promoter.

A different approach for Ad capsid modification is Ad5Luc1-CK (also termed AdCK-2; Glasgow et al, 2004) displaying genetic xeno-fiber knob replacement via the fiber knob of the canine Ad serotype 2. The cell entry mechanism of Ad5Luc1-CK involves both the putative cellular receptor(s) of the canine Ad serotype 2²¹ and CAR. The control Ad vector for Ad5Luc1-CK was the isogenic, capsid-unmodified Ad5Luc1. Thus, we used two groups of viral vectors, whereby a distinct untargeted Ad5 vector served as an isogenic control to the corresponding retargeted Ad vectors (Fig. 1). All viruses were rescued on 293 cells and purified by using a standard CsCl gradient protocol. The number of viral particles was determined using a conversion factor of 1.1×10^{12} viral particles (vp) per absorbance unit at 260 nm. The titers of these viruses were as follows: Ad5: 3.1×10^{12} vp/ml, Ad5.RGD: 2.1×10^{12} vp/ml, Ad5.RGD.pk7: 7.8×10^{11} vp/ml, Ad.pk7: 1.0×10^{12} vp/ml, Ad5.luc1: 3.7×10^{12} vp/ml, Ad5.luc1-CK: 9.7×10^{11} vp/ml.

Flow Cytometry

Glioma cells were rinsed with phosphate-buffered saline (PBS), harvested by versene incubation, and resuspended in PBS containing 1% bovine serum albumin (Sigma Chemical Co.). For antibody incubation, 2×10^5 cells (for VU-28, 1×10^5 cells) were incubated with the monoclonal mouse anti-human CAR antibody, RmcB (produced by Dr. J.T. Douglas from the hybridoma CRL-2379 cell line, ATCC), at 1:80 for 1 h at 4°C. An isotype-matched normal mouse IgG₁ (1:80) was used as a negative control. After incubation, cells were rinsed with PBS-bovine serum albumin and incubated with a 1:100 dilution of fluorescein isothiocyanate (FITC)-labeled goat anti-mouse IgG (Alexa 488, Molecular Probes, Eugene, OR, USA) for 1 h at 4°C. After another PBS rinse, labeled cells were fixed with 1% paraformaldehyde solution and analyzed by flow cytometry.

Relative mean fluorescence intensity was calculated as the ratio of the mean fluorescence intensity of the sample of interest to that of the corresponding negative control. The FITC-positive cell population for each cell line was determined by gating cells incubated with 1% buffer only (negative control).

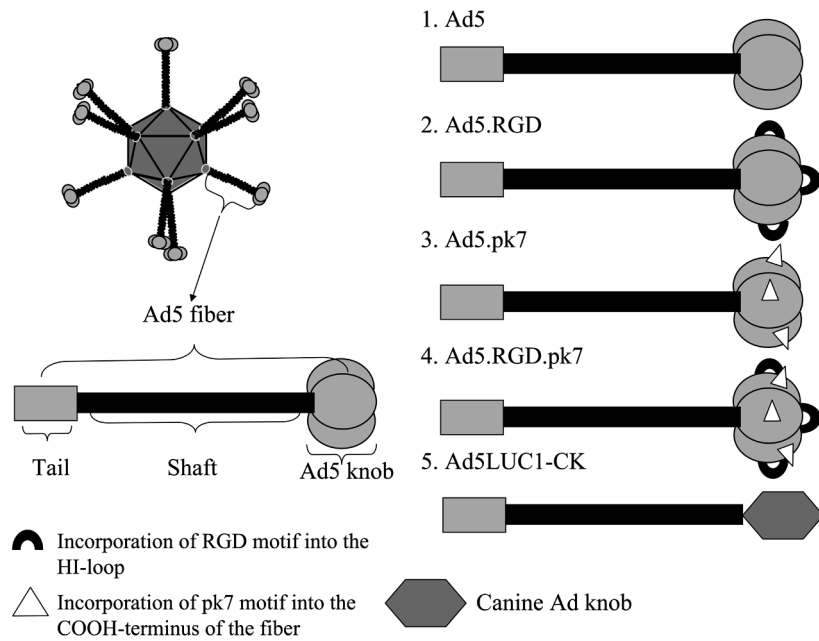


Figure 1. Diagram of the various capsid-modified Ad vectors used in the study.

Fluorescence Microscopy

U118 glioma cells were plated in six-well plates (10^5 cells/well). Two days later, cells were infected for 1 h with either the control Ad5 vector or the retargeted vector Ad5.Pk7 or Ad5.Pk7.RGD, at a multiplicity of infection (MOI) of 1000 vp/cell. Fluorescence microscopy was performed 2 days later with an Olympus IX70 inverted epifluorescence microscope. All samples were photographed and processed under the same conditions.

Luciferase Assays

Cells were seeded in 24-well plates (50,000 cells/well, 25,000 cells/well for VU-28), with each well containing 0.5 ml of growth medium. After 24 h, cells were infected at an MOI of 40, 200, and 1000 in 500 μ l of infection medium. After 1 h, the infection medium was replaced with growth medium. Twenty-four hours later, the growth medium was aspirated, and the cells were washed and lysed with 100 μ l of lysis buffer (Promega, Madison, WI, USA) and mechanically harvested. Ten microliters of each sample was then mixed with 50 μ l of luciferase assay reagent (Promega) and measured for relative light units (RLU) with Berthold Lumat LB9501 luminometer. Standardization between cell lines and MOIs was accomplished by setting the values obtained with the relevant Ad5 control vector as 100%.

Competitive Inhibition Assays

U118 cells were plated in 12-well plates at a density of 10^5 cells/well the day before infection. An MOI of 200 was used for each infection. Ad5.Pk7 and Ad5.RGD.Pk7 were pre-incubated with unfractionated heparin (heparin sodium salt from porcine in intestinal mucosa, Sigma, 0.1, 1, or 10 $\mu\text{g}/\text{ml}$), to block the heparin sulfate proteoglycan (HSPG) cellular entry mechanism, as described before (Wu, et al, 2002).

To block the putative cellular receptor for canine Ad, U87 cells were pre-incubated with recombinant canine knob (0.5, 5, or 50 $\mu\text{g}/\text{ml}$) and then infected with Ad5Luc1-CK at an MOI of 200. Luciferase assays were used to evaluate the efficiency of infection.

In Vivo Glioma Xenograft Model and Luciferase Imaging

All animal experiments were approved by the Institutional Animal Care and Use Committee of the University of Alabama at Birmingham and performed according to their guidelines. The glioma xenograft models were established in female athymic nude mice (National Cancer Institute-Frederick Animal Production Area, Frederick, MD, USA) by stereotactical injection of glioma cells into the mouse brain at the region of the caudate putamen nucleus. Glioma cells that stably express firefly luciferase (Luc⁺ U87MG) and regular glioma cells including high-CAR D54MG cells and low-CAR U87MG cells were used in the experiments. For each mouse, 5×10^5 glioma cells in a 5- μl volume were injected into the brain. Two weeks later, 10^{10} viral particles of each Ad vector were injected into the brain tumors that were established with regular U87MG or D54MG cells. Noninvasive, live luciferase imaging was performed at different days after viral injection to follow the transgene (luciferase reporter) expression. The experimental design of the *in vivo* glioma xenograft model is depicted in Table 1. Luciferase imaging was performed using a custom-built noninvasive optical imaging system similar to the Roper Scientific ChemiPro imaging system. For live imaging, the mice were anesthetized with isoflurane inhalation. Following intraperitoneal injection of D-luciferin (2.5 mg/100 μl per mouse), the bioluminescent signals in live mice were captured with a highly sensitive back-illuminated VersArray:1KB CCD camera (Princeton Instruments) that was equipped with a Nikkor 1.2 lens. Images were acquired with WinView /32 (Roper Scientific) and analyzed with ImageTool 3.0 (The University of Texas Health Science Center in San Antonio) and Photoshop 7.0 (Adobe).

Table 1. Experimental design for *in vivo* evaluation of infectivity-modified Ad5 vectors

Tumor model	1) High-CAR: D54MG 2) Low-CAR: U87MG
Mouse	Athymic nude mice, five mice per vector per model
Vectors	Ad5, Ad5.Pk7, Ad5.RGD.Pk7, Ad5Luc1, Ad5Luc1-CK
Tumor inoculation	5×10^5 cells in a 5- μl volume were injected stereotactically into the mouse brain at the region of caudate putamen nucleus.
Vector injection	Fourteen days after tumor inoculation, 10^{10} vp of each vector were stereotactically injected into each brain tumor model.
Luc imaging	Twice a week following vector injection, for 2 weeks.

Statistical Methods

Student's *t*-test was used to compare the efficiency of gene delivery by the various Ad vectors in glioma cells *in vitro* or in the *in vivo* glioma tumor models; $p < 0.05$ was considered significant. The Wilcoxon two-sample test was used to confirm statistical significance.

Results

Heterogeneous CAR Expression in Established Glioma Cells

CAR expression is a critical determinant of the efficiency of Ad entry into glioma cancer cells grown in monolayer²²⁻²⁴. Therefore, to evaluate the utility of our retargeting strategies, we first measured CAR expression in a panel of established glioma cells. We found that CAR expression in glioma cells was heterogeneous and could be grouped into three major groups: low-, medium-, or high-CAR expression (Fig. 2). Of note, the medium level of CAR expression in the established glioma cell lines D65 and M59K was derived from two distinct populations, i.e., low- and high-CAR cells. Thus, within the established glioma cell lines there was considerable variation in CAR expression.

Superiority of Retargeted Ad Vectors in Established Low-CAR Glioma Cell Lines

To evaluate the hypothesis that the novel genetic strategies for tropism modification of Ad vectors could circumvent the resistance of low-CAR glioma cells to Ad5 infection, we employed three retargeted Ad vectors. The first strategy was based on a chimeric Ad vector composed of the human Ad5 shaft flanked by the canine Ad knob (Ad5Luc1-CK). The second Ad retargeting strategy was based on incorporation of a polylysine motif into the C-terminus of the Ad5 fiber (Ad5.Pk7). The third Ad vector was based on dual targeting, with both a polylysine motif and an RGD4C peptide inserted into the Ad5 C-terminus fiber gene and HI loop of the knob, respectively (Ad5.RGD.Pk7). Ad5Luc1-CK, Ad5.Pk7, and Ad5.RGD.Pk7 were designed to target the respective alternative Ad receptors, the putative receptor for canine Ad, HSPG, or both HSPG and cell surface integrins. Of note, an isogenic Ad.RGD vector was less efficient in enhancing gene delivery into glioma cells and was further used only as a specific control for Ad5.RGD.Pk7 (data not shown).

When low-CAR glioma cell lines were tested for susceptibility to Ad infection, the three retargeting strategies proved to be superior to regular Ad5 vectors with no capsid modification (Fig. 3A-C). Specifically, in the low-CAR U118 and U87 cells, substantially higher levels of gene delivery could be achieved by all three retargeted vectors. In the medium-CAR glioma cell lines D65 and M59K, the infectivity enhancement of the retargeted Ad vectors was lower than in the low-CAR cells. In high-CAR cells, there was no consistent advantage for CAR-independent infection. Of note, the degree of infectivity enhancement of the retargeted Ad vectors varied in the D65 and M59K cell lines, in accordance with the two distinct cell populations in regard to CAR expression, as shown in Fig. 2. While the double-modified Ad5.RGD.Pk7 showed more efficient CAR-independent cell entry in the low-CAR primary glioma cells and in U118 cells, Ad5.pk7 infection was more efficient in the low-CAR U87 cells, possibly indicating variable HSPG and integrin cell surface expression in different glioma cell lines. In low-CAR cells, Ad5.RGD.Pk7 was superior to Ad5.RGD vector (Fig. 3C), which was previously shown to enhance infectivity in glioma cells (Yoshida, et al 1998; Grill,

et al 2001). Thus, the novel retargeted Ad vectors Ad5CK-2, Ad5.Pk7, and Ad5.RGD.Pk7 augment Ad-based gene delivery into established low-CAR glioma cell lines.

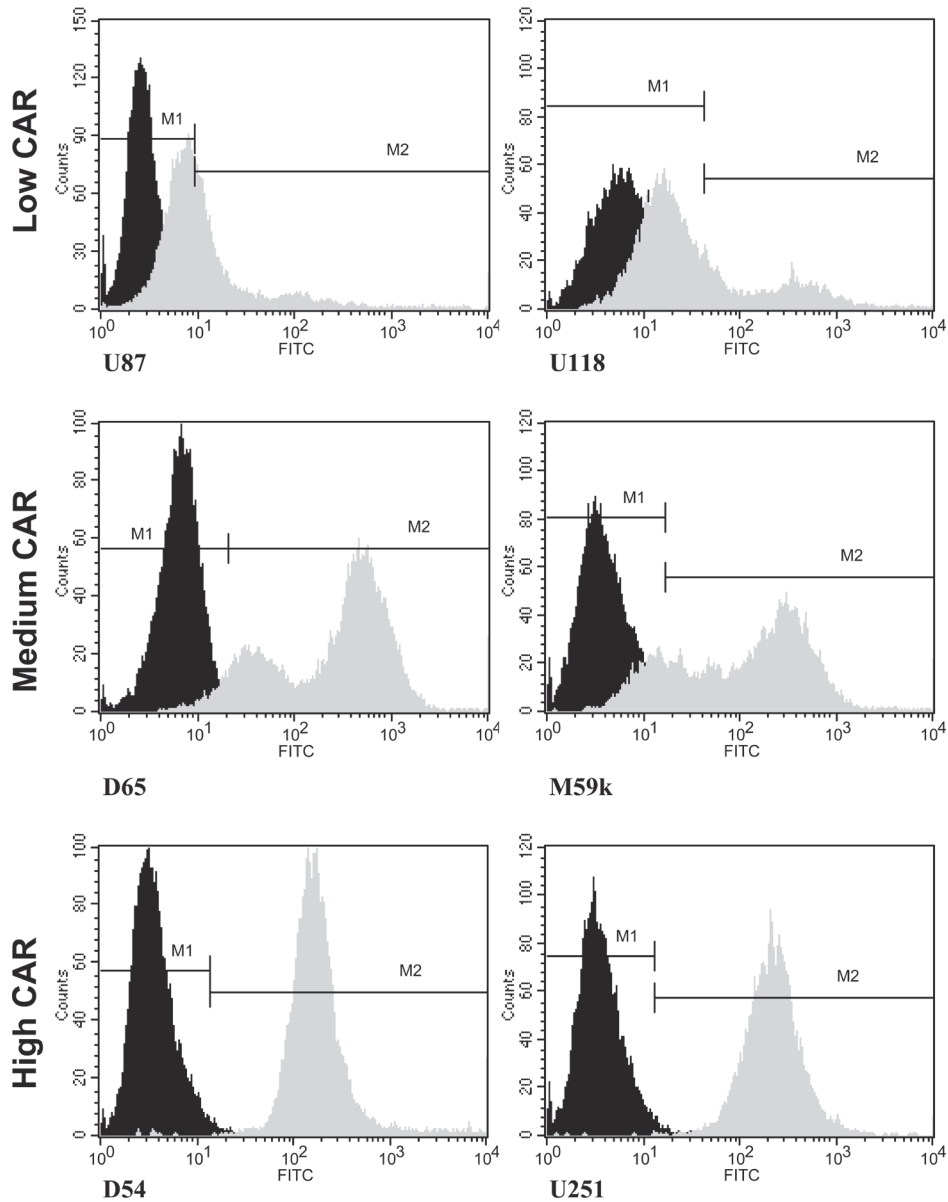


Figure 2. CAR expression in established glioma cells. Expression of CAR (*gray*) was measured in the established human glioma cell lines U87, U118, D65, M59K, D54, and U251 with indirect flow cytometry. Cells were first incubated with the monoclonal anti-CAR Ab RmcB, followed by detection with FITC-labeled secondary antibody. An IgG-matched isotype antibody was used as a control (*black*).

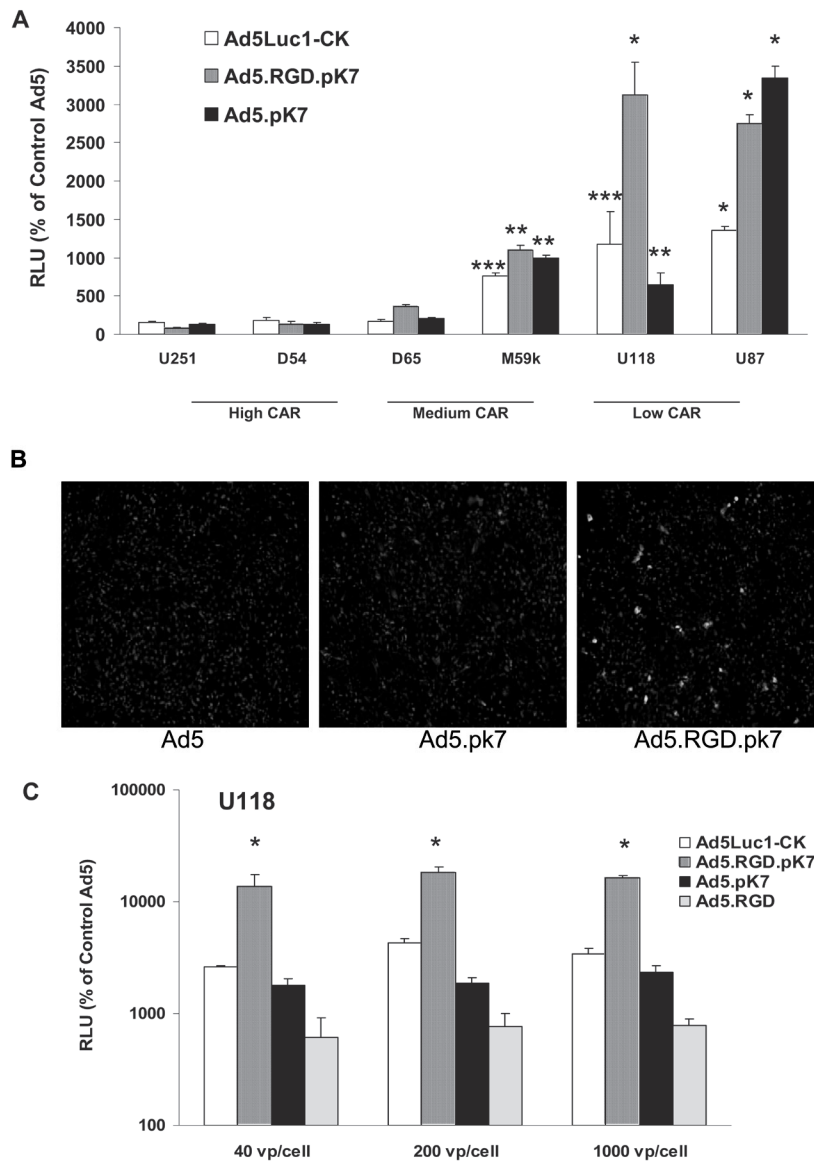


Figure 3. Retargeted Ad vectors confer infectivity enhancement in established glioma cells expressing low or medium CAR levels. **A.** Analysis of low-CAR glioma cells infected by Ad vectors expressing luciferase. Glioma monolayers were infected at an MOI of 200 with either the retargeted Ad5Luc1-CK and its corresponding control vector Ad5Luc1 or with the retargeted Ad5 vector Ad5.Pk7 or Ad5.RGD.Pk7 and their corresponding control vector Ad5. Note that the mean relative light units (RLU) are shown graphically as the percentage of the relevant capsid-unmodified control Ad5 vector. Results are representative of multiple experiments with MOIs of 40, 200, and 1000. * $p < 0.0005$, ** $p < 0.005$, *** $p < 0.05$ (retargeted Ad vectors compared with their corresponding Ad5 control). **B.** Analysis of low-CAR glioma cells infected by Ad vectors expressing green

fluorescent protein (GFP). U118 cells were infected at an MOI of 1000 with either the control Ad5 vector or with the retargeted vector Ad5.Pk7 or Ad5.RGD.Pk7. Fluorescence microscopy was performed 2 days later. Nuclei were stained with Hoechst (red). The fluorescent signal is green (weak signal) to yellow (very strong signal). C. Ad5.RGD.Pk7 confers higher levels of infectivity enhancement than the previously reported retargeted vector Ad5.RGD in established low-CAR glioma cells. U118 cells were infected at MOIs of 40, 200, or 1000 with either the control Ad5 vector; the novel retargeted vector Ad5Luc1-CK, Ad5.Pk7, or Ad5.Pk7.RGD; or the previously reported retargeted vector Ad5.RGD. Note that the mean relative light units (RLU) are shown graphically as the percentage of the relevant Ad5 control vector. * $p < 0.005$ for Ad5.RGD.Pk7 vs. Ad5.RGD. See page 195 for color figure

Capsid-modified Ad Vectors Infect Glioma Cells via Specific, Non-CAR-mediated, Cell Entry Pathways

To evaluate the relevant cell entry mechanism into glioma cells, competitive blocking assays were performed for Ad5.Pk7, Ad5.RGD.Pk7, and Ad5Luc1-CK. To this end, we employed heparin or the recombinant knob protein of the canine Ad serotype 2 to block either the HSPG pathway or the putative cellular receptor for canine 2 Ad, respectively. Our results show that specific blockers of these cellular entry pathways could inhibit the infection of glioma cells by the capsid-modified vectors (Fig. 4).

Specifically, heparin could block Ad5.pk7 efficiently but could block Ad5.RGD.Pk7 only to a much lower extent (Fig. 4A), indicating the significance of integrins in the CAR-independent cell entry of Ad5.RGD.Pk7. The canine knob protein could partially block Ad5Luc1-CK (Fig. 4B). We have previously shown that blockade of the Ad5/CAR cellular entry pathway with Ad5 knob does not inhibit infection with Ad5Luc1-CK, Ad5.Pk7, or Ad5.RGD.Pk7 (Wu et al, 2002). These previous findings, together with our current findings of the specific inhibition of the respective cellular entry mechanisms, seem to indicate that Ad5Luc1-CK, Ad5.Pk7, and Ad5.RGD.Pk7 infect low-CAR glioma cells via CAR-independent cellular entry pathways. Of note, Ad5.RGD.Pk7 seems to have a broader spectrum for cell entry in consideration of its relative resistance to heparin and its promiscuous infection profile, unless both the integrins and HSPG pathways are blocked, as previously demonstrated²⁵.

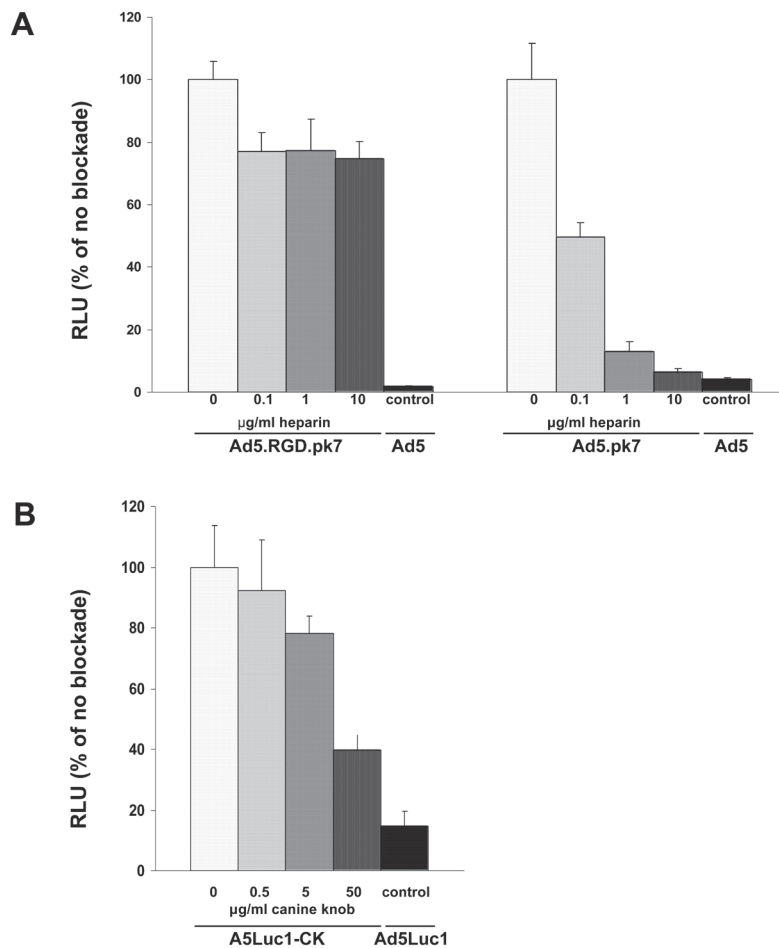


Figure 4. Competitive inhibition can partially block infection with retargeted Ad vectors in low-CAR glioma cells. A. U118 cells were infected with the control Ad5 vector, Ad5.Pk7, or Ad5Pk7.RGD at an MOI of 200, after preincubation of the viral vectors with the indicated concentrations of heparin. The infectivity was assessed by luciferase activity. Similar results were obtained with U87 cells. B. U87 cells were infected with the control Ad5Luc1 vector or the retargeted Ad5Luc1-CK at an MOI of 200, following incubation of the cells with the canine Ad knob at the indicated concentrations. Similar results were obtained with U118 cells.

Retargeting Ad Vectors Enhances Infectivity in Primary, Low-passage Glioma Cells

Glioma cells freshly isolated from tumor samples of patients (referred to here as primary glioma cells) better reflect the true nature of tumor cells than cell lines which have been grown for years. Therefore, we further evaluated the utility of the three retargeting strategies in four primary glioma cell lines, all before their eighth passage. First, we classified the primary glioma cells on the basis of their CAR expression (Fig. 5A). Next, we evaluated the utility of the various retargeted Ad vectors as gene delivery vehicles into the primary glioma cells. Our findings indicate that in low-CAR primary glioma cells, all three retargeting strategies could augment gene delivery. Of

note, the efficiency of Ad5.RGD.Pk7 was substantially higher than those of the other vectors (Fig. 5B). In parallel to the established glioma cell lines, infectivity enhancement correlated inversely with the level of CAR expression in primary glioma cell lines. However, while the level of infectivity enhancement obtained by Ad5.RGD.Pk7 in established low-CAR glioma cell lines was approximately 30-fold (Fig. 3A), in primary low-CAR glioma cells it was up to 270-fold (Fig. 5B), thereby showing the relevance of CAR-independent infection in glioma cells in monolayer culture.

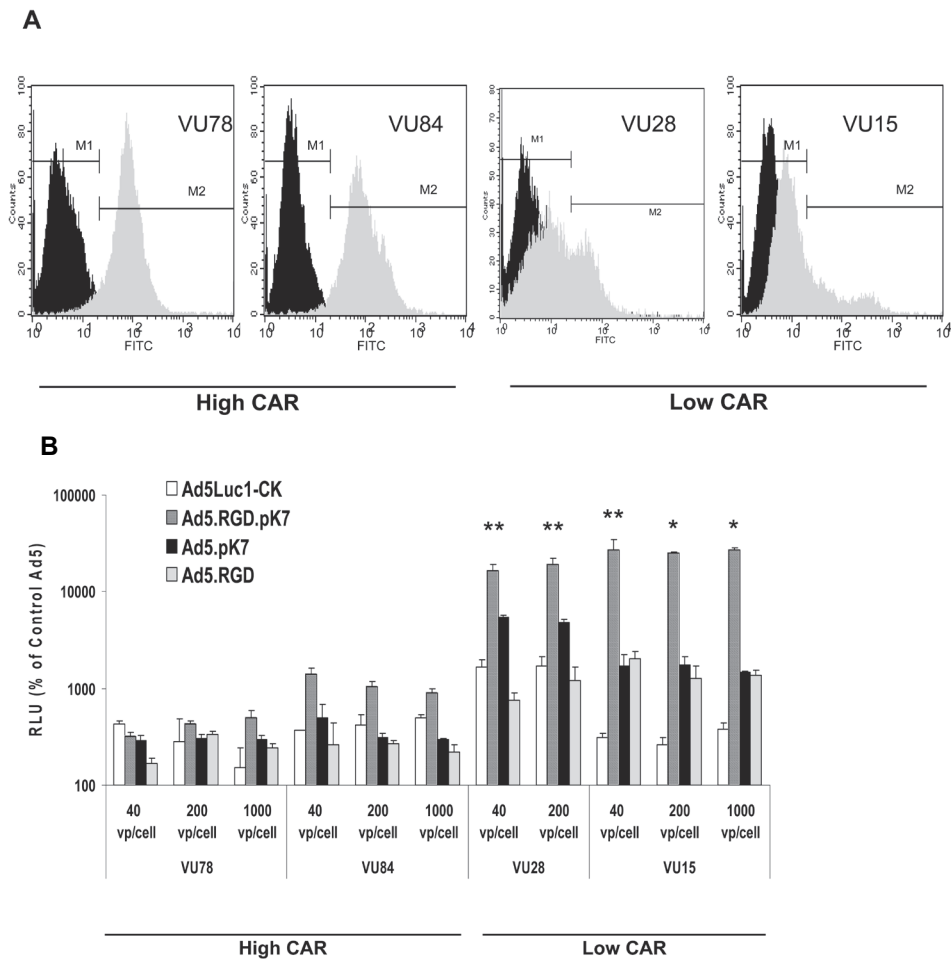


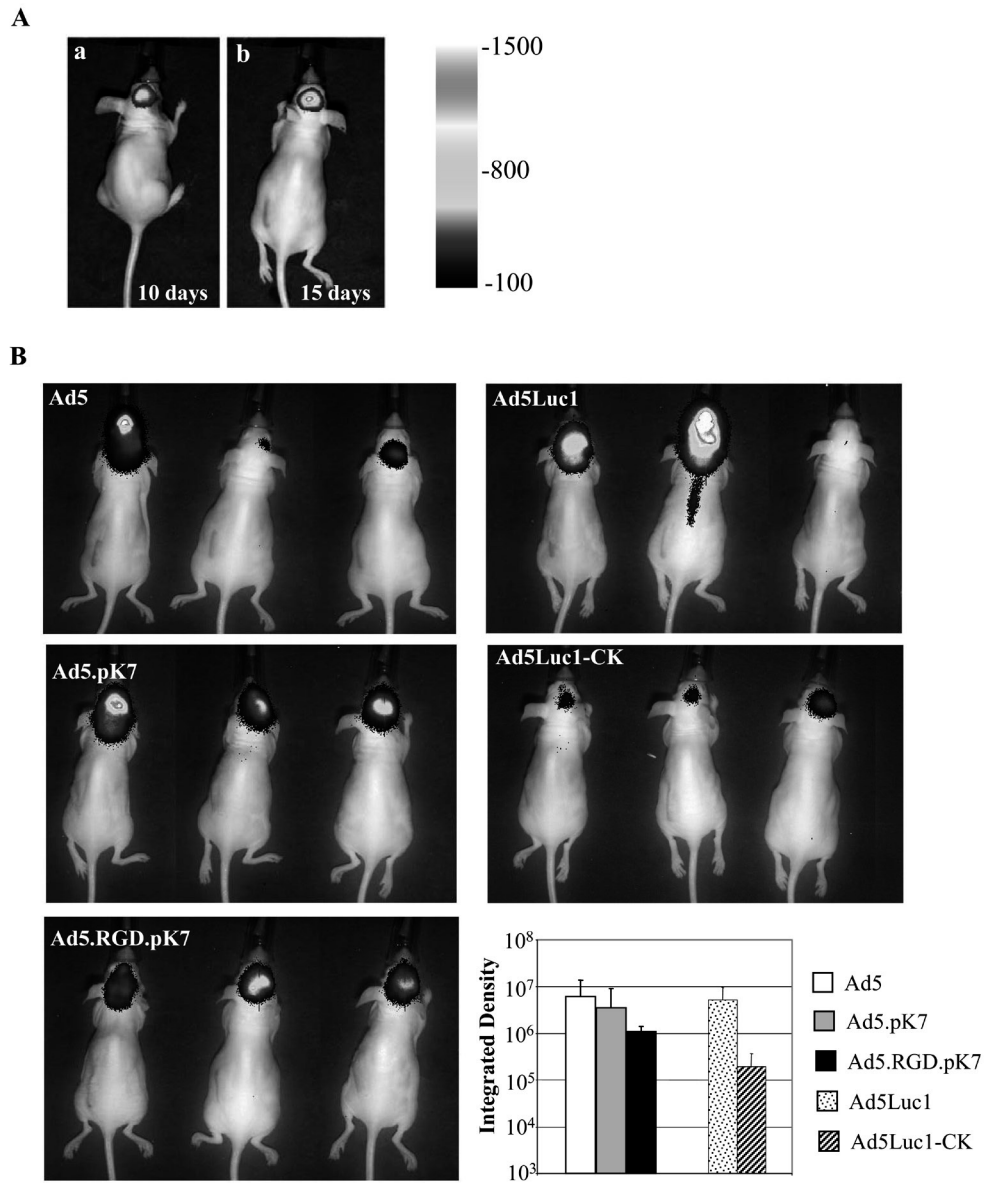
Figure 5. Retargeted Ad vectors confer infectivity enhancement in primary, low-passage CAR-deficient glioma cells. A. Expression of CAR (gray) was measured in the primary human glioma cells VU-78, VU-84, VU-28, and VU-15 with indirect flow cytometry. Cells were first incubated with the monoclonal anti-CAR Ab RmCB, followed by detection with FITC-labeled secondary antibody. IgG-matched isotype antibody was used as a control (black). B. Analysis of primary glioma cells infected by Ad vectors expressing luciferase. The primary human glioma cells VU-78, VU-84, and VU-15 were infected at MOIs of 40, 200, and 1000,

whereas VU-28 cells were infected at MOIs of 40 and 200 with either the retargeted Ad5Luc1-CK and its corresponding control vector Ad5luc1 or with the retargeted Ad5 vector Ad5.Pk7 or Ad5.RGD.Pk7 and the corresponding control vector Ad5. Note that the mean relative light units (RLU) are shown graphically as the percentage of the relevant Ad5 control vector. * $p < 0.0005$, ** $p < 0.005$.

Infectivity Enhancement of Ad Vectors Is Compromised *In Vivo* in Glioma Xenografts

We next examined whether the CAR-independent Ad infection attained *in vitro* may predict *in vivo* gene delivery. To this end, we pre-established orthotopic human glioma xenografts in mice, followed by direct intracranial injection of the various Ad vectors. To directly evaluate gene delivery in real time, we studied live animals in which luciferase activity in the tumors was imaged using a CCD camera to quantitatively measure light emission. To validate transcranial measurement of gene expression, we first confirmed intracranial light signaling from glioma xenograft tumors consisting of glioma cells constitutively expressing luciferase (Fig. 6A). The increasing luciferase signals at day 15 compared with day 10 after tumor inoculation were compatible with active tumor growth, thereby confirming the establishment of the glioma xenograft model. Next, we pre-implanted two different types of orthotopic human glioma xenografts (Luc-) in nude mice, followed by intratumoral injection of either the three retargeted Ad vectors or the unmodified Ad5 isogenic control vector (Table 1). The *in vivo* gene delivery efficiency was evaluated by noninvasive Luc imaging since the vectors contained the firefly luciferase reporter. Of note, the two xenograft types were composed of human glioma cells with either low (U87) or high (D54) levels of CAR expression.

As also found under the *in vitro* conditions, in high-CAR glioma tumors we observed no infectivity enhancement: the capsid-modified Ad5.Pk7 and Ad5.RGD.Pk7 vectors showed no significant difference from the control Ad5 vector with regard to *in vivo* gene delivery efficiency ($p > 0.05$), whereas the Ad5Luc1-CK vector was significantly less efficient than the isogenic control vector ($p < 0.05$) (Fig. 6B). Unlike in the two-dimensional glioma cell monolayers, however, in low-CAR glioma tumors *in vivo* the unmodified Ad vectors were not inferior to the capsid-modified Ad ($p > 0.05$) (Fig. 6C). Thus, in human glioma xenografts, *in vitro* CAR-independence does not necessarily predict enhanced gene delivery *in vivo*.



See page 194 for color figure

C

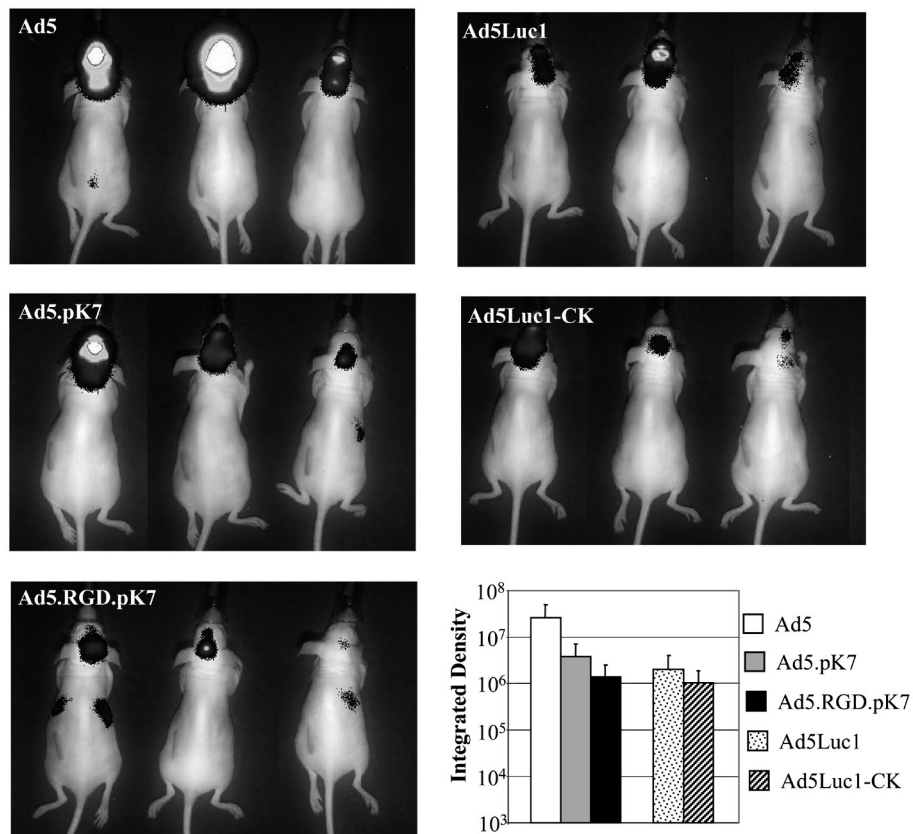


Figure 6. Retargeted Ad vectors do not confer infectivity enhancement in glioma xenografts in mice. A. Noninvasive imaging to establish the mouse xenograft glioma model. Fifty thousand U87MG glioma cells constitutively expressing luciferase (Luc⁺-U87MG) were stereotactically injected into the brain of a nude mouse. Luciferase imaging was performed at days 10 and 15 after tumor inoculation. B. *In vivo* evaluation of gene transfer efficacy of the retargeted Ad5 vectors in high-CAR glioma xenografts. The glioma models were pre-established as above with the high-CAR D54MG cells (Luc⁺) in nude mice. Two weeks later, 10¹⁰ viral particles of the Ad5 vectors were injected into each tumor stereotactically. Five mice were used in each group. Noninvasive imaging was used to follow transgene expression. Shown here are representative images taken at day 3 after viral injection. Quantitative imaging signals (with integrated density) showed that Ad5Luc1-CK was significantly less efficient in gene delivery into the D54 glioma xenografts than the unmodified control vector ($p < 0.05$), whereas Ad5.Pk7 and Ad5.RGD.Pk7 showed no significant differences relative to the corresponding control Ad5 vector ($p > 0.05$). * $p < 0.05$. C. *In vivo* evaluation of gene transfer efficacy of the retargeted Ad5 vectors in low-CAR glioma mouse models. The glioma models were pre-established with the low-CAR U87MG cells (Luc⁺) in nude mice, and experiments were performed as above in Fig. 6B. Representative images taken at day 6 after viral injection are shown. Statistical analysis of the quantified imaging signals indicated that there was no significant difference between the modified Ad5 vectors and their unmodified Ad5 control vectors. Quantified data are presented individually for each vector. See page 195 for color figure

Discussion

The use of Ad-based gene therapy against gliomas may be feasible for several reasons. First, local intracranial injection is feasible using surgical and stereotactic techniques. Second, prognosis of aggressive glioma is dismal. Finally, clinical gene therapy studies have shown that Ad-mediated brain toxicity is very low, despite the capacity of Ad5 vectors to infect a number of normal brain cell populations, such as neurons, astrocytes, and ependymal cells²⁶ Puumalainen, et al., 1998). It is therefore not surprising that Ad have been previously found to be efficient gene delivery vectors in several glioma models²⁷⁻²⁹. However, a major factor limiting the assessment of Ad-based gene therapy strategies for glioma is the inadequacy of currently available human tumor models. For example, data derived from monolayer cell culture clearly do not reflect the tumor microenvironment.

Previously, genetic strategies to modify the Ad fiber have been reported to augment infectivity in glioma cells (Yoshida, et al 1998; Shinoura, et al 1999). In this study, we revisited the hypothesis that Ad-based gene delivery into gliomas could be enhanced by genetic retargeting of the vectors to alternative cellular Ad receptors. To address this issue, we performed *in vitro* and *in vivo* studies with three distinct approaches for Ad retargeting. *In vitro*, we first showed that CAR expression varies considerably among glioma cell lines. CAR expression was quantified as low, medium, or high. We next demonstrated that in established and primary low-CAR glioma cell lines, all three genetic approaches could enhance Ad infection, independently of CAR.

Of note, in the low-CAR U118 glioma cell line and in primary low-CAR glioma cells, double targeting of HSPG and integrins could augment Ad infectivity (Fig. 3A and Fig. 5B), whereas in the low-CAR U87 glioma cell line double targeting of HSPG and integrins was less efficient than HSPG-based cell entry alone. Furthermore, as shown in Fig. 4A, competitive inhibition of HSPG-mediated cell entry with heparin in U118 cells could efficiently block Ad5.Pk7 infection but not Ad5.RGD.Pk7 infection. These results indicate that, in U118 glioma cells, integrins may play an important role as mediators of cell entry for Ad5.RGD.Pk7 but not for Ad5.pk7. Because Ad5.RGD.Pk7 can potentially utilize both HSPG and integrins for cell entry, variable expression of these cell surface receptors in distinct cell lines may account for the different capacity to achieve CAR-independent infectivity enhancement. In this regard, it has been suggested that double modification of the Ad fiber may cause conformational ligand changes (Wu et al, 2002) that may affect Ad cell entry differentially in different cell lines.

A major finding of our *in vivo* studies in glioma xenografts was the lack of infectivity enhancement of Ad5.RGD.Pk7 (Fig. 6C), in contrast to our *in vivo* studies in monolayer cultures. This observation is compatible with results of previous *in vivo* studies in which, in an intraperitoneal ovarian cancer model, Ad5.RGD.pk7 was less efficient than Ad5.pk7 and did not enhance infectivity over Ad5. In contrast, in a subcutaneous ovarian tumor xenograft, Ad5.RGD.pk7, but not Ad5.pk7 or Ad5.RGD, enhanced infectivity³⁰. The variable nature of tumors was also demonstrated *in vivo* in a syngeneic melanoma tumor model in which another capsid-modified Ad vector incorporating both RGD and pk7 ligands could confer infectivity enhancement *in vitro* but not *in vivo*³¹. Thus, in addition to the levels of CAR expression, other factors clearly play significant roles in the susceptibility of glioma tumors to Ad vectors.

These other factors may include intratumoral restriction of vector distribution within the tumor mass by 1) high tumor cell density and intratumoral connective tissue³²; 2) limited availability of vectors within the “infection zone,” corresponding to up to five layers of tumor cells around the needle track³³; 3) size of virions (Sauthoff, et al., 2003); 4) host immune response, augmented by display of charged ligands³⁴; 5) tumor inactivation of viral DNA after inoculation³⁵; 6) charged ligands promoting binding to extracellular matrix proteins, e.g., integrins and HSPGs^{36, 37}; 7) a gradient of viral infection that results in a high MOI primarily around the needle track; and 8) attenuation of vectors for safety reasons. Altogether, inefficient intratumoral diffusion probably accounts for the limited distribution of Ad-mediated gene delivery in human glioma tumors, as observed in previous human clinical trials³⁸. Some of these obstacles may be addressed by replication-competent oncolytic viruses or via combined therapeutic modalities^{39, 40}. In conclusion, although novel strategies for CAR-independent ad infection could confer infectivity enhancement of primary and established low-CAR glioma cell lines *in vitro*, these approaches were less efficient *in vivo*. Thus, gene delivery into glioma cell monolayers, inclusive of primary glioma cells, cannot predict gene delivery in complex, heterogenic three-dimensional tumors. Further research is required to characterize and overcome the factors impeding gene delivery into glioma tumors.

References

1. Elliott,W.L., Roberts,B.J., Howard,C.T., & Leopold,W.R. Chemotherapy with [Sp-4-3-(R)]-[1,1-Cyclobutanedicarboxylato(2-)](2-Methyl-1,4-Butanediamine-N,N')Platinum (Ci-973, Nk121) in Combination with Standard Agents Against Murine Tumors In-Vivo. *Cancer Research* 54, 4412-4418 (1994).
2. Schmitt,C.A. et al. A senescence program controlled by p53 and p16(INK4a) contributes to the outcome of cancer therapy. *Cell* 109, 335-346 (2002).
3. Eck,S.L. et al. Clinical protocol - Treatment of advanced CNS malignancies with the recombinant adenovirus H5.010RSVTK: A phase I trial. *Human Gene Therapy* 7, 1465-1482 (1996).
4. Sandmair,A.M., Vapalahti,M., & Yla-Herttuala,S. Adenovirus-mediated herpes simplex thymidine kinase gene therapy for brain tumors. *Cancer Gene Therapy* 465, 163-170 (2000).
5. Trask,T.W. et al. Phase I study of adenoviral delivery of the HSV-tk gene and ganciclovir administration in patients with recurrent malignant brain tumors. *Molecular Therapy* 1, 195-203 (2000).
6. Puumalainen,A.M. et al. beta-galactosidase gene transfer to human malignant glioma in vivo using replication-deficient retroviruses and adenoviruses. *Human Gene Therapy* 9, 1769-1774 (1998).
7. Staba,M.J., Wickham,T.J., Kovesdi,I., & Hallahan,D.E. Modifications of the fiber in adenovirus vectors increase tropism for malignant glioma models. *Cancer Gene Therapy* 7, 13-19 (2000).
8. Miller,C.R. et al. Differential susceptibility of primary and established human glioma cells to adenovirus infection: Targeting via the epidermal growth factor receptor achieves fiber receptor-independent gene transfer. *Cancer Research* 58, 5738-5748 (1998).
9. Asaoka,K., Tada,M., Sawamura,Y., Ikeda,J., & Abe,H. Dependence of efficient adenoviral gene delivery in malignant glioma cells on the expression levels of the Coxsackievirus and adenovirus receptor. *Journal of Neurosurgery* 92, 1002-1008 (2000).
10. Douglas,J.T., Kim,M., Sumerel,L.A., Carey,D.E., & Curiel,D.T. Efficient oncolysis by a replicating adenovirus (Ad) in vivo is critically dependent on tumor expression of primary ad receptors. *Cancer Research* 61, 813-817 (2001).
11. Tsugawa,T. et al. Sequential delivery of interferon-alpha gene and DCs to intracranial gliomas promotes an effective antitumor response. *Gene Therapy* 11, 1551-1558 (2004).
12. Immonen,A. et al. AdvHSV-tk gene therapy with intravenous ganciclovir improves survival in human malignant glioma: A randomised, controlled study. *Molecular Therapy* 10, 967-972 (2004).
13. Fueyo,J. et al. A mutant oncolytic adenovirus targeting the Rb pathway produces anti-glioma effect in vivo. *Oncogene* 19, 2-12 (2000).
14. Parr,M.J. et al. Tumor-selective transgene expression in vivo mediated by an E2F-responsive adenoviral vector. *Nature Medicine* 3, 1145-1149 (1997).
15. Franklin,R.J.M., Quick,M.M., & Haase,G. Adenoviral vectors for in vivo gene delivery to oligodendrocytes: transgene expression and cytopathic consequences. *Gene Therapy* 6, 1360-1367 (1999).
16. Lamfers,M.L.M. et al. Potential of the conditionally replicative adenovirus Ad5-Delta 24RGD in the treatment of malignant gliomas and its enhanced effect with radiotherapy. *Cancer Research* 62, 5736-5742 (2002).
17. Dirven,C.M.F. et al. Gene therapy for meningioma: improved gene delivery with targeted adenoviruses. *Journal of Neurosurgery* 97, 441-449 (2002).
18. Krasnykh,V.N., Mikheeva,G.V., Douglas,J.T., & Curiel,D.T. Generation of recombinant adenovirus vectors with modified fibers for altering viral tropism. *Journal of Virology* 70, 6839-6846 (1996).
19. Dmitriev,I. et al. An adenovirus vector with genetically modified fibers demonstrates expanded tropism via utilization of a coxsackievirus and adenovirus receptor-independent cell entry mechanism. *Journal of Virology* 72, 9706-9713 (1998).
20. Krasnykh,V. et al. Characterization of an adenovirus vector containing heterologous peptide epitope in the HI loop of the fiber knob. *Journal of Virology* 72, 1844-1852 (1998).
21. Glasgow,J.N. et al. An adenovirus vector with a chimeric fiber derived from canine adenovirus type 2 displays novel tropism. *Virology* 324, 103-116 (2004).
22. Yoshida,Y. et al. Generation of fiber-mutant recombinant adenoviruses for gene therapy of malignant glioma. *Human Gene Therapy* 9, 2503-2515 (1998).

23. Grill,J. et al. Combined targeting of adenoviruses to integrins and epidermal growth factor receptors increases gene transfer into primary glioma cells and spheroids. *Clinical Cancer Research* 7, 641-650 (2001).
24. Shinoura,N. et al. Highly augmented cytopathic effect of a fiber-mutant E1B-defective adenovirus for gene therapy of gliomas. *Cancer Research* 59, 3411-3416 (1999).
25. Wu,H.J. et al. Double modification of adenovirus fiber with RGD and polylysine motifs improves coxsackievirus-adenovirus receptor-independent gene transfer efficiency. *Human Gene Therapy* 13, 1647-1653 (2002).
26. Alemany,R. et al. Gene therapy for gliomas: Molecular targets, adenoviral vectors, and oncolytic adenoviruses. *Experimental Cell Research* 252, 1-12 (1999).
27. Tsugawa,T. et al. Sequential delivery of interferon-alpha gene and DCs to intracranial gliomas promotes an effective antitumor response. *Gene Therapy* 11, 1551-1558 (2004).
28. Immonen,A. et al. AdvHSV-tk gene therapy with intravenous ganciclovir improves survival in human malignant glioma: A randomised, controlled study. *Molecular Therapy* 10, 967-972 (2004).
29. Fueyo,J. et al. A mutant oncolytic adenovirus targeting the Rb pathway produces anti-glioma effect in vivo. *Oncogene* 19, 2-12 (2000).
30. Wu,H. et al. Preclinical evaluation of a class of infectivity-enhanced adenoviral vectors in ovarian cancer gene therapy. *Gene Therapy* 11, 874-878 (2004).
31. Koizumi,N., Mizuguchi,H., Utoguchi,N., Watanabe,Y., & Hayakawa,T. Generation of fiber-modified adenovirus vectors containing heterologous peptides in both the HI loop and C terminus of the fiber knob. *Journal of Gene Medicine* 5, 267-276 (2003).
32. Sauthoff,H. et al. Intratumoral spread of wild-type adenovirus is limited after local injection of human xenograft tumors: Virus persists and spreads systemically at late time points. *Human Gene Therapy* 14, 425-433 (2003).
33. Jia,W. & Zhou,Q. Viral vectors for cancer gene therapy: Viral dissemination and tumor targeting. *Current Gene Therapy* 5, 133-142 (2005).
34. Liu,Q. & Muruve,D.A. Molecular basis of the inflammatory response to adenovirus vectors. *Gene Therapy* 10, 935-940 (2003).
35. Nemunaitis,J. et al. Phase II trial of intratumoral administration of ONYX-015, a replication-selective adenovirus, in patients with refractory head and neck cancer. *Journal of Clinical Oncology* 19, 289-298 (2001).
36. Thomas,C.E., Edwards,P., Wickham,T.J., Castro,M.G., & Lowenstein,P.R. Adenovirus binding to the coxsackievirus and adenovirus receptor or integrins is not required to elicit brain inflammation but is necessary to transduce specific neural cell types. *Journal of Virology* 76, 3452-3460 (2002).
37. Haviv,Y.S. & Curiel,D.T. Conditional gene targeting for cancer gene therapy. *Advanced Drug Delivery Reviews* 53, 135-154 (2001).
38. Pulkkanen,K.J. & Yla-Herttuala,S. Gene therapy for malignant glioma: Current clinical status. *Molecular Therapy* 12, 585-598 (2005).
39. Lam,J.T. et al. Inter-patient variation in efficacy of five oncolytic adenovirus candidates for ovarian cancer therapy. *Journal of Gene Medicine* 6, 1333-1342 (2004).
40. Haviv,Y.S. et al. Adenoviral gene therapy for renal cancer requires retargeting to alternative cellular receptors. *Cancer Research* 62, 4273-4281 (2002).

— |

— |



3

The human survivin promoter: a novel transcriptional targeting strategy for treatment of glioma

Winan J. van Houdt, Yosef S. Haviv, Baogen Lu, Minghui Wang, Angel A. Rivera, Ilya V. Ulasov, Martine L. M. Lamfers, Daniel Rein, Maciej S. Lesniak, Gene P. Siegal, Clemens M. F. Dirven, David T. Curiel and Zeng B. Zhu

Journal of Neurosurgery, 2006 Apr;104(4):583-92

Abstract

Object. Malignant brain tumors have been proved to be resistant to standard treatments and therefore require new therapeutic strategies. Survivin, a recently described member of the inhibitor of apoptosis protein family, is overexpressed in several human brain tumors, primarily gliomas, but is downregulated in normal tissues. The authors hypothesized that the expression of tumor-specific survivin could be exploited for treatment of gliomas by targeting the tumors with gene therapy vectors.

Methods. Following confirmation of survivin expression in glioma cell lines, an adenoviral vector containing the survivin promoter and the reporter gene *luciferase* was tested in established and primary glioma cells, normal astrocytic cells, and normal human brain tissues. High levels of reporter gene expression were observed in established tumor and primary tumor cell lines and low levels of expression in astrocytes and normal human brain tissue. To test oncolytic potency, the authors constructed survivin promoter–based conditionally replicative adenoviruses (CRAds), composed of survivin promoter–regulated *E1* gene expression and an RGD-4C capsid modification. These CRAds could efficiently replicate within and kill a variety of established glioma tumor cells, but were inactive in a normal human liver organ culture. Finally, survivin promoter–based CRAds significantly inhibited the growth of glioma xenografts in vivo.

Conclusions. Together these data indicate that the survivin promoter is a promising tumor-specific promoter for transcriptional targeting of adenovirus-based vectors and CRAds for malignant gliomas. The strategy of using surviving-CRAds may thus translate into an experimental therapeutic approach that can be used in human clinical trials.

Introduction

Malignant gliomas are the most common tumor in the central nervous system. Despite recent advances in treatment, their prognosis remains poor. The 5-year survival rate in patients harboring a GBM, the most common and malignant glioma subtype, is less than 3%, whereas the 5-year survival rate for patients with a lower grade astrocytoma is 30%.^{3,6,7,38} Therefore, the identification of novel therapeutic strategies for malignant gliomas merits a high priority. In this regard, gene therapy with adenoviral vectors is a promising new modality for the treatment of glioma.^{9,10,23,26} Adenoviral vectors may be genetically designed to express therapeutic genes in cancer cells. To this end, tumor-selective transgene expression is critical and can be obtained by placing the transgene under the control of a TSP.^{12,13,29,31,35} Specifically, to achieve a high therapeutic index with adenoviral vectors in vivo, repression of TSPs in normal tissues, primarily those of the liver, emerges as the most critical predictor of a high tumor/normal tissue ratio.¹² Current TSP candidates for glioma targeting do not fully meet these criteria,²¹ and therefore novel TSPs are required for transcriptional targeting of gliomas. The recently discovered *survivin* gene encodes the surviving protein, a member of the IAP protein family, which plays an important role in the survival of cancer cells and the progression of malignancy. Members of the IAP family directly inhibit terminal effector caspases through baculovirus IAP repeat-dependent recognition, thereby preventing apoptosis.^{4,24} Survivin is normally expressed during embryogenesis and is undetectable in fully differentiated adult tissues.⁶ In contrast, survivin is repeatedly expressed in a broad spectrum of human cancers including brain, breast, pancreas, esophageal, and ovarian tumors. Survivin-mediated suppression of apoptosis and growth factor-independent cell survival is implicated in the resistance of the tumor to standard therapy. In this regard, 80% of GBM cells demonstrate abundant survivin expression,⁵ and a clear correlation is seen between the histological grade of a glioma and the fraction of survivin-positive tumor samples. In glioma tumors, survivin expression is also correlated with a resistance to chemo- and radiotherapy and with poor prognosis.^{6,15,34} Given this promising role for survivin, we developed a survivin promoter-based adenoviral vector for the purpose of transcriptional targeting of gliomas. We hypothesized that this strategy of tumor-specific regulation of gene expression could provide a novel transcriptional targeting approach for human gliomas. Furthermore, we used this surviving TSP approach in the context of CRAds use for tumor-selective viral replication and oncolysis. To achieve this goal, a TSP is required to control *E1* gene expression in the adenovirus. Although other TSPs have been previously suggested in the context of glioma, such as hTERT,^{19,20} *oncostatin-M* promoter (a hematopoietic cytokine), the *vascular endothelial growth factor* promoter,³⁰ the *c-Myc* promoter activated in medulloblastoma,³⁷ and *gas1*,⁴⁴ in this study we identified the survivin promoter as a uniquely transcriptional targeting strategy for human glioma.

Materials and Methods

Cells, Tissues, and Animals

Samples of the human glioma tumor cell lines U251MG, U87MG, U373MG, D54MG, and D65MG were kind gifts from Dr. G. Y. Gillespie (Department of Neurosurgery, University of Alabama at Birmingham). Samples of the M59K and U118MG cell lines were obtained from the American Type Culture Collection (Manassas, VA). Cells of the U87MG line were cultured in minimal essential medium (Mediatech, Herndon, VA) containing 15% FBS (HyClone, Logan, UT), 2 mM L-glutamine, penicillin (100 IU/ml), and streptomycin (100 mg/ml). The other cell lines—U251MG, D54MG, U118MG, M59K, and D65MG—were cultured in DMEM–Ham F12 50:50 (Mediatech) containing 10% FBS and supplemented with L-glutamine, penicillin, and streptomycin as previously described. In addition, 911 cells (a kind gift from Dr. Van Der Eb, Leiden University, The Netherlands) were maintained in DMEM. Each medium was also supplemented with fetal calf serum, penicillin, and streptomycin. Astrocyte cells, a kind gift from Dr. Charles Bonus, were cultured in DMEM and supplemented with 10% FBS, penicillin, and streptomycin. Three primary glioma tumor cells, VU84, VU119, and VU78,²³ were cultured in DMEM with 10 to 15% FBS, L-glutamine, and antibiotic agents. The cells were incubated at 37°C in a 95% air/5% CO₂ environment under humidified conditions. Human liver samples were separated from donor hepatectomy remnants that had been obtained during liver transplantation; the study was approved by the local internal review board. To generate human liver organ cultures, the tissue was serially dissected into 0.5-mm-thick slices by using a Krumdieck tissue slicer (Alabama Research Development, Munford, AL). Next, the liver tissue was cultured in 24-well plates in RPMI medium supplemented with 10% FBS, 100 U/ml penicillin, 100 mg/ml streptomycin, and 5 mg/ml insulin. The tissue cultures were maintained at 37°C in a humidified atmosphere of 95% air/5% CO₂. Three tissue slices were examined per group. Female C57BL/6 mice and female BALB/c nude mice (6–8 weeks of age; Charles River, Wilmington, MA) were used in the *in vivo* experiments. All animals received humane care based on guidelines established by the American Veterinary Association. All experimental protocols involving live animals were reviewed and approved by the Institutional Animal Care and Use Committee of the University of Alabama at Birmingham.

Adenoviral Vectors

The following recombinant adenoviral vectors and CRAds were constructed in our lab. The recombinant adenoviral vectors reAdGL3BCox2 (or Ad-Cox2),⁴² reAdGL3Midkine (or Ad-Mk),¹ reAdGL3BSurvivin (or Ad-S),⁴⁵ and reAdGL3BCMV (or Ad-CMV), each of which was used in this experiment, are all isogenic in that they are composed of the pGL3B plasmid adenoviral backbone, which carries the same *luciferase* cassette but under the control of different promoters, that is, Cox-2, midkine, survivin, or CMV, respectively. Two CRAds—CRAd-S-S and CRAd-S-L—were generated by our group and have been described elsewhere.⁴⁷ In these CRAds, the adenoviral native E1 promoter was completely deleted and the AD5 *E1* gene was regulated by a short survivin promoter, S-S (nucleotides 2230 to 130), or a longer segment, S-L (nucleotides 21430 to 130). To increase the killing of glioma cancer cells, these CRAd genomes also contain a capsid modification, RGD-4C, which was inserted genetically into the viral capsid. As a replicative control for the survivin-CRAds, we used a wild-type adenovirus (Adwt). The viral particle/plate forming unit ratio for each virus was 34 for CRAd-S-S and 16 for CRAd-S-L.

Analysis of Survivin Promoter Activity in Glioma Cells

A recombinant adenoviral vector, AdSurvivin, was used in this study as reported previously.⁴⁵ To determine the transcriptional activity of the survivin promoter, 5×10^4 cells of each established glioma cancer cell line (U87MG, M59K, U251MG, U118MG, D65MG, and D54MG), primary glioma cells, and normal controls (primary mesothelial cells, derived in our department from ascites fluid, and keratinocytes), were plated into 24-well tissue plates and infected with Ad-CMV, Ad-Cox2, Ad-Mk, or Ad-S at an MOI of 100 (100 vp/cell) in 200 ml of growth medium containing 2% FBS (infection medium). The infection medium was replaced by fresh medium containing 10% FBS after 2 hours. Twenty-four hours postinfection, luciferase activity was determined using the Reporter Lysis Buffer and Luciferase Assay System (Promega, Madison, WI) following the manufacturer's protocol. Experiments were performed in triplicate, and luciferase activities are presented as relative light units normalized to the CMV promoter activity.

Quantitative Real-Time PCR for Detection of the Human Survivin Gene and Ad5 *E4* Gene Expression

Total cellular RNA or DNA was extracted from cell cultures in 6-well plates by using the RNeasy mini RNA extraction kit or the blood DNA kit (Qiagen, Valencia, CA). Both RNA and DNA samples were treated with RNase-free DNase and DNase-free RNase, respectively, to remove possible contamination. The *survivin* gene transcripts were detected in RNA samples by using an oligo pair (forward primer 5'TGGAAGGCTGGGAGCCA and reverse primer 5'GAAAGCGCAACCGGACG) and the probe (ORF6TGACGACCCATAGAGGAACATAAAAAGCAT); the Ad5 *E4* gene was detected in DNA samples by using an oligo pair (forward primer 5'GGAGTGCGCCGAGACAAC and reverse primer 5'ACTACGTCCGGCGTTCCAT) and the probe (ORF6TGGCATGACAC TACGACCAACACGATCT). The oligos were designed using Primer Express (version 1.0; Perkin-Elmer, Foster City, CA) and synthesized by Applied Biosystems. Specifics of the real-time PCR reaction have been described by us elsewhere.^{45,46} Negative controls without templates were included in each reaction series, and an internal control (human GAPDH or b-actin) was used to normalize the copy number for the *survivin* and *E4* genes.

Survivin Promoter Activity in Normal Human Brain Tissue

Specimens of normal human brain were obtained following approval from our internal review board and consisted of 200-mm slices of gray matter from the temporal lobe, which were acquired during surgery for epilepsy. The brain slices were prepared as previously described by Verwer, et al.⁴⁰ Experiments were performed on normal brain slices excised from two patients with epilepsy. On Day 2, the brain specimens were infected in quadruplicate with 2×10^8 vp of Ad-S or Ad-CMV. On Day 5, the brain specimens were harvested and the luciferase assays were performed.

Analysis of CRAd Replication in Tumor Cell Lines

Glioma cells (10^5 /well) were cultured in the manner described earlier, infected with 100 vp/cell of CRAd-S-S, CRAd-S-L, Adwt, or Ad-S in infection medium containing 2% FBS, and incubated at 37°C in a 95% air/5% CO₂ environment. After 2 hours in incubation, the infection medium was removed, the cells were washed three times with PBS, and the cells were placed in fresh culture medium with 10% FBS. Media from triplicate wells were collected 1, 3, and 9 days postinfection; DNA was extracted from 200 ml of media by using the DNeasy Tissue Kit (Qiagen), and quantitative real-time PCR was performed in the manner described earlier. The adenovirus *E4* gene copy numbers were detected.

Replication of CRAd in the Human Liver

Human liver organ cultures, described earlier, were infected with CRAd-S-S, CRAd-S-L, Adwt, or Ad-S (10^8 vp/slice, ~ 500 vp/cell) and incubated at 37°C in a humidified atmosphere of 95% air/5% CO₂. Three tissue slices were included per group. After a 2-day incubation, total DNA was extracted from the human liver organ cultures by using the DNeasy Tissue Kit (Qiagen). The DNA samples were treated with DNase-free RNase to remove possible RNA contamination and were stored at 280°C until use. The Ad5 *E4* gene copy numbers were detected and normalized by referral to human GAPDH.

Analysis of In Vitro Glioma Cell Killing

The in vitro cytotoxic effects of CRAd-S-S and CRAd-S-L were analyzed by performing crystal violet staining. Briefly, 25,000 cells (including D65MG, U251MG, U373MG, U87MG, U118MG, or OV4, an ovarian cancer cell line used as a control) per well were plated onto a 24-well plate, and the cells were infected at 100, 10, 1, and 0 vp/cell with CRAd-S-S, CRAd-S-L, or Ad-S in infection medium. Two hours later, the infection medium was replaced with complete medium. After 10 more days of culture, the cells were fixed with 10% buffered formalin for 10 minutes and stained with 1% crystal violet in 70% ethanol for 20 minutes, followed by washing three times with tap water and air drying. Trypan blue exclusion experiments also were performed.

Analysis of CRAd Replication in Glioma Xenografts

The U118MG glioma cells were injected into the flanks of nude mice (5×10^6 cells in 200 ml PBS per tumor, five animals/group). When the resulting tumors reached 5 mm in diameter, 5×10^8 vp of CRAd-S-S or Adwt diluted in 50 ml PBS were injected into each tumor. On Days 1 and 7 postinjection, the tumors were collected and snap-frozen with dry ice/ethanol. The DNA was extracted, and the relative *E4* copy numbers were determined.

Antitumor Effect of CRAd on Mouse Xenografts

Five BALB/c nude mice in each group were inoculated in the flanks with 5×10^6 U118MG cells. The tumor cells were verified to have 95% viability by Trypan blue exclusion. When the tumor reached 5 mm in its widest diameter, 10^9 vp of viral vector (CRAd-S-S, CRAd-S-L, or Ad-S) or PBS was injected intratumorally. The vector Ad-S was used as a nonreplicative control virus with an identical viral backbone. The same dose was repeated after 1 week.

Tumor volumes were monitored twice a week, and the volumes were calculated by using the formula $\frac{1}{2}xy^2$, where x is the longest diameter and y the shortest diameter of the tumor. Based on the determined volume, the following equations were applied. Tumor volume ratio = tumor volume at Day 30/tumor volume at Day 1 x 100%. Tumor growth inhibition rate = 100% - (tumor volume at Day 30/ tumor volume at Day 1 x 100%).

Statistical Analysis

The luciferase activities measured in this study were analyzed by performing the Student t-test using commercial software (Statistics Analysis Software version 8.2; SAS Inc., Cary, NC). A probability value less than 0.05 was considered statistically significant.

Results

Survivin Promoter is Active in Both Established and Primary Glioma Cells

Four recombinant adenoviral vectors, Ad-Cox2, Ad-Mk, Ad-S, and Ad-CMV, were used in these experiments. All recombinant adenoviruses are isogenic, thereby allowing the determination of promoter activity via reporter gene expression. The CMV promoter in Ad-CMV is constitutively active, thereby serving as a positive control to allow normalization for each given cell line. The data shown in Fig. 1 represent promoter activity in established and primary low-passage glioma cells. Of all three TSPs, the survivin promoter exhibited the highest activity in the established glioma cell lines, with a mean of 11.2% of the activity of the CMV promoter. In contrast, both the Cox-2 and midkine promoters were relatively inactive, showing less than 4% of the activity of the CMV promoter. The differences were significant (p, 0.01). All three promoters were inactive in both normal primary mesothelial cells and the normal keratinocyte cell line. Because established cancer cell lines may not reflect the true nature of cancer cells, we repeated these experiments in primary low-passage glioma cells. Again, we observed that the survivin promoter was the most active of all three promoters in three primary glioma cells. The mean survivin promoter activity was 20% of the activity of the CMV promoter in three primary cells, but with wide variation among the three cell types (5, 12.5, and 42.5% of the activity of the CMV promoter in VU84, VU119, and VU78 cells, respectively). The mean Cox-2 and midkine promoter activities were less than 5% of the CMV promoter. Thus, the survivin promoter is repressed in normal cells and is active in both established and primary glioma cells.

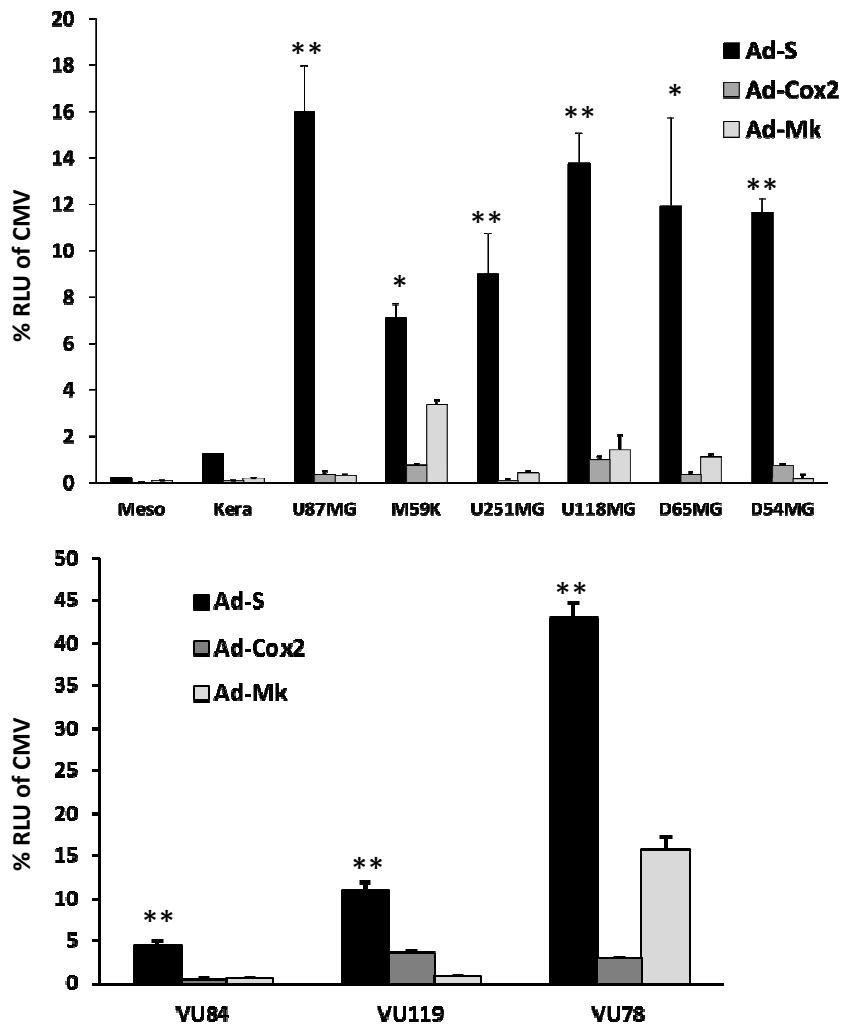


Figure 1. Bar graphs demonstrating that the human survivin promoter is selectively active in established glioma cell lines and in primary cells. *Upper:* Survivin promoter activity in glioma cell lines and control normal cells shown as percentages of CMV promoter activity. Cells from six glioma cell lines (U87MG, M59K, U251MG, U118MG, D65MG, and D54MG) and two normal control cell lines (mesothelial cells [Meso] and keratinocytes [Kera]) were infected with Ad-S, Ad-Cox-2, Ad-Mk, or Ad-CMV at an MOI of 100. The respective promoter activities were evaluated by measuring *luciferase* gene expression 2 days after infection. Data are presented as relative light units (RLU), which have been standardized as a percentage of CMV promoter activity. *Lower:* Survivin promoter activity in primary glioma cells shown as percentages of CMV activity. Primary, low-passage human glioma cells (VU84, VU78, and VU119) were infected with adenoviral agents as described in the legend to the *upper* panel. Luciferase activity was analyzed after 2 days and is presented as percentages of CMV promoter activity. The values represent the mean values of triplicate assays, and each point represents the mean and standard deviation (SD) of three determinations. *p, 0.05 and **p, 0.01 in comparisons of survivin promoter activity and both Cox-2 and midkine activities.

Survivin Promoter is Less Active in Normal Astrocytes and Normal Human Brain

A critical determinant of any candidate transcriptional targeting approach for glioma is tumor specificity. In the previous section, we described our study of survivin promoter activity in glioma cells. Next, we tested whether this promoter may be applicable to glioma gene therapy, that is, whether it is inactive in the normal brain. To this end, we evaluated survivin promoter activity in normal astrocytes and normal brain tissue. First, D65MG glioma cells and astrocytes were infected with either Ad-S or Ad-CMV (Fig. 2 *upper right*). The survivin promoter activity in the D65MG glioma cell line (12.6% of the activity of the CMV promoter) was 12-fold higher than that in astrocytes (1% of the activity of the CMV promoter). This pattern correlates well with *survivin* gene expression (Fig. 2 *upper left*). The transcript levels of the *survivin* gene were sixfold higher in the D65MG glioma cell line (310 copies/ng RNA) than in primary astrocytes (48 copies/ng RNA). Thus, high levels of *survivin* gene expression and survivin promoter activity were observed in glioma cells but not in normal astrocytes. To examine the tumor selectivity of the survivin promoter more fully, normal human cerebral cortex tissues, which were excised during epilepsy surgeries performed in two patients, were evaluated for survivin promoter activity (Fig. 2 *lower*). Normal human cerebral cortex displayed less activity, showing only 0.26% of the activity of the CMV promoter ($p < 0.01$). Thus, the survivin promoter is downregulated in the normal human brain.

Survivin-CRAds Induce Cytotoxicity in Glioma Cell Lines

Encouraged by the glioma-specific activity of the surviving promoter, we used two CRAds that had been constructed by this group and described previously⁴⁷ as oncolytic antiglioma agents. The short segment of the surviving promoter, CRAd-S-S, and the long segment of the survivin promoter, CRAd-S-L, were evaluated to determine their cell-killing effect in a variety of glioma cell lines. Cytotoxicity was evaluated after 10 days of incubation by staining the tissue with crystal violet (Fig. 3). Although the replication-incompetent Ad-S vector had no cytotoxic effect even at 100 vp/cell, the survivin-based CRAds induced cytotoxicity in all glioma cancer cell lines. Oncolytic efficiency, however, varied in the glioma cell lines tested. While survivin-based CRAds were highly efficient even at 1 vp/cell in D65MG cells, cytotoxicity was observed at 10 vp/cell for CRAd-S-S and 100 vp/cell for CRAd-S-L in U251MG, U87MG, and U118MG cells; and cytotoxicity was observed for both CRAds only at 100 vp/cell in U373MG cells. In contrast, the OV4 ovarian cancer cells were resistant to the survivin-based CRAds. Thus, both CRAd-S-S and CRAd-S-L show substantial oncolytic activity in established glioma cell lines.

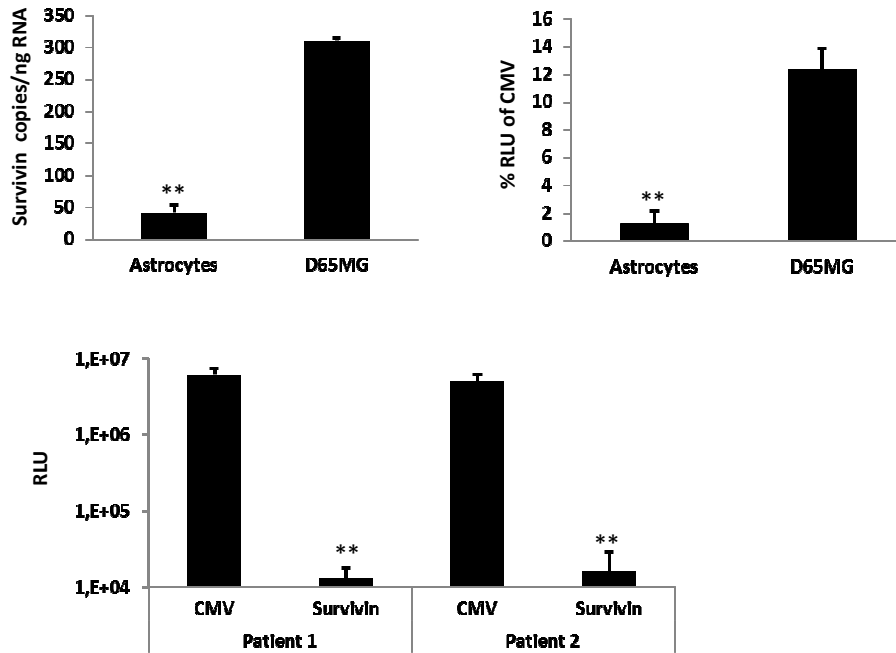


Figure 2. Expression of the *survivin* gene in glioma cells. *Upper Left:* Basal *survivin* gene expression is increased in glioma D65MG cells and is decreased in astrocytes. The results were obtained by performing quantitative real-time PCR for *survivin* transcripts. Total RNA was extracted from 10^6 cells. Real-time PCR reactions for transcripts of the human *survivin* gene or the control housekeeping gene *GAPDH* or *b-actin* were performed under conditions described in *Materials and Methods*. The *survivin* transcriptional levels in both the D65MG cells and astrocytes were normalized to *GAPDH* levels and expressed as *survivin* copies per nanogram of RNA. **p*, 0.05 and ***p*, 0.01 for a comparison of *survivin* transcripts in normal astrocytes and D65MG glioma cells. *Upper Right:* Specific *survivin* promoter activity orrelates with basal *survivin* gene expression. Glioma D65MG cells and normal astrocytes were infected with Ad-S or Ad-CMV, respectively, at an MOI of 100. Luciferase activity was analyzed after 2 days of infection and is presented as percentages of CMV promoter activity. The values represent mean values of triplicate assays, and each point represents the mean and SD from three determinations. **p*, 0.05 and ***p*, 0.01 for a comparison of *survivin* promoter activities in normal astrocytes and D65MG glioma cells. *Lower:* *Survivin* promoter activity is decreased in normal human brain. *Survivin* promoter activity was measured in human brain specimens excised from two patients during epilepsy surgeries. Normal brain specimens were infected in quadruplicate with either Ad-S or Ad-CMV. After a 72-hour incubation, luciferase activity was measured. Each point represents the mean and the SD from four determinations. ***p*, 0.01 for a comparison of *survivin* and CMV promoter activities.

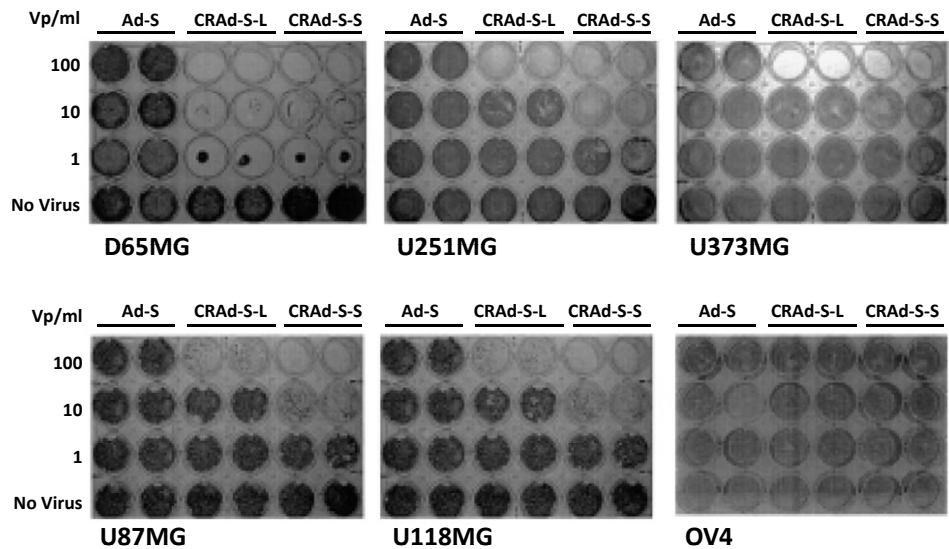


Figure 3. Tissue cultures stained with crystal violet showing that survivin-based CRAds induce glioma cell killing. Cytotoxic effects of CRAd-S-S, CRAd-S-L, and the negative control Ad-S in a variety of glioma cell lines and an ovarian cell line, OV4. Cells (5×10^4) from each cell line—D65MG, U251MG, U373MG, U87MG, U118MG, and OV4—were placed in 24-well plates and infected with adenoviral vector at the indicated MOIs or were mock infected. After a 10-day infection period, the cells were stained with crystal violet as described in *Materials and Methods*.

Survivin Promoter-Regulated CRAds are Inactive in the Human Liver

Due to the fact that adenoviral replication is species specific and because the major adenoviral toxicity in gene therapy trials is hepatic, we tested the replication of survivin-CRAds in human liver specimens in organ cultures. To evaluate viral replication indirectly, we measured *E4* gene copy numbers with quantitative real-time PCR, performed on DNA isolated from human liver slices 2 days after infection with CRAd-S-S, CRAd-S-L, or Adwt (Fig. 4). The *E4* copy numbers of the CRAd-S-S and CRAd-S-L agents were 1.5 and 2.5 orders of magnitude fewer than that of Adwt, respectively. Thus, survivin promoter-regulated CRAds exhibit a “liver-off” profile, especially CRAd-S-L.

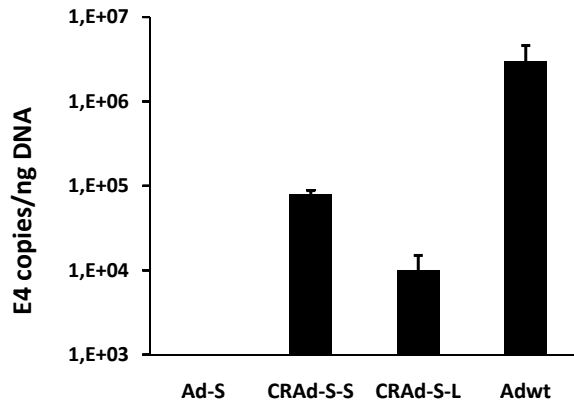


Figure 4. Bar graph demonstrating that the replication of surviving based CRAds is repressed in human liver organ cultures. The replication of survivin-based CRAds was evaluated in human liver lices, which had been infected with 500 vp/cell of an adenovirus (Adwt, Ad-S, CRAd-S-S, or CRAd-S-L). Two days following infection, DNA was isolated from each human liver slice and the Ad5 *E4* levels were determined by performing quantitative PCR. The data are expressed as the adenoviral *E4* copy number per nanogram DNA following normalization to GAPDH.

Replication of Survivin–CRAds In Vitro and In Vivo

Next, CRAd-S-S and CRAd-S-L replications were compared in vitro to Adwt replication in D65MG glioma cells. Viral replication was determined indirectly by examining the *E4* gene copy numbers on Days 1, 3, and 9 postinfection (Fig. 5 *upper*). The *E4* copy numbers of CRAd-S-S (3.2 million copies on Day 3 and 12.8 million copies on Day 9) were higher than both CRAd-S-L (1.1 million copies on Day 3 and 2.3 million copies on Day 9) and Adwt (0.34 and 2.86 million copies on Days 3 and 9, respectively). On a time scale, the replication rates increased twofold, fourfold, and 8.3-fold from Day 3 to Day 9 for CRAd-S-L, CRAd-S-S, and Adwt, respectively. Thus, despite their decreased replication in the human liver, CRAd-S-L and CRAd-S-S maintain their replicative potential in glioma cells. Because no established glioma xenograft animal models involve the use of D65MG cells, we used U118MG glioma cells. Xenografts of U118MG cells were injected with either Adwt or CRAd-S-S, and harvested either on Day 1 or Day 7 after injection. Next, DNA was extracted from tumor samples and the *E4* gene copy numbers were measured using quantitative real-time PCR (Fig. 5 *lower*). The *E4* copy numbers increased to 815 copies/ng DNA in tumors injected with Adwt and 2574 copies/ng DNA in tumors injected with CRAd-S-S; these increases constitute a 50-fold and a 160-fold increase in the replication rate on Day 7 for cells treated with Adwt and CRAd-S-S, respectively. Thus, although both Adwt and CRAd replicate well in vivo in a glioma xenograft model, survivin promoter–regulated CRAd replication was superior to that of Adwt.

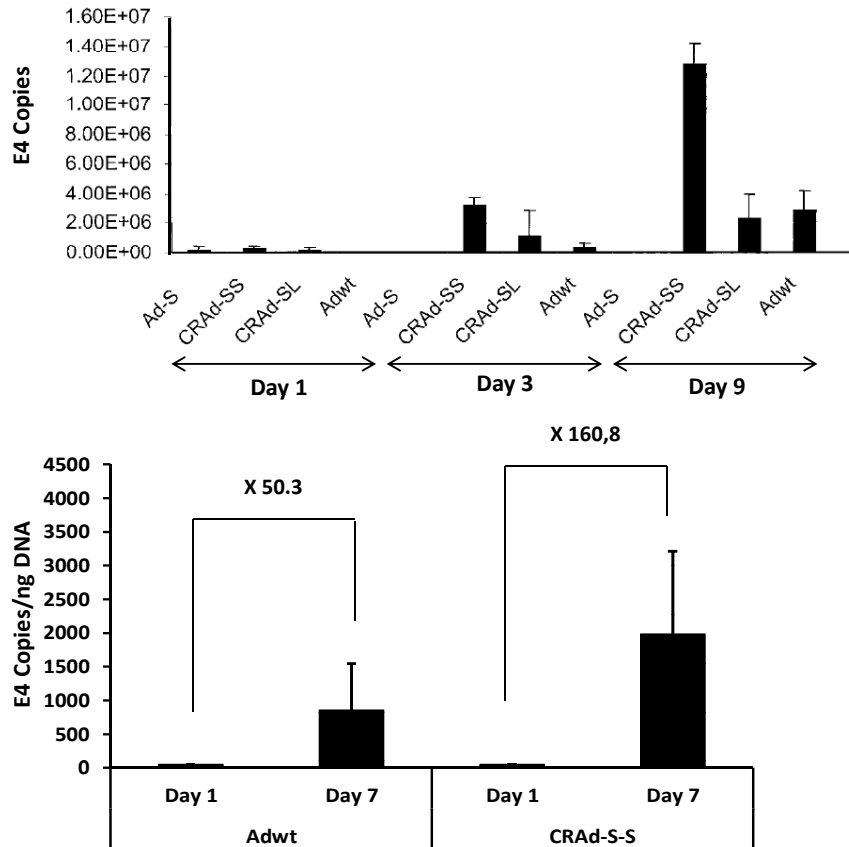


Figure 5. Bar graphs demonstrating survivin-based CRAds replication in glioma cell lines. *Upper:* Replication of CRAd agents in vitro. The D65MG glioma cells (5×10^4) were placed in 24-well plates and infected with CRAd-S-S, CRAd-S-L, Adwt, or a nonreplicating adenovirus, Ad-S, at an MOI of 100. Two hundred microliters of medium was removed from each well on Days 1, 3, and 9. The DNA was isolated using a Qiagen column, and the amount of *E4* gene was determined using quantitative PCR as described in *Materials and Methods*. The *E4* gene levels are shown as copy numbers on the y axis. All experiments in each group were performed in triplicate. *Lower:* Replication of CRAd-survivin-RGD in vivo. Tumor cells (5×10^6) were injected in both flanks. Ten days later, 5×10^8 vp of CRAd-S-S or Adwt were injected intratumorally. The tumors were collected 1 and 7 days postinjection; the Ad5 *E4* gene copy number was detected using quantitative real-time PCR and normalized to b-actin levels.

Antitumor Effects of Survivin-CRAds

The antitumor effects of CRAd-S-S and CRAd-S-L were analyzed in vivo in the U118MG xenograft model (Fig. 6). A follow-up examination of tumor volume showed that both survivin-based CRAds could significantly inhibit tumor growth. As Fig. 6 *upper* demonstrates, tumor volumes were $37.5 \pm 6.7 \text{ mm}^3$, $35.4 \pm 14.1 \text{ mm}^3$, $119.3 \pm 35 \text{ mm}^3$, and $167.6 \pm 49 \text{ mm}^3$ 30 days after the animals were injected with CRAd-S-S, CRAd-S-L, Ad-S, and PBS, respectively. When tumor

volumes were compared with those on Day 1 (Fig. 6 lower), a 62.1% volume reduction rate was observed for tumors treated with CRAd-S-S and a 67.2% volume reduction rate for tumors treated with CRAd-S-L after 30 days. In contrast, relative tumor volumes increased to 160% in the non-replicative virus-treated group and 225% in the PBS-treated group. There is a statistically significant difference (p , 0.01) between treatment groups and control groups. Thus, although the antitumor effects did not differ between the two survivin-based CRAds, both CRAds exhibited a strong antitumor effect in the U118MG glioma xenograft model.

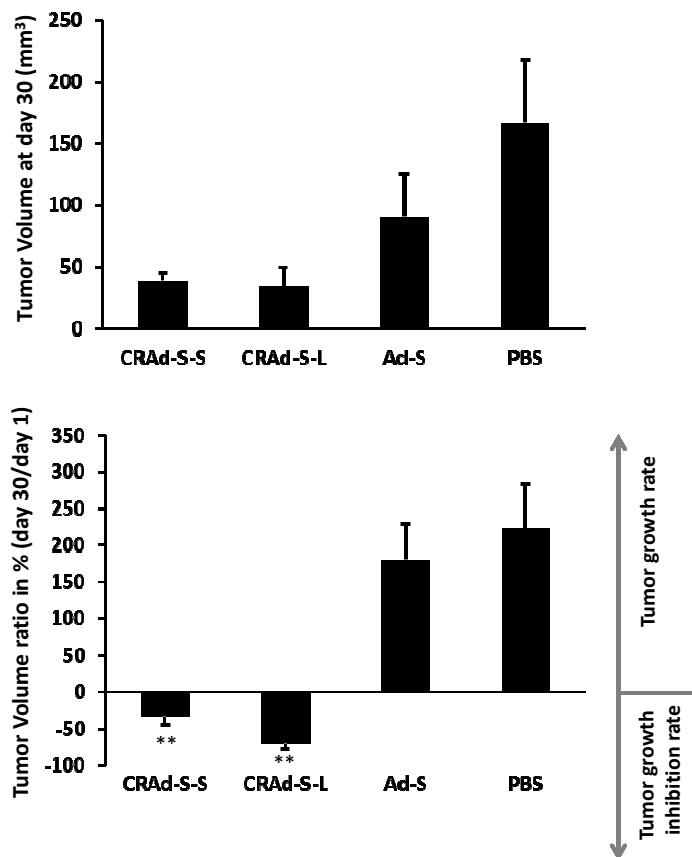


Figure 6. Bar graphs depicting the antitumor effect of CRAd agents on a murine glioma xenograft model. *Upper:* Antitumor effects of CRAd agents. The U118MG glioma cells (5×10^6) were injected subcutaneously into both flanks of nude mice. When the tumor reached 5 mm in diameter, administration of adenoviral vectors (10^9 vp) including a nonreplicative adenovirus, Ad-S, or PBS was performed by intratumoral injection. A second administration of adenoviral vectors or PBS was given 1 week later. The tumor volume was calculated using the formula $1/2 xy^2$, in which x = the longest dimension of the tumor and y = the shortest dimension of the tumor. *Lower:* Relative volume ratios of the antitumor effects of various CRAd agents, nonreplicative adenovirus (Ad-S), and PBS. The tumor growth rate and the tumor growth inhibition rate are described in *Materials and Methods*. ** p , 0.01.

Discussion

Malignant gliomas (GBM and anaplastic astrocytoma) are the most common types of primary central nervous system tumors and together have an incidence of 5 to 8 per 100,000 persons. The median survival of patients with malignant glioma varies from 14 weeks among those who receive conservative treatment to 40 to 59 weeks for those who receive aggressive therapy.^{8,14,32,33} Because survival in patients with malignant glioma remains poor, novel strategies are urgently required. In this regard, oncolytic virotherapy with CRAd agents is a promising and emerging approach that is already used in other types of cancer.^{16,28} The hallmark of oncolytic virotherapy is the potential for tumor-specific replication and cell killing. To this end, transcriptional targeting is essential. In our previous reports we identified the survivin promoter as an excellent TSP that exhibits a “tumor-on” and “liver-off” profile.⁴⁵ In this study, we focused on the survivin promoter as a key regulatory TSP for glioma. First, we demonstrated, in a recombinant adenoviral vector background, that the survivin promoter is active in a variety of established and primary glioma cells. This promoter activity correlated well with the native *survivin* gene expression pattern in these glioma cells. Encouraged by these findings, we used survivin promoter-regulated CRAds, in which the *E1* gene was driven by the human survivin promoter, to achieve tumor-specific oncolysis. Although these survivin-CRAds demonstrated a glioma cell-killing capacity in vitro as well as in vivo, we detected only minimal viral transcription in normal human cells including astrocytes. Consequently, survivin-based promoter transcriptional regulation emerges as a potentially applicable antitumor approach for glioma. Other promoters have been proposed for glioma-specific therapy, such as glial fibrillary acidic protein (a brain-specific expression but not a TSP) and the hTERT TSP.^{19,20} In this study, the Cox-2 and midkine promoters were compared with the survivin promoter on the basis of their proven potential for glioma.^{2,18,27} Although all three TSPs were repressed in normal cells, the survivin promoter demonstrated superior activity in both established glioma cell lines (with a mean 11.2% of the activity of the CMV promoter compared with a mean of , 4% activity of the CMV promoter for the Cox-2 and midkine promoters; Fig. 1 upper). More importantly, the activity in primary glioma cells was 20% of the activity of the CMV promoter compared with a mean of less than 5% activity of the CMV promoter for the Cox-2 and midkine promoters (Fig. 1 lower). Although decreased expression of *survivin* gene in normal tissues is expected,⁵ it is encouraging that the promoter is expressed in glioma cells, especially in view of the correlation between survivin expression levels and the prognosis of glioma.⁶ Moreover, the increasing expression of survivin in progressive grades of astrocytic tumors has important clinical application, as survivin-based therapies can be implemented across a spectrum of malignant brain tumors.¹⁵ Given that replication-incompetent vectors have proved to be inefficient as antitumor agents, replication-selective viruses have emerged as potentially powerful anticancer agents.¹⁷ Based on their capacity for gene amplification and intratumoral production of viral progeny, the intrinsic cell killing of adenoviruses has been diverted into CRAd oncolysis. These attributes of CRAds have recently been applied in the context of glioma.^{25,36} In this study, we constructed two novel CRAd agents, CRAd-S-S (nucleotides 2230 to 130 of the human *survivin* gene) and CRAd-S-L (nucleotides 21430 to 130 of the human *survivin* gene), in which the survivin promoter regulated Ad5 *E1* gene expression and viral infectivity was enhanced by capsid modification, that is, genetic insertion of the RGD-4C ligand. Of note, the *E3* gene

was retained in these CRAds for improved cell killing. Nevertheless, despite the cell killing attributes of our survivin-based CRAds, they maintained safe profiles in both normal brain and liver. Because the liver manifests a 95% uptake rate of adenovirus when delivered systemically,²² thereby potentially compromising liver function,³⁹ the safety profile of survivin-based CRAds in liver tissue (1.5 and 2.5 orders of magnitude fewer *E4* copies than those found in Adwt, CRAd-S-S, and CRAd-SL, respectively) is especially encouraging. Furthermore, because malignant gliomas do not metastasize, local CRAd injection may be applicable on the basis of dramatic repression of the survivin promoter in normal human astrocytes and brain tissue.

The in vitro oncolytic effects of CRAd-S-S and CRAd-SL were translated into antitumor effects in a glioma xenograft model and correlated with intratumoral replication rates. The difference we observed between the short and long versions of the survivin promoter in the CRAd context was that the long version of the survivin promoter was less hepatotoxic than the short version. These data are reminiscent of the Cox-2 promoter versions previously described.^{41,43} Thus, CRAd-S-L maintains an antitumor effect, while minimizing hepatotoxicity to increase the therapeutic index, an important parameter in cancer gene therapy. In this study, the viral replication of CRAds was regulated by a tumor-specific promoter, the survivin promoter. Thus, viral replication was limited to tumor cells and minimized in normal host cells. However, adenoviruses are able to kill normal cells as well as cancer cells by leaking vectors, leading to host toxicity.¹¹ The potential of killing normal cells relates to the promoter activity in normal cells. For this reason, we tested the promoter activity in human brain tissue. The data shown in Fig. 2 *lower* revealed only 0.26% of the activity of the CMV promoter, indicating that the toxicity of leakage of these agents to brain tissue is low because of the TSP.

Conclusions

We identified the human survivin promoter as a tumorspecific regulatory element for glioma. It is activated in established and primary glioma cells and is downregulated in normal astrocytes and human brain and liver tissues. The survivin promoter therefore represents a promising transcriptional targeting approach for gliomas. Survivin-based CRAds significantly kill glioma cells in vitro and inhibit the growth of glioma xenografts in vivo. On this basis, the surviving promoter in recombinant adenovirus and CRAd contexts may have potential use for future experimental clinical applications in the treatment of glioma.

References

1. Adachi Y, Reynolds PN, Yamamoto M, Grizzle WE, Overturf K, Matsubara S, et al: Midkine promoter-based adenoviral vector gene delivery for pediatric solid tumors. *Cancer Res* 60: 4305–4310, 2000
2. Akasaki Y, Liu G, Chung NH, Ehtesham M, Black KL, Yu JS: Induction of a CD4+ T regulatory type 1 response by cyclooxygenase-2-overexpressing glioma. *J Immunol* 173:4352–4359, 2004
3. Alemany R, Gomez-Manzano C, Balague C, Yung WKA, Curiel DT, Kyritsis AP, et al: Gene therapy for gliomas: molecular targets, adenoviral vectors, and oncolytic adenoviruses. *Exp Cell Res* 252:1–12, 1999
4. Ambrosini G, Adida C, Altieri DC: A novel anti-apoptosis gene, survivin, expressed in cancer and lymphoma. *Nat Med* 3: 917–921, 1997
5. Bao R, Connolly DC, Murphy M, Green J, Weinstein JK, Pisarcik DA, et al: Activation of cancer-specific gene expression by the survivin promoter. *J Natl Cancer Inst* 94:522–528, 2002
6. Chakravarti A, Noll E, Black PM, Finkelstein DF, Finkelstein DM, Dyson NJ, et al: Quantitatively determined survivin expression levels are of prognostic value in human gliomas. *J Clin Oncol* 20:1063–1068, 2002
7. Davis FG, McCarthy BJ: Epidemiology of brain tumors. *Curr Opin Neurol* 13:635–640, 2000
8. Fine HA, Dear KB, Loeffler JS, Black PM, Canellos GP: Metaanalysis of radiation therapy with and without adjuvant chemotherapy for malignant gliomas in adults. *Cancer* 71:2585–2597, 1993
9. Fueyo J, Alemany R, Gomez-Manzano C, Fuller GN, Khan A, Conrad CA, et al: Preclinical characterization of the antiglioma activity of a tropism-enhanced adenovirus targeted to the retinoblastoma pathway. *J Natl Cancer Inst* 95:652–660, 2003
10. Fueyo J, Gomez-Manzano C, Alemany R, Lee PSY, McDonnell TJ, Mitlianga P, et al: A mutant oncolytic adenovirus targeting the Rb pathway produces anti-glioma effect in vivo. *Oncogene* 19: 2–12, 2000
11. Fueyo J, Gomez-Manzano C, Yung WK, Kyritsis AP: Targeting in gene therapy for gliomas. *Arch Neurol* 56:445–448, 1999
12. Haviv YS, Curiel DT: Conditional gene targeting for cancer gene therapy. *Adv Drug Deliv Rev* 53:135–154, 2001
13. Huang CJ, Nazarian R, Lee J, Zhao PM, Espinosa-Jeffrey A, de Vellis J: Tumor necrosis factor modulates transcription of myelin basic protein gene through nuclear factor kappa B in a human oligodendrogloma cell line. *Int J Dev Neurosci* 20:289–296, 2002
14. Huncharek M, Muscat J: Treatment of recurrent high grade astrocytoma; results of a systematic review of 1,415 patients. *Anticancer Res* 18:1303–1311, 1998
15. Kajiwara Y, Yamasaki F, Hama S, Yahara K, Yoshioka H, Sugiyama K, et al: Expression of survivin in astrocytic tumors: correlation with malignant grade and prognosis. *Cancer* 97:1077–1083, 2003
16. Khuri FR, Nemunaitis J, Ganly I, Arseneau J, Tannock IF, Romel L, et al: A controlled trial of intratumoral ONYX-015, a selectively-replicating adenovirus, in combination with cisplatin and 5-fluorouracil in patients with recurrent head and neck cancer. *Nat Med* 6:879–885, 2000
17. Kirn D, Martuza RL, Zwiebel J: Replication-selective virotherapy for cancer: biological principles, risk management and future directions. *Nat Med* 7:781–787, 2001
18. Kohno S, Nakagawa K, Hamada K, Harada H, Yamasaki K, Hashimoto K, et al: Midkine promoter-based conditionally replicative adenovirus for malignant glioma therapy. *Oncol Rep* 12: 73–78, 2004
19. Komata T, Koga S, Hirohata S, Takakura M, Germano IM, Inoue M, et al: A novel treatment of human malignant gliomas in vitro and in vivo: FADD gene transfer under the control of the human telomerase reverse transcriptase gene promoter. *Int J Oncol* 19: 1015–1020, 2001
20. Komata T, Kondo Y, Kanzawa T, Hirohata S, Koga S, Sumiyoshi H, et al: Treatment of malignant glioma cells with the transfer of constitutively active caspase-6 using the human telomerase catalytic subunit (human telomerase reverse transcriptase) gene promoter. *Cancer Res* 61:5796–5802, 2001
21. Komata T, Kondo Y, Kanzawa T, Ito H, Hirohata S, Koga S, et al: Caspase-8 gene therapy using the human telomerase reverse transcriptase promoter for malignant glioma cells. *Hum Gene Ther* 13:1015–1025, 2002
22. Krut FA, Curiel DT: Toward a new generation of conditionally replicating adenoviruses: pairing tumor selectivity with maximal oncolysis. *Hum Gene Ther* 13:485–495, 2002
23. Lamfers MLM, Grill J, Dirven CMF, van Beusechem VW, Georger B, Van Den Berg J, et al: Potential of the conditionally replicative adenovirus Ad5-delta24RGD in the treatment of malignant gliomas and its enhanced effect with radiotherapy. *Cancer Res* 62:5736–5742, 2002

24. Li F, Ambrosini G, Chu EY, Plescia J, Tognin S, Marchisio PC, et al: Control of apoptosis and mitotic spindle checkpoint by survivin. *Nature* 396:580–584, 1998
25. Lou E: Oncolytic viral therapy and immunotherapy of malignant brain tumors: two potential new approaches of translational research. *Ann Med* 36:2–8, 2004
26. Manome Y, Kunieda T, Wen PY, Koga T, Kufe DW, Ohno T: Transgene expression in malignant glioma using a replicationdefective adenoviral vector containing the Egr-1 promoter: activation by ionizing radiation or uptake of radioactive iododeoxyuridine. *Hum Gene Ther* 9:1409–1417, 1998
27. Mishima K, Asai A, Kadomatsu K, Ino Y, Nomura K, Narita Y, et al: Increased expression of midkine during the progression of human astrocytomas. *Neurosci Lett* 233:29–32, 1997
28. Morris JC, Wildner O: Therapy of head and neck squamous cell carcinoma with an oncolytic adenovirus expressing HSV-tk. *Mol Ther* 1:56–62, 2000
29. Nanda D, Vogels R, Havenga M, Avezaat CJ, Bout A, Smitt PS: Treatment of malignant gliomas with a replicating adenoviral vector expressing herpes simplex virus-thymidine kinase. *Cancer Res* 61:8743–8750, 2001
30. Repovic P, Fears CY, Gladson CL, Benveniste EN: Oncostatin-M induction of vascular endothelial growth factor expression in astroglioma cells. *Oncogene* 22:8117–8124, 2003
31. Ruan H, Su H, Hu L, Lamborn KR, Kan YW, Deen DF: A hypoxia- regulated adeno-associated virus vector for cancer-specific gene therapy. *Neoplasia* 3:255–263, 2001
32. Salzman M: Survival in glioblastoma: historical perspective. *Neurosurgery* 7:435–439, 1980
33. Salzman M, Scholtz H, Kaplan RS, Kulik S: Long-term survival in patients with malignant astrocytoma. *Neurosurgery* 34:213–220, 1994
34. Sasaki T, Lopes MBS, Hankins GR, Helm GA: Expression of survivin, an inhibitor of apoptosis protein, in tumors of the nervous system. *Acta Neuropathol* 104:105–109, 2002
35. Segovia J, Vergara P, Brenner M: Differentiation-dependent expression of transgenes in engineered astrocyte cell lines. *Neurosci Lett* 242:172–176, 1998
36. Shah AC, Benos D, Gillespie GY, Markert JM: Oncolytic viruses: clinical applications as vectors for the treatment of malignant gliomas. *J Neurooncol* 65:203–226, 2003
37. Siu IM, Lal A, Blankenship JR, Aldosari N, Riggins GJ: c-Myc promoter activation in medulloblastoma. *Cancer Res* 63:4773–4776, 2003
38. Surawicz TS, Davis F, Freels S, Laws ER Jr, Menck HR: Brain tumor survival: results from the National Cancer Data Base. *J Neurooncol* 40:151–160, 1998
39. van der Eb MM, Cramer SJ, Vergouwe Y, Schagen FH, van Krieken JH, van der Eb AJ, et al: Severe hepatic dysfunction after adenovirus- mediated transfer of the herpes simplex virus thymidine kinase gene and ganciclovir administration. *Gene Ther* 5:451–458, 1998
40. Verwer RW, Hermens WT, Dijkhuizen P, Ter Brake O, Baker RE, Salehi A, et al: Cells in human postmortem brain tissue slices remain alive for several weeks in culture. *FASEB J* 16:54–60, 2002
41. Wesseling JG, Yamamoto M, Adachi Y, Bosma PJ, van Wijland M, Blackwell JL, et al: Midkine and cyclooxygenase-2 promoters are promising for adenoviral vector gene delivery of pancreatic carcinoma. *Cancer Gene Ther* 8:990–996, 2001
42. Yamamoto M, Alemany R, Adachi Y, Grizzle WE, Curiel DT: Characterization of the cyclooxygenase-2 promoter in an adenoviral vector and its application for the mitigation of toxicity in suicide gene therapy of gastrointestinal cancers. *Mol Ther* 3:385–394, 2001
43. Yamamoto M, Davydova J, Wang M, Siegal GP, Krasnykh V, Vickers SM, et al: Infectivity enhanced, cyclooxygenase-2 promoter- based conditionally replicative adenovirus for pancreatic cancer. *Gastroenterology* 125:1203–1218, 2003
44. Zamorano A, Lamas M, Vergara P, Naranjo JR, Segovia J: Transcriptionally mediated gene targeting of gas 1 to glioma cells elicits growth arrest and apoptosis. *J Neurosci Res* 71:256–263, 2003
45. Zhu ZB, Makhija SK, Lu B, Wang M, Kaliberova L, Liu B, et al: Transcriptional targeting of adenoviral vector through the CXCR4 tumor-specific promoter. *Gene Ther* 11:645–648, 2004
46. Zhu ZB, Makhija SK, Lu B, Wang M, Rivera AA, Kim-Park S, et al: Incorporating the survivin promoter in an infectivity enhanced CRAd-analysis of oncolysis and anti-tumor effects in vitro and in vivo. *Int J Oncol* 27:237–246, 2005
47. Zhu ZB, Makhija SK, Lu BG, Wang M, Kaliberova L, Liu B, et al: Transcriptional targeting of tumors with a novel tumor-specific survivin promoter. *Cancer Gene Ther* 11:256–262, 2004

4

Transient infection of freshly isolated human colorectal tumor cells by Reovirus T3D intermediate subviral particles

Winan. J. van Houdt, Niels Smakman, Diana M. van den Wollenberg, Benjamin L. Emmink, Liesbeth M. Veenendaal, Paul J. van Diest, Rob C. Hoeben, Inne H.M. Borel Rinkes, and Onno Kranenburg

Cancer Gene Therapy, 2008 May;15(5):284-92

Abstract

Reovirus T3D preferentially kills tumor cells expressing Ras oncogenes and has shown great promise as an anti-cancer agent in various pre-clinical tumor models. Here we investigated whether Reovirus can infect and kill tumor cell cultures and tissue fragments isolated from resected human colorectal tumors, and whether this was affected by the presence of endogenous oncogenic KRAS. Tissue fragments and single cell populations isolated from human colorectal tumor biopsies were infected with Reovirus virions or with intermediate subviral particles (ISVPs). Reovirus virions were incapable of infecting single-cell tumor cell populations, nor small fragments of intact viable tumor tissue. However, infection of tumor cells with ISVPs resulted in transient viral protein synthesis, irrespective of the presence of oncogenic KRAS, but this did not lead to the production of infectious virus particles, and tumor cell viability was largely unaffected. ISVPs failed to infect intact tissue fragments. Thermolysin treatment of tumor tissue liberated single cells from the tissue and allowed infection with ISVPs but this did not result in the production of infectious virus particles. Immunohistochemistry on tissue microarrays showed that JAM1, the major cellular Reovirus receptor, was improperly localized in the cytoplasm of colorectal tumor cells and was expressed at very low levels in liver metastases. This may contribute to the observed resistance of tumor cells to Reovirus T3D virions. We conclude that infection of human colorectal tumor cells by Reovirus T3D requires processing of virions to ISVPs but that oncolysis is prevented by a tumor cell response that aborts viral protein synthesis and the generation of infectious viral particles, irrespective of KRAS mutation status.

Introduction

Activating mutations in the KRAS proto-oncogene are found in approximately 30% of all human tumors. Recent evidence suggests that the sustained presence of oncogenic KRAS is required for maintenance of the transformed and malignant properties of several types of tumor cells¹⁻³. This makes KRAS, or KRAS-activated signaling intermediates, attractive targets for therapeutic intervention. Reovirus T3D is an oncolytic virus that kills susceptible cells by inducing apoptosis⁴. We have recently shown that oncogenic KRAS sensitizes human and mouse colorectal tumor cells to apoptosis induction by Reovirus T3D^{5,6}. Alternatively, KRAS may facilitate virus replication⁷. Reovirus T3D has shown great pre-clinical therapeutic efficacy in the treatment of several types of subcutaneous tumors and metastatic lesions formed by tumor cell lines⁸⁻¹². Based on this pre-clinical evidence, the anti-tumor activity of Reovirus T3D is currently being tested in clinical trials¹³.

Many novel therapeutics that show great promise as anti-tumor compounds in pre-clinical experiments fail to fulfill this promise in clinical trials. Work from our own group and from others has shown that Reovirus T3D can efficiently kill colorectal tumor cell lines and cell line-derived tumors in mice^{5,6,9,12}. In the present report we have evaluated the potential of Reovirus T3D to infect and kill tumor cells and tissue fragments freshly isolated from primary human colorectal tumors and their liver metastases. Furthermore, we have assessed whether virus replication and tumor cell killing are associated with the presence of oncogenic KRAS. Finally, we determined the expression and localization of the major Reovirus receptor, junction adhesion molecule 1 (JAM-1)¹⁴ in normal colon and in primary human colorectal tumors and their paired liver metastases.

Materials and Methods

Tumor samples

Patients who underwent a resection for primary colon cancer or for colorectal liver metastases from January 2004 to August 2006 were included in the study. The study was approved by the medical ethical committee of our institute. All patients gave their informed consent to the use of their tumor tissue for the purpose of this study. Directly following resection, the specimens were taken to the pathology department where a part of the tumor was excised for experimentation. The biopsy was mechanically dissociated using scalpels and vigorous trituration to yield small fragments (<1 mm³) and single cells. In some cases, where indicated, the tissue fragments were incubated with thermolysin (0.05% in 10 mM HEPES pH7.2, 37°C, 1 hour). The suspension was then filtered through a 70 µm pore size nylon cell strainer to separate the tissue fragments from the single cells. Tissue fragments and single cells were cultured separately in 96-well plates in Dulbecco's Modified Eagle's Medium/Ham F12 (1/1) (Dulbecco, ICN Pharmaceuticals, Costa Mesa, CA, USA) supplemented with 15% (v/v) fetal calf serum, 2mM glutamine, 0.1 mg/ml streptomycin, 100 U/ml penicillin and 2% Ultrosor G (PALL Life Sciences, Portsmouth, UK) at 37°C in a humidified atmosphere containing 5% CO₂.

Cell line, virus and intermediate subviral particles (ISVPs)

The human colorectal cancer cell line HCT116 was purchased from ATCC (CCL-247). HCT 116 cells were cultured in Dulbecco's Modified Eagle's Medium (DMEM; Dulbecco) supplemented with 5% (v/v) fetal calf serum, 2 mM glutamine, 0,1 mg/ml streptomycin, and 100 U/ml penicillin. All cells were kept at 37°C in a humidified atmosphere containing 5% CO₂. Reovirus T3D was purchased from ATCC (Teddington, UK) (VR-824). The virus was propagated and purified as previously described⁵. ISVPs were freshly prepared by treating purified virions with chymotrypsin just prior to infection (200µg/ml, Roche Diagnostics, Penzberg, Germany) for 60 minutes at 37°C. Digestion was stopped by the addition of PMSF (Calbiochem, Amsterdam, The Netherlands) to 2,5 mM at 4°C.

FACS analysis

Primary tumor cells (2×10^5) were washed twice with PBS containing 2% FCS and were resuspended in PBS-FCS 2% containing anti-hEpCam/Trop1 (R&D systems, Abingdon, UK) (1:200) or isotype control antibody. After 1h incubation at 4°C, the cells were washed twice with 2% FCS-PBS and were resuspended in 2%FCS-PBS containing goat-anti mouse Fab2-488 (Dako, (Heverlee, Belgium) (1:200). Following a 1h incubation at 4°C, the samples were washed twice and were immediately analyzed by flow cytometry using a FACScalibur (BD Biosciences, San Diego, USA).

Western Blotting

To 10 µl of a Reovirus or ISVP stock, sample buffer was added and the samples were run on a 10% sodium dodecyl sulphate - polyacrylamide gel (SDS-PAGE) for western blotting. After blotting, the membrane was washed and incubated for 1 hour with polyclonal rabbit anti-reovirus serotype 3 serum. After washing, the membrane was incubated for 1 hour with swine-anti-rabbit-RPO (Dako) (1:5000). The signals were visualized using an enhanced chemiluminescence system (Roche)

Reovirus infection and replication

Viable tumor tissue fragments were infected with Reovirus T3D (5×10^7 pfu/fragment) or control vehicle. Primary tumor cells or cell lines were infected with Reovirus T3D, ISVP (MOI 20 unless indicated otherwise) or control vehicle. Viral protein synthesis and replication was tested daily from post-operative day (pod) 1-3 by [³⁵S]-methionine (200µCi/ml, Amersham, city, country) labeling experiments. Cells were harvested 24h after labeling and cell extracts or tumor fragments were prepared in sample buffer and were analyzed with electrophoresis on long 45 cm SDS-PAGE. Gels were dried and exposed to radiographic film. Quantity One (Biorad, Hercules, USA) software was used to quantify the signal intensities. The ratios between the viral σ band and the cellular protein running ~5kDa above σ were calculated in each case.

Plaque assay

Plaque assays were performed exactly as described⁵.

Viability assay

Cells were plated on 96 wells plates and calcein (Invitrogen, Leek, The Netherlands) was added to 2,5 μM on day 1, 2, 3 and 4 (15 minutes, 37 $^{\circ}\text{C}$). Cells were harvested and washed once with PBS and were resuspended in PBS. The percentage viable (fluorescent) cells was analyzed by flow cytometry.

DNA extraction, PCR and sequence analysis

Genomic DNA was extracted from frozen tumor specimens corresponding to the tissue fragments and cell populations that were analyzed for Reovirus replication. The dissected tissue was suspended in extraction buffer (1M Tris, 0,5M EDTA, 10% SDS) containing proteinase K (1mg/ml) and was incubated at 56 $^{\circ}\text{C}$ for 48 hours. Proteinase K was freshly added every 12 hours. The solution was extracted twice with a 25:24:1 mixture of phenol-chloroform-isoamylalcohol. Genomic DNA was precipitated with ethanol, pelleted and resuspended in TE (Tris-HCl 10mM, EDTA 1mM). Target sequences encompassing codons 12, 13 and 61 of the KRAS gene and codon 600 of the BRAF gene were amplified by nested PCR in 384-well plates. Sequencing was performed using the Big Dye terminator Cycle Sequencing Ready Reaction Kit (Applied Biosystems, Warrington UK), according to the manufacturer's instructions. Analysis of the products was performed on an ABI Prism 377 DNA Sequencer (PE Biosystems). All target sequences were amplified in duplicate by independent PCR reactions and sequencing was done with both the forward and reverse sequencing primer. Only if a mutation was found in both independently amplified fragments, it was considered a real mutation and not a PCR artifact. The primer sequences will be supplied upon request.

Tissue microarray (TMA)

A tissue microarray (TMA) was made to analyze the expression of JAM-1 in normal colon epithelium and in CRC cells in the primary tumor and the corresponding liver metastasis. We collected representative paraffin embedded tissue blocks from neoplastic and non-neoplastic regions and the TMA was constructed as previously described in detail¹⁵. In brief, samples from surgical resections of 61 patients of whom normal colon, primary CRC, and corresponding CRC liver metastasis were available were selected for preparing a TMA. For each patient, nine cylindrical tissue cores were included in the TMA; three from the normal colon, three from the primary CRC and three from the corresponding liver metastasis. Immunostaining was performed using standard procedures. After incubation with 3% hydrogen peroxide, antigen retrieval was achieved by boiling in 10 mM citrate buffer pH 6.0. Sections were blocked with 5% goat serum in TBS and incubated with an anti-JAM-1 antibody (H-80, sc-25629 Santa Cruz Biotech., Heidelberg, Germany) at 4 $^{\circ}\text{C}$ overnight. HRP-conjugated secondary antibodies (DPVM-55HRP, Immunologic, Duiven, The Netherlands) were detected with 3,3'-diaminobenzidine substrate (D4418, Sigma, Saint Louis, USA). Slides were counterstained with hematoxylin and rinsed with water, dehydrated in ethanol, cleared in xylene and coverslipped. The localization and intensity of JAM-1 staining was determined in each separate tissue core by two independent experienced observers blinded to the cores' identities. Membranous staining of JAM-1 was scored as positive or negative. When a tissue core displayed weak and focal positivity in less than 5% of the total number of tumor cells, it was classified as negative. Cytoplasmic staining was scored as 0: no staining, 1: weak staining, 2: moderate staining and 3: strong staining. The average scores of the 3 biopsies were calculated.

Results

Isolation and culture of tumor-derived single cell cultures and tissue fragments

Biopsies of primary colorectal tumors or colorectal liver metastases were obtained immediately following tumor resection. The biopsies were processed into small tumor tissue fragments (<1mm³) and into single cell suspensions. The percentage of tumor cells in these cultures was determined by FACS analysis, using an antibody directed against the epithelial cell surface marker EpCAM. In general, approximately 60-85% of the cells in tumor-derived single cell populations are epithelial (tumor) cells. An example is shown in Figure 1a. Viability of the single cell populations was measured by FACS analysis of calcein-stained cells and did not change over the 4 day culture period (91±5% viable cells on day 1 versus 89±4% viable cells on day 4). Over time, the single cell populations continued to express CK20, demonstrating their epithelial (tumor) origin (Figure 1a). The tumor tissue fragments were small enough to allow diffusion of oxygen and nutrients, thus preserving the viability of tumor and stromal cells for the duration of the experiments. H&E-stained paraffin-embedded tissue fragment sections showed that tissue architecture was largely preserved over a 4-day culture period (Figure 1b). Furthermore, Western blot analysis of cytokeratin 20 (CK20) expression in the tissue fragments revealed that the fraction of tumor cells in the fragments remained constant throughout the culture period (Figure 1b).

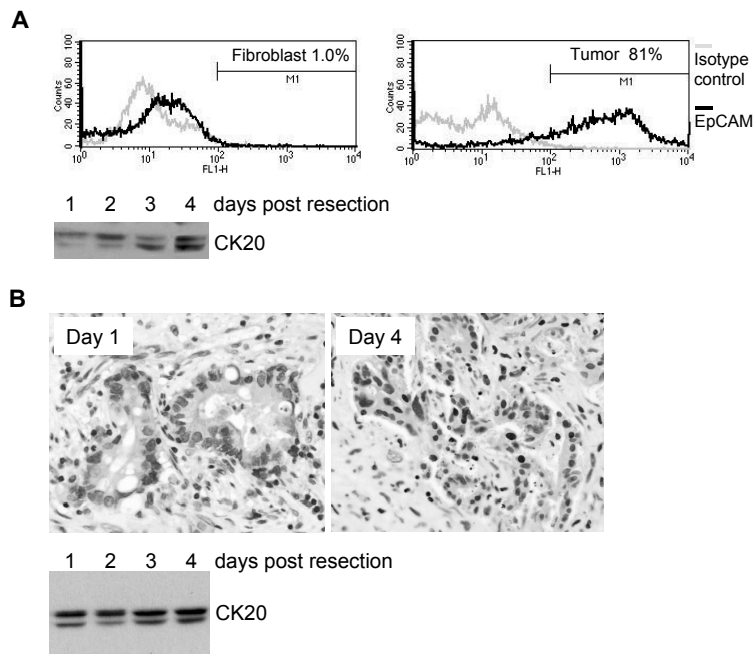


Figure 1. Tumor-derived single-cell cultures and tissue fragments. (A) Biopsies of resected primary colorectal tumors or colorectal liver metastases were processed as described in the Materials and Methods section. Single cell populations derived from colorectal tumor biopsies were analyzed by FACS for the percentage of EpCAM-positive cells. Typically 60-85% of single tumor cell preparations are EpCAM-positive.

A representative example is shown. Cultures of primary human fibroblasts were used as a negative control. Western blot analysis of CK20 expression demonstrates the maintenance of epithelial (tumor) cells in the single cell populations over time. (B) Cultured tissue fragments were fixed in formalin and were processed for haematoxylin and eosin-staining. Sections of paraffin-embedded tissue fragments after 1 and 4 days of culturing show that tissue architecture and cell viability is largely maintained. Western blot analysis of CK20 expression demonstrates the maintenance of epithelial (tumor) cells in the cultured tissue fragments over time. Representative examples are shown. *See page 196 for color figure*

Single cell cultures from human colorectal tumors are resistant to infection by Reovirus T3D.

The freshly isolated single cell populations were infected with increasing doses of Reovirus T3D (0-400 pfu/cell) and Reovirus protein synthesis was assessed by [³⁵S]-methionine labeling experiments. Figure 2 shows that Reovirus protein synthesis was only detectable at the highest concentration tested (400 pfu/cell), but not at any of the lower concentrations. In contrast, all human CRC cell lines tested so far in our lab, including HCT116 (Figure 2) are readily infected at 20 pfu/cell. At 20 pfu/cell, we found no evidence for virus replication in any of the tumor cell populations tested (n=13, Figure 4b) even though 5 out of 12 tumors (42%) contained activating mutations in KRAS (G13D (3x), G12V (1x) G12D (1x)). Thus, the tumor cell populations are relatively resistant to Reovirus infection despite the presence of oncogenic KRAS.

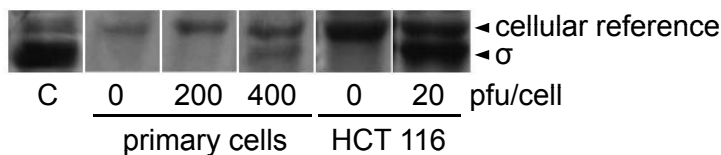


Figure 2. Tumor-derived single-cell populations are relatively resistant to infection by Reovirus T3D. Freshly isolated single-cell populations derived from colorectal tumors, or cells from an established colorectal cancer cell line (HCT116) were infected with Reovirus T3D at the indicated concentrations. A previously successfully infected HCT116 population served as a control for migration of the Reovirus proteins. Viral protein synthesis was then assessed by [³⁵S]-methionine labeling. The figure shows Reovirus σ protein synthesis 2 days following infection.

Virion processing to ISVPs facilitates tumor cell infection in single cell cultures

Next, we tested whether the relative resistance of colorectal tumor cells to infection could be overcome by infecting them with intermediate subviral particles (ISVPs). ISVPs were successfully generated by incubating Reovirus virions with chymotrypsin, as judged by the disappearance of μ and the appearance of the protease-resistant δ fragment (Figure 3a). One day following infection with Reovirus virions or with ISVPs (5 pfu/cell), HCT116 cells were labeled with [³⁵S]-methionine. Figure 3b shows that the ISVPs displayed a far greater infectivity than the virions, as measured by Reovirus protein synthesis. Furthermore, ISVP-infected cells amplified the input dosage of infectious viral particles 149-fold over a period of 4 days, whereas virion-infected cells amplified the input dosage less efficiently (40-fold) (Figure 4c).

Next, single cell cultures freshly isolated from tumor biopsies were infected either with virions or with ISVPs (20 pfu/cell) and Reovirus protein synthesis was assessed over time. Reovirus protein synthesis could clearly be detected 1 day after infection of the tumor cell cultures with ISVPs, but not with virions (Figure 4a and 4b). Infection with ISVPs yielded robust Reovirus protein synthesis 1 day after infection in 6 out of 8 tumor cell populations tested. However, in all these cultures Reovirus protein synthesis had dropped dramatically on day 2 and was undetectable by day 3 (Figure 4a and 4b). Despite the fact that viral protein synthesis was clearly detectable in ISVP-infected tumor cells, they showed only a marginal non-significant increase in the production of infectious virus particles over a period of 4 days (1.4 fold amplification of the input dose) (Figure 4c). Similarly, virion-infected tumor cells did not significantly amplify the input dose (1.8-fold) (Figure 4c). Interestingly, only 1 of the 6 tumor cell populations that sustained temporary Reovirus replication also showed a temporary loss of cell viability as measured by FACScan analysis of calcein-stained cells (Figure 4d). Thus, when compared to virions, Reovirus ISVPs show a greatly enhanced ability to infect single cell cultures of colorectal tumors, but viral protein synthesis is rapidly aborted, which allows most tumor cell cultures to survive infection.

Freshly isolated tumor tissue is resistant to infection with Reovirus virions and ISVPs..

Next, we tested whether tumor cells in the context of tumor tissue could be infected with Reovirus virions or ISVPs. Following infection, viral protein synthesis was assessed by [³⁵S]-methionine labeling experiments. Tumor fragments from 30 independent colorectal tumors were tested, and none of the tumors showed detectable Reovirus protein synthesis following infection with either virions or ISVPs (Figure 3c). In 8 of these tumors (27%) we detected activating mutations in KRAS (G12D (3x), G12V (2x), G13D (1x), G12S (1x), G12R (1x)), while 2 tumors harbored an activated BRAF allele (V600E (2x); 7%). Also at later time points (up to 8 days) we failed to detect Reovirus protein synthesis in any of the virion- or ISVP-infected tissue fragments. Thus, ISVPs can infect single cell cultures of freshly isolated tumor cells, but they fail to penetrate tumor tissue.

Finally, we tested whether degradation of the extracellular matrix in tumor tissue fragments by the protease thermolysin would allow tumor cell infection by Reovirus. Thermolysin was previously successfully used for the isolation of primary epithelial cells from human intestinal tissue¹⁶. Thermolysin treatment greatly increased the yield of single tumor cells from tumor tissue (not shown), and allowed infection of the isolated single cells with ISVPs but not with virions (Figure 4f). Thus, thermolysin treatment of tumor tissue liberates single cells from the tissue and makes them available for infection with ISVPs. However single cell populations isolated with or without thermolysin-treatment did not show differences in their ability to sustain Reovirus protein synthesis, or in their ability to produce infectious virus particles (Figures 4f-g). Thus, even in the absence of extracellular matrix and stromal tissue, freshly isolated primary colorectal cancer cells are very inefficient in sustaining Reovirus replication and virus production. Furthermore, the relatively inefficient generation of virus progeny by freshly isolated tumor cells (Figure 4c) was unaffected by inclusion of thermolysin in the isolation procedure (Figure 4g). Rather, virus yield in the thermolysin-treated samples was even lower than that in the non-treated samples, although these differences were not statistically significant.

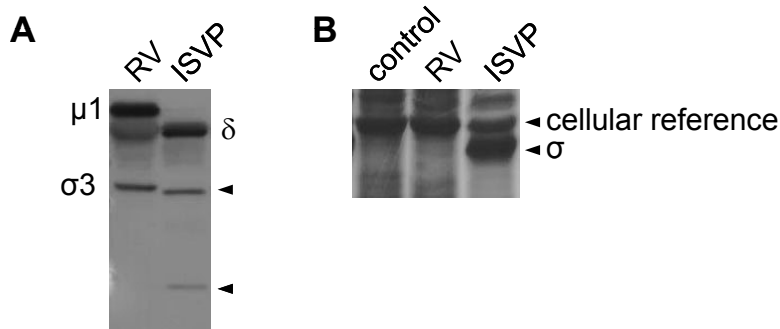


Figure 3. Generation of ISVPs. (A) Purified Reovirus T3D virions were incubated with chymotrypsin for 1h at 37°C and the reaction was stopped with PMSF. Equal amounts of virions and ISVPs were then analyzed by Western blotting using a polyclonal anti-Reovirus T3D antibody. ISVPs are characterized by cleavage of $\mu 1$ and by the appearance of the chymotrypsin-resistant fragment δ (generated from $\mu 1$). The arrowheads denote additional chymotrypsin-resistant proteolytic fragments recognized by our polyclonal antibody. (B) Virions and ISVPs were then used to infect HCT116 cells at low MOI (5 pfu/cell) and viral protein synthesis was assessed by [35 S]-methionine labeling 24 hours later.

Human primary colorectal tumors and liver metastases display aberrant localization of JAM-1

The major Reovirus virion receptor is a tight junction molecule called junction adhesion molecule 1 (JAM1). JAM1 localizes to cell-cell contacts in layers of epithelial and endothelial cells and its expression is a major determinant of cellular sensitivity to Reovirus infection¹⁴. In contrast, ISVPs infect target cells independently of JAM1, as the JAM1-binding head domain of the viral $s1$ attachment protein is lost during ISVP generation¹⁷. The finding that freshly isolated colorectal tumor cells are resistant to infection with virions but not ISVPs, prompted us to test JAM1 expression in a series of primary human colorectal carcinomas and paired liver metastases. Normal colon tissue adjacent to the primary tumor was used as a positive control. Paired samples of 61 patients were available from the Pathology database. After construction and evaluation of the TMA, a total of 52 normal colon samples, 61 primary tumor samples and 53 liver metastasis samples were available for analysis. Immunohistochemical analysis of JAM1 expression on the TMA revealed that JAM1 is localized at epithelial cell-cell contacts in normal colonic enterocytes, as expected (Figure 5). In contrast, JAM1 staining was predominantly cytoplasmic in primary colorectal tumors and in liver metastases, but it was not observed at the cell-cell contacts between tumor cells (Figure 5). Only 4/61 primary tumors and 2/53 liver metastases displayed weak focal JAM1 staining at cell-cell contacts. Finally, JAM1 expression was markedly and significantly lower in the liver metastases than in the paired primary tumors and in control colon tissue. This is relevant because novel therapeutics are required for the treatment of (liver) metastases rather than primary tumors. Thus, mislocalization and low level expression of JAM1 may contribute to the resistance of human colorectal tumor cells to Reovirus T3D.

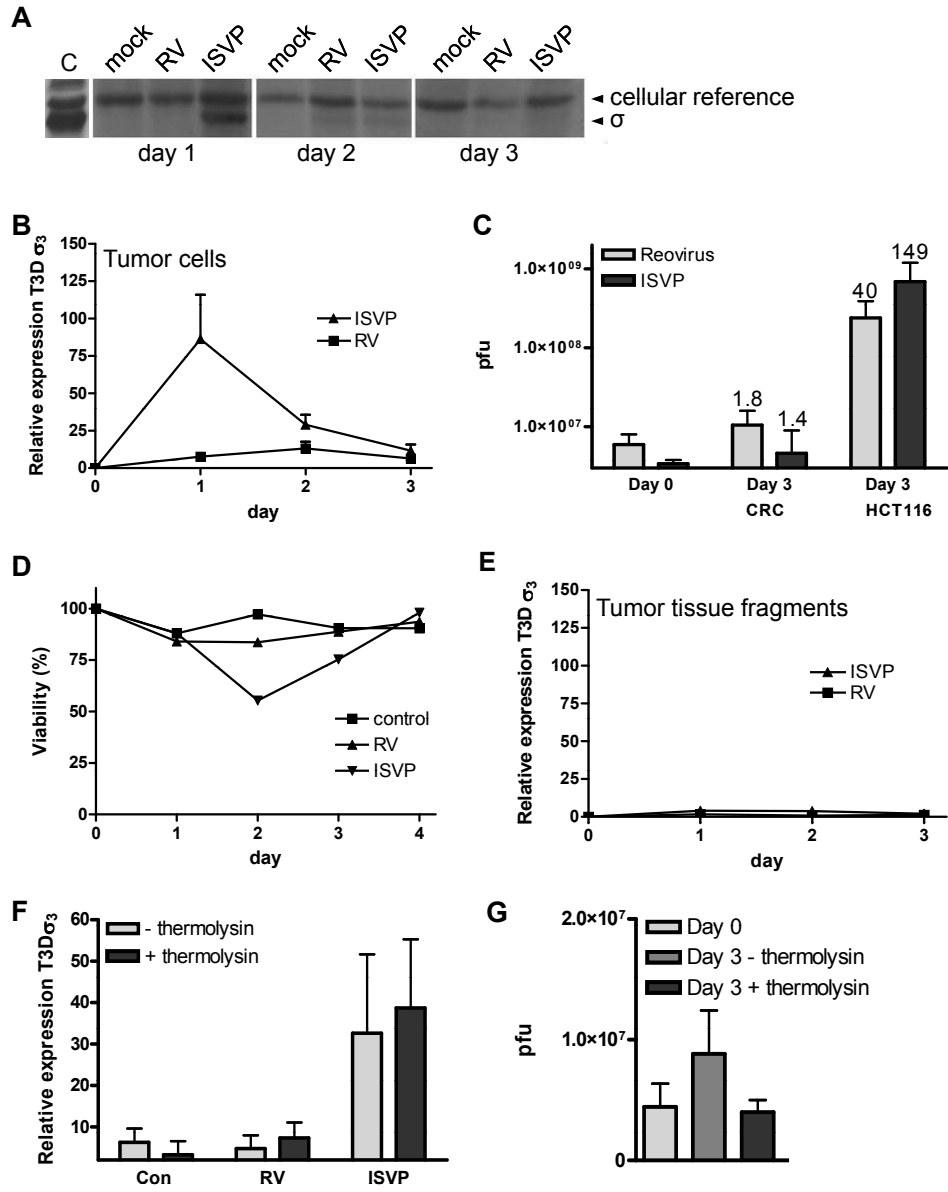


Figure 4. Transient infection of single cell populations by ISVPs. (A,B) Freshly isolated human colorectal tumor cells were infected with Reovirus virions or with ISVPs as indicated (20 pfu/cell). Viral protein synthesis was then followed over time by [³⁵S]-methionine labeling. The radiographic exposures of all tumor cell populations infected with Reovirus (n=30) or ISVPs (n=8) over time were used to scan the intensity of the viral s₃ band when compared to that of a cellular reference protein running immediately above s₃. Similar results were obtained when the λ or m1 bands were used for quantification (not shown). The relative density of s₃ (when compared to the cellular reference protein) was then plotted over time. (C) Analysis of plaque forming units (PFU) produced by HCT116 cells, and by 3 independent freshly isolated CRC tumor cell populations infected either with virions or with ISVPs. HCT116 cells generate virus progeny when infected by virions (40-fold amplification of the input) or by ISVPs (149-fold), but all three CRC populations failed to do so (1.8-fold amplification (virions) and 1.4 fold amplification (ISVPs)). Averages of duplicate samples are shown. The values of the three independently infected freshly isolated CRC populations were pooled and plotted (D). Cell viability analysis showed that only 1 of the 6 successfully infected tumor cell populations showed a temporary loss of cell viability (to 50%) which was rapidly restored following clearance of the virus. The time course of this particular tumor infected with control vehicle, virions, or ISVPs is shown. The rest of the infected tumor cell populations did not show this phenomenon. (E) Tissue fragments from 30 independent colorectal tumors were infected with virions or ISVPs and were analyzed in parallel. Reovirus protein synthesis was observed in none of the fragments analyzed. (F) Reovirus protein synthesis in CRC cultures isolated with or without thermolysin treatment from three distinct CRC tumors and infected with virions or ISVPs, was analyzed by [³⁵S]-methionine labeling and plotted as in (a). Thermolysin treatment did not affect Reovirus protein synthesis. (G) CRC cultures isolated with or without thermolysin treatment from three distinct CRC tumors and infected with virions were tested for their ability to produce infectious virus particles as in (c). Thermolysin treatment did not promote the production of infectious virus particles.

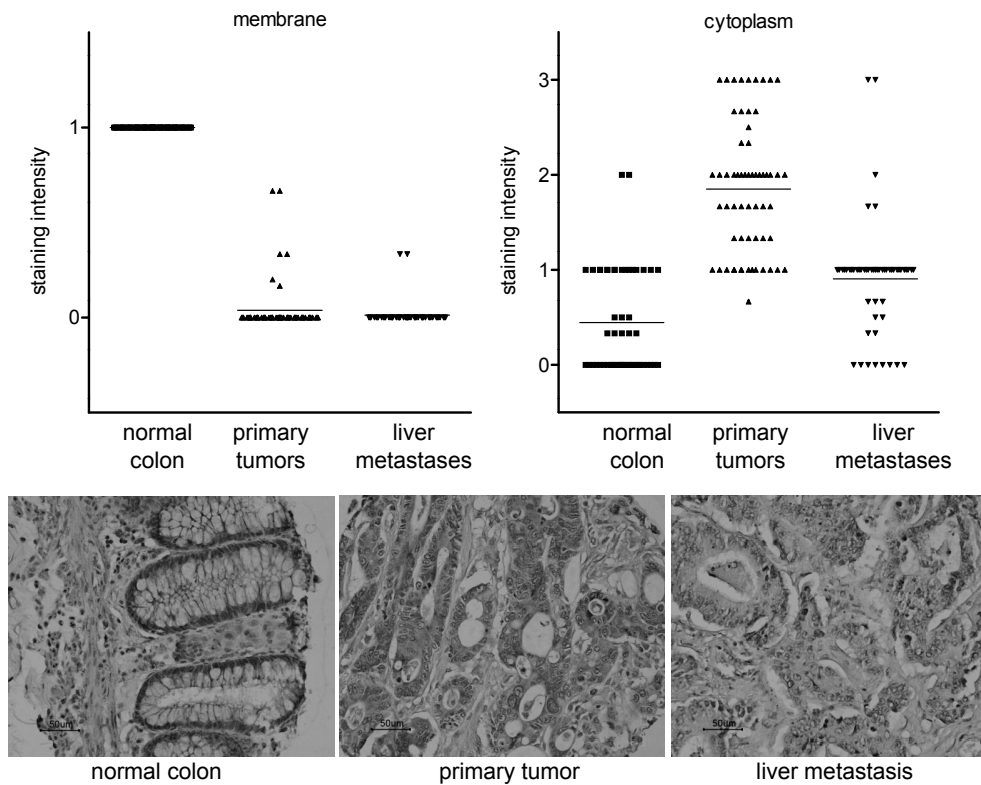


Figure 5. Mislocalization of JAM1 in human colorectal tumors. A paraffin-embedded tissue microarray containing samples of normal human colon, primary colorectal carcinomas and colorectal liver metastases from the same patients was processed for immunohistochemistry using an antibody directed against human JAM1. JAM1 localized to cell-cell contacts in normal human colon, as expected. However, JAM1 in primary human colorectal carcinomas and in liver metastases was not observed at cell-cell contacts, but in the cytoplasm. In addition, the over-all staining intensity in liver metastases was markedly and significantly lower than in the primary tumors ($p < 0.001$). Membrane staining was scored as positive (1) or negative (0). Cytoplasmic staining was scored as 0: no staining, 1: weak staining, 2: moderate staining and 3: strong staining. The average scores of 3 biopsies per tumor were calculated and plotted. See page 196 for color figure

Discussion

Reovirus infects target cells through interaction of the head domain of the attachment protein s1 with JAM1¹⁴. However, our results show that JAM1 is localized in the cytoplasm of colorectal tumor cells. This is in contrast to normal epithelial cells where JAM1 is localized at the cell surface, notably at intercellular tight junctions. At present it is not known to what extent JAM1 contributes to the determination of cell and tissue tropism displayed by Reovirus T3D, and to what extent JAM1 is accessible to Reovirus within tight junctions¹⁸. Nevertheless, JAM1 remains the best characterized Reovirus T3D receptor to date¹⁴. Therefore, further work is needed to establish a functional link between aberrant JAM1 localization and expression in CRC tumors and the resistance of CRC cells to Reovirus infection *in vitro* and *in vivo*. Infection of colorectal tumor cells independently of JAM1 could be established by proteolytic processing of Reovirus virions to ISVPs. The C-terminal head fragment of the s1 viral attachment protein which binds JAM1¹⁴ is released during this process¹⁷, whereas the s1 tail domain, which binds to sialic acid (SA) moieties on cell surface glycoproteins and/or glycolipids^{19;20} is retained. SA binding is likely to be critical in the JAM1-independent infection of tumor cells by ISVPs and, moreover, it is essential for the induction of apoptosis in tumor cells²¹. During the generation of ISVPs the SA-binding capacity, as measured by erythrocyte agglutinating activity, is markedly stimulated¹⁷ and this may explain why ISVPs, but not virions, can infect freshly isolated colorectal tumor cells, although they fail to kill them.

The intestinal epithelium produces a mucinous layer of cell surface sialic acid-rich glycoconjugates which acts as a physical barrier to pathogen invasion. Indeed, most epithelial cells lining the digestive tract are protected from Reovirus infections by the mucus layer and only the M-cells in the Peyer's patches which are devoid of a mucus layer are prone to be infected. Many colorectal tumors retain the capacity to form a mucus layer^{22;23} and this may interfere with the infection of tumor cells by oncolytic viruses like Reovirus T3D²⁴. Interestingly, s1 from Reovirus T3D possesses a latent glycosyl hydrolase activity which is uncovered during the generation of ISVPs. It has been suggested that ISVPs utilize this activity to hydrolyze (part of) the glycosidic portion of the mucus layer to allow infection of otherwise resistant cells.²⁵ It is presently not known how this activity affects binding of Reovirus to SA moieties within the mucus layer. Taken together, we propose that ISVP generation may be a prerequisite for efficient tumor cell infection and oncolysis of colorectal tumors *in vivo*. However, our results also show that even if it is feasible to infect tumor cells with ISVPs, tumor cell killing is prevented by the rapid shutdown of viral protein synthesis. In the series of freshly isolated tumor cell cultures analyzed here, the presence of oncogenic KRAS could not prevent the shutdown of Reovirus protein synthesis. The extracellular matrix and stromal cell populations form an additional physical barrier for viral access to tumor cells that neither virions nor ISVPs can breach.

In conclusion, our results suggest that the infection of colorectal tumor cells in tumor tissue is hindered by at least 3 independent barriers (Figure 6). First, stromal tissue forms a physical barrier between virus particles and tumor cells. Second, tumor cells are resistant to infection by Reovirus virions, possibly due to aberrant JAM1 localization and/or expression. This can be overcome by virion processing into ISVPs. Third, colorectal tumor cells rapidly abort Reovirus protein synthesis and fail to produce infectious virus progeny. The presence of oncogenic KRAS

does not prevent the shutdown of viral protein synthesis, but is more likely to affect the course of a productive infection by facilitating apoptosis induction^{5,6,26}.

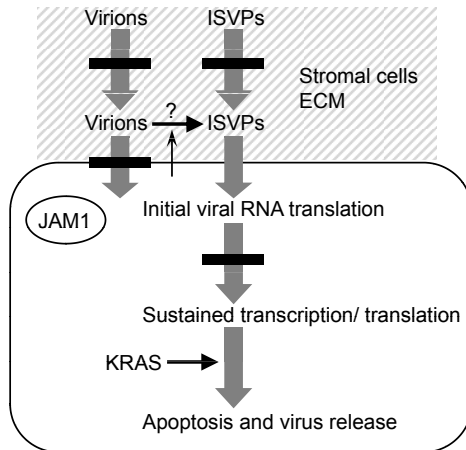


Figure 6. Barriers to successful oncolysis of colorectal tumors by Reovirus T3D. Stromal tissue hinders virus particles (either virions or ISVPs) to reach tumor cells in the context of tumor tissue. Virus particles that do reach tumor cells are incapable of infecting them, possibly as a result of improper JAM1 localization or low expression. Tumors that produce proteases that can process virions to ISVPs, may allow subsequent tumor cell infection. Once infected, colorectal tumor cells rapidly abort Reovirus protein synthesis. The presence of oncogenic KRAS is not sufficient to allow sustained Reovirus protein synthesis. Rather, activated KRAS is more likely to affect the late stages of a productive infection by facilitating apoptosis induction (^{5,6}).

References

1. Brummelkamp TR, Bernards R, Agami R. Stable suppression of tumorigenicity by virus-mediated RNA interference. *Cancer Cell*. 2002;2:243-247.
2. Shirasawa S, Furuse M, Yokoyama N, Sasazuki T. Altered growth of human colon cancer cell lines disrupted at activated Ki-ras. *Science*. 1993;260:85-88.
3. Smakman N, Veenendaal LM, van Diest P, Bos R, Offringa R, Borel Rinkes IH et al. Dual effect of Kras(D12) knockdown on tumorigenesis: increased immune-mediated tumor clearance and abrogation of tumor malignancy. *Oncogene*. 2005;24:8338-8342.
4. Clarke P, Debiase RL, Goody R, Hoyt CC, Richardson-Burns S, Tyler KL. Mechanisms of reovirus-induced cell death and tissue injury: role of apoptosis and virus-induced perturbation of host-cell signaling and transcription factor activation. *Viral Immunol*. 2005;18:89-115.
5. Smakman N, van den Wollenberg DJ, Borel Rinkes IH, Hoebe RC, Kranenburg O. Sensitization to apoptosis underlies KrasD12-dependent oncolysis of murine C26 colorectal carcinoma cells by reovirus T3D. *J Virol*. 2005;79:14981-14985.
6. Smakman N, van den Wollenberg DJ, Elias SG, Sasazuki T, Shirasawa S, Hoebe RC, et al. KRAS(D13) Promotes apoptosis of human colorectal tumor cells by ReovirusT3D and oxaliplatin but not by tumor necrosis factor-related apoptosis-inducing ligand. *Cancer Res*. 2006;66:5403-5408.
7. Strong JE, Coffey MC, Tang D, Sabin P, Lee PW. The molecular basis of viral oncolysis: usurpation of the Ras signaling pathway by reovirus. *EMBO J*. 1998;17:3351-3362.
8. Coffey MC, Strong JE, Forsyth PA, Lee PW. Reovirus therapy of tumors with activated Ras pathway. *Science*. 1998;282:1332-1334.
9. Hirasawa K, Nishikawa SG, Norman KL, Alain T, Kossakowska A, Lee PW. Oncolytic reovirus against ovarian and colon cancer. *Cancer Res*. 2002;62:1696-1701.
10. Hirasawa K, Nishikawa SG, Norman KL, Coffey MC, Thompson BG, Yoon, CS, et al. Systemic reovirus therapy of metastatic cancer in immune-competent mice. *Cancer Res*. 2003;63:348-353.
11. Norman KL, Coffey MC, Hirasawa K, Demetrick DJ, Nishikawa SG, Difrancesco LM et al. Reovirus oncolysis of human breast cancer. *Hum Gene Ther*. 2002;13:641-652.
12. Smakman N, van der Bilt JD, van den Wollenberg DJ, Hoebe RC, Borel Rinkes IH, Kranenburg O. Immunosuppression promotes reovirus therapy of colorectal liver metastases. *Cancer Gene Ther*. 2006;13:815-818.
13. Norman KL, Lee PW. Not all viruses are bad guys: the case for reovirus in cancer therapy. *Drug Discov Today*. 2005;10:847-855.
14. Barton ES, Forrest JC, Connolly JL, Chappell JD, Liu Y, Schnell FJ et al. Junction adhesion molecule is a receptor for reovirus. *Cell*. 2001;104:441-451.
15. Kononen J, Bubendorf L, Kallioniemi A, Barlund M, Schraml P, Leighton S et al. Tissue microarrays for high-throughput molecular profiling of tumor specimens. *Nat Med*. 1998;4:844-847.
16. Perreault N, Jean-Francois B. Use of the dissociating enzyme thermolysin to generate viable human normal intestinal epithelial cell cultures. *Exp Cell Res*. 1996;224:354-364.
17. Nibert ML, Chappell JD, Dermody TS. Infectious subviral particles of reovirus type 3 Dearing exhibit a loss in infectivity and contain a cleaved sigma 1 protein. *J Virol*. 1995;69:5057-5067.
18. Tyler KL, Clarke P, Debiase RL, Kominsky D, Poggioli GJ. Reoviruses and the host cell. *Trends Microbiol*. 2001;9:560-564.
19. Chappell JD, Gunn VL, Wetzell JD, Baer GS, Dermody TS. Mutations in type 3 reovirus that determine binding to sialic acid are contained in the fibrous tail domain of viral attachment protein sigma1. *J Virol*. 1997;71:1834-1841.
20. Chappell JD, Duong JL, Wright BW, Dermody TS. Identification of carbohydrate-binding domains in the attachment proteins of type 1 and type 3 reoviruses. *J Virol*. 2000;74:8472-8479.
21. Connolly JL, Barton ES, Dermody TS. Reovirus binding to cell surface sialic acid potentiates virus-induced apoptosis. *J Virol*. 2001;75:4029-4039.
22. Byrd JC, Bresalier RS. Mucins and mucin binding proteins in colorectal cancer. *Cancer Metastasis Rev*. 2004;23:77-99.

23. Hollingsworth MA, Swanson BJ. Mucins in cancer: protection and control of the cell surface. *Nat Rev Cancer*. 2004;4:45-60.
24. Helander A, Silvey KJ, Mantis NJ, Hutchings AB, Chandran K, Lucas WT et al. The viral sigma1 protein and glycoconjugates containing alpha2-3-linked sialic acid are involved in type 1 reovirus adherence to M cell apical surfaces. *J Virol*. 2003;77:7964-7977.
25. Bisaillon M, Senechal S, Bernier L, Lemay G. A glycosyl hydrolase activity of mammalian reovirus sigma1 protein can contribute to viral infection through a mucus layer. *J Mol Biol*. 1999;286:759-773.
26. Marcato P, Shmulevitz M, Pan D, Stolz D, Lee PW. Ras transformation mediates reovirus oncolysis by enhancing virus uncoating, particle infectivity, and apoptosis-dependent release. *Mol Ther*. 2007;15:1522-1530.

5

Oncogenic KRAS Desensitizes Colorectal Tumor Cells to EGFR Inhibition and Activation

Winan J. van Houdt, Frederik J.H. Hoogwater, Menno T. de Bruijn, Benjamin L. Emmink,
Maarten W. Nijkamp, Danielle A.E. Raats, Petra van der Groep, Paul van Diest,
Inne H.M. Borel Rinkes, and Onno Kranenburg

Neoplasia, 2010 Jun;12(6):443-52

Abstract

EGFR-targeting therapeutics have shown efficacy in the treatment of colorectal cancer (CRC) patients. Clinical studies have revealed that activating mutations in the *KRAS* proto-oncogene predict resistance to EGFR-targeted therapy. However, the causality between mutant *KRAS* and resistance to EGFR inhibition has so far not been demonstrated. Here we show that deletion of the oncogenic *KRAS* allele from colorectal tumor cells re-sensitizes those cells to EGFR inhibitors. Re-sensitization was accompanied by an acquired dependency on the EGFR for maintaining basal ERK activity. Deletion of oncogenic *KRAS* not only re-sensitized tumor cells to EGFR inhibition but also promoted EGF-induced NRAS activation, ERK and AKT phosphorylation, and c-FOS transcription. The poor responsiveness of mutant *KRAS* tumor cells to EGFR inhibition and activation was accompanied by a reduced capacity of these cells to bind and internalize EGF and by a failure to retain EGFR at the plasma membrane. Out of 16 human colorectal tumors with activating mutations in *KRAS*, 15 displayed loss of basolateral EGFR localization. Plasma membrane localization of the EGFR could be restored *in vitro* by suppressing receptor endocytosis through Rho kinase inhibition. This caused an EGFR-dependent increase in basal and EGF-stimulated ERK phosphorylation, but failed to restore tumor cell sensitivity to EGFR inhibition. Our results demonstrate a causal role for oncogenic *KRAS* in desensitizing tumor cells not only to EGFR inhibitors, but also to EGF itself.

Introduction

The epidermal growth factor receptor (EGFR) is widely expressed in the gastrointestinal tract and stimulates proliferation of a range of cell types, including epithelial cells¹. The vast majority of colorectal tumors are initiated by inactivating mutations in the tumor suppressor gene APC². Loss of functional APC is sufficient to initiate the formation of intestinal polyps in mice, and this is accompanied by increased EGFR expression and activity³. Partial loss of EGFR function, or pharmacological inhibition of the EGFR, greatly reduces polyp development in this model⁴. The EGFR is also frequently overexpressed in human colorectal tumors when compared to normal intestinal tissue, and this is associated with increased metastatic potential and poor prognosis⁵⁻⁷. EGFR-targeting therapeutics have shown promising clinical activity in a minority of colorectal cancer patients⁸⁻¹². The presence of activating mutations in the *KRAS* gene in these tumors is a reliable predictor of tumor resistance to anti-EGFR therapy^{13,14}. Conversely, high expression of EGFR ligands predicts response to anti-EGFR therapy, but only in the subset of wildtype *KRAS* tumors^{15,16}. Although these clinical studies have firmly associated activating mutations in *KRAS* with resistance to EGFR-targeted therapy, it has so far not been demonstrated that signalling by the *KRAS* oncoprotein is the underlying cause of resistance to EGFR inhibition. For instance, it is possible that colorectal tumors with *KRAS* mutations preferentially develop in an (epi)genetic background of EGFR-independence. Such EGFR-independence has previously been shown in a minority of tumors that are driven by APC loss only⁴. Constitutive activation of *KRAS* and its downstream signalling pathways may reduce the dependency on upstream activators like the EGFR. However, the EGFR activates multiple distinct mitogenic signalling pathways of which the GRB2/SOS/RAS pathway is only one¹⁷. In addition, activation of the ERK pathway by EGFR ligands is very different in time and amplitude than activation of this pathway by a constitutively active endogenous *KRAS* mutant protein. For those reasons we set out to assess the causal relationship between the presence of endogenous oncogenic *KRAS* and EGFR independence.

Materials and Methods

Cell culture

The colorectal cancer cell lines HCT116, CT26 and DLD1 were purchased from ATCC. The HCT116 cells lacking *KRAS*^{D13} (HKH2) with their own HCT116 control and the DLD1 cells lacking *KRAS*^{D13} (DKO4) with their own DLD1 control were obtained from Dr. Shirasawa and were previously described¹⁸. We previously established CT26 cell lines in which the endogenous *Kras*^{D12} allele is stably suppressed by mutant specific RNA interference, using a lentiviral vector (CT26-KrasKD)¹⁹. Control CT26 cells were transduced with a lentiviral shRNA construct targeting luciferase (see below). All these cell lines were cultured in Dulbecco's Modified Eagle's Medium (DMEM; Dulbecco, ICN Pharmaceuticals) supplemented with 5% (v/v) fetal calf serum, 2 mM glutamine, 0,1 mg/ml streptomycin, and 100 U/ml penicillin. L145 cells were derived directly from a tumor biopsy of a patient operated for colorectal liver metastases in our hospital. The tissue fragment was washed with PBS and was mechanically dissociated. Enzymatic digestion (thermolysin (Sigma) 0.05%; 2hr; 37°C;) was performed in DMEM/F12. Single cell suspensions

were obtained by filtering through a 40- μ m-pore size nylon cell strainer (BD Falcon). Spheroids formed spontaneously by culturing in DMEM/F12 (Gibco) supplemented with 0,6% glucose (BDH Lab. Supplies), 2 mM L-glutamine (Biowhittaker), 9.6 μ g/ml putrescin (Sigma), 6.3 ng/ml progesterone (Sigma), 5.2 ng/ml sodium selenite (Sigma), 25 μ g/ml insulin (Sigma), 100 μ g/ml apotransferrin (Sigma), 5 mM hepes (Gibco), 0,005 μ g/ml trace element A (Cellgro), 0,01 μ g/ml trace element B (Cellgro), 0,01 μ g/ml trace element C (Cellgro), 100 μ M β -mercapto ethanol (Merck), 10 ml antibiotic-antimycotic (Gibco), 4 μ g/ml gentamicine (Invitrogen), 0.002% lipid mixture (Sigma), 5 μ g/ml glutathione (Roche) and 4 μ g/ml Heparin (Sigma). The HIEC cells were a kind gift from Dr. Beaulieu and have been described before ²⁰. All cells were kept at 37°C in a humidified atmosphere containing 5% CO₂.

Antibodies and inhibitors

The following antibodies were from Cell Signaling Technology Inc.: rabbit α nti-phospho-mapk p44/42 (thr 202/tyr 204), rabbit anti-phospho-Akt (ser 473), rabbit anti-EGFR (#2232; used for HCT116 and HKH2 cells) and rabbit anti phospho-EGFR antibodies (tyr 845, 992, 1068, 1045) (#2231, #2234, #2235, #2237). EGFR phosphorylation status was determined by probing the Western blots with a mixture of antibodies 2231, 2234, 2235 and 2237. For EGFR detection in mouse CT26 and CT26-KrasKD cells we used rat anti-mEGFR (Clone 176436; R&D systems). Goat α nti-Akt1 was obtained from Santa Cruz. Secondary peroxidase-conjugated α ntibodies were from Dako.

Gefitinib (Iressa/ZD1839) was kindly provided by AstraZeneca (Macclesfield, United Kingdom). Cetuximab was kindly provided by Merck (Darmstadt, Germany). Erlotinib (Tarceva/OSI1774) was purchased from LC laboratories (Woburn, MA, USA). The MEK inhibitor U0126 was from Promega (Madison, WI, USA), the PI3K inhibitor LY 294002 and the Rac inhibitor Y27632 from Sigma (Saint Louis, MO, USA), and the Rac inhibitor (Rac1-Inh) from Calbiochem (Darmstadt, Germany).

Viability assay

Cells were plated at a density of 5000 cells/well in DMEM containing 5% FCS in 96 wells plates. Cell viability of treated or mock treated cells was then analyzed for 3-6 consecutive days by standard 3-(4,5 dimethylthiazolyl-2)]-2,5-diphenyltetrazoleumbromide (MTT) assays (Roche Diagnostics) according to the manufacturer's instructions.

Analysis of EGF signaling

Cells were plated at day 0 at a density of 200.000 cells/well on 6 wells plates. After overnight incubation in serum free medium, the cells were stimulated with the indicated concentrations of EGF, and were harvested after the indicated periods of stimulation. Western blotting was performed according to standard procedures. Quantity One (Biorad, Hercules, USA) software was used to quantify the signal intensities and ratios between samples loaded on the same gel.

Ras assay

The RAS-binding domain of RAF1 fused to glutathione-S-transferase (GST) and coupled to glutathione-sepharose was used as an affinity matrix for activated RAS. The assay and subsequent Western blotting with isoform-specific antibodies was performed exactly as described ²¹.

RT PCR

Cells were plated at day 0 at a density of $2 \cdot 10^6$ cells on 10 cm disks. After overnight serum-starvation cells were stimulated with EGF and RT-PCR was performed. RNA was isolated using the Trizol method, and cDNA was synthesized by Superscript 2 (Invitrogen). The primers used were: c-FOS forward: 5'-GTCTTCACCACCATGGAG-3' and c-FOS reverse: 5'-CCACCTTCTTGATGTCATC-3', GAPDH forward: 5'-CCTACCCAGCTCTGCTTCAC-3', and GAPDH reverse: 5'-GTGGGAATGAAGTTGGCACT-3'.

Live cell imaging

Cells were seeded in a Lab-Tek® Chambered #1.0 Borosilicate Coverglass System (Nalge Nunc International, Rochester, NY14625, USA) and were mounted on a Zeiss Axiovert 200M microscope for live cell imaging under 5% CO₂ at 37°C overnight. LysoTracker and Alexa-488-labelled EGF (Invitrogen, Molecular Probes, Leiden, The Netherlands) was added to the wells and images were captured every 10 seconds using a Photometrics Coolsnap HQ charged-coupled device (CCD) camera (Scientific, Tucson, AZ). Images were processed using Metamorph software (Universal Imaging, Downingtown, PA).

Immunofluorescence

Cells were grown on glass cover slips and were either stimulated with EGF or were left unstimulated. Cells were fixed by addition of 3.7% formaldehyde to the culture medium for 10 minutes. Cells were then permeabilized with 0.05% Triton X-100 in 1% PBS/BSA. Coverslips were blocked in PBS with 3% BSA for 1 h. Anti-EGFR primary antibodies were incubated at room temperature overnight. Secondary antibodies were incubated for 1 hour at room temperature. Coverslips were mounted using Vectashield with DAPI (H-1200, Vectorlabs). Confocal images were acquired using a Zeiss Meta Axiovert 200M confocal microscope, with a 40X 1,3 N.A. objective.

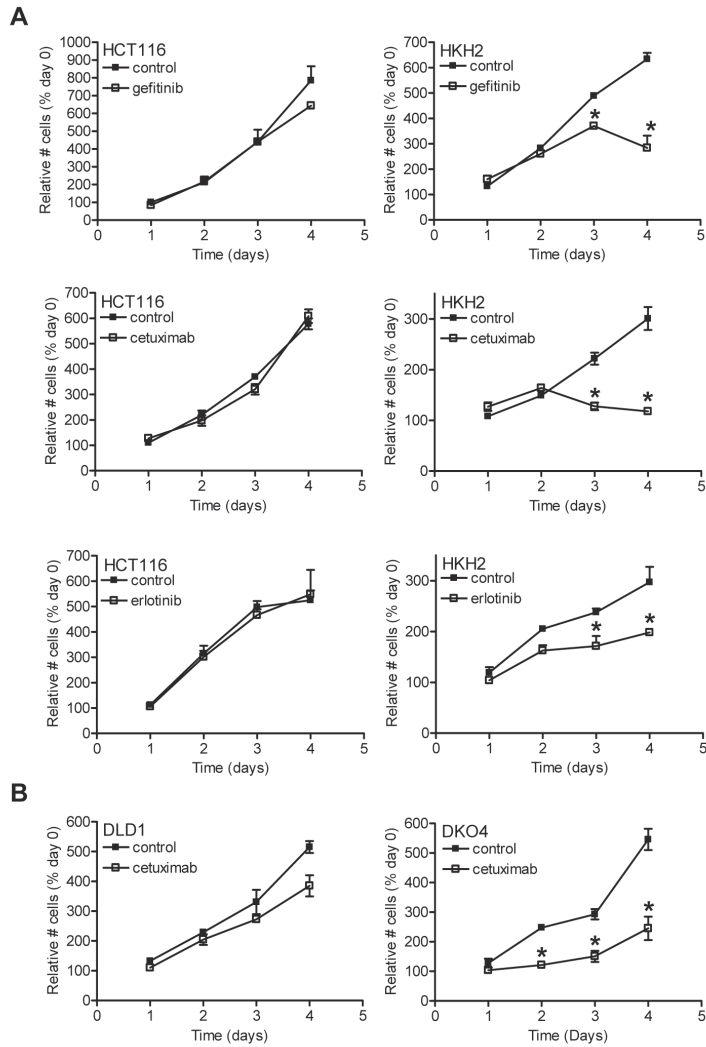
Tissue microarray (TMA)

A tissue microarray (TMA) was used to analyze the expression of EGFR in colorectal tumors. The TMA was constructed as previously described in detail²². In brief, samples from surgical resections of 55 patients with colorectal cancer with known KRAS mutation status were selected for the TMA. For each sample three different cylindrical tissue cores were included in the TMA. Immunostaining was performed using standard procedures. After incubation with 3% hydrogen peroxide, antigen retrieval was achieved by boiling in 10 mM citrate buffer pH 6.0. Sections were blocked with 5% goat serum in TBS and incubated with a rabbit α -EGFR (Cell signaling #2232), at 4°C overnight. The HRP-conjugated secondary antibody (DPVM-55HRP, Immunologic, Duiven, The Netherlands) was detected with 3,3'-diaminobenzidine substrate (D4418, Sigma, Saint Louis, USA). Slides were counterstained with hematoxylin and rinsed with water, dehydrated in ethanol, cleared in xylene and mounted on coverslips. The intensity and localization of EGFR staining and the percentage of positive cells were determined in each separate tissue core by two independent experienced observers blinded to the cores' identities. Staining intensity was scored as follows: 0=negative, 1=weak, 2=moderate, 3=strong, 4=very strong. The percentages of positive cells were categorized as follows: <1 % as 0, 1-25 % as 1, 25-50% as 2, >50% as 3. The staining coefficient was determined as the product of the staining intensity and the percentage category, so with a maximum score of 12. The EGFR antibody was validated by Western blotting using lysates of colorectal cancer cells, and by immunohistochemistry on formalin-fixed paraffin-

embedded sections of normal human colon and skin tissue. The staining and scoring procedure was independently repeated by a third independent observer.

Statistical analysis

Differences between the distinct treatment groups were evaluated using the student's t-test. Asterisks indicate statistical significance, based on two-tailed analyses of the data sets. Differences with p-values <0.05 were considered statistically significant.



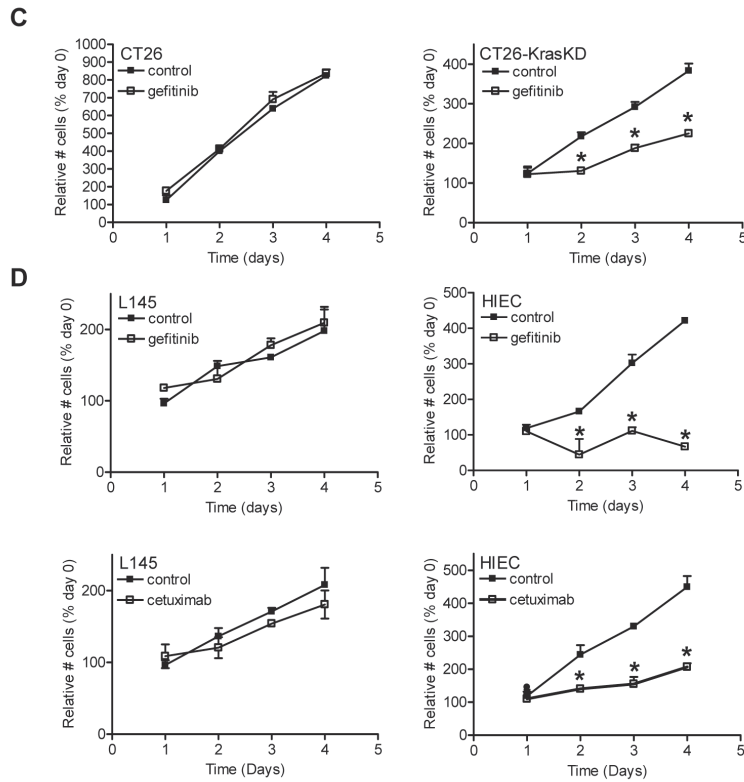


Figure 1. Deletion of oncogenic KRAS sensitizes colorectal tumor cells to EGFR inhibition. (A) HCT116 and HKH2 cells were seeded in 96-well plates and were treated with cetuximab (20 μ g/ml), erlotinib (5 μ M), or gefitinib (2 μ M) for four consecutive days in triplicate. Mitochondrial activity was determined by MTT assays. (B) The experiment was performed as in A, using cetuximab (20 μ g/ml) to treat DLD1 and DKO4 cells. (C) The experiment was performed as in A, using gefitinib (2 μ M) to treat CT26 cells expressing luciferase-targeting shRNA's (CT26) and CT26 cells in which endogenous Kras^{D12} is stably suppressed by RNAi¹⁹. (D) The experiment was performed as in A, using cetuximab (20 μ g/ml) or gefitinib (2 μ M) on L145 cells. L145 cells were freshly established from a liver metastasis harbouring a KRAS^{D12} mutation. Primary human epithelial cells (HIEC; ²⁰) express only wildtype KRAS. *denotes statically significant differences (p<0.05).

Results

Loss of oncogenic KRAS sensitizes tumor cells to EGFR inhibition

To assess the causal relationship between oncogenic KRAS and EGFR independency, we made use of colorectal cancer cell lines with an activating mutation in KRAS (HCT116, DLD1, CT26) and their isogenic derivatives lacking oncogenic KRAS (HKH2, DKO4, CT26-KrasKD)^{18,19}. Treatment of HCT116 and HKH2 cells with the anti-EGFR antibody cetuximab, or with the small molecule inhibitors gefitinib or erlotinib had no effect on parental (KRAS-mutant) HCT116 cells, but strongly reduced cell proliferation of KRAS-wildtype HKH2 cells (Figure 1A). In addition, cetuximab only marginally affected DLD1 cell proliferation, but strongly inhibited DKO4 proliferation (Figure 1B). Likewise, gefitinib had no effect on control CT26 cells, but suppressed cell proliferation upon knockdown of the mutant KRAS allele (Figure 1C). Cetuximab could not be used in this cell system as it does not recognize mouse EGFR. Gefitinib and cetuximab also strongly reduced the proliferation of primary human intestinal epithelial cells (HIECs²⁰) expressing wildtype KRAS. In contrast, neither gefitinib nor cetuximab had any effect on proliferation of freshly isolated colorectal cancer stem cells with an activating mutation in KRAS (L145; KRAS^{D12}) (Figure 1D). In all these cases, the cells expressing mutant KRAS were significantly more resistant to cell growth inhibition by EGFR-targeting therapeutics than their isogenic KRAS-deleted/suppressed counterparts (Supplemental Figure 1). Cell death was not observed in any of the above experiments. These results suggest that oncogenic KRAS is causally involved in reducing tumor cell dependency on EGFR activity.

Oncogenic KRAS reduces EGFR control of ERK phosphorylation

The classical RAS/RAF/MEK/ERK pathway is one of the mitogenic signalling pathways that is activated in response to EGFR stimulation. We first assessed the contribution of EGFR activity to basal levels of ERK phosphorylation. Treatment of cells lacking oncogenic KRAS (HKH2, CT26-KrasKD, HIEC) with either cetuximab or gefitinib caused a strong decrease in the levels of basal ERK phosphorylation, which corresponds with the observed reduction in cell proliferation (Figure 2A-C and Supplemental Figure 1). In contrast, basal ERK phosphorylation was unaffected in tumor cells expressing mutant KRAS (Figure 2A-C). Thus, EGFR is a major determinant of basal ERK phosphorylation in the absence but not in the presence of oncogenic KRAS.

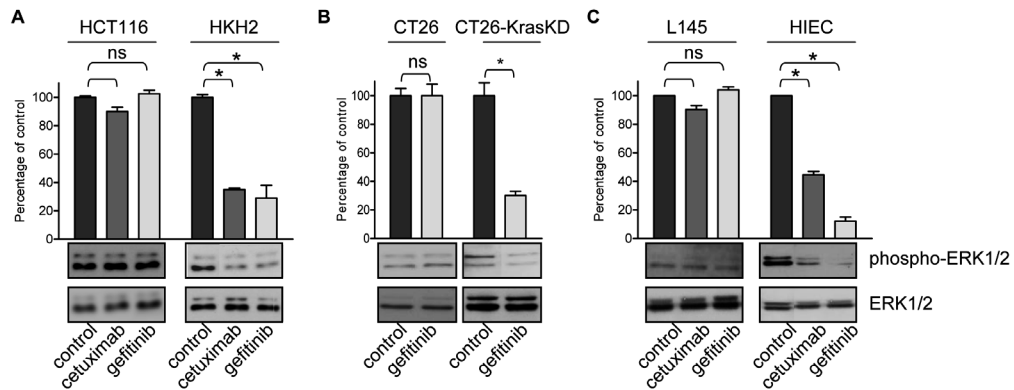


Figure 2. EGFR activity is required for maintenance of ERK phosphorylation in wild type KRAS cells but not in mutant KRAS cells. (A) HCT116 cells and HKH2 cells were treated overnight with the indicated EGFR inhibitors, and phosphorylated and total ERK levels were assessed by Western blotting. Bar diagrams represent means and standard error of the mean (SEM) of 3 independent experiments. (B) As in A, using CT26 cells expressing Luciferase-targeting shRNA's (CT26) and CT26-KrasKD. (C) As in A, using L145 cells and HIEC. *denotes statically significant differences ($p < 0.05$).

EGF stimulation of HCT116 and HKH2 cells showed that the immediate early response gene *c-FOS* was readily induced in HKH2 cells but not in HCT116 cells (Figure 3A). Oncogenic KRAS strongly suppressed EGF-stimulated activation of ERK phosphorylation (Figure 3B). Since NRAS is an efficient activator of the ERK pathway, we examined how oncogenic KRAS affected EGF stimulation of (wildtype) NRAS activity. EGF strongly stimulated NRAS activity in cells expressing wildtype or no KRAS, but not in the parental cells expressing oncogenic KRAS (Figure 3C). This suggests that the desensitizing effect of oncogenic KRAS on EGF-stimulated ERK pathway activation lies upstream of RAS activation. Indeed, receptor-independent ERK pathway activation at the level of RAF by the phorbol ester TPA was unaffected, or even more pronounced, in the presence of oncogenic KRAS (Figure 3D). We conclude that oncogenic KRAS strongly reduces the impact of both EGFR inhibition and activation on ERK phosphorylation.

Next, we tested whether oncogenic KRAS selectively suppressed EGF-stimulated ERK pathway activation, or whether other pathways were suppressed as well. Tyrosine-phosphorylated (activated) EGFR binds the p85 subunit of PI(3)-kinase, which results in activation of AKT. EGF stimulation of KRAS wildtype and mutant cells shows that also this pathway is strongly suppressed by oncogenic KRAS (Figure 3E).

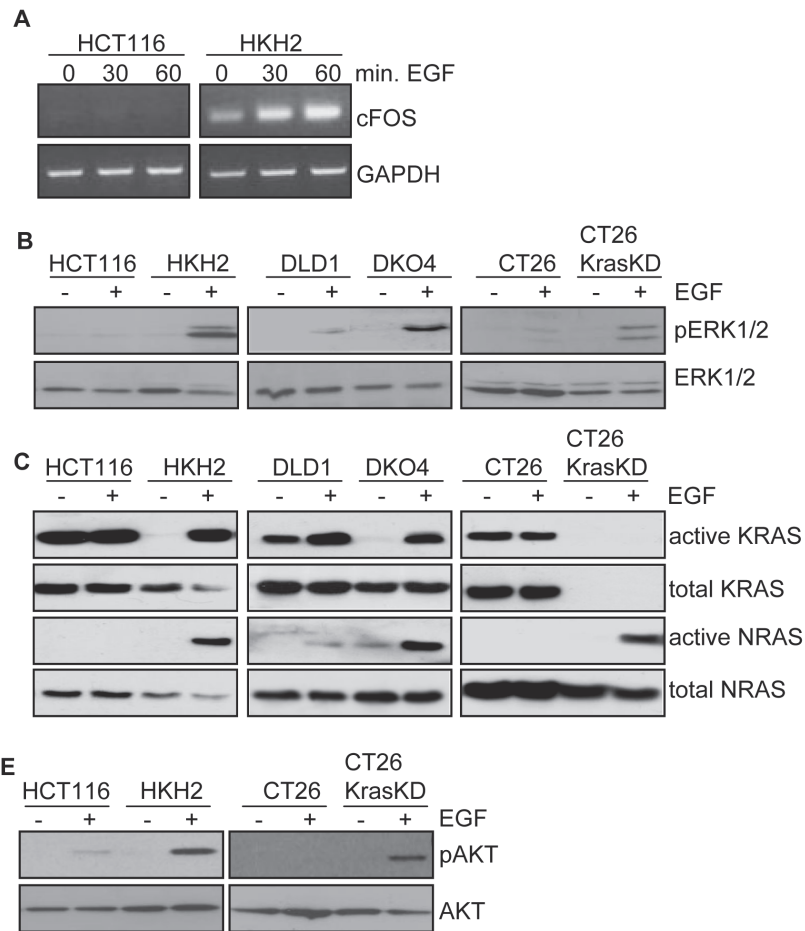


Figure 3. Oncogenic KRAS suppresses EGFR signalling. (A) Serum-starved HCT116 and HKH2 cells were stimulated with 20 ng/ml EGF for 0, 30 and 60 minutes. cFos mRNA levels were determined using RT-PCR. (B) Serum-starved HCT116, DLD1, and CT26 cells and their isogenic derivatives lacking oncogenic KRAS (HKH2, DKO4, CT26-KrasKD) were stimulated with 20 ng/ml EGF for 5 minutes. The levels of phosphorylated and total ERK were determined by Western blotting. (C) Cells were cultured and stimulated as in B. Ras activity assays were performed using the Ras-binding domain (RBD) of Raf1 fused to GST immobilized on glutathione sepharose. Lysates and RBD-Raf1-bound proteins were analyzed for the presence of NRAS and KRAS by Western blotting. (D) Cells were cultured as above and stimulated with the phorbol ester TPA (5 nM) for 5 minutes. The levels of phosphorylated and total ERK were determined by Western blotting. (E) Cells were cultured as above and stimulated with 20 ng/ml EGF for 5 minutes. The levels of phosphorylated and total AKT were determined by Western blotting.

KRAS alters EGFR localization and reduces EGF binding and internalization

The above results suggest that oncogenic KRAS desensitizes cells to EGF at the level of the EGFR. Indeed, basal and EGF-stimulated EGFR phosphorylation was strongly impaired in the presence of oncogenic KRAS (Figure 4A). Live cell imaging using Alexa-488-labelled EGF showed that HKH2 cells readily bound and internalized EGF. A large proportion of EGF ended up in the lysosomes as expected (Figure 4B). In contrast, whereas parental HCT116 cells express EGFR (Fig. 4A), they bound and internalized far less fluorescent EGF, although some internalization could still be observed (Figure 4B). Therefore, we examined the localization of the EGFR by immunofluorescence analysis. Strikingly, in parental HCT116 cells the majority of the EGFR was found in intracellular vesicles (Figure 4C), and its distribution did not change following receptor stimulation (Figure 4D). In HKH2 cells however, the EGFR predominantly localized to the plasma membrane (Figure 4C) and was internalized following stimulation with EGF (Figure 4B, D), or after re-expression of *KRAS*^{G12D}. In line with these results, prolonged stimulation with EGF, or with cetuximab, caused downregulation of the EGFR in cells expressing wildtype KRAS, but not in cell expressing mutant KRAS (Figure 4E). Also in the CT26 cell system we found that suppression of the oncogenic *Kras*^{D12} allele restored plasma membrane localization of the EGFR (Figure 5A). Stimulation of CT26 cells did not affect intracellular localization of the EGFR. However, stimulation of CT26-KrasKD cells caused EGFR clustering and internalization, similar to what was observed in HKH2 cells (Figure 5A). In line with these results, CT26-KrasKD cells, but not CT26 cells, efficiently internalized fluorescent EGF (Figure 5B).

Next, we tested whether the relationship between oncogenic KRAS and altered EGFR localization was also observed in human colorectal tumors. To this end, we analyzed EGFR localization in a panel of 55 colorectal carcinomas with known KRAS mutation status using antibody #2232 from Cell Signalling (Figure 6 and Supplemental Figure 3). Of these tumors, 12 showed normal basolateral EGFR staining, 32 showed diffuse staining throughout the tumor cells, and 11 were negative (Figure 6A,B). In this panel, 16 tumors had an activating mutation in KRAS. Strikingly, only one of these tumors displayed normal basolateral staining, ten displayed diffuse staining and five had lost EGFR staining altogether (Figure 6B). A chi-square test revealed that the unequal distribution of *KRAS* mutations in tumors with basolateral EGFR staining (1/12) versus tumors with either negative or diffuse staining (15/43) showed a trend towards statistical significance ($p=0.073$). This result suggests that KRAS mutations may be associated with loss of normal basolateral EGFR localization in human colorectal tumors, which could influence the responsiveness of these tumors to EGFR ligands.

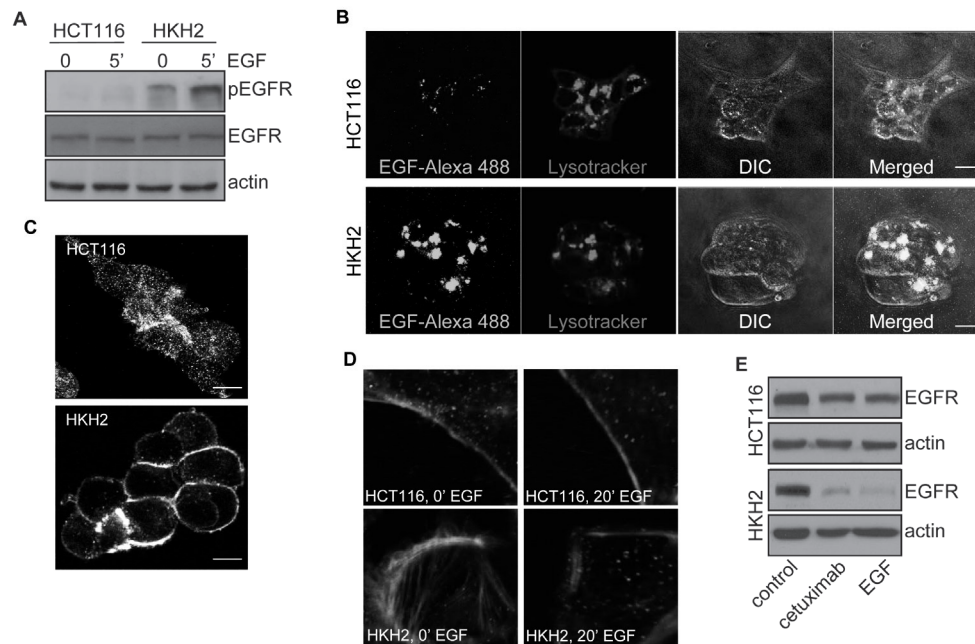


Figure 4. Aberrant EGFR localization and reduced EGF internalization in HCT116 cells. (A) Serum-starved HCT116 and HKH2 cells were stimulated with 20 ng/ml EGF for 0 or 5 minutes. Total and phosphorylated EGFR levels were determined by Western blotting. (B) Serum-starved HCT116 and HKH2 cells were stimulated with Alexa 488-conjugated EGF (30 ng/ml; 20 min) in the presence of lysotracker. The uptake of fluorescent EGF and its trafficking to lysosomes was analyzed by live cell imaging. Final images are shown. (C) HCT116 cells were grown on glass coverslips and EGFR localization was studied by immunofluorescence analysis. (D) Serum-starved HCT116 cells were stimulated with 20 ng/ml EGF (0 or 20 minutes). EGFR (green) and f-actin (red) distribution was then analyzed by immunofluorescence. (E) HCT116 cells were incubated overnight with EGF (20 ng/ml) or cetuximab (20 μ g/ml) under serum-free conditions. EGFR and actin levels were determined by Western blotting. *See page 196 for color figure*

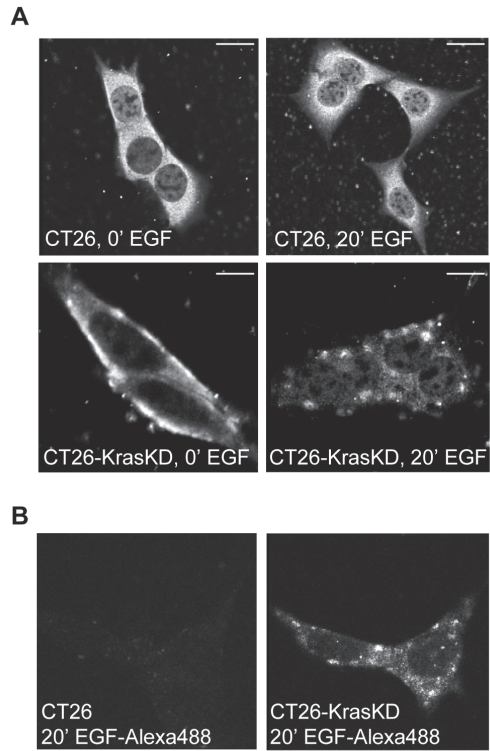


Figure 5. Aberrant EGFR localization and reduced EGF internalization in CT26 cells. (A) CT26 control cells and CT26-KrasKD cells were grown on glass coverslips. Cells were serum-starved overnight and were subsequently stimulated with 20 ng/ml EGF for 20 minutes. Coverslips were then stained for EGFR and were analyzed by immunofluorescence. (B) CT26 and CT26-KrasKD cells were stimulated with Alexa 488-conjugated EGF (30 ng/ml; 20 min). Cells were then fixed and analyzed for the uptake of fluorescent EGF by confocal microscopy.

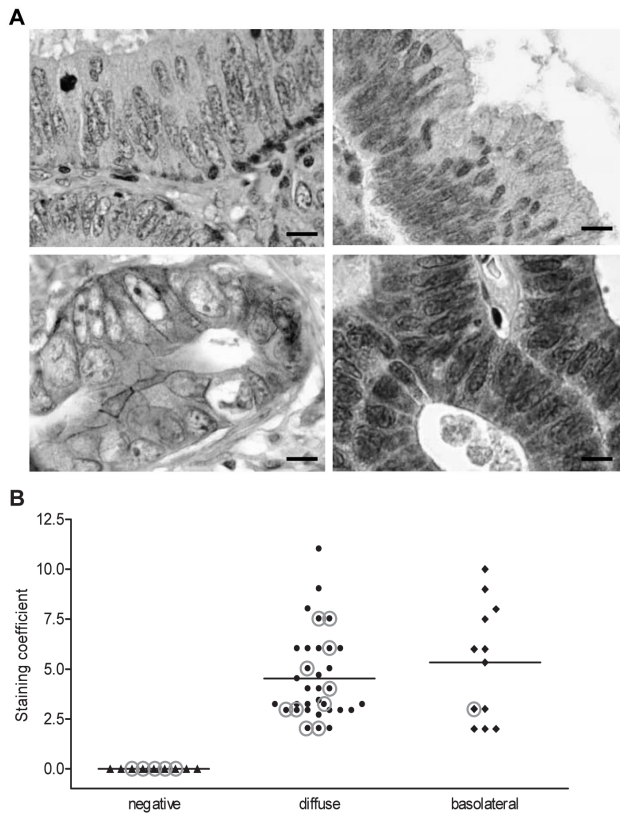


Figure 6. Aberrant localization of the EGFR in colorectal tumors expressing oncogenic KRAS. A tissue microarray containing a panel of colorectal tumors with known KRAS mutation status was used to study EGFR localization. (A) We distinguished three types of staining. 1) Basolateral and membranous; examples are shown in the left upper and lower images. 2) Negative; an example is shown in the right upper image. 3) Diffuse throughout the tumor cells with negative membrane staining; an example is shown in the right lower image. (B) The staining coefficient was determined as the product of the staining intensity on a 0-4 scale (with 0=negative, 1=weak, 2=moderate, 3=strong, 4=very strong) and the percentage positive cells on a 0-3 scale (with <1%=0, 1-25%=1, 25-50%=2, >50%=3). The staining scores for all tumors (with a maximum score of 12) was then plotted. The tumors with activating mutations in KRAS are circled in red. See page 197 for color figure

Rho kinase inhibition restores EGFR plasma membrane localization and EGF signalling, but not EGFR dependency

The above results suggest that desensitization of HCT116 and CT26 cells to EGF could be due to loss of EGFR localization from the plasma membrane. We reasoned that inhibition of KRAS signalling could restore EGFR plasma membrane localization. Therefore, we treated HCT116 cells with inhibitors targeting MEK, Rac, PI(3)K, and Rho kinase (ROK), and evaluated the response of these cells to EGF.

PI(3)kinase or Rac inhibition completely abolished AKT (but not ERK) phosphorylation, but did not sensitize the tumor cells to EGF. Likewise, MEK inhibition abolished ERK (but not AKT) phosphorylation, but did not sensitize the tumor cells to EGF. However, inhibition of ROK sensitized cells to EGF-stimulated phosphorylation of ERK1/2 and AKT, albeit not as efficiently as following deletion of mutant KRAS (Figure 7A,B). ROK inhibition also restored EGF-induced tyrosine phosphorylation of the EGFR (Figure 7C). Furthermore, immunofluorescence analysis showed that the sensitization of HCT116 cells to EGF by ROK inhibition was accompanied by restoration of EGFR localization to the plasma membrane (Figure 7D). Next, we tested whether restoration of EGF signalling in ROK-inhibited cells would be accompanied by a newly acquired dependency on EGFR signalling. To this end, HCT116 cells were treated with cetuximab or gefitinib and the ROK inhibitor Y27632, either alone or in combination. Figure 7E shows that the proliferation of HCT116 cells was not significantly affected by treatment with the drugs, either alone or in combination, even though both the ROK and EGFR inhibitors were effective in inducing and suppressing EGFR-dependent ERK phosphorylation respectively. Next we tested the effect of ROK inhibition on EGF signalling in CT26 cells. In line with the results above, ROK inhibition by Y27632 promoted ERK phosphorylation by EGF (Figure 7F) and restored EGFR plasma membrane localization in CT26 cells (Figure 7G). Also in this cell system Y27632 did not restore tumor cell sensitivity to EGFR inhibition by gefitinib (Figure 7H). Taken together, the results suggest that ROK inhibition restores EGFR plasma membrane localization and EGF signalling, but it does not restore tumor cell-dependency on EGFR activity.

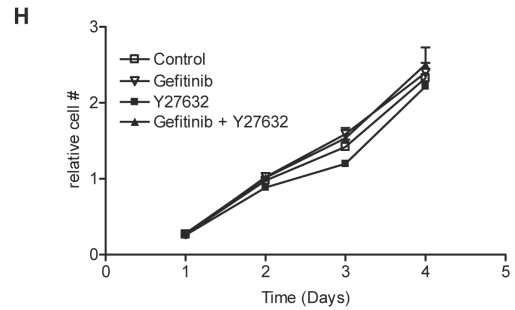
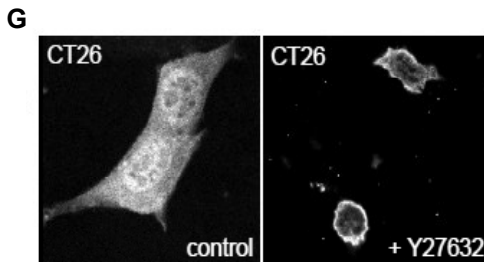
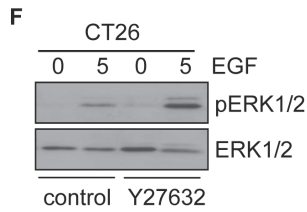
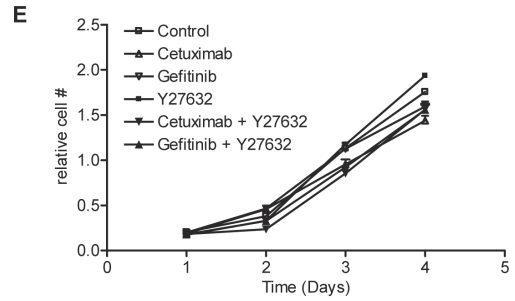
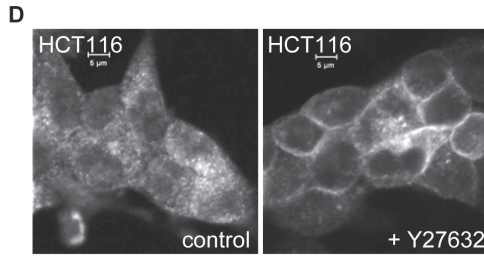
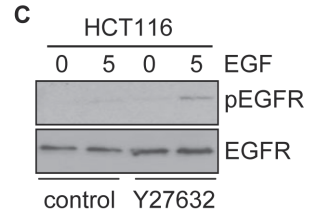
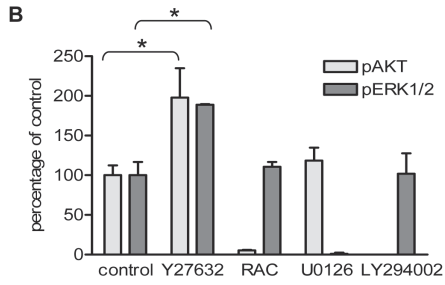
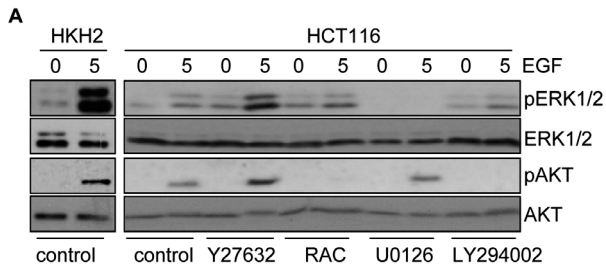


Figure 7. Rho kinase inhibition restores EGFR localization and signalling, but not EGFR dependency. (A) HCT116 cells were serum-starved overnight in the presence of 20 μ M Y27632, 10 mM Rac-inh, 10 μ M U0126 or 10 μ M LY294002, or in the absence of inhibitors (control). HKH2 cells served as a positive control. The cells were then stimulated with 20 ng/ml EGF for 5 minutes (5), or were left unstimulated (0). ERK1/2 and AKT phosphorylation were then determined by Western blotting. (B) The intensities of the pERK1/2 and pAKT signals before and after EGF stimulation were measured using Quantity One software. The percentage of signal intensities (n=3) in treated *versus* untreated cells was then plotted. (C) HCT116 cells were serum-starved overnight in the presence or absence of 20 μ M Y27632. The cells were then stimulated with 20 ng/ml EGF for 5 minutes (5), or were left unstimulated (0). EGFR expression and phosphorylation was determined by Western blotting. (D) HCT116 cells were grown on glass coverslips in the presence or absence 20 μ M Y27632. EGFR localization was then determined by immunofluorescence. (E) HCT116 cells were treated for 4 days with 20 μ g/ml cetuximab or 2 μ M gefitinib either alone or in combination with 20 μ M Y27632. Mitochondrial activity was then assessed by MTT assays. All data points represent means of triplicates \pm SEM. (F) CT26 cells were serum-starved overnight in the presence or absence of 20 μ M Y27632. The cells were then stimulated with 20 ng/ml EGF for 5 minutes (5), or were left unstimulated (0). ERK expression and phosphorylation was then determined by Western blotting. (G) CT26 cells were grown on glass coverslips in the presence or absence 20 μ M Y27632. EGFR localization was then determined by immunofluorescence. (H) CT26 cells were treated for 4 days with 2 μ M gefitinib either alone or in combination with 20 μ M Y27632. Mitochondrial activity was then assessed by MTT assays. All data points represent means of triplicates \pm SEM.

Discussion

The association of KRAS mutations with resistance to EGFR inhibitors has been demonstrated in a large number of clinical studies, both in patients with colorectal cancer and lung cancer¹⁴. Our study shows that oncogenic KRAS is causally involved in mediating resistance to EGFR-targeted therapeutics. Constitutive signalling by oncogenic KRAS may reduce the requirement for EGFR activity as an upstream RAS activator. Although we did not observe reduced basal phosphorylation of the ERK or AKT protein kinases following deletion of oncogenic KRAS, maintenance of the activity of these pathways became dependent on EGFR signalling. This lends support to the hypothesis that KRAS renders cells less dependent on the EGFR for maintaining the activity of these critical signalling pathways, albeit at relatively low basal levels.

Oncogenic KRAS desensitized cells not only to EGFR inhibition, but also to EGFR activation by altering its intracellular localization. EGFR localization, internalization and trafficking is controlled by a complex network of signalling molecules^{23, 24}. Following EGF stimulation, the EGFR is downregulated via ubiquitination and lysosomal degradation. Alternatively, internalized EGFR can recycle back to the plasma membrane, or be retained inside the cell. The reduction in cell surface EGFR in KRAS mutant cells limits its availability to EGF and to EGFR-targeting antibodies. We have so far not been able to identify the KRAS effector pathway(s) that cause(s) altered EGFR localization. Although suppression of ROK signalling partially restored EGFR localization to the plasma membrane and EGF responsiveness, the activity of RhoA or ROK was reduced rather than elevated in mutant KRAS cells when compared to wt KRAS cells (WvH and MdB, unpublished observations). This suggests that basal ROK activity is required for EGFR internalization, but that mutant KRAS does not stimulate this pathway to accelerate EGFR internalization.

RNA interference (ERK1, ERK2, ERK1+ERK2, ARAF, BRAF, CRAF, RalA, RalB) and inhibitor studies (Sorafenib, U0126, LY, Rac1) failed to implicate these classical KRAS effector pathways in desensitizing HCT116 and/or CT26 cells to EGF (WvH, unpublished results). Possibly, a combination of effectors, or subtle alterations in effector protein activity or localization are required for altering EGFR localization, rather than robust changes in expression levels or activity.

From clinical studies it has become clear that wild-type BRAF is required for response to EGFR therapy in metastatic colorectal cancer²⁵. In addition, the Raf/VEGFR inhibitor Sorafenib has been used in combination with EGFR inhibitors in the treatment of several solid malignancies²⁶. The rationale for this was to simultaneously target the tumor cells (EGFR inhibition) and the vasculature (VEGFR inhibition). However, Sorafenib is also a potent RAF kinase inhibitor and RAF kinases are critical KRAS-activated signal transducers in lung cancer cells²⁷. Therefore, it is possible that Sorafenib could sensitize colorectal tumor cells to EGFR inhibition by suppressing KRAS/RAF signalling. Our *in vitro* results do not support such a simple mechanism, since neither Sorafenib treatment, nor RNAi-mediated suppression of RAF kinases could restore tumor cell sensitivity to EGF or EGFR inhibition (WvH unpublished observations). This suggests that other RAS effector pathways and/or a combination of effector pathways mediate KRAS-dependent resistance to EGFR inhibition.

Taken together, mutant KRAS causes intracellular retention of the EGFR which dampens the tumor cell response to EGF. Interestingly, high levels of EGFR ligands predict tumor responsiveness to cetuximab, but only in tumors with wild type KRAS^{28, 29}. Our results suggest that in mutant KRAS

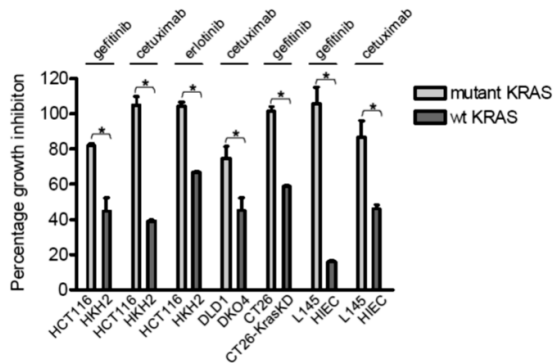
tumors the EGFR is likely to be a relatively inefficient signal transducer due to its absence from the basolateral membrane. We propose that oncogenic KRAS fixes the activation state of its effector pathways at levels that are relatively low when compared to those achieved following EGF stimulation of KRAS wild type cells, but high enough to sustain cell proliferation and viability. EGFR protein levels, as determined by immunohistochemistry, are not associated with the response of colorectal tumors to cetuximab^{30,31}. Our results show that a minor population of human CRC tumors with wildtype KRAS shows proper polarized basal/basolateral localization of the EGFR, similar to what is observed in normal colon tissue. Interestingly, the effect of EGFR activation or inhibition on colorectal cancer cell proliferation was previously shown to be dependent on cell polarity: Only when stimulated or inhibited at the basolateral side does modulation of EGFR activity affect tumor cell proliferation³². Possibly, polarized EGFR staining, rather than total protein levels, may identify a subset of wildtype KRAS tumors that respond to EGFR-targeted therapy. This hypothesis should be tested in the tumors of cetuximab-treated cohorts of colorectal cancer patients.

Restoration of proper EGFR localization and signalling in colorectal cancer cells with oncogenic KRAS is possible (by ROK inhibition) but this does not restore tumor cell dependency on EGFR signalling. EGFR unresponsiveness is therefore uncoupled from EGFR independency. The results suggest that the combination of ROK inhibitors with EGFR inhibitors does not seem to be a logical combination strategy to pursue in the clinic at the moment. Identification of (the combination of) KRAS-activated effector pathways that mediate EGFR independency remains a major challenge for future studies.

References

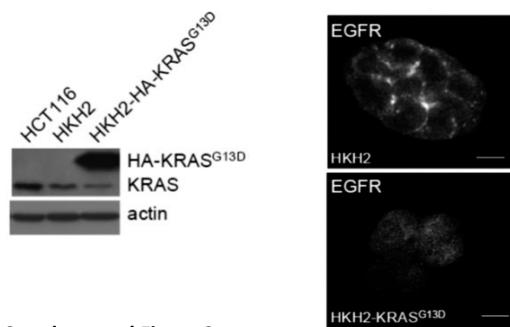
1. Dignass, A.U. & Sturm, A. Peptide growth factors in the intestine. *Eur. J. Gastroenterol. Hepatol.* 13, 763-770 (2001).
2. Kinzler, K.W. & Vogelstein, B. Lessons from hereditary colorectal cancer. *Cell* 87, 159-170 (1996).
3. Moran, A.E. et al. Apc deficiency is associated with increased Egfr activity in the intestinal enterocytes and adenomas of C57BL/6J-Min/+ mice. *J. Biol. Chem.* 279, 43261-43272 (2004).
4. Roberts, R.B. et al. Importance of epidermal growth factor receptor signaling in establishment of adenomas and maintenance of carcinomas during intestinal tumorigenesis. *Proc. Natl. Acad. Sci. U. S. A.* 99, 1521-1526 (2002).
5. Nicholson, R.I., Gee, J.M., & Harper, M.E. EGFR and cancer prognosis. *Eur. J. Cancer* 37 Suppl 4, S9-15 (2001).
6. O'Dwyer, P.J. & Benson, A.B., III Epidermal growth factor receptor-targeted therapy in colorectal cancer. *Semin. Oncol.* 29, 10-17 (2002).
7. Radinsky, R. et al. Level and function of epidermal growth factor receptor predict the metastatic potential of human colon carcinoma cells. *Clin. Cancer Res.* 1, 19-31 (1995).
8. Amado, R.G. et al. Wild-type KRAS is required for panitumumab efficacy in patients with metastatic colorectal cancer. *J. Clin. Oncol.* 26, 1626-1634 (2008).
9. Bokemeyer, C. et al. Fluorouracil, leucovorin, and oxaliplatin with and without cetuximab in the first-line treatment of metastatic colorectal cancer. *J. Clin. Oncol.* 27, 663-671 (2009).
10. De, R.W. et al. KRAS wild-type state predicts survival and is associated to early radiological response in metastatic colorectal cancer treated with cetuximab. *Ann. Oncol.* 19, 508-515 (2008).
11. Karapetis, C.S. et al. K-ras mutations and benefit from cetuximab in advanced colorectal cancer. *N. Engl. J. Med.* 359, 1757-1765 (2008).
12. Van, C.E. et al. Cetuximab and chemotherapy as initial treatment for metastatic colorectal cancer. *N. Engl. J. Med.* 360, 1408-1417 (2009).
13. Allegra, C.J. et al. American Society of Clinical Oncology provisional clinical opinion: testing for KRAS gene mutations in patients with metastatic colorectal carcinoma to predict response to anti-epidermal growth factor receptor monoclonal antibody therapy. *J. Clin. Oncol.* 27, 2091-2096 (2009).
14. Linardou, H. et al. Assessment of somatic k-RAS mutations as a mechanism associated with resistance to EGFR-targeted agents: a systematic review and meta-analysis of studies in advanced non-small-cell lung cancer and metastatic colorectal cancer. *Lancet Oncol.* 9, 962-972 (2008).
15. Jacobs, B. et al. Amphiregulin and epiregulin mRNA expression in primary tumors predicts outcome in metastatic colorectal cancer treated with cetuximab. *J. Clin. Oncol.* 27, 5068-5074 (2009).
16. Khambata-Ford, S. et al. Expression of epiregulin and amphiregulin and K-ras mutation status predict disease control in metastatic colorectal cancer patients treated with cetuximab. *J. Clin. Oncol.* 25, 3230-3237 (2007).
17. Jorissen, R.N. et al. Epidermal growth factor receptor: mechanisms of activation and signalling. *Exp. Cell Res.* 284, 31-53 (2003).
18. Shirasawa, S., Furuse, M., Yokoyama, N., & Sasazuki, T. Altered growth of human colon cancer cell lines disrupted at activated Ki-ras. *Science* 260, 85-88 (1993).
19. Smakman, N. et al. Dual effect of Kras(D12) knockdown on tumorigenesis: increased immune-mediated tumor clearance and abrogation of tumor malignancy. *Oncogene* 24, 8338-8342 (2005).
20. Perreault, N. & Beaulieu, J.F. Primary cultures of fully differentiated and pure human intestinal epithelial cells. *Exp. Cell Res.* 245, 34-42 (1998).
21. Kranenburg, O., Verlaan, I., & Moolenaar, W.H. Regulating c-Ras function. cholesterol depletion affects caveolin association, GTP loading, and signaling. *Curr. Biol.* 11, 1880-1884 (2001).
22. Veenendaal, L.M. et al. Differential Notch and TGFbeta signaling in primary colorectal tumors and their corresponding metastases. *Cell Oncol.* 30, 1-11 (2008).
23. Mosesson, Y., Mills, G.B., & Yarden, Y. Derailed endocytosis: an emerging feature of cancer. *Nat. Rev. Cancer* 8, 835-850 (2008).
24. Sorkin, A. & Goh, L.K. Endocytosis and intracellular trafficking of ErbBs. *Exp. Cell Res.* 315, 683-696 (2009).

25. Di,N.F. et al. Wild-type BRAF is required for response to panitumumab or cetuximab in metastatic colorectal cancer. *J. Clin. Oncol.* 26, 5705-5712 (2008).
26. Quintela-Fandino,M. et al. Phase I combination of sorafenib and erlotinib therapy in solid tumors: safety, pharmacokinetic, and pharmacodynamic evaluation from an expansion cohort. *Mol. Cancer Ther.* 9, 751-760 (2010).
27. Takezawa,K. et al. Sorafenib inhibits non-small cell lung cancer cell growth by targeting B-RAF in KRAS wild-type cells and C-RAF in KRAS mutant cells. *Cancer Res.* 69, 6515-6521 (2009).
28. Jacobs,B. et al. Amphiregulin and epiregulin mRNA expression in primary tumors predicts outcome in metastatic colorectal cancer treated with cetuximab. *J. Clin. Oncol.* 27, 5068-5074 (2009).
29. Khambata-Ford,S. et al. Expression of epiregulin and amphiregulin and K-ras mutation status predict disease control in metastatic colorectal cancer patients treated with cetuximab. *J. Clin. Oncol.* 25, 3230-3237 (2007).
30. Cunningham,D. et al. Cetuximab monotherapy and cetuximab plus irinotecan in irinotecan-refractory metastatic colorectal cancer. *N. Engl. J. Med.* 351, 337-345 (2004).
31. Saltz,L.B. et al. Phase II trial of cetuximab in patients with refractory colorectal cancer that expresses the epidermal growth factor receptor. *J. Clin. Oncol.* 22, 1201-1208 (2004).
32. Damstrup,L. et al. Amphiregulin acts as an autocrine growth factor in two human polarizing colon cancer lines that exhibit domain selective EGF receptor mitogenesis. *Br. J. Cancer* 80, 1012-1019 (1999).



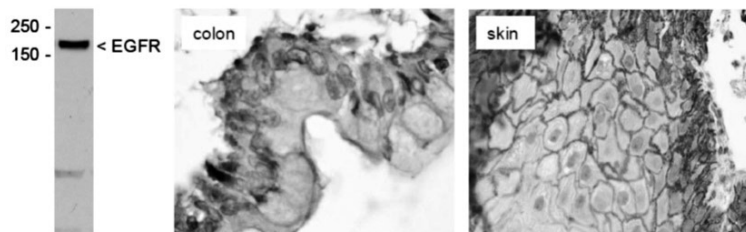
Supplemental Figure 1.

Deletion of oncogenic KRAS allows growth inhibition by EGFR-targeting therapeutics. Cells were treated for 4 days with the indicated compounds (See Figure 1). MTT values of inhibitor-treated cells were then plotted as % of untreated controls. The effect of EGFR inhibition in KRAS mutant cells was minimal (20% at most), while KRAS deletion/suppression allowed growth inhibition in all cases. All differences between isogenic wildtype and mutant KRAS cell lines were statistically significant (* $p < 0.05$).



Supplemental Figure 2.

KRAS^{G13D} expression causes loss of EGFR membrane localization in HKH2 cells. HKH2-KRAS^{G13D} cells and control-transfected HKH2 cells were analyzed by Western blotting for expression of KRAS (upper panel) and for EGFR localization by immunofluorescence analysis using rabbit anti-human EGFR (Cell Signalling #2232) (lower panel).



Supplemental Figure 3.

Validation of anti-EGFR antibody #2232. (A) Western blot analysis of 50 micrograms of a HCT116 cell lysate. (B) Immunohistochemistry of skin and normal colon, showing membrane (skin) and polarized basal (colon) staining. See page 197 for color figure

6

Oncogenic K-ras activates p38 to maintain colorectal cancer cell proliferation during MEK inhibition

Winan J. van Houdt, Menno T. de Bruijn, Danielle Raats, Frederik J.H. Hoogwater, Inne H.M. Borel Rinkes, and Onno Kranenburg

Cellular Oncology, 2010 Jan1;32(4):245-57

Abstract

Background: Colon carcinomas frequently contain activating mutations in the *K-ras* proto-oncogene. *K-ras* itself is a poor drug target and drug development efforts have mostly focused on components of the classical Ras-activated MEK/ERK pathway. Here we have studied whether endogenous oncogenic *K-ras* affects the dependency of colorectal tumor cells on MEK/ERK signaling.

Methods: *K-ras* mutant colorectal tumor cell lines C26, HCT116 and L169 were used. *K-Ras* or components of the MEK/ERK and p38 pathway were suppressed by RNA interference (RNAi). MEK was inhibited by U0126. p38 was inhibited by SB203850.

Results: MEK inhibition, or suppression of MEK1/2 or ERK1/2 by RNA interference, reduced the proliferation rate of all colorectal cancer cell lines. However, cell proliferation returned to normal after two weeks of chronic inhibition, despite the continued suppression of MEK or ERK. In contrast, *K-ras*-suppressed tumor cells entered an irreversible senescent-like state following ERK pathway inhibition. MEK inhibition or ERK1/2 suppression caused activation of p38 α in a *K-ras*-dependent manner. Inhibition or suppression of p38 α prevented the recovery of *K-ras* mutant tumor cells during prolonged MEK inhibition.

Conclusion: Oncogenic *K-Ras* activates p38 α to maintain cell proliferation during MEK inhibition. MEK-targeting therapeutics can create an acquired tumor cell dependency on p38 α .

1. Introduction

Activating mutations in the *KRAS/K-ras* proto-oncogene are found in approximately 40% of colorectal tumors. Deletion or suppression of endogenous oncogenic *Ras* alleles from human and mouse colon tumor cells strongly reduces their tumorigenic potential¹⁻⁴. Efforts to generate effective *Ras* oncoprotein inhibitors have so far remained unsuccessful^{5,6}. *Ras*-activated signaling intermediates may serve as alternative targets for therapy. Indeed, components of the classical *Ras*-activated MEK/ERK pathway, in particular RAF and MEK, have served as targets for the development of novel anti-cancer drugs⁷⁻⁹. MEK inhibitors are especially effective in tumor cells with activating mutations in the *BRAF* oncogene¹⁰. However, tumor cell lines with activating mutations in *KRAS/K-ras* display a highly variable response to MEK inhibitors¹⁰⁻¹⁴. Furthermore, the levels of steady state ERK phosphorylation in these cell lines also vary extensively and do not predict response to MEK inhibition¹⁴. In mice, intestine-specific expression of *K-ras^{D12}* induces hyperplasia which depends on activation of the ERK pathway^{15,16}. However, the ERK pathway is no longer activated in intestinal tumors generated by oncogenic *Kras* in cooperation with mutant APC and these tumors fail to respond to MEK inhibitors^{15,16}. In colon cancer patients, the majority of tumors display elevated levels of phosphorylated ERK and MEK when compared to normal mucosa^{17,18}. Although MEK inhibitors can effectively suppress ERK phosphorylation in human tumors, this does not correlate with robust anti-tumor responses^{19,20}. This demonstrates the existence of resistance mechanisms also in human tumors^{19,20}. The mechanisms underlying resistance to MEK-targeted therapy are incompletely understood. Recent work has shown that activation of the PI(3)-kinase pathway, by activating mutations in *PIK3CA* or inactivating mutations in *PTEN*, is a major cause of tumor cell resistance to MEK inhibitors²¹. The aim of this study was to assess whether tumor cells that are dependent on endogenous *KRAS/K-ras*, also depend on the MEK/ERK pathway. We show that oncogenic *Ras* does not cause addiction to this pathway, but allows tumor cells to recover from its inhibition by activating p38 α . The finding that ERK pathway inhibition can create an acquired dependency on p38 α may have implications for the use of MEK and p38-targeted therapeutics.

2. Materials and Methods

Cell lines

The colorectal cancer cell lines C26 (*Kras^{G12D}*) and HCT116 (*KRAS^{G13D}*) were obtained from ATCC. L145 and L169 were freshly isolated from colorectal liver metastases, and were established as spheroid cultures. Both spheroid populations contain a mutant *KRAS^{G12D}* allele. We previously established C26 cell lines in which the endogenous *K-ras^{D12}* allele is stably suppressed by mutant specific RNA interference, using a lentiviral vector (C26-*KrasKD*)³. Control C26 cells were transduced with a lentiviral shRNA construct targeting luciferase (see below). C26, all its derivatives, and HCT116 cells were cultured in Dulbecco's Modified Eagle's Medium (DMEM; Dulbecco, ICN Pharmaceuticals, Costa Mesa, CA, USA) supplemented with 5% (v/v) fetal calf serum, 2 mM glutamine, 0,1 mg/ml streptomycin, and 100 U/ml penicillin. Human intestinal epithelial cells (HIEC) were kindly provided by Prof JF Beaulieu.

Human colorectal tumor specimens were obtained in accordance with the ethical standards of the institutional committee on human experimentation from patients undergoing a colon or liver resection for metastatic adenocarcinoma. Informed consent was obtained from both patients. The spheroid cells were cultured in advanced DMEM/F12 (Gibco) supplemented with 0,6% glucose (BDH Lab. Supplies), 2 mM L-glutamine (Biowhittaker), 9.6 µg/ml putrescin (Sigma), 6.3 ng/ml progesterone (Sigma), 5.2 ng/ml sodium selenite (Sigma), 25 µg/ml insulin (Sigma), 100 µg/ml apotransferrin (Sigma), 5 mM hepes (Gibco), 0,005 µg/ml trace element A (Cellgro), 0,01 µg/ml trace element B (Cellgro), 0,01 µg/ml trace element C (Cellgro), 100 µM β-mercapto ethanol (Merck), 10 ml antibiotic-antimycotic (Gibco), 4 µg/ml gentamicine (Invitrogen), 0.002% lipid mixture (Sigma), 5 µg/ml glutathione (Roche) and 4 µg/ml Heparin (Sigma). Growth factors (20 ng/ml EGF (Invitrogen) and 10 ng/ml b-FGF (Abcam)) were added to the cell culture medium freshly each week. All cell culture was carried out in non-tissue culture treated flasks (BD Falcon) at 37° C in a 5% CO₂ humidified incubator. Spheroid cultures were maintained in lowadhesion flasks in stem cell medium without serum.

Two-monthly mycoplasma tests confirmed that all experiments were performed in mycoplasma-free cell cultures.

Antibodies and inhibitors

The following antibodies were obtained from Cell Signaling Technology Inc, Danvers, MA, USA: rabbit anti-pERK p44/42 (thr 202/tyr 204), rabbit anti-pAKT (ser 473), rabbit anti-pMEK1/2 (#9121) and the secondary antibody peroxidase conjugated anti-rabbit IgG. The following antibodies were all obtained from Santa Cruz biotechnology, Heidelberg, Germany: rabbit anti-MEK1 (sc219), rabbit antiMEK2 (sc524), rabbit anti-p21 (sc397), mouse anti-cyclin D1 (sc450), goat antiphospho-pRb (sc12901), mouse anti-p53 (sc126), rabbit anti-p16 (sc468), and goat anti-AKT1 (sc1618). Anti-p38a (#9218) and phospho-p38 (T180/T182) (#9211) were from Cell Signalling. Anti-phospho-MPM2 was from Millipore (#05-368). Anti-p27 (#554069) was from BD Biosciences (Alphen aan den Rijn, The Netherlands) and anti-actin (NB 600501) was from Novus Biological (Littleton, CO, USA.) The MEK inhibitor U0126 was from Promega, Madison, WI, USA and the PI3K inhibitor LY 294002 and the p38α/β inhibitor SB203850 were from Sigma, Saint Louis, MO, USA.

Lentiviral constructs

To stably knock down ERK1, ERK2, MEK1 and MEK2 we used short hairpin RNAs (shRNAs) expressed by lentiviral vectors. The ERK1 and ERK2 constructs were kindly provided by Dr. Brambilla and were previously described²². For knockdown of MEK1 and MEK2, we obtained lentiviral constructs from the TRC-library (Open Biosystems, Huntsville, AL, USA). For MEK1 and MEK2 we used the target sets NM_008927 and NM_023138. TRCN0000025214 and TRCN0000055063 produced the most effective MEK1 and MEK2 knock down respectively and were used for all subsequent experiments. For p38 we used the target set NM_011951 of which TRCN0000055223 produced the most effective knock down. The lentiviral construct targeting luciferase (control) harbored the targeting sequence TGACCAGGCATTACAGAAAT. Lentivirus production was performed as described before²³. Lentiviral infection was performed according to the Open Biosystems protocol.

Western blotting

Western blotting was performed as described in ²⁴, using 50 µg of cell lysate.

Proliferation and population doubling assays

Cells were plated at a density of 5000 cells/well in 96-well plates. The relative number of viable cells in each well was then analyzed for 3-6 consecutive days by standard 3-(4,5-dimethylthiazolyl-2)-2,5-diphenyltetrazoleumbromide (MTT) assays (Roche Diagnostics) according to the manufacturer's instructions. All proliferation assays were performed at least two times in triplicate. For population doubling assays the cells were seeded at a density of 50,000 cells/well on 6 wells plates and each well was passed at confluence in a 1:4 dilution (2 population doublings). The inhibitors U0126, LY 294002 and SB were used at a concentration of 10µM, unless stated otherwise. All population doubling experiments were performed at least twice. For measuring growth rates the [# population doublings / # days] was determined for all control and inhibitor-treated cell populations. The mean growth rate in control-treated cell populations was set to 100% and was used to calculate the relative growth rate in inhibitor-treated cell populations.

Statistical analysis

Differences between the distinct treatment groups were evaluated using the student's t-test. Asterisks indicate statistical significance, based on two-tailed analyses of the data sets. Differences with p-values <0.05 were considered statistically significant.

3. Results

Suppression of oncogenic K-ras sensitizes C26 colon tumor cells to MEK/ERK inhibition

First, we tested whether K-ras^{D12}-dependent C26 colon tumor cells ³ are also dependent on MEK/ERK pathway activity. Pharmacologic inhibition of MEK by U0126 reduced the rate of cell proliferation and caused extensive cell flattening (Figure 1A and B left upper and middle panel). U0126-treated C26 cells displayed strongly reduced levels of phosphorylated ERK1 and ERK2 as expected (Figure 1C), and accumulated in G1 with a concomitant reduction in S and M-phase cells (Figure 1D and E). Cell viability was not affected by U0126 treatment (Figure 1B and D). After approximately 2 weeks of chronic MEK inhibition C26 cell proliferation returned to normal and this was accompanied by a partial restoration of the original cell morphology, despite continued suppression of ERK1/2 phosphorylation (Figure 1AC). Strikingly, U0126 treatment of C26 cells in which oncogenic K-ras is suppressed (C26-KrasKD ³) caused extensive cell flattening and a complete loss of cell proliferation from which the cells did not recover (Figure 1A-C). Similarly, U0126 treatment of primary human intestinal epithelial cells caused a lasting growth inhibition from which cells were unable to recover (Supplementary Figure 1).

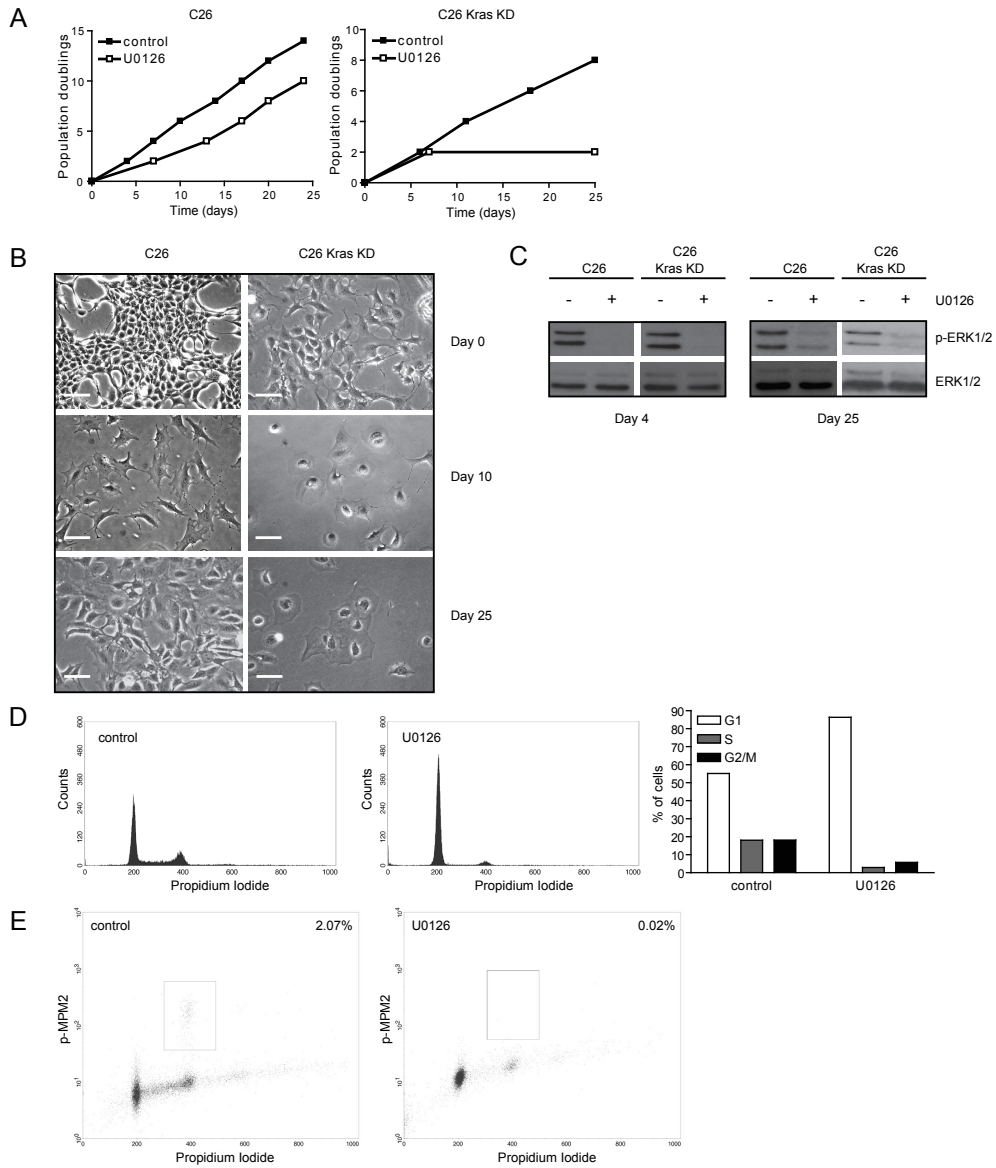


Figure 1. Oncogenic K-ras reduces C26 tumor cell dependency on MEK activity. (A) C26 and C26-KrasKD cells were treated with 10 μ M U0126, which was refreshed every 3 days. Cells were passed 1:4 at confluence so that each passage correlates with 2 population doublings. The graphs show population doublings of control and U0126 treated cells over time. The selective recovery of C26 cells from U0126-mediated growth arrest was observed in four independent experiments. A representative experiment is shown. (B) Photomicrographs showing C26 and C26KrasKD cells (left and right panels) treated with 10 μ M U0126 for three days (middle panels) and 25 days (lower panels). (C) C26 and C26-KrasKD cells were treated as in A

and the phosphorylation of ERK1 and ERK2 was assessed by anti-phosphoERK1/2 Western blot analysis. (D) C26 cells were treated with 10 μ M U0126 for 2 days and the cell cycle profile was assessed by FACS analysis of propidium-iodidestained cells. U0126-induced accumulation of C26 cells in G1 was observed in four independent experiments. A representative experiment is shown. (E) Cells were treated as in D, and the number of mitotic cells was assessed by FACS analysis for phospho-MPM2.

Next we tested whether K-ras suppression would similarly sensitize cells to inhibition of other Ras-effector pathways. To this end, C26 and C26-KrasKD cells were treated with the PI(3)K inhibitor LY294002 and cell proliferation was followed over time. LY294002 reduced the rate of cell proliferation in both cell types to a similar extent (by approximately 30%), without inducing gross alterations in cell morphology and without affecting cell viability (Supplementary Figure 2A and B). The levels of pAKT were stably suppressed in both cell types during the course of the experiment (Supplementary Figure 2C). These results show that endogenous oncogenic K-ras provides resistance to MEK inhibition, but not to PI3K inhibition.

Oncogenic K-ras reduces tumor cell dependency on MEK and ERK

We next assessed the relative importance of MEK1 and MEK2 in maintaining proliferation of tumor cells in the presence or absence of K-ras^{D12}. To this end, expression of either MEK1 or MEK2 was suppressed by using lentiviral RNA interference (RNAi) vectors. Stable knockdown of either MEK1 or MEK2 had no effect on the proliferation of C26 cells (Figure 2A and B). In contrast, knockdown of either MEK1 or MEK2 had a profound and lasting inhibitory effect on the proliferation of K-ras^{D12}-suppressed cells (Figure 2A and B), although the effect was less dramatic than that observed following U0126 treatment (Figure 1A). In both cell types MEK1 and MEK2 expression were successfully and stably suppressed (Figure 2B).

The classical MEK targets are ERK1 and ERK2. Suppression of either kinase by RNA interference had a transient but reproducible inhibitory effect on the proliferation of C26 cells, but cell proliferation returned to normal after approximately two weeks of cell culture (Figure 2C and D). However, ERK1 or ERK2 knockdown had a far more dramatic effect on K-ras^{D12}-suppressed cells, causing profound and long-term inhibition of cell proliferation (Figure 2C and D). Taken together, the results show that endogenous K-ras^{D12} reduces the dependency of C26 cells on MEK and ERK.

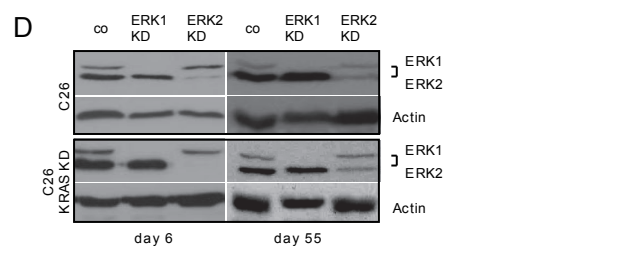
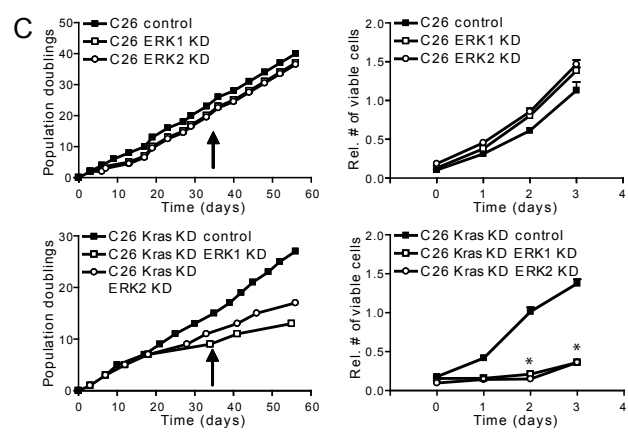
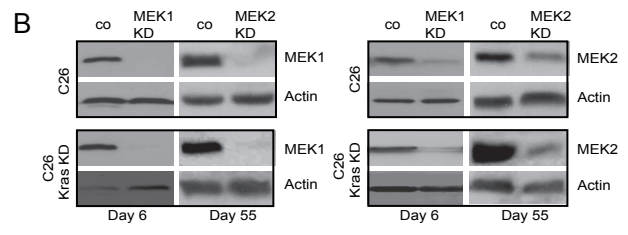
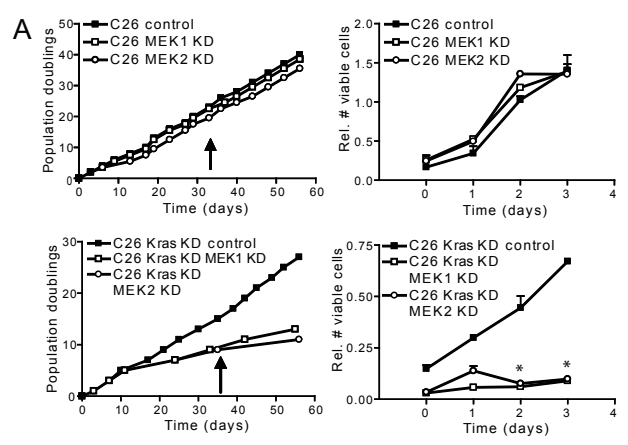


Figure 2. Oncogenic K-ras reduces C26 tumor cell dependency on MEK1&2 and ERK1&2. (A) C26 and C26-KrasKD cells were transduced with lentiviral shRNA constructs targeting MEK1, MEK2 or firefly luciferase (control). After puromycin selection population doubling assays were performed. The selective proliferation-suppressing effect of MEK1 and MEK2 knockdown in the C26-KrasKD cells was observed in four independent experiments. A representative experiment is shown. Short-term mitochondrial activity assays (MTT) were carried out 35 days postselection in triplicate (indicated by the arrow). *indicates statistically significant differences ($p < 0.01$). (B) At the indicated times following puromycin selection cell lysates were prepared and expression of MEK1 and MEK2 were determined by Western blotting. (C) C26 and C26-KrasKD cells were transduced with lentiviral shRNA constructs targeting ERK1, ERK2 or firefly luciferase (control). After puromycin selection population doubling assays were performed. The selective proliferation-suppressing effect of ERK1 and ERK2 knockdown in the C26-KrasKD cells was observed in four independent experiments. A representative experiment is shown. Short-term mitochondrial activity assays (MTT) were carried out 35 days post-selection in triplicate (indicated by the arrow). *indicates statistically significant differences ($p < 0.01$). (D) At the indicated times following puromycin selection cell lysates were prepared and expression of ERK1 and ERK2 were determined by Western blotting.

Oncogenic K-ras prevents senescence induction following ERK silencing

The inhibition of MEK in cells lacking K-ras^{D12} resulted in complete cessation of cell proliferation, but did not induce cell death (Figure 1A). This prompted us to investigate whether the suppression of ERK1 and ERK2 in the absence of K-ras^{D12} would be sufficient to induce senescence. To this end, C26 cells and C26-KrasKD cells were transduced with a combination of the ERK1 and ERK2-targeting RNAi vectors. Combined knockdown of ERK1 and ERK2 induced cell flattening and reduced cell proliferation in C26 cells (Figure 3A-C), similar to U0126 treatment (Figure 1A). Cell proliferation returned to normal after approximately two weeks of cell culture similar to what was observed following treatment with U0126, or after single ERK1 or ERK2 knockdown. However, the combined knockdown of ERK1 and ERK2 in C26-KrasKD cells caused a complete cessation of cell proliferation after a single passage three days after initiation of selection (Figure 3A-C). The cells did not die but obtained a morphology that was reminiscent of the morphology of senescent cells (i.e. large flattened pancake-shaped cells; Figure 3B). An important hallmark of senescent cells is their inability to respond to growth factors. Indeed, EGF-stimulated MEK and AKT phosphorylation in control C26-KrasKD cells, but failed to do so in the senescent-like ERK1/2 knockdown cells (Figure 3D). In addition, the senescence-like cells also displayed loss of cyclin D1 expression and reduced phosphorylation of the retinoblastoma tumor suppressor protein pRb (Figure 3E). Although the cyclinD/cdk4 inhibitor p16 is usually strongly expressed in senescent cells its expression was lost in ERK1/2-suppressed cells, which further implicates ERK1/2 signaling in the control of p16 expression²⁵. The senescence-like cells also displayed activation of the p53 tumor suppressor and its target p21, and of the related cell cycle inhibitor p27 (Figure 3E). Taken together the data show that oncogenic K-ras prevents senescence induction as a result of ERK silencing.

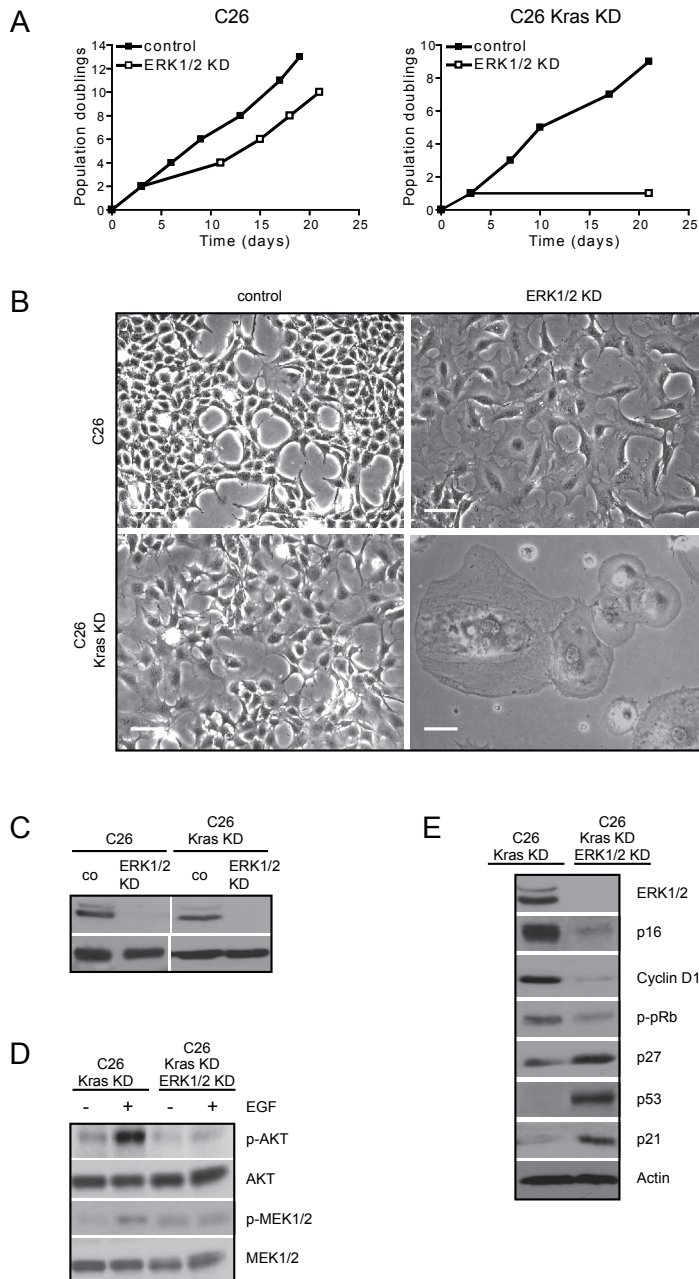


Figure 3. Oncogenic K-ras prevents senescence induction following ERK silencing. (A) C26 and C26-KrasKD cells were transduced with lentiviral shRNA constructs targeting ERK1 plus ERK2 (ERK1/2 KD) or targeting firefly luciferase (control). After puromycin selection population doubling assays were performed. The proliferation of ERK1/2-suppressed C26-KrasKD cells was completely abrogated after a single passage three

days after initiation of selection. The selective proliferation-suppressing effect of ERK1/2 knockdown in the C26-KrasKD cells was observed in four independent experiments. A representative experiment is shown. (B) Photomicrographs of C26 and C26-KrasKD cells fourteen days after targeting luciferase (control) or ERK1/2. Bars 50 μ m. (C) The cells in B were lysed and expression of ERK and ERK2 was assessed by Western blotting using a polyclonal anti-ERK1/ERK2 antibody. (D) Fourteen days after transduction of the control (luciferase) and ERK1/2 targeting shRNA vectors, the cells were stimulated with EGF (20 ng/ml, 3 minutes) and analyzed for AKT and MEK phosphorylation by Western blotting using phospho-specific antibodies. (E) C26-KrasKD control and senescent-like cells were lysed and analyzed for expression of the indicated markers of cell cycle arrest and senescence by Western blotting.

Ras-dependent activation of p38 α allows cell proliferation during ERK suppression

We next tested whether recovery of C26 cells from the U0126-imposed cell cycle arrest was correlated with activation of other MAP kinase pathways. Indeed, we found that MEK inhibition by U0126 or ERK1/2 suppression increased the phosphorylation of p38 α in a K-Ras^{D12}-dependent manner, both in C26 cells and in HCT116 cells (Figure 4). To assess whether p38 α activation was involved in mediating recovery from MEK/ERK inhibition we generated stable p38 α knockdown cells and made use of the p38 inhibitor SB203580. Knockdown of p38 α or treatment with SB203580 had no discernable effect on cell proliferation or on the cell cycle profile of C26 cells (Figure 5A-C). In addition, SB203580 had no effect on long-term proliferation of two additional human colorectal cancer cell lines expressing endogenous oncogenic K-Ras (HCT116 and L169) (Figure 5A). U0126 treatment caused a temporary decrease in the growth rate of all three colorectal cancer cell lines (C26, HCT116, L145) (Figure 5A). However, all three cell types recovered from growth inhibition during chronic exposure to U0126 (Figure 5A). Strikingly, combination treatment with U0126 and the p38 α / β inhibitor SB203580 completely prevented the recovery from U0126-induced growth inhibition in all three cell types (Figure 5A-C). In addition, specific knockdown of p38 α completely prevented recovery from U0126-induced growth inhibition (Figure 5A and B), similar to p38 inhibition by SB203580.

FACS analysis of cell cycle profiles showed that U0126 caused a G1 arrest in C26 cells from which they recovered within 3 weeks (Figure 5C). Recovery was accompanied by the re-appearance of mitotic (p-MPM2-positive) cells in U0126-treated cultures (Figure 5D). Co-treatment of tumor cells with U0126 and SB203580 prevented cell cycle normalization and the appearance of mitotic cells (Figure 5C and 5D). Together, these studies indicate that p38 α plays an important role in the recovery of colorectal cancer cells from U0126-imposed cell cycle arrest.

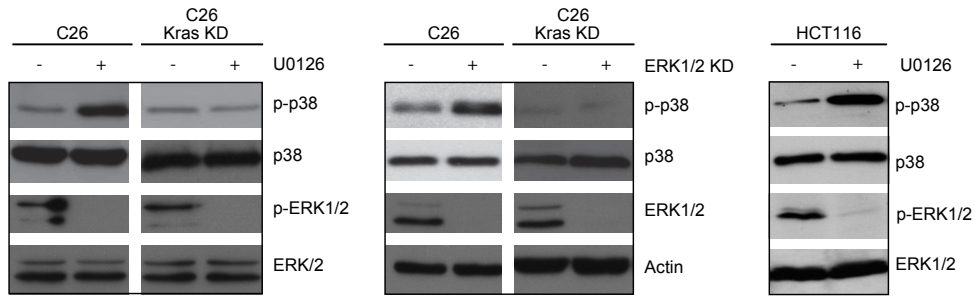
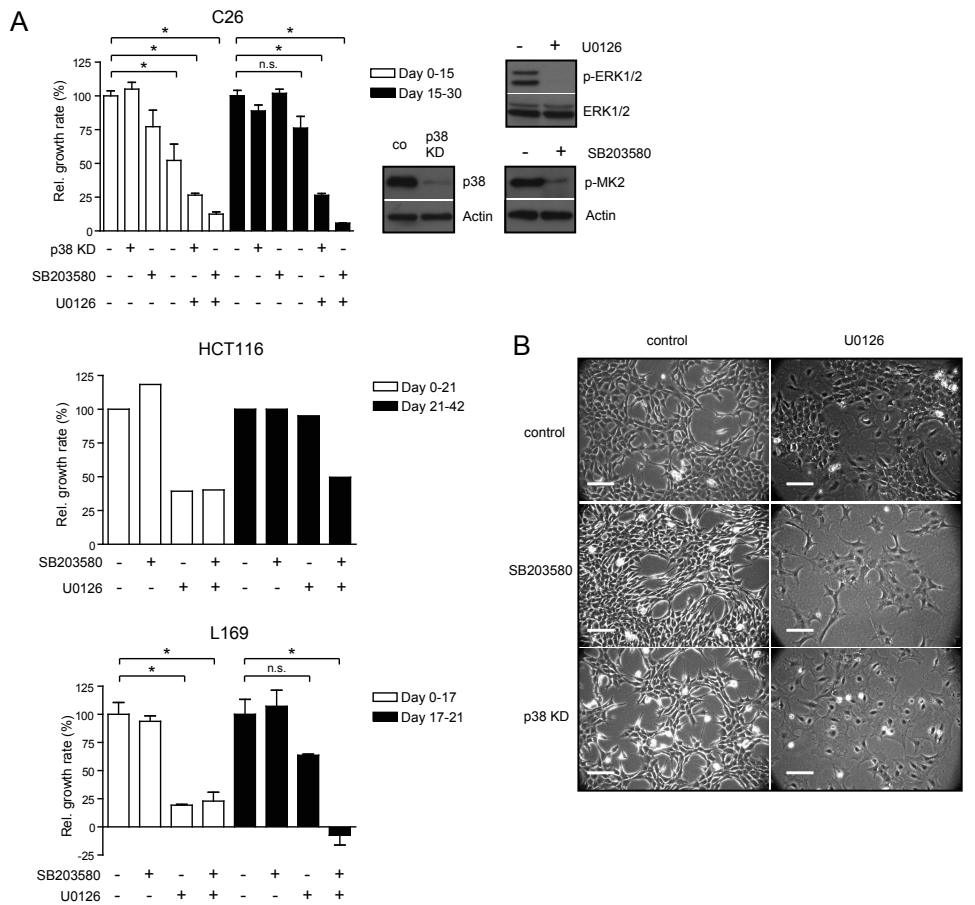
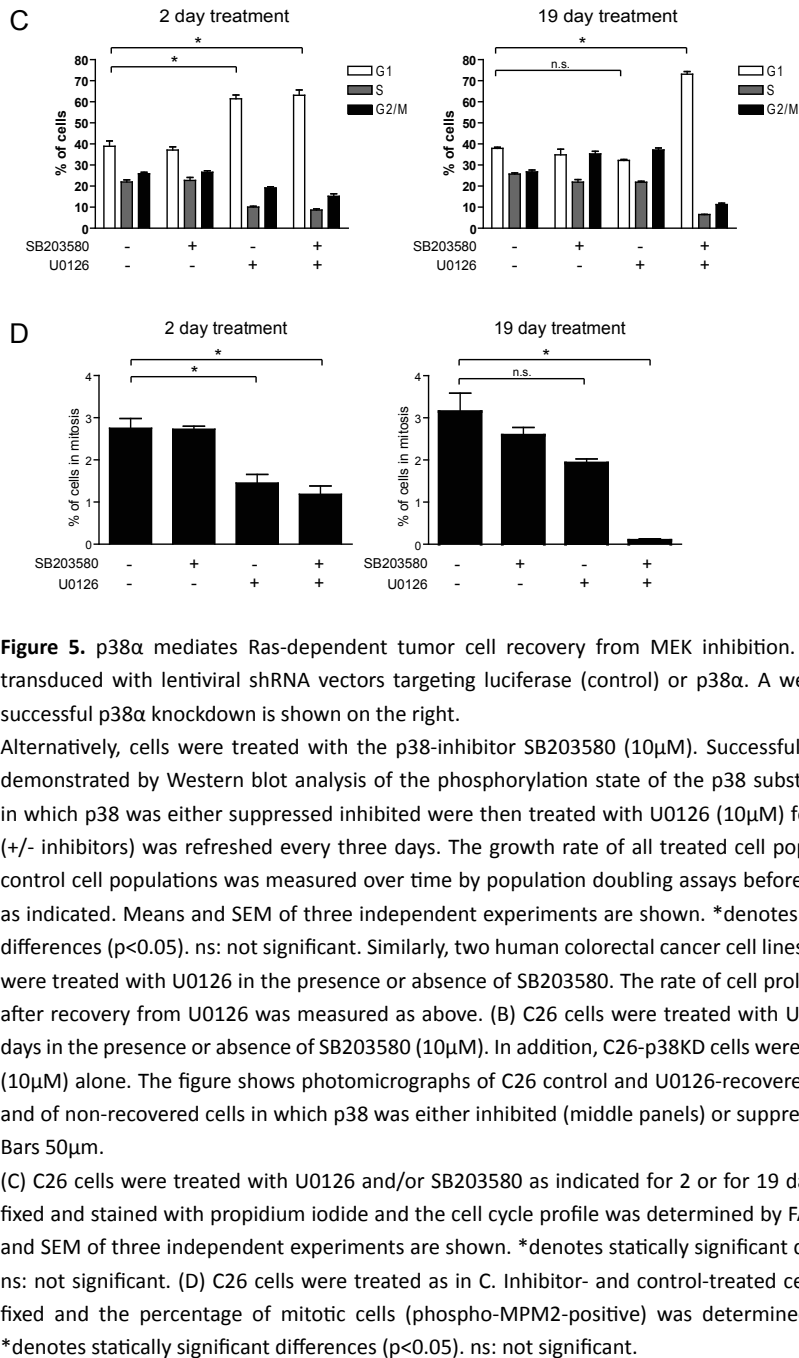


Figure 4. MEK/ERK inhibition causes K-Ras-dependent p38 α phosphorylation. C26, C26-KrasKD and HCT116 cells were treated overnight with U0126 as indicated. Alternatively, C26 and C26-KrasKD cells were transduced with shRNA vectors targeting luciferase (control) or ERK1 and ERK2 (ERK1/2) as indicated. After puromycin selection, cells were lysed and analyzed for the levels of total and phosphorylated p38 α , ERK1 and ERK2. Both experiments were performed three times with similar results.





4. Discussion

Our results show that oncogenic K-ras reduces the dependency of colon tumor cells on ERK pathway activity and that it prevents senescence induction as a result of MEK inhibition. The results from clinical studies so far indicate that treatment of cancer patients with MEK inhibitors can effectively lower the levels of pERK1/2 in different tumor types, including those of colorectal origin, but that this is not clearly correlated with changes in tumor cell proliferation or tumor progression^{19;20}. Tumor cells with oncogenic *Ras* depend on the continued presence of this oncogene for maintaining tumorigenic potential¹⁻⁴. However, its presence does not make tumor cells dependent on MEK/ERK pathway activity, but can even cause resistance to inhibition of this pathway^{13;21}. Identification of the K-ras-activated pathway(s) that desensitize(s) colon tumor cells to ERK pathway inhibition may therefore be the key to effective MEK-targeted therapy. A recent study showed that suppression of the PI(3)K pathway is an important determinant of colorectal tumor cell sensitivity to MEK inhibitors and that its inhibition greatly sensitizes tumor cells with oncogenic *Kras* to MEK inhibition²¹. Our study identifies the p38 α pathway as a second K-ras activated resistance pathway to MEK inhibitors. p38 α was activated as a result of MEK inhibition in a Ras-dependent manner. Furthermore, this was required for recovery from cell cycle arrest and restoration of proliferative capacity in three independent colorectal cancer cell lines. The effect of p38 α on cell cycle inhibition or progression is highly context-dependent²⁶. Most studies indicate that p38 α primarily acts as a tumor suppressor (reviewed in²⁶). The mechanisms of tumor suppression by p38 α may vary under different conditions and in different cell types²⁷⁻²⁹ and include suppression of EGFR signaling^{29;30}, JNK/c-Jun signaling^{28;31} and activation of p53^{27;32}. Indeed, p38 α -suppression caused increased JNK phosphorylation and EGFR signaling in our cells (MdB, unpublished results) but this had no discernable stimulatory effect on tumor cell proliferation. p38 α also plays a role in the G2/M checkpoint that halts cell cycle progression after DNA damage^{33;34}. The latter function of p38 may be less relevant in the context of MEK/ERK suppression which causes accumulation of cells in G1. Furthermore, we did not observe an increased number of cells entering mitosis following inhibition or suppression of p38 α .

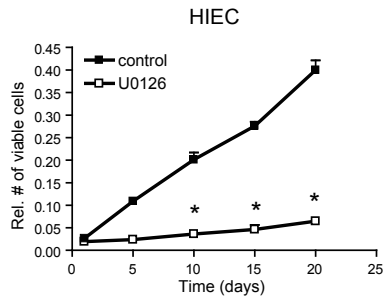
In addition to its tumor-suppressive activity, p38 α can also stimulate cell proliferation. This is mostly observed in established tumor cell lines, for instance by contributing to cyclin D1 and cyclin E expression³⁵⁻⁴¹. In colorectal HT29 cells p38 α contributes to cell proliferation and cyclin E expression³⁵. These authors also demonstrated that p38 α inhibition ultimately caused autophagic cell death in colorectal cancer cell lines and suggested that p38 α could serve as a target for therapy in colorectal cancer³⁵. In addition to p38 α , p38 γ may also promote colorectal tumor cell proliferation, as its inhibition reduced cell proliferation in HCT116 cells⁴². However, p38 γ is insensitive to SB203580 and its expression requires ERK pathway activity⁴², suggesting that it does not play a role during recovery from MEK inhibition.

Future research should elucidate under which (stressed) circumstances colorectal tumor cells come to rely on p38 α . The results presented here suggest that ERK inhibition can induce an acquired dependency on p38 α , which offers a possibility for therapeutic exploitation.

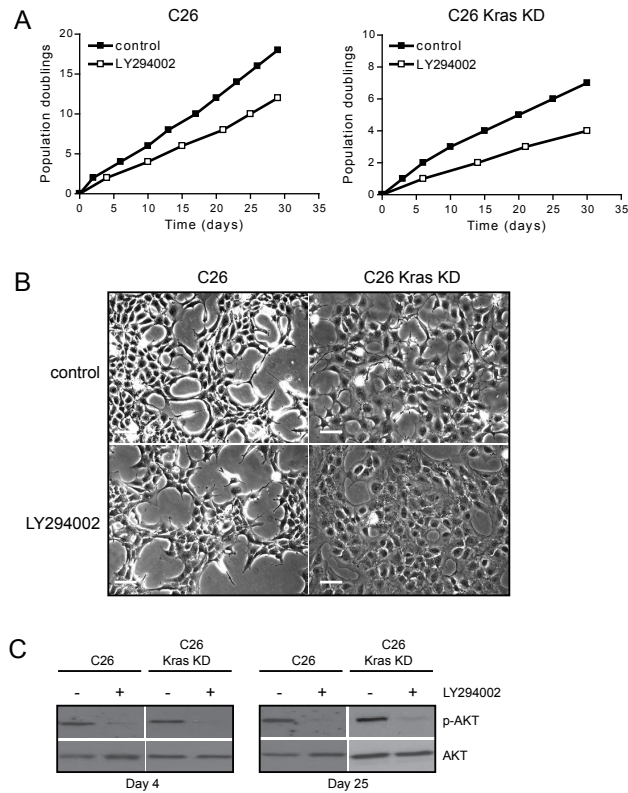
References

1. T.R.Brummelkamp, R.Bernards, and R.Agami, Stable suppression of tumorigenicity by virus-mediated RNA interference. *Cancer Cell* 2 (2002) 243-247.
2. S.Shirasawa, M.Furuse, N.Yokoyama, and T.Sasazuki, Altered growth of human colon cancer cell lines disrupted at activated Ki-ras. *Science* 260 (1993) 85-88.
3. N.Smakman, L.M.Veenendaal, P.van Diest, R.Bos, R.Offringa, R.Borel, I, and O.Kranenburg, Dual effect of Kras(D12) knockdown on tumorigenesis: increased immune-mediated tumor clearance and abrogation of tumor malignancy. *Oncogene* 24 (2005) 8338-8342.
4. T.Tokunaga, T.Tsuchida, H.Kijima, K.Okamoto, Y.Oshika, N.Sawa, Y.Ohnishi, H.Yamazaki, S.Miura, Y.Ueyama, and M.Nakamura, Ribozymemediated inactivation of mutant K-ras oncogene in a colon cancer cell line. *Br.J.Cancer* 83 (2000) 833-839.
5. J.Downward, Targeting RAS signalling pathways in cancer therapy. *Nat.Rev.Cancer* 3 (2003) 11-22.
6. B.B.Friday and A.A.Adjei, K-ras as a target for cancer therapy. *Biochim.Biophys.Acta* 1756 (2005) 127-144.
7. B.B.Friday and A.A.Adjei, Advances in targeting the Ras/Raf/MEK/Erkmitogen-activated protein kinase cascade with MEK inhibitors for cancertherapy. *Clin.Cancer Res.* 14 (2008) 342-346.
8. P.J.Roberts and C.J.Der, Targeting the Raf-MEK-ERK mitogen-activated protein kinase cascade for the treatment of cancer. *Oncogene* 26 (2007) 3291-3310.
9. J.S.Sebolt-Leopold, Advances in the development of cancer therapeutics directed against the RAS-mitogen-activated protein kinase pathway. *Clin.Cancer Res.* 14 (2008) 3651-3656.
10. D.B.Solit, L.A.Garraway, C.A.Pratilas, A.Sawai, G.Getz, A.Basso, Q.Ye, J.M.Lobo, Y.She, I.Osman, T.R.Golub, J.Sebolt-Leopold, W.R.Sellers, and N.Rosen, BRAF mutation predicts sensitivity to MEK inhibition. *Nature* 439 (2006) 358-362.
11. B.R.Davies, A.Logie, J.S.McKay, P.Martin, S.Steele, R.Jenkins, M.Cockerill, S.Cartlidge, and P.D.Smith, AZD6244 (ARRY-142886), a potent inhibitor of mitogen-activated protein kinase/extracellular signal-regulated kinase 1/2 kinases: mechanism of action in vivo, pharmacokinetic/pharmacodynamic relationship, and potential for combination in preclinical models. *Mol.Cancer Ther.* 6 (2007) 2209-2219.
12. G.Pohl, C.L.Ho, R.J.Kurman, R.Bristow, T.L.Wang, and I.Shih, Inactivation of the mitogen-activated protein kinase pathway as a potential target-based therapy in ovarian serous tumors with KRAS or BRAF mutations. *Cancer Res.* 65 (2005) 1994-2000.
13. Y.Wang, B.K.Van, P.Jiang, S.Przybranowski, C.Omer, and J.Sebolt-Leopold, A role for K-ras in conferring resistance to the MEK inhibitor, CI-1040. *Neoplasia.* 7 (2005) 336-347.
14. J.J.Yeh, E.D.Routh, T.Rubinas, J.Peacock, T.D.Martin, X.J.Shen, R.S.Sandler, H.J.Kim, T.O.Keku, and C.J.Der, KRAS/BRAF mutation status and ERK1/2 activation as biomarkers for MEK1/2 inhibitor therapy in colorectal cancer. *Mol.Cancer Ther.* 8 (2009) 834-843.
15. K.M.Haigis, K.R.Kendall, Y.Wang, A.Cheung, M.C.Haigis, J.N.Glickman, M.Niwa-Kawakita, A.Sweet-Cordero, J.Sebolt-Leopold, K.M.Shannon, J.Settleman, M.Giovannini, and T.Jacks, Differential effects of oncogenic K-Ras and N-Ras on proliferation, differentiation and tumor progression in the colon. *Nat. Genet.* 40 (2008) 600-608.
16. D.A.Tuveson, A.T.Shaw, N.A.Willis, D.P.Silver, E.L.Jackson, S.Chang, K.L.Mercer, R.Grochow, H.Hock, D.Crowley, S.R.Hingorani, T.Zaks, C.King, M.A.Jacobetz, L.Wang, R.T.Bronson, S.H.Orkin, R.A.Depinho, and T.Jacks, Endogenous oncogenic K-ras(G12D) stimulates proliferation and widespread neoplastic and developmental defects. *Cancer Cell* 5 (2004) 375-387.
17. R.Hoshino, Y.Chatani, T.Yamori, T.Tsuruo, H.Oka, O.Yoshida, Y.Shimada, Ari-i S, H.Wada, J.Fujimoto, and M.Kohno, Constitutive activation of the 41/43-kDa mitogen-activated protein kinase signaling pathway in human tumors. *Oncogene* 18 (1999) 813-822.
18. S.H.Lee, J.W.Lee, Y.H.Soung, S.Y.Kim, S.W.Nam, W.S.Park, S.H.Kim, N.J.Yoo, and J.Y.Lee, Colorectal tumors frequently express phosphorylated mitogen-activated protein kinase. *APMIS* 112 (2004) 233-238.
19. A.A.Adjei, R.B.Cohen, W.Franklin, C.Morris, D.Wilson, J.R.Molina, L.J.Hanson, L.Gore, L.Chow, S.Leong, L.Maloney, G.Gordon, H.Simmons, A.Marlow, K.Litwiler, S.Brown, G.Poch, K.Kane, J.Haney, and S.G.Eckhardt, Phase I pharmacokinetic and pharmacodynamic study of the oral, smallmolecule mitogen-activated protein kinase kinase 1/2 inhibitor AZD6244 (ARRY-142886) in patients with advanced cancers. *J.Clin.Oncol.* 26 (2008) 2139-2146.

20. J.Rinehart, A.A.Adjei, P.M.Lorusso, D.Waterhouse, J.R.Hecht, R.B.Natale, O.Hamid, M.Varterasian, P.Asbury, E.P.Kaldjian, S.Gulyas, D.Y.Mitchell, R.Herrera, J.S.Sebolt-Leopold, and M.B.Meyer, Multicenter phase II study of the oral MEK inhibitor, CI-1040, in patients with advanced non-small-cell lung, breast, colon, and pancreatic cancer. *J.Clin.Oncol.* 22 (2004) 4456-4462.
21. S.Wee, Z.Jagani, K.X.Xiang, A.Loo, M.Dorsch, Y.M.Yao, W.R.Sellers, C.Lengauer, and F.Stegmeier, PI3K Pathway Activation Mediates Resistance to MEK Inhibitors in KRAS Mutant Cancers. *Cancer Res.* 2009.
22. C.Vantaggiato, I.Formentini, A.Bondanza, C.Bonini, L.Naldini, and R.Brambilla, ERK1 and ERK2 mitogen-activated protein kinases affect Rasdependent cell signaling differentially. *J.Biol.* 5 (2006) 14.
23. N.Smakman, A.Martens, O.Kranenburg, and R.Borel, I, Validation of bioluminescence imaging of colorectal liver metastases in the mouse. *J.Surg.Res.* 122 (2004) 225-230.
24. O.Kranenburg, I.Verlaan, and W.H.Moolenaar, Regulating c-Ras function. cholesterol depletion affects caveolin association, GTP loading, and signaling. *Curr.Biol.* 11 (2001) 1880-1884.
25. A.W.Lin, M.Barradas, J.C.Stone, A.L.van, M.Serrano, and S.W.Lowe, Premature senescence involving p53 and p16 is activated in response to constitutive MEK/MAPK mitogenic signaling. *Genes Dev.* 12 (1998) 30083019.
26. E.F.Wagner and A.R.Nebreda, Signal integration by JNK and p38 MAPK pathways in cancer development. *Nat.Rev.Cancer* 9 (2009) 537-549.
27. D.V.Bulavin and A.J.Fornace, Jr., p38 MAP kinase's emerging role as a tumor suppressor. *Adv.Cancer Res.* 92 (2004) 95-118.
28. L.Hui, L.Bakiri, E.Stepniak, and E.F.Wagner, p38alpha: a suppressor of cell proliferation and tumorigenesis. *Cell Cycle* 6 (2007) 2429-2433.
29. K.Pruitt, W.M.Pruitt, G.K.Bilter, J.K.Westwick, and C.J.Der, Raf-independent deregulation of p38 and JNK mitogen-activated protein kinases are critical for Ras transformation. *J.Biol.Chem.* 277 (2002) 31808-31817.
30. Y.Zwang and Y.Yarden, p38 MAP kinase mediates stress-induced internalization of EGFR: implications for cancer chemotherapy. *EMBO J.* 25 (2006) 4195-4206.
31. L.Hui, L.Bakiri, A.Mairhorfer, N.Schweifer, C.Haslinger, L.Kenner, V.Komnenovic, H.Scheuch, H.Beug, and E.F.Wagner, p38alpha suppresses normal and cancer cell proliferation by antagonizing the JNK-c-Jun pathway. *Nat.Genet.* 39 (2007) 741-749.
32. J.Han and P.Sun, The pathways to tumor suppression via route p38. *Trends Biochem.Sci.* 32 (2007) 364-371.
33. D.V.Bulavin, S.A.Amundson, and A.J.Fornace, p38 and Chk1 kinases: different conductors for the G(2)/M checkpoint symphony. *Curr.Opin.Genet.Dev.* 12 (2002) 92-97.
34. A.Mikhailov, M.Shinohara, and C.L.Rieder, The p38-mediated stressactivated checkpoint. A rapid response system for delaying progression through antephasis and entry into mitosis. *Cell Cycle* 4 (2005) 57-62.
35. F.Comes, A.Matrone, P.Lastella, B.Nico, F.C.Susca, R.Bagnulo, G.Ingravallo, S.Modica, S.G.Lo, A.Moschetta, G.Guanti, and C.Simone, A novel cell typespecific role of p38alpha in the control of autophagy and cell death in colorectal cancer cells. *Cell Death.Differ.* 14 (2007) 693-702.
36. L.Fan, X.Yang, J.Du, M.Marshall, K.Blanchard, and X.Ye, A novel role of p38 alpha MAPK in mitotic progression independent of its kinase activity. *Cell Cycle* 4 (2005) 1616-1624.
37. D.Halawani, R.Mondeh, L.A.Stanton, and F.Beier, p38 MAP kinase signaling is necessary for rat chondrosarcoma cell proliferation. *Oncogene* 23 (2004) 3726-3731.
38. R.J.Lee, C.Albanese, R.J.Stenger, G.Watanabe, G.Inghirami, G.K.Haines, III, M.Webster, W.J.Muller, J.S.Brugge, R.J.Davis, and R.G.Pestell, pp60(v-src) induction of cyclin D1 requires collaborative interactions between the extracellular signal-regulated kinase, p38, and Jun kinase pathways. A role for cAMP response element-binding protein and activating transcription factor-2 in pp60(v-src) signaling in breast cancer cells. *J.Biol.Chem.* 274 (1999) 7341-7350.
39. L.C.Plataniias, Map kinase signaling pathways and hematologic malignancies. *Blood* 101 (2003) 4667-4679.
40. J.A.Recio and G.Merlino, Hepatocyte growth factor/scatter factor activates proliferation in melanoma cells through p38 MAPK, ATF-2 and cyclin D1. *Oncogene* 21 (2002) 1000-1008.
41. M.Ricote, I.Garcia-Tunon, F.Bethencourt, B.Fraile, P.Onsurbe, R.Paniagua, and M.Royuela, The p38 transduction pathway in prostatic neoplasia. *J.Pathol.* 208 (2006) 401-407.
42. J.Tang, X.Qi, D.Mercola, J.Han, and G.Chen, Essential role of p38gamma in K-Ras transformation independent of phosphorylation. *J.Biol.Chem.* 280 (2005) 23910-23917.



Supplementary Figure 1. Human intestinal epithelial cells were exposed to U0126 (5 μ M) and were cultured for 20 days. At the indicated timepoints mitochondrial activity was analyzed by MTT assays, as a measure for the relative number of viable cells. The graph shows means and SEM of triplicate analyses. * denotes statistical significance ($p < 0.01$). Apoptosis was not observed in these cultures.



Supplementary Figure 2. Oncogenic Ras does not confer resistance to the PI(3)-kinase inhibitor LY294002. (A) C26 and C26-KrasKD cells were treated with 10 μ M LY294002. Cell proliferation was then followed over time by population doubling assays. (B), Photomicrographs showing control cells and cells treated with 10 μ M LY294002 for three weeks. Bars 50 μ m. (C), After four and twenty-five days all cells were lysed and analyzed for the presence of phosphorylated AKT by Western blotting.

7

Differentiated Human Colorectal Cancer Cells Protect Tumor- Initiating Cells From Irinotecan

Winan J. van Houdt, Benjamin L. Emmink, Robert G. Vries, Frederik J.H. Hoogwater,
Klaas M. Govaert, Andre Verheem, Maarten W. Nijkamp, Ernst J.A. Steller, Connie R. Jimenez,
Hans Clevers, Inne H.M. Borel Rinkes and Onno Kranenburg

Gastroenterology, 2011 March 31 (epub ahead of print)

Abstract

Background: Normal tissue stem cells possess resistance mechanisms that allow them to endure a lifetime of genotoxic insults. By inheriting these traits, tumor-initiating cells are thought to be endowed with an intrinsic resistance to chemotherapy. However, the relationship between chemoresistance and tumor-initiating potential is poorly understood. Here we studied how resistance to the topoisomerase I inhibitor irinotecan is related to tumor-initiating potential in colorectal cancer.

Methods: Colonosphere cultures were established from resected primary tumors and liver metastases. Stem cell and differentiation markers were analyzed by Western blotting and FACS. Clone- and tumor-initiating capacity was assessed by single cell cloning and subcutaneous injections into immunodeficient mice. Sensitivity to irinotecan was assessed *in vitro* and in tumor-bearing immune-deficient mice. The relationship between drug resistance and tumor-initiating capacity was tested by FACS-sorting colonosphere cells on the basis of ABCB1 expression and aldehyde dehydrogenase (ALDH) activity.

Results: Colonosphere cultures displayed high tumor-initiating capacity and resistance to irinotecan. However, drug resistance was mediated by a small subpopulation of differentiated cells expressing the drug efflux pump ABCB1. The ABCB1 inhibitor PSC-833 allowed ablation of tumor-initiating potential by irinotecan. Drug-resistant ABCB1⁺ cells were proliferation-competent but unable to initiate the formation of clones or tumors. Conversely, tumor-initiating cells, identified by high aldehyde dehydrogenase (ALDH)-activity, were ABCB1-negative and drug-sensitive. Tumorigenic ALDH^{high} cells could generate non-tumorigenic ABCB1-positive drug-resistant offspring *in vitro* and in tumor xenografts. Finally, PSC-833 strongly enhanced the therapeutic efficacy of irinotecan in tumor-bearing mice.

Conclusion: The resistance of colorectal tumors to irinotecan requires the cooperative action of drug-sensitive ALDH^{high} tumor-initiating cells and their ABCB1-expressing drug-resistant differentiated offspring.

Keywords: Aldehyde dehydrogenase; ABCB1; differentiation

Introduction

Intestinal stem cells drive normal tissue turnover by generating daughter stem cells and a rapidly proliferating pool of progenitor cells that give rise to differentiated cell types with specialized functions¹. This functional hierarchy is preserved in colon tumors in which a small tumor-initiating cell compartment drives the formation of proliferating and differentiated cell types with reduced tumorigenic potential²⁻⁵. Normal tissue stem cells have recently been identified as the cells of origin of several tumor types, including those of intestinal origin⁶⁻¹⁰. Preservation of the resistance mechanisms that characterise normal tissue stem cells during oncogenic transformation would provide the resulting tumor-initiating cells with an innate resistance to genotoxic agents. Therefore, tumor-initiating cells may not only drive tumor progression, but may also be responsible for resistance to chemotherapy and for subsequent tumor recurrence¹¹⁻¹³. Indeed, tumor-initiating cells from a diverse range of tumors were found to display intrinsic chemo-resistance¹³⁻¹⁸.

Chemotherapy of colorectal tumors is primarily based on 5-fluorouracil (5-FU), oxaliplatin and irinotecan¹⁹. However, colorectal tumors frequently fail to respond to chemotherapy, leaving the majority of tumor cells to survive treatment. Response rates are limited to 40-50%¹⁹. It is presently unknown how these clinical observations fit a model in which chemo-resistance is mediated by the small fraction of tumor cells with tumor-initiating capacity. Furthermore, drug efflux capacity does not appear to mark intestinal or colorectal tumor-initiating cells^{20,21}. Nevertheless, chemotherapy does enrich the population of clonogenic cancer cells in colorectal xenograft models, suggesting that these cells do display some form of selective drug resistance^{4,22}.

Here, we studied the relationship between tumor-initiating potential and irinotecan resistance by using a series of highly clonogenic and tumorigenic colonosphere cultures isolated from freshly resected primary colorectal tumors and liver metastases.

Materials and Methods

Collection of Tumor Specimens

Human colorectal tumor specimens were obtained from 28 patients undergoing a colon or liver resection for primary or metastatic adenocarcinoma, in accordance with the ethical committee on human experimentation. Informed consent was obtained from all patients. Diagnosis of tumor type and grade was based on histological examination.

Isolation and Expansion of Colorectal Tumor-Initiating Cell Cultures

A detailed procedure describing the isolation and expansion of colorectal tumor-initiating cell cultures is given in the supplementary material.

Colonosphere-Forming Efficiency (CFE)

Single cell suspensions derived from colonospheres and differentiated tumor cell cultures were counted, suspended in Matrigel (100 cells in 100 μ l) and allowed to set in 48-well plates. After setting, stem cell medium with fresh growth factors was added. Clone formation was analyzed after three weeks of culture. Colonies were counted using a Leica DM IRBE microscope and the

colonsphere-forming efficiency (CFE) was calculated as the percentage of seeded cells that formed colonspheres.

Irinotecan Sensitivity Assay

Both colonsphere cultures and their differentiated derivatives were cultured in stem cell medium in the presence of irinotecan (Campo, Pfizer) at the indicated concentrations for five days. In addition colonsphere cultures were cultured in the presence of the ABCB1 inhibitor PSC833 (2 μ M; Novartis, Basel Switzerland), the ABCG2 inhibitor Ko143 (200 nM; kindly provided by Dr. Alfred Schinkel, NKI, the Netherlands) and the ABCC1 inhibitor MK571 (30 μ M; Sigma) either alone, or in combination with 50 μ g/ml irinotecan for three consecutive days. Mitochondrial activity was evaluated using CellTiter 96 Aqueous One Solution Cell Proliferation Assay (MTS) (Promega). All absorbance values are expressed as percentages of vehicle-treated control wells.

Immunofluorescence and immunohistochemistry

Immunofluorescence were performed according to standard procedures, as specified in the supplementary material.

Statistical Analysis

The student's t test (unpaired, two-tailed) was performed to analyze statistically significant differences between groups. Outcome variables are depicted as point estimates, with a 95% confidence interval. In vivo tumor formation and drug treatment experiments were analyzed by one-way ANOVA followed by a Bonferroni multiple comparison test using GraphPad Prism software (GraphPad San Diego, CA). Differences with a p value of <0.05 were considered to be statistically significant.

Results

A novel series of undifferentiated colonsphere cultures from primary colorectal tumors and liver metastases

To study the relationship between tumor-initiating capacity and irinotecan resistance, we established a series of colonsphere cultures isolated from freshly resected primary colorectal tumors and liver metastases. Immediately following surgery, biopsies were obtained from the resection specimens. Single cell cultures were prepared from the biopsies and these were cultured in serum-free stem cell medium in low-adherence flasks. Colonspheres formed in 8/20 of these cultures, four originating from primary CRC tumors and four originating from liver metastases (supplementary Table 1). Single cell suspensions of all eight colonsphere cultures displayed high colonsphere-forming efficiency (CFE) ranging from 20-62% (supplementary Table 1). Furthermore, these cells were highly tumorigenic when injected into immune deficient mice (supplementary Table 1). Flow cytometry and Western blot analysis for the expression of published markers for tumor-initiating cells^{2, 3, 5, 22-24} showed that all colonspheres were positive for CD44 (50-100% of the cells) and ALDH1, while expression of CD133 and CD166 was more variable, ranging from 0-100% CD133-positive cells, and from 15-100% CD166-positive cells (supplementary Table 1). Colonsphere-initiated xenografts displayed extensive differentiation

and were histologically similar to the tumors from which they were derived (Supplementary Figure 1).

When exposed to serum-containing medium the colonospheres attached to the culture dish and grew out to form adherent cultures with heterogeneous morphology (Figure 1A). A subpopulation of cells was positive in the periodic acid-Schiff (PAS) stain for mucin-producing Goblet cells (Figure 1A) and all adherent cultures expressed the differentiation marker cytokeratin 20 (CK20) (Figure 1B). Distinct subpopulations of the adherent tumor cell populations expressed CK20 and the enterocyte brush border marker phospho-ezrin (Figure 1C).

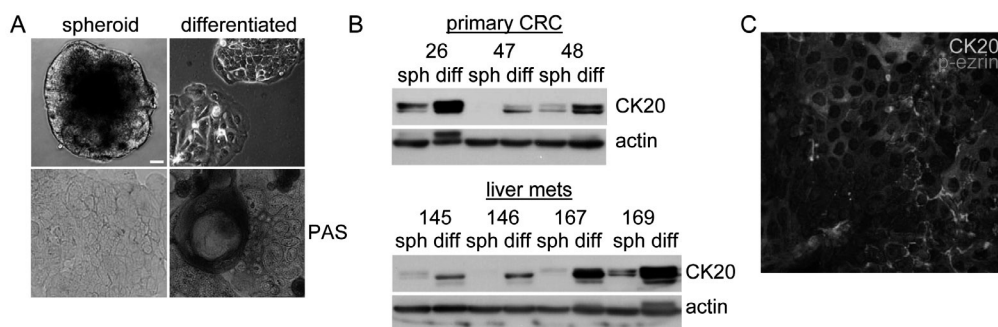


Figure 1. Differentiation of colonosphere-forming cells from human colorectal tumors. (A) Light microscopic images of a representative colonosphere and a population of colonosphere-derived adherent tumor cells. Bar 20 μ m. The lower panel shows Periodic Acid Schiff-stained cultures. (B) Western blot analysis of the expression of cytokeratin 20 (CK20) and actin in isogenic colonosphere and adherent tumor cell cultures. (C) Adherent tumor cells were grown on glass coverslips and were analyzed by immunofluorescence to detect the differentiation markers CK20 (in green) and phospho-ezrin (in red). Bar 20 μ m. See page 197 for color figure

An unbiased proteomics screen of the tumorigenic and non-tumorigenic differentiated tumor cell populations revealed that aldehyde dehydrogenase 1 (ALDH1) was strongly expressed in all tumor-initiating cell-enriched cultures, but not in the differentiated cultures. Western blot analysis confirmed the selective expression of ALDH1 in the colonosphere cultures (Figure 2A). Colonosphere-derived single cell populations displayed heterogeneous ALDH activity as measured by Aldefluor[®] (Supplementary Figure 2), and cells with high ALDH activity displayed a significantly higher clone-forming potential when compared to cells with low ALDH activity (56% versus 14%, difference = 42%; 95% CI = 34% to 49%, $p < 0.0001$) (Figure 2B). Co-staining with Aldefluor[®] and CD44 showed that the vast majority (>96%) of Aldefluor[®]-positive colonosphere cells were also positive for CD44 (Supplementary Figure 2). Importantly, serial transplantation of ALDH^{high} cells into immune-deficient mice revealed their capacity to self-renew and to form tumors (Figure 2C, Supplementary Figure 3). Upon *in vitro* differentiation, ALDH1-expression dropped, and this was accompanied by a drastic reduction in clone- and tumor-forming potential (supplementary Table 1, Figure 2 D-E). ALDH1 expression in spheroid-initiated xenografts dropped to similarly low levels as those obtained following *in vitro* differentiation (Supplementary Figure 1). These results are in line with recent reports identifying ALDH1 as a marker for colorectal tumor-initiating cells^{22, 23}. Taken together, we have established an *in vitro* culture system for the maintenance of ALDH1-positive, differentiation-competent colorectal tumor-initiating cells.

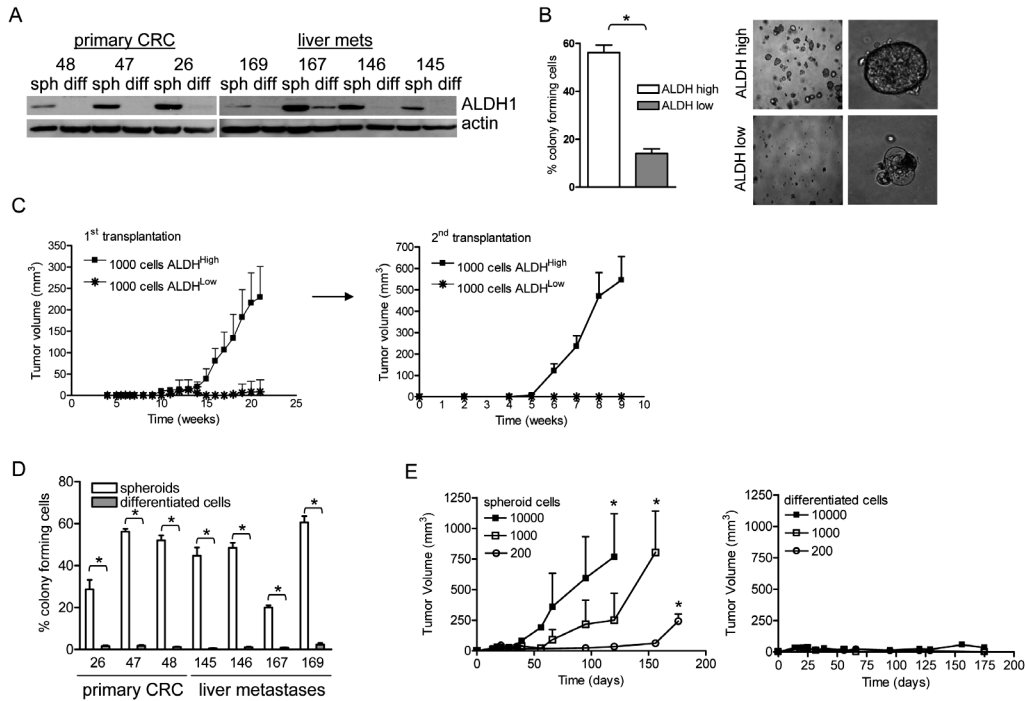


Figure 2. ALDH1 marks tumor-initiating cells in colonospheres. (A) Lysates of paired colonosphere and differentiated cultures derived from primary colorectal tumors and liver metastases were analyzed for the expression of ALDH1 by Western blotting. (B) Cultures enriched for tumor-initiating cells were analyzed for ALDH activity. Clone forming potential of cells with high and low ALDH activity was determined after 3 weeks. Representative examples of clones formed in ALDH-high and ALDH-low cultures are shown. (C) ALDH^{high} and ALDH^{low} cell populations within the spheroids were separated by making use of the fluorescent ALDH substrate Aldefluor®. ALDH^{high} and ALDH^{low} cells (1000) were injected into the flanks of nude mice (n=8). Tumors generated by ALDH^{high} cells were harvested and processed to generate single cell suspensions. Again ALDH^{high} and ALDH^{low} cell populations were separated by FACS sorting and these were injected into the flanks of nude mice (1000 cells). Tumor growth was analyzed by caliper measurements. The mean tumor volume of all tumors is shown. (D) Single cell populations were generated from the indicated colonosphere lines and from adherent tumor cell cultures and these were suspended in Matrigel at 1000 cells/ml. Equal numbers of Matrigel-embedded cells (n=100 in 100 μ l) were allowed to set in 48-well plates and clone formation was analyzed after three weeks of culture. (E) Single cell populations were generated from L145 colonospheres and from adherent tumor cell cultures and these were suspended in Matrigel. Mice were injected with 10.000 (n=3), 1000 (n=3), or 200 (n=3) tumor cells as indicated and tumor growth was followed over time by calliper measurements. *denotes statistical significance (Unpaired, 2-tailed t test: p<0.05).

Colonsphere cultures display resistance to irinotecan

We next used the metastasis-derived pairs of tumorigenic colonosphere and non-tumorigenic differentiated tumor cell populations to assess their relative sensitivity to irinotecan, a frequently used chemotherapeutic agent in the treatment of metastasized colorectal cancer¹⁹. Mitochondrial activity assays revealed that all colonosphere cultures were significantly more resistant to irinotecan than differentiated tumor cells (Figure 3A). Irinotecan treatment of differentiated tumor cells caused loss of BrdU incorporation (Figure 3B), rapid stabilization of p53 and processing of caspase 3 (Figure 3C), reflecting cell cycle arrest and apoptosis. In colonosphere cultures irinotecan reduced BrdU incorporation by ~50% (Figure 3B), similar to the reduction in mitochondrial activity (Figure 3A), but p53 stabilization or caspase 3 processing were not observed (Figure 3C).

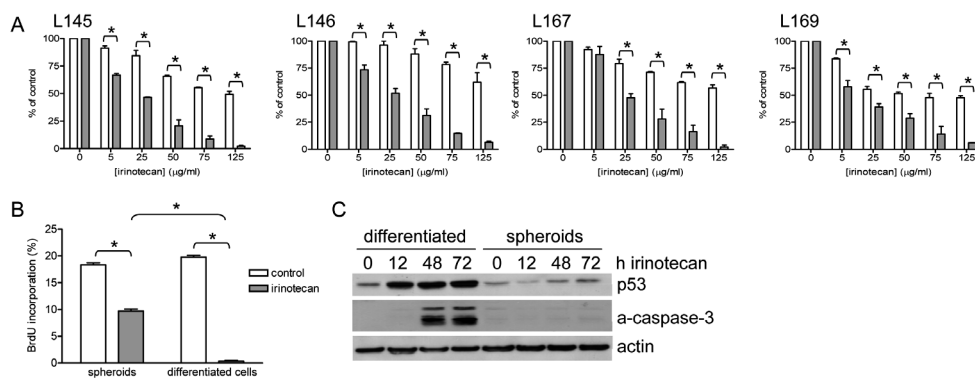


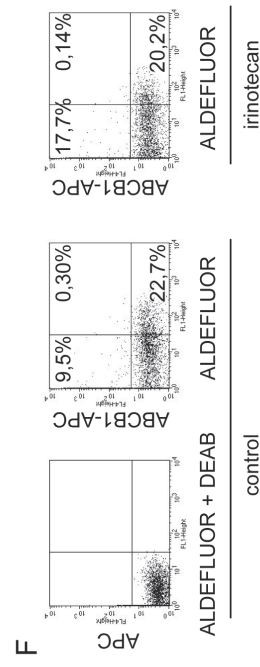
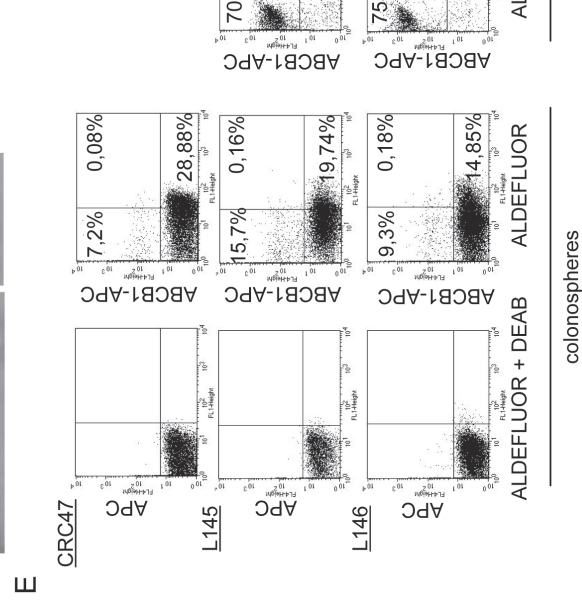
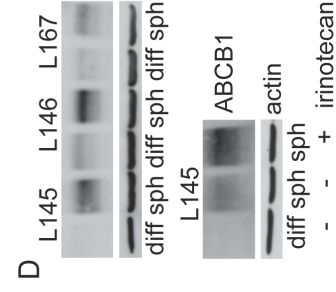
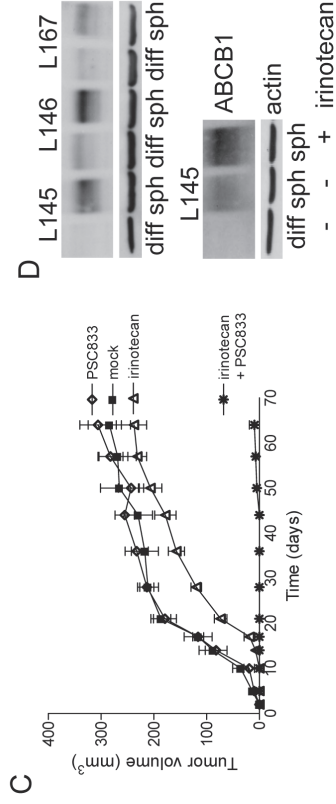
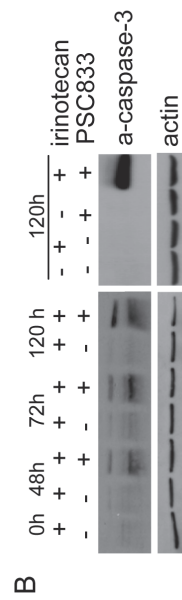
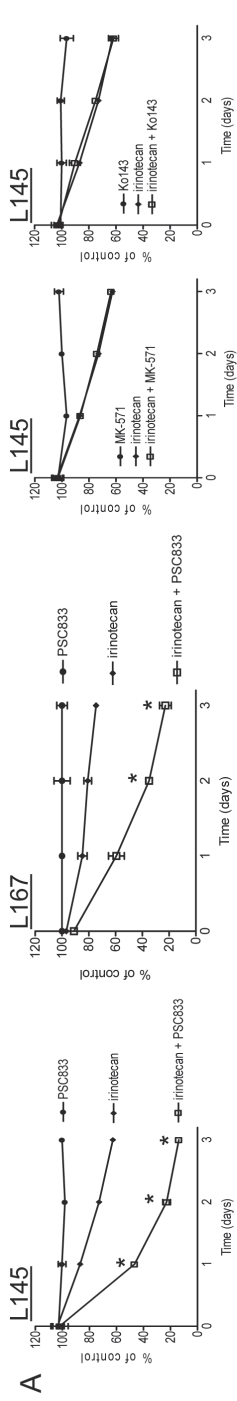
Figure 3. Colonosphere resistance to irinotecan. (A) Colonospheres (open bars) and isogenic differentiated tumor cells (closed bars) were seeded in 48-well plates in triplicate and were exposed to the indicated concentrations of irinotecan for five days. Mitochondrial activity was then tested by standard MTS assays. Absorbance values are expressed as percentages of vehicle-treated control wells. (B) L145 colonospheres and differentiated tumor cells were treated either with vehicle (open bars) or with 125 µg/ml irinotecan (closed bars) for 72 hours. The cells were then pulse-labelled with BrdU for 30 minutes and the percentage of BrdU-positive cells was determined by FACS analysis. (C) L145 colonospheres and differentiated tumor cells were treated with irinotecan for the indicated periods of time. Cell lysates were prepared and were analyzed for the presence of p53 and activated (cleaved) caspase-3 (a-caspase-3). *denotes statistical significance (Unpaired, 2-tailed t test: $p < 0.05$).

Irinotecan resistance is mediated by ABCB1

An important mechanism of resistance to irinotecan is the expression of drug efflux pumps of the ABC transporter family²⁵. The fluorescent DNA-binding dye Hoechst-33342 is a good substrate for the ABC pumps, offering a convenient assay for relevant ABC transporter activity. Hoechst-33342 readily stained the differentiated cell populations, but colonospheres failed to retain the dye (supplementary Figure 4). Verapamil, a relatively non-selective inhibitor of ABCB1, ABCG2, and to a lesser extent ABCC1, allowed Hoechst retention throughout the colonospheres, without affecting cell viability (supplementary Figure 4). To assess whether irinotecan resistance

is caused by ABC transporter activity, the colonosphere cultures were exposed to irinotecan in combination with selective inhibitors of ABCB1 (PSC833), ABCG2 (Ko143) and ABCC1 (MK-571). Only PSC833 sensitized the colonosphere cultures to irinotecan (Figure 4A and supplementary Figure 8), which was accompanied by caspase 3 cleavage and apoptosis induction (Figure 4B). Only the combination treatment, but neither irinotecan alone nor PSC833 alone, caused caspase-3 processing (Figure 4B). The irinotecan-related fluorescent drug topotecan was also excluded from colonospheres, but PSC833 allowed its uptake and retention (Supplementary Figure 5). These results suggest that co-treatment of colonospheres with PSC-833 and irinotecan suffices to kill tumor-initiating cells. To test this directly, colonospheres were treated with vehicle, PSC-833 alone, irinotecan alone or with the drug combination. The resulting cell populations were then injected into nude mice to assess tumor-initiating potential. PSC833-treatment did not affect tumor formation or latency time, when compared to treatment with vehicle. Irinotecan treatment did not affect tumor incidence, although latency time was ~1 week longer. However, co-treatment with PSC-833 and irinotecan completely abolished tumor-initiating potential. The PSC833-target ABCB1 was highly expressed in colonosphere cultures, but not in differentiated tumor cells (Figure 4D). Irinotecan treatment further increased ABCB1 expression (Figure 4D). Strikingly, FACS analysis showed that only ~12% of the colonosphere cell population expressed ABCB1 (supplementary Figure 6), even though the entire population displayed irinotecan resistance. FACS analysis of colonospheres and colonosphere-initiated tumors for ABCB1 and ALDH activity showed that these markers were expressed in a mutually exclusive fashion, with less than 0.3% double positive cells (Figure 4E). Exposure to irinotecan did not cause an increase in the percentage of ABCB1/ALDH^{high} double-positive cells, although ABCB1 single-positive cells were somewhat increased (Figure 4F, supplementary Figure 6).

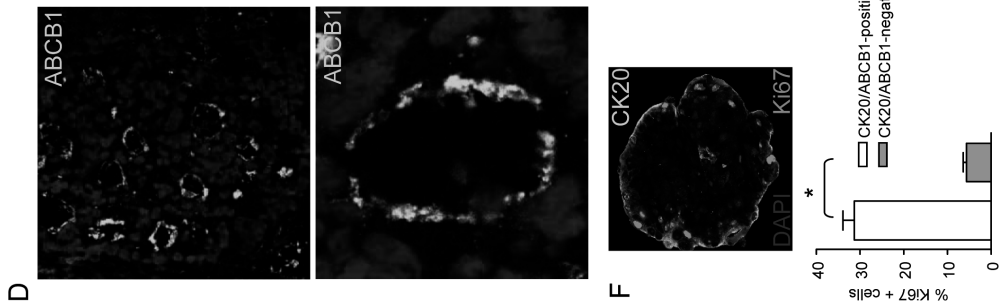
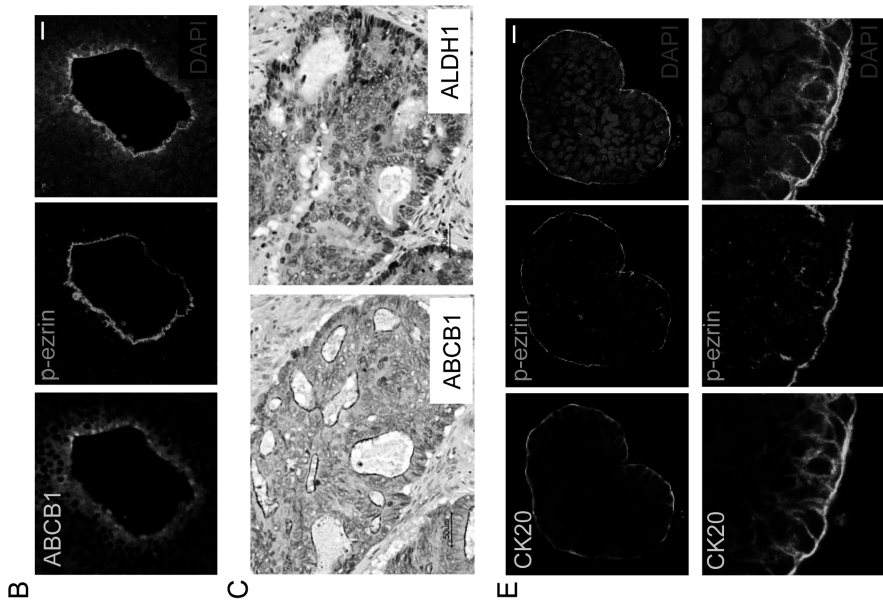
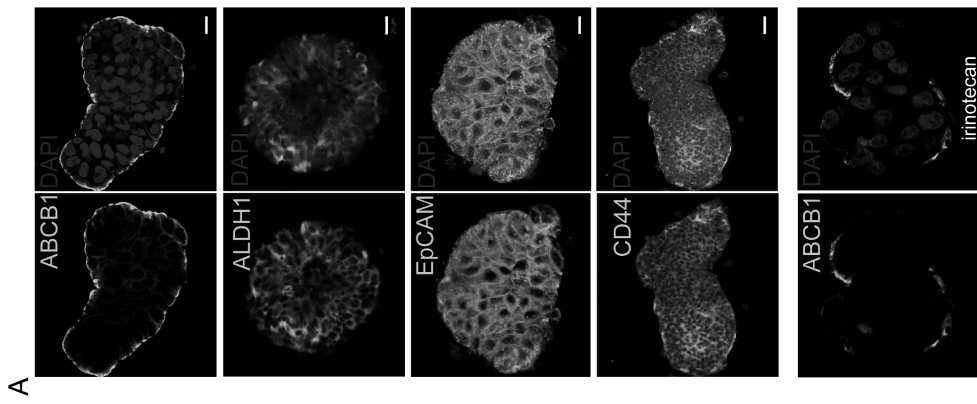
Figure 4. Irinotecan resistance is mediated by a subpopulation of tumor cells expressing ABCB1. (A) L145 and L167 colonospheres were cultured in the presence of irinotecan (50 µg/ml) the ABCB1 inhibitor PSC833 (2 µM), the ABCG2 inhibitor Ko143 (200 nM), or the ABCC1 inhibitor MK571 (30 µM), either alone or in combination as indicated. Mitochondrial activity was then assessed by MTS assays for three consecutive days. Absorbance values are expressed as percentages of vehicle-treated control wells. *denotes statistical significance (Unpaired, 2-tailed t test: p<0.05). (B) L145 colonospheres were cultured in the presence of irinotecan either in the absence or presence of the ABCB1 inhibitor PSC833. Cell lysates were prepared at the indicated periods of time and these were analyzed for the presence of activated (cleaved) caspase-3 (a-caspase-3). (C) L145 colonospheres were treated with vehicle, PSC833 alone (2 µM), irinotecan alone (75 µg/ml) or with the combination. The resulting cell populations were injected into the flanks of nude mice to assess tumor-initiating potential. Tumor growth was measured by calliper measurements. (D) Cell lysates of colonosphere cultures and differentiated tumor cells of the indicated tumors were lysed and analyzed for the presence of ABCB1 by Western blotting. L145 colonospheres were treated with vehicle or with irinotecan for 72 hours and lysates were prepared for analysis of ABCB1 expression by Western blotting. (E) FACS analysis of ABCB1 and Aldefluor[®] in three different colonosphere lines and in two spheroid-initiated tumors. (F) FACS analysis of ABCB1 and Aldefluor[®] in irinotecan-treated L145 colonosphere cultures (75 µg/ml; 24 h).

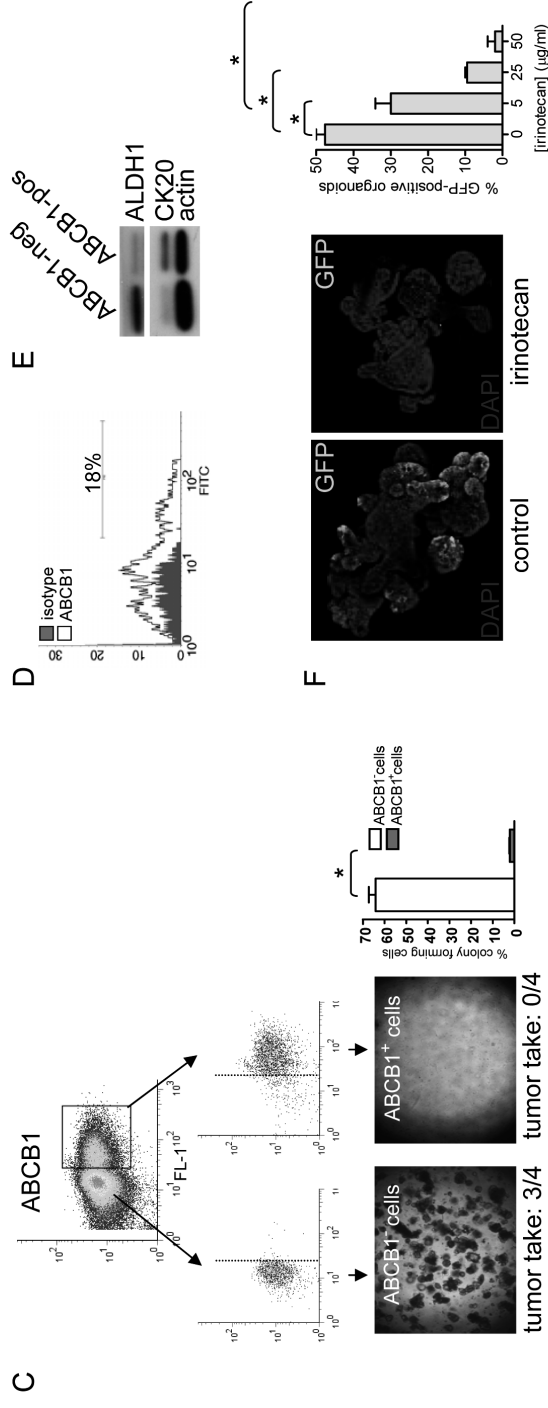
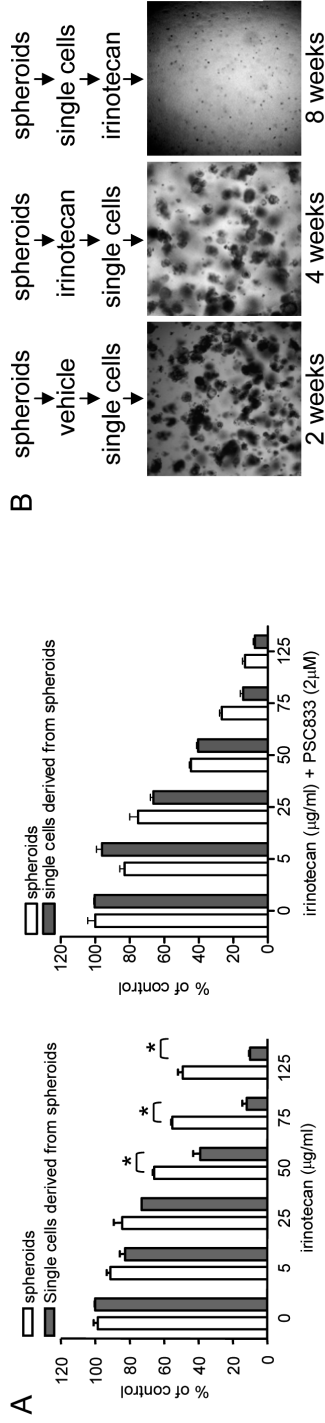


ABCB1 marks a differentiated non-tumorigenic minor subpopulation of colonosphere cells

Immunofluorescence analysis showed that ABCB1 expression was restricted to the apical membrane of the single outer cell layer of L145 and CRC26 colonospheres, whereas CD44 and EpCAM showed a homogeneous staining pattern (Figure 5A and supplementary Figure 8). Similar results were obtained for L146, L167 and L169. Furthermore, ABCB1 was also strongly expressed on cells forming tubules inside large colonospheres (Figure 5B). These cells co-expressed the brush border marker phospho-ezrin. Irinotecan exposure did not alter the pattern of expression throughout the colonosphere (Figure 5A, lower panel). In human colorectal liver metastases ABCB1 predominantly localized to the luminal side of differentiated tubule-forming cells (Figure 5C,D). ALDH1-positive cells were predominantly localized in undifferentiated areas of the tumor and were generally not a part of the ABCB1-positive tubules (Figure 5C). In L145 colonospheres the ABCB1-positive cells also expressed cytokeratin-20 and the enterocyte brush border marker phospho-ezrin (Figure 5E), but were negative in the PAS stain (Figure 1A). Similar results were obtained for L146, L167 and L169. While normal intestinal enterocytes are post-mitotic, approximately 30% of the enterocyte-like colonosphere cells expressed the proliferation marker Ki67 (Figure 5F). Similarly, ABCB1-positive tubule-forming cells in human colorectal liver metastases express Ki67. Cell proliferation in the inner cell mass of the colonospheres was significantly lower (27% versus 7%, difference=20%; 95% CI=10 to 29, $p=0.002$) (Figure 5F). ABCB1 therefore marks a population of differentiated, yet proliferation-competent tumor cells. These cells are clearly distinct from the stably differentiated adherent cultures that were obtained after serum stimulation and that lack expression of ABCB1.

Figure 5. ABCB1 marks a population of proliferating tubule-forming cells displaying enterocyte-like differentiation. (A) L145 colonospheres were fixed in formalin and processed for immunofluorescence using validated antibodies directed at ABCB1, CD44 and EpCAM. Irinotecan-treated cultures (75 $\mu\text{g}/\text{ml}$; 72h) were also analyzed for ABCB1 localization (lower panel). (B) Large colonospheres with signs of intra-sphere tubule formation were fixed and stained for ABCB1 and phospho-ezrin as in A. (C) Paraffin-embedded (left panels) and frozen (right panels) tissue sections of the same region in human colorectal tumor tissue (L150) were stained for expression of ABCB1 and ALDH1. Representative images are shown. ABCB1 is mainly found on the apical membrane of tubule forming cells. ALDH1 is expressed by non-tubule-forming cells in poorly differentiated tumor areas which lie between the tubule-forming cells. Bar 50 μm . (D) Colonospheres were fixed in formalin and processed for immunofluorescence using validated antibodies directed at cytokeratin 20 (CK20) and phospho-ezrin (p-ezrin). A representative L145 sphere is shown. (E) Expression of the proliferation marker Ki67 in the CK20/ABCB1/p-ezrin-positive outer cell layer relative to inner sphere cells was assessed by immunofluorescence as in A. Quantification was performed by counting the number of outer and inner cells displaying Ki67 expression. A representative example is shown in the left panel, quantification of Ki67 in the two cell compartments was based on analysis of 16 spheres from L145, L146 and L150 each. *denotes statistical significance ($p=0.0002$). All bars 20 μm . See page 198 for color figure





tumor take: 3/4

tumor take: 0/4

Figure 6. Separation of irinotecan-resistance and tumor-initiating potential on the basis of ABCB1 expression. (A) L145 colonospheres and sphere-derived single cell populations were treated either with vehicle or with irinotecan in the presence or absence of PSC-833 for five days at the indicated concentrations. Mitochondrial activity was then assessed by MTS assays for three consecutive days. Absorbance values are expressed as percentages of vehicle-treated control wells. (B) L145 colonospheres were either left as spheres or were processed to generate single cell populations. Colonospheres and single cell populations were then treated with irinotecan. All cultures were washed and the spheres were processed to generate single cell populations. All single cell populations were resuspended in Matrigel at 1000 live cells/ml. Equal numbers of Matrigel-embedded cells (n=100 in 100 μ l) were allowed to set in 48-well plates and clone formation was analyzed after two weeks (left panel) 4 weeks (middle panel) or 8 weeks (right panel) of cell culture. (C) Single cell cultures were derived from L145 colonospheres and these cells were stained for expression of ABCB1 by using 2 independent antibodies (MM4.17 and F4; see also Supplementary Figure 7). The ABCB1-positive and ABCB1-negative subpopulations were separated by FACS sorting and analyzed for clone-forming and tumor-initiating capacity as above. Part of the cells was re-sorted to assess their proper separation. (D) The clones generated by the ABCB1-negative cells were recovered from the Matrigel and single cell populations were prepared and analyzed for ABCB1 expression by FACS analysis. (E) Tumors were excised and processed to generate single cell suspensions. ABCB1-positive and -negative epithelial (EpCAM+) cells were separated by FACS sorting and analyzed for expression of ALDH1 and CK20 by Western blotting. (F) Intestinal organoid cultures from *Lgr5-EGFP-ires-CreERT2* mice²⁷ (n=3, each containing 25-50 organoids) were treated for 24 hours with the indicated concentrations of irinotecan. The number of GFP-positive organoids was assessed by fluorescence microscopy using DAPI as counterstain for healthy cells. *denotes statistical significance (Unpaired, 2-tailed t test: p<0.05). See page 199 for color figure

Differentiated ABCB1-positive cells protect ALDH1-positive tumor-initiating cells from irinotecan

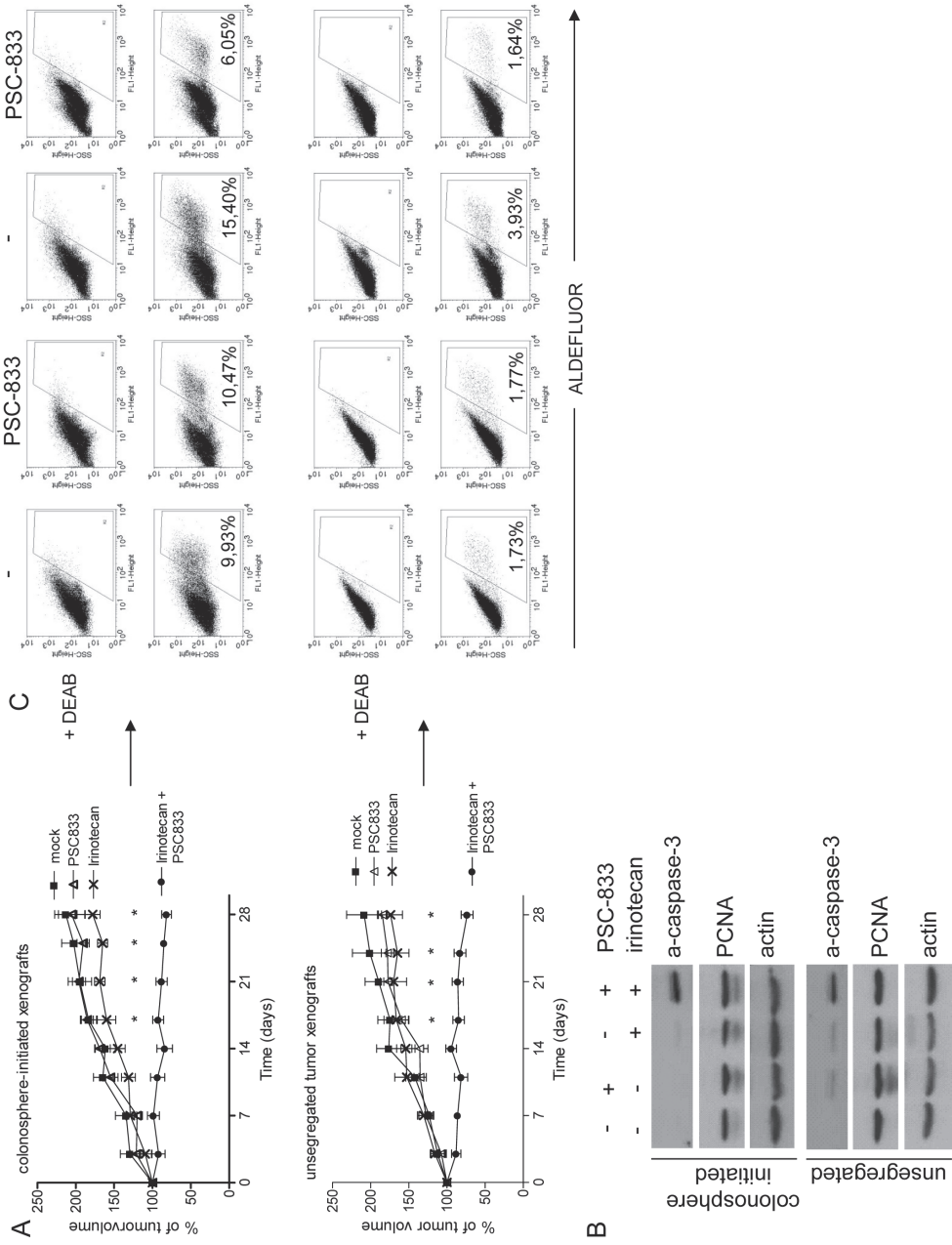
To test whether the ABCB1-expressing outer cell layer protects the inner cell mass from irinotecan, colonospheres were dissociated and single cell suspensions were exposed to irinotecan in the presence or absence of PSC-833. The vast majority of colonosphere-derived single cells (~90%) were killed by irinotecan, while intact colonospheres displayed resistance (Figure 6A; see also Figure 3A). The remaining live cells following single cell treatment were unable to form new clones (Figure 6B). By contrast, irinotecan-treated colonospheres retained their clone-forming potential (Figure 6B). PSC-833 treatment allowed irinotecan to kill colonospheres with similar efficiency as single cell cultures (Figure 6A). This suggests that ABCB1-mediated drug efflux is the major determinant of colonosphere resistance to irinotecan. To further assess the relationship between drug resistance (ABCB1 expression) and tumor-initiating potential, the ABCB1-positive and ABCB1-negative cells were separated by FACS sorting using two independent antibodies (MM-4.17 and F4). ABCB1-negative cells were highly clonogenic, but ABCB1-positive cells failed to form clones (Figure 6C, supplementary Figures 7 & 8) (64% versus 2%, difference 62%; 95% CI = 55.18% to 68.83%, p<0.0001). Furthermore, ABCB1-negative cells induced tumor formation in immunodeficient mice (3/4), but ABCB1-positive cells failed to do so (0/4). FACS analysis of the clones generated by ABCB1-negative cells revealed that they were composed of subpopulations of ABCB1-positive and ABCB1-negative cells with a distribution similar to the colonospheres from which they were derived (Figure 6D). Thus, ABCB1-negative cells were able to generate ABCB1-

positive cells, but not *vice versa*. Interestingly, ABCB1-negative tumor cells were characterized by expression of the cancer stem cell marker ALDH1, while non-tumorigenic ABCB1-positive cells expressed the differentiation marker CK20 (Figure 6E).

Normal intestinal stem cells are the cells of origin of intestinal tumors^{6,10} and express low levels of ABC transporters²⁶. This predicts that intestinal stem cells could also be sensitive to irinotecan. To test this we employed the recently described organoid culture system in which intestinal stem cells are marked by *Lgr5* promoter-driven expression of green fluorescent protein (GFP)²⁷. Fluorescence microscopy showed that irinotecan treatment caused a rapid depletion of GFP-positive stem cells from the organoid cultures (Figure 6E). Washed and re-plated populations of irinotecan-treated organoids failed to form new organoids, demonstrating the loss of tissue stem cells with regenerative potential.

Finally, we evaluated whether PSC833 could enhance the therapeutic efficacy of irinotecan against human colorectal tumor xenografts initiated by injection of either colonospheres or of unsegregated human tumor tissue. Tumor growth was observed in all injected animals. Tumor-bearing mice were treated with vehicle, irinotecan alone, PSC-833 alone, or the combination. Only the combination treatment had a robust anti-tumor effect against both types of xenograft (Figure 7A). In complete accordance with the *in vitro* findings, tumor cell apoptosis (active caspase-3) was only observed in tumors treated with the combination therapy (Figure 7B). FACS analysis of the treated xenografts further showed that irinotecan treatment alone enhanced the percentage of Aldefluor^{high} cells, but that co-treatment with PSC-833 caused a marked reduction in the percentage of Aldefluor^{high} cells (Figure 7C). The percentage of Aldefluor^{high} cells in xenografts treated with irinotecan and PSC-833 does not differ from that in mock-treated tumors. However, the absolute number of Aldefluor^{high} cells is reduced 3-6 fold when compared to single compound or mock-treated tumors (Supplementary Table 7). This is due to the lower tumor volume selectively in combination-treated animals.

Figure 7. PSC-833 enhances the anti-tumor efficacy of irinotecan. (A) Subcutaneous tumor xenografts were generated by injection of colonospheres (n=8) or by transplantation of unsegregated biopsies from a freshly resected human colorectal liver metastasis (n=8). Tumor growth was observed in all injected animals. Treatment (vehicle, irinotecan, PSC-833, or the combination) was started (day 0) after tumors reached a volume of 250-350 mm³. Tumor volume was analyzed by calliper measurements. Tumors were harvested and pooled samples of each group were analyzed (B) for active caspase-3 by Western blotting, or (C) for ALDH activity by FACS analysis, using Aldefluor®.



Discussion

The generation of colonosphere cultures from resection specimens is currently believed to be the most relevant cell culture system for colorectal tumors available. In this report we provide evidence that the maintenance of tumorigenic colonosphere cells following irinotecan exposure requires two types of tumor cells: First, a drug-sensitive cell population with intrinsic tumor-initiating capacity and second, a drug-resistant non-tumorigenic differentiated cell population that provides protection to the tumor-initiating cells from which they originated. To our knowledge this is the first example of how differentiated tumor cells and tumor-initiating cells display functional cooperation. Current models of chemo-resistance have implicated intrinsically drug-resistant tumor-initiating cells as the driving force behind tumor recurrence following chemotherapy^{11, 12, 28}. This is based on the fact that normal tissue stem cells generally express high levels of ABC transporters and DNA repair enzymes and are relatively resistant to apoptosis, and on more recent reports showing that tissue stem cells are the cells of origin of a number of different tumor types⁶⁻¹⁰.

Recently, it has been shown that treatment of colon cancer xenografts with irinotecan caused a minor increase in the percentage of cells co-expressing the 'cancer stem cell' markers CD44 and CD166²². However, the vast majority of tumor cells surviving treatment (>90%) were negative for these markers²². This suggests that mechanisms other than intrinsically drug-resistant tumor-initiating cells must play a major role in determining the resistance of colorectal tumors to irinotecan. Furthermore, the clinical observation that colorectal tumors frequently fail to respond to cytotoxic chemotherapeutics at all²⁹⁻³¹ is hard to reconcile with the idea that a small fraction of drug-resistant tumor-initiating cells is the primary cause of chemoresistance. The relationship between drug resistance and tumor-initiating potential is most likely dependent on the specific drug and on the mechanism(s) of resistance to that drug. For instance, ALDH^{high} tumor-initiating cells are intrinsically resistant to cyclophosphamide due to direct detoxification of this drug by ALDH1²², but they are not intrinsically resistant to irinotecan due to low level ABCB1 expression (this report). These relationships need to be clarified for all relevant chemotherapeutic drugs.

Irinotecan is a good substrate for the ABC transporters ABCB1 and ABCG2²⁵. The contribution of the various ABC transporters to primary and acquired irinotecan resistance in colon cancer patients is currently unknown. The expression of ABCG2 increases following irinotecan exposure³², but whether this represents a major resistance mechanism has not been tested. 'Reversal trials' using ABC transporter inhibitors in combination with chemotherapeutics have generated disappointing results. This is possibly due to the fact that mechanisms other than ABC transporter-mediated drug clearance also play an important role in determining drug resistance. These include inadequate drug delivery to tumor cells within a tumor mass, metabolic drug conversion and cell intrinsic properties such as increased levels of DNA repair enzymes³³. Several reversal trials have been performed in colorectal cancer patients, but none of these involved irinotecan^{33, 34}. Future work should clarify whether inhibition of ABCB1 activity is sufficient to kill tumor-initiating cells by irinotecan in the context of human colorectal tumor tissue. Irinotecan/PSC-833 combination therapy greatly reduced the total number of residual Aldefluor^{high} cells and also the percentage of these cells when compared to tumors treated with irinotecan alone. This may have clinical relevance as it is most likely the total number of residual tumor-initiating cells which determines the time-to-progression in chemotherapy-treated cancer patients. Since not all residual tumor-

initiating cells are eliminated by irinotecan/PSC-833 combination treatment, ABC transporter-unrelated resistance mechanisms, such as those discussed above, must play a role as well.

In normal intestinal tissue, expression of ABC transporters is restricted to the top compartment of differentiated cells facing the lumen²⁶. This not only prevents the entry of toxic substances across the intestinal barrier, but also expels intravenously delivered drugs, such as irinotecan, into the gastrointestinal lumen. In contrast, ABC transporter expression in the crypt stem cell compartment is very low²⁶. In line with this, we find that Lgr5-positive intestinal stem cells are readily eradicated by irinotecan. One of the major dose-limiting toxicities associated with irinotecan-based chemotherapy is severe diarrhea. This is observed in up to 82% of the patients, and is associated with morphological and functional changes in the intestinal mucosa^{19, 35-37}. While acute diarrhea is short-lasting and manageable, delayed onset diarrhea (from three days onwards) is more difficult to treat, and its causes are obscure³⁶. Our results suggest that depletion of the ABCB1-negative intestinal stem cell population by irinotecan and a consequent disturbance of intestinal homeostasis may contribute to delayed onset intestinal toxicity.

Taken together, we have shown that tumor-initiating potential and irinotecan resistance are separable traits in colonosphere cultures. In recent years the identification of tumor-initiating cells and the pathways on which they depend has received an enormous amount of attention. Our work suggests that the conventional anti-cancer drug irinotecan can reduce the total number of colorectal tumor-initiating cells, as long as the non-tumorigenic ABCB1-expressing cells are targeted simultaneously.

References

1. van der Flier LG, Clevers H. Stem cells, self-renewal, and differentiation in the intestinal epithelium. *Annu Rev Physiol* 2009;71:241-260.
2. O'Brien CA, Pollett A, Gallinger S, Dick JE. A human colon cancer cell capable of initiating tumour growth in immunodeficient mice. *Nature* 2007;445:106-110.
3. Ricci-Vitiani L, Lombardi DG, Pilozzi E, Biffoni M, Todaro M, Peschle C, De Maria R. Identification and expansion of human colon-cancer-initiating cells. *Nature* 2007;445:111-115.
4. Todaro M, Alea MP, Di Stefano AB, Cammareri P, Vermeulen L, Iovino F, Tripodo C, Russo A, Gulotta G, Medema JP, Stassi G. Colon cancer stem cells dictate tumor growth and resist cell death by production of interleukin-4. *Cell Stem Cell* 2007;1:389-402.
5. Vermeulen L, Todaro M, de Sousa MF, Sprick MR, Kemper K, Perez AM, Richel DJ, Stassi G, Medema JP. Single-cell cloning of colon cancer stem cells reveals a multi-lineage differentiation capacity. *Proc Natl Acad Sci U S A* 2008;105:13427-13432.
6. Barker N, Ridgway RA, van Es JH, van de WM, Begthel H, van den BM, Danenberg E, Clarke AR, Sansom OJ, Clevers H. Crypt stem cells as the cells-of-origin of intestinal cancer. *Nature* 2009;457:608-611.
7. Kim CF, Jackson EL, Woolfenden AE, Lawrence S, Babar I, Vogel S, Crowley D, Bronson RT, Jacks T. Identification of bronchioalveolar stem cells in normal lung and lung cancer. *Cell* 2005;121:823-835.
8. Le LQ, Shipman T, Burns DK, Parada LF. Cell of origin and microenvironment contribution for NF1-associated dermal neurofibromas. *Cell Stem Cell* 2009;4:453-463.
9. Perez-Caro M, Cobaleda C, Gonzalez-Herrero I, Vicente-Duenas C, Bermejo-Rodriguez C, Sanchez-Beato M, Orfao A, Pintado B, Flores T, Sanchez-Martin M, Jimenez R, Piris MA, Sanchez-Garcia I. Cancer induction by restriction of oncogene expression to the stem cell compartment. *EMBO J* 2009;28:8-20.
10. Zhu L, Gibson P, Currie DS, Tong Y, Richardson RJ, Bayazitov IT, Poppleton H, Zakharenko S, Ellison DW, Gilbertson RJ. Prominin 1 marks intestinal stem cells that are susceptible to neoplastic transformation. *Nature* 2009;457:603-607.
11. Dean M, Fojo T, Bates S. Tumour stem cells and drug resistance. *Nat Rev Cancer* 2005;5:275-284.
12. Donnenberg VS, Donnenberg AD. Multiple drug resistance in cancer revisited: the cancer stem cell hypothesis. *J Clin Pharmacol* 2005;45:872-877.
13. Eyler CE, Rich JN. Survival of the fittest: cancer stem cells in therapeutic resistance and angiogenesis. *J Clin Oncol* 2008;26:2839-2845.
14. Hermann PC, Huber SL, Herrler T, Aicher A, Ellwart JW, Guba M, Bruns CJ, Heeschen C. Distinct populations of cancer stem cells determine tumor growth and metastatic activity in human pancreatic cancer. *Cell Stem Cell* 2007;1:313-323.
15. Hirschmann-Jax C, Foster AE, Wulf GG, Nuchtern JG, Jax TW, Gobel U, Goodell MA, Brenner MK. A distinct "side population" of cells with high drug efflux capacity in human tumor cells. *Proc Natl Acad Sci U S A* 2004;101:14228-14233.
16. Li X, Lewis MT, Huang J, Gutierrez C, Osborne CK, Wu MF, Hilsenbeck SG, Pavlick A, Zhang X, Chamness GC, Wong H, Rosen J, Chang JC. Intrinsic resistance of tumorigenic breast cancer cells to chemotherapy. *J Natl Cancer Inst* 2008;100:672-679.
17. Liu G, Yuan X, Zeng Z, Tunici P, Ng H, Abdulkadir IR, Lu L, Irvin D, Black KL, Yu JS. Analysis of gene expression and chemoresistance of CD133+ cancer stem cells in glioblastoma. *Mol Cancer* 2006;5:67.
18. Ma S, Lee TK, Zheng BJ, Chan KW, Guan XY. CD133+ HCC cancer stem cells confer chemoresistance by preferential expression of the Akt/PKB survival pathway. *Oncogene* 2008;27:1749-1758.
19. Chau I, Cunningham D. Treatment in advanced colorectal cancer: what, when and how? *Br J Cancer* 2009.
20. Alison MR, Poulosom R, Brittan M, Schier S, Burkert J, Wright NA. Isolation of gut SP cells does not automatically enrich for stem cells. *Gastroenterology* 2006;130:1012-1013.
21. Burkert J, Otto WR, Wright NA. Side populations of gastrointestinal cancers are not enriched in stem cells. *J Pathol* 2008;214:564-573.
22. Dylla SJ, Beviglia L, Park IK, Chartier C, Raval J, Ngan L, Pickell K, Aguilar J, Lazetic S, Smith-Berdan S, Clarke MF, Hoey T, Lewicki J, Gurney AL. Colorectal cancer stem cells are enriched in xenogeneic tumors following chemotherapy. *PLoS ONE* 2008;3:e2428.

23. Huang EH, Hynes MJ, Zhang T, Ginestier C, Dontu G, Appelman H, Fields JZ, Wicha MS, Boman BM. Aldehyde dehydrogenase 1 is a marker for normal and malignant human colonic stem cells (SC) and tracks SC overpopulation during colon tumorigenesis. *Cancer Res* 2009;69:3382-3389.
24. Dalerba P, Dylla SJ, Park IK, Liu R, Wang X, Cho RW, Hoey T, Gurney A, Huang EH, Simeone DM, Shelton AA, Parmiani G, Castelli C, Clarke MF. Phenotypic characterization of human colorectal cancer stem cells. *Proc Natl Acad Sci U S A* 2007;104:10158-10163.
25. Smith NF, Figg WD, Sparreboom A. Pharmacogenetics of irinotecan metabolism and transport: an update. *Toxicol In Vitro* 2006;20:163-175.
26. Kosinski C, Li VS, Chan AS, Zhang J, Ho C, Tsui WY, Chan TL, Mifflin RC, Powell DW, Yuen ST, Leung SY, Chen X. Gene expression patterns of human colon tops and basal crypts and BMP antagonists as intestinal stem cell niche factors. *Proc Natl Acad Sci U S A* 2007;104:15418-15423.
27. Sato T, Vries RG, Snippert HJ, van de WM, Barker N, Stange DE, van Es JH, Abo A, Kujala P, Peters PJ, Clevers H. Single Lgr5 stem cells build crypt-villus structures in vitro without a mesenchymal niche. *Nature* 2009;459:262-265.
28. Dean M. ABC transporters, drug resistance, and cancer stem cells. *J Mammary Gland Biol Neoplasia* 2009;14:3-9.
29. Alberts SR, Wagman LD. Chemotherapy for colorectal cancer liver metastases. *Oncologist* 2008;13:1063-1073.
30. Mitry E, Douillard JY, Van CE, Cunningham D, Magherini E, Mery-Mignard D, Awad L, Rougier P. Predictive factors of survival in patients with advanced colorectal cancer: an individual data analysis of 602 patients included in irinotecan phase III trials. *Ann Oncol* 2004;15:1013-1017.
31. Douillard JY, Cunningham D, Roth AD, Navarro M, James RD, Karasek P, Jandik P, Iveson T, Carmichael J, Alakl M, Gruia G, Awad L, Rougier P. Irinotecan combined with fluorouracil compared with fluorouracil alone as first-line treatment for metastatic colorectal cancer: a multicentre randomised trial. *Lancet* 2000;355:1041-1047.
32. Candeil L, Gourdier I, Peyron D, Vezzio N, Copois V, Bibeau F, Orsetti B, Scheffer GL, Ychou M, Khan QA, Pommier Y, Pau B, Martineau P, Del RM. ABCG2 overexpression in colon cancer cells resistant to SN38 and in irinotecan-treated metastases. *Int J Cancer* 2004;109:848-854.
33. Bradshaw DM, Arceci RJ. Clinical relevance of transmembrane drug efflux as a mechanism of multidrug resistance. *J Clin Oncol* 1998;16:3674-3690.
34. Linn SC, Giaccone G. MDR1/P-glycoprotein expression in colorectal cancer. *Eur J Cancer* 1995;31A:1291-1294.
35. Ikuno N, Soda H, Watanabe M, Oka M. Irinotecan (CPT-11) and characteristic mucosal changes in the mouse ileum and cecum. *J Natl Cancer Inst* 1995;87:1876-1883.
36. Saliba F, Hagipantelli R, Misset JL, Bastian G, Vassal G, Bonnay M, Herait P, Cote C, Mahjoubi M, Mignard D, Cvitkovic E. Pathophysiology and therapy of irinotecan-induced delayed-onset diarrhea in patients with advanced colorectal cancer: a prospective assessment. *J Clin Oncol* 1998;16:2745-2751.
37. Di FF, Van CE. Acute and long-term gastrointestinal consequences of chemotherapy. *Best Pract Res Clin Gastroenterol* 2009;23:113-124.

Supplementary Materials and Methods

Isolation and Expansion of Colorectal Tumor-Initiating Cell Cultures

The obtained tissue fragments were washed extensively with PBS and were mechanically dissociated using scalpels and vigorous trituration to yield small fragments (<1mm³) and single cells. Enzymatic digestion was performed using thermolysin 0.05% (Sigma, Type X) in DMEM/F12 containing 5 mM Hepes (Gibco) for 2hr at 37°C. The suspension was then filtered through a 40-µm-pore size nylon cell strainer (BD Falcon) to separate the tissue fragments from the single cells. The single cell suspension was cultured in advanced DMEM/F12 (Gibco) supplemented with 0,6% glucose (BDH Lab. Supplies), 2 mM L-glutamine (Biowhittaker), 9.6 µg/ml putrescin (Sigma), 6.3 ng/ml progesterone (Sigma), 5.2 ng/ml sodium selenite (Sigma), 25 µg/ml insulin (Sigma), 100 µg/ml apotransferrin (Sigma), 5 mM hepes (Gibco), 0,005 µg/ml trace element A (Cellgro), 0,01 µg/ml trace element B (Cellgro), 0,01 µg/ml trace element C (Cellgro), 100 µM β-mercapto ethanol (Merck), 10 ml antibiotic-antimycotic (Gibco), 4 µg/ml gentamicine (Invitrogen), 0.002% lipid mixture (Sigma), 5 µg/ml glutathione (Roche) and 4 µg/ml Heparin (Sigma). Growth factors (20 ng/ml EGF (Invitrogen) and 10 ng/ml b-FGF (Abcam)) were added to the cell culture medium freshly each week. All cell culture was carried out in non-tissue culture treated flasks (BD Falcon) at 37° C in a 5% CO₂ humidified incubator. In vitro differentiation was induced by culturing colon colonospheres for 3 weeks on collagen-coated dishes in DMEM-F12 (GIBCO) supplemented with 20% fetal bovine serum.

Antibodies

The antibodies used in this study are anti human epithelial antigen (Ep-CAM, clone BER-EP4; Dako), anti human CD133/1 - APC (clone AC133; Miltenyi Biotec), anti human CD44 – APC (clone G44-26; BD Pharmingen), anti human CD166 – PE (clone 3A6; BD Pharmingen), anti human MDR-1 (Ab2, clone F4; Neomarkers). Anti-human MDR-1 (clone MM4.17; Chemicon), anti-MRP1 (MRPm6; Alexis Biochemicals), anti-ABCG2 (BXP-21; Abcam), anti-cleaved-caspase-3 (Cell Signaling), anti-p53 (DO-1; Santa Cruz), anti-ALDH1 (#44; BD Biosciences), anti-cytokeratin 20 (Ks20.8; Dako), anti-β-actin (AC-15; Novis Biologicals), anti-phospho-ezrin (Thr567) (Cell Signaling), and Ki67 (SP6, Neomarkers). The Aldefluor™ reagent was purchased from StemCell Technologies and used according to the manufacturer's instruction.

Hoechst and Topotecan Uptake Assay

Colonospheres and differentiated progeny were stained with Hoechst 33342 (5 µg/ml; 90 min) (Cambrex) and were visualized using a Leica DM IRBE microscope. Images were captured using a QImaging Retiga EXi CCD digital camera. Verapamil (Fluka) (50 µM) was added for 30 min and Hoechst uptake by the same colonospheres was assessed by fluorescence microscopy. Cell viability was assessed by adding 10µg/ml propidium iodide (PI) to the medium. PI-excluding cells were considered viable. Colonosphere cultures were incubated with 20 µM topotecan (Hycamtin, GlaxoSmithKline) with or without 2 µM PSC833 for 90 minutes at 37°C. After incubation, the colonospheres were gently washed twice with medium before analysis of fluorescence uptake by confocal microscopy at 405 nm (Zeiss LSM 510 Meta).

Immunofluorescence

Immunofluorescence staining was performed on colonospheres and their differentiated derivatives. Colonospheres growing in suspension were attached to coverslips by cytospin (800 rpm, 5 minutes). Cells were fixed in 3.7% formaldehyde and permeabilized with ice-cold (-20°C) methanol. After blocking with PBS-1%BSA, cells were incubated overnight at 4°C with primary antibodies. Secondary antibodies (incubated overnight at 4°C) goat anti-rabbit Alexa fluor 568 (Invitrogen) or chicken anti-mouse Alexa fluor 488 (Invitrogen), mixed with 0.5 µg/mL DAPI were used. Confocal microscopy was performed using the Zeiss LSM510 META microscope and Zeiss LSM5 Software.

Immunohistochemistry

Immunohistochemistry was performed using anti-ABCB1 Ab-5 (clone C494; Neomarkers, Lab Vision Corp, Fremont, CA, USA) and anti-ALDH1 (BD Transduction Laboratories). For detection goat anti Ms/Rb/Rt-poly-HRP (Powersvision, Immunologic, Immunovision Technologies, Brisbane, USA) was used. All slides were developed with diaminobenzidine followed by hematoxylin counterstaining. Frozen tissue sections were fixed with acetone for 20 minutes at room temperature, followed by a permeabilization and blocking step. Slides were incubated overnight at 4°C with anti-ABCB1 (clone 494; Neomarkers, Lab Vision Corp, Fremont, CA, USA) and chicken anti-mouse Alexa fluor 488 (Invitrogen), mixed with 0.5 µg/mL DAPI. Confocal microscopy was performed using the Zeiss LSM510 META microscope and Zeiss LSM5 Software.

Tumor formation and drug treatment

Single cell populations were diluted to 200, 1000 and 10.000 live spheroid-derived cells, mixed with BD Matrigel (BD Biosciences) at a 1:1 ratio (total volume 100 µl) and injected subcutaneous into the flanks of 6 weeks old BALB/c^{nu/nu} mice. The same procedure was followed after FACS sorting experiments in which ABCB1-positive and -negative or Aldefluor® (Stemcell Technologies, Grenoble, France) -positive and -negative cell populations were mixed with Matrigel (BD Biosciences) at 1000 cells/50 µl and injected into the flanks of BALB/c^{nu/nu} mice.

For drug treatment experiments mice were inoculated either with colonospheres mixed with Matrigel (1:1) or with 4x4 mm fragments of unsegregated colorectal tumors. Treatment was started (day 0) after tumors reached a volume ($V=AxB^2 \times 0.5263$) of 250-350 mm³. Valspodar (PSC833 (100 mg/kg oral gavage); Novartis, Basel Switzerland) and irinotecan (Campo, Pfizer; 50 mg/kg intraperitoneal (colonosphere-initiated tumors) or 15 mg/kg (biopsy-initiated tumors)) were given once weekly. Valspodar was given two hours prior to irinotecan. Control mice received vehicle only.

Tumor growth in all treated and untreated mice was followed for up to 5 months or when tumors reached a maximum of 1 cm³. Mice were sacrificed by cervical dislocation. All experiments involving the use of animals were performed in accordance with University of Utrecht institutional animal welfare guidelines.

Isolation of single cells from xenografts and colonospheres

Tumor xenografts were mechanically dissociated to yield small fragments that were further dissociated using dispasell (Roche)/collagenaseXI (Sigma; 30 min 37°C). The cells were washed once with PBS and were subsequently incubated with TrypLE express (Invitrogen) including 2,000 U/ml DNase (Sigma; 30 min 37°C). To obtain single cell suspensions from colonospheres, they were incubated with Accumax (Innovative Cell Technologies) plus 2 U/ml DNase1 (Sigma) for 10 minutes in a rotary incubator at 37°C. Both types of cell suspensions were then filtered through a 40- μ m-pore size nylon cell strainer (BD Falcon) to obtain single cells.

Flow Cytometry and Cell Sorting

The expression of a panel of cell surface markers was analyzed using a FACScalibur (BD Biosciences, San Diego, USA). All antibody incubation steps were carried out at 4°C. Dead cells were excluded using viability marker 7-aminoactinomycin D (7-AAD) and cell doublets and clumps were excluded using doublet discrimination gating. For analysis of xenografts, anti-EpCAM (1/1000) was always included as a marker for epithelial cells. Aldefluor[®]-positive cells were analyzed according to the manufacturer's protocol by using the ALDH substrate BAAA (1 μ mol/l per 1×10^6 cells). Negative control samples were co-incubated with diethylaminobenzaldehyde (DEAB; 50 mM). The cell sorting experiments were conducted with DAKO-Cytomation MoFlo High Speed Sorter.

For FACS-based cell cycle analysis, cells were incubated for 30 minutes with 1 μ M BrdU at 37°C. BrdU-positive cells were detected with an anti-BrdU-FITC antibody (BD Bioscience) according to the manufacturer's protocol. For determination of DNA content 10 μ g/ml propidium iodide (PI) was added in the presence of 250 μ g/ml RNase.

Supplementary table 1. Expression of stem cell markers and clone- and tumor-forming potential of human colorectal colonosphere cultures. Upper part: Tumor characteristics. Lower part: Expression of stem cell markers is depicted as % positive cells, based on FACS analysis. -: 0%; +: 1-25%; ++: 26-50%; +++: 51-75%; ++++: 76-100%. ND: not determined. # CRC29 cells were unable to form differentiated progeny under these experimental conditions. * Histological examination revealed that this was a cyst-like fluid-filled structure, rather than a tumor.

Case	Tumor site	Tumor type	Tumor stage	Differentiation
CRC26	Sigmoid	Adenocarcinoma	T3N2M1	Moderate
CRC29	Right colon	Adenocarcinoma	T3N0Mx	Poor
CRC47	Sigmoid	Adenocarcinoma	T3N1MX	Poor
CRC48	Right colon	Adenocarcinoma	T3N1M1	Moderate
L145	Liver segment VII	Adenocarcinoma		ND
L146	Liver segment IV	Adenocarcinoma		ND
L167	Liver segment II-IV	Adenocarcinoma		ND
L169	Liver segment	Adenocarcinoma		ND

Tumor	Stem Cell Markers			Clone formation %	Tumor formation colonosphere cells			
	<i>CD133</i>	<i>CD44</i>	<i>CD166</i>		200	1.000	10.000	10.000
CRC26	++++	+++	++	30	0/3	1/3	3/3	0/3
CRC29	++++	++++	+	59	3/3	3/3	3/3	#
CRC47	++	++++	++++	59	1/3	2/3	3/3	1/3*
CRC48	+++	+++	++	58	3/3	3/3	3/3	0/3
L145	-	++++	++++	46	3/3	3/3	3/3	0/3
L146	+++	++++	++++	50	2/3	2/3	2/3	0/3
L167	++	++	++	20	0/3	1/3	2/3	0/3
L169	-	++++	+++	62	1/3	2/3	3/3	ND

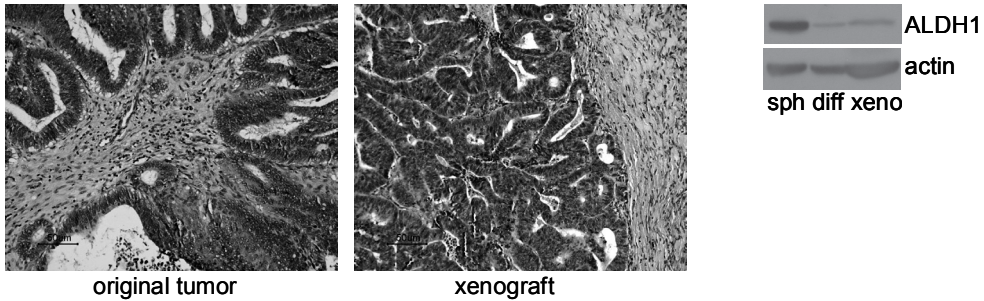
Supplementary table 2. Influence of PSC 833 on tumor volume and total number of Aldefluor^{high} cells. From the data presented in Figure 7 the fold change in tumor volume and the change in total numbers of Aldefluor^{high} cells was calculated for each treatment group. In both types of xenografts the combination treatment reduced tumor volume as well as the total number of Aldefluor^{high} cells.

Spheroid-initiated xenografts

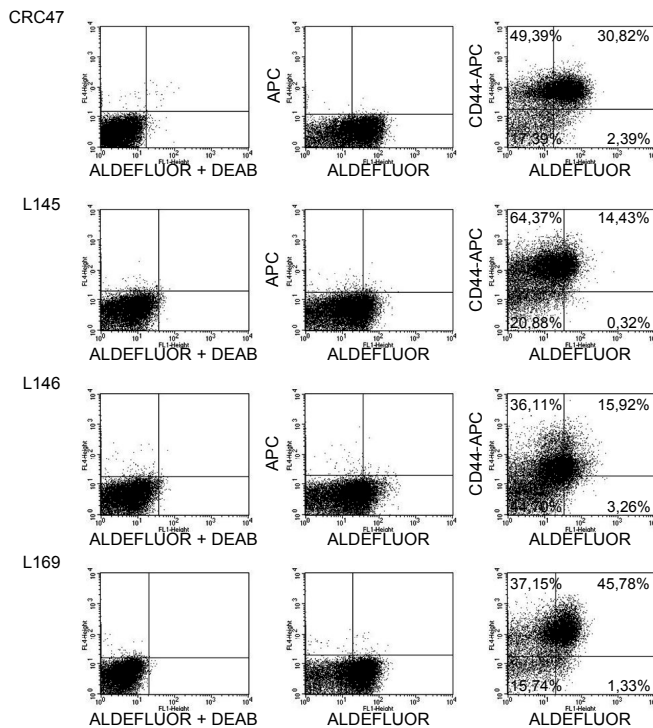
	Tumor volume (fold change)	Total # Aldefluor ^{high} cells (fold change)
Mock vs. PSC (P)	-1,04	1,09
Mock vs. irinotecan (I)	-1,2	1,86
Mock vs. I+P	-2,63	-4,32
PSC vs. irinotecan	-1,16	1,71
PSC vs. I+P	-2,53	-4,37
Irinotecan vs. I+P	-2,19	-5,57

Unsegregated xenografts

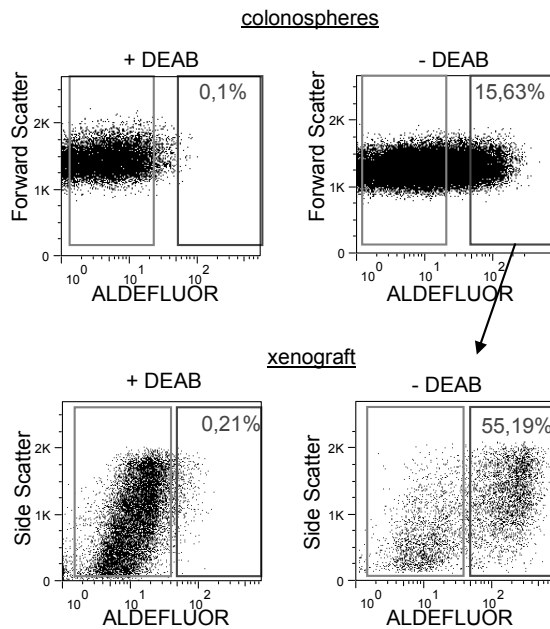
	Tumor volume (fold change)	Total # Aldefluor ^{high} cells (fold change)
Mock vs. PSC (P)	-1,12	1,15
Mock vs. irinotecan (I)	-1,19	2,7
Mock vs. I+P	-2,86	-3,02
PSC vs. irinotecan	-1,06	2,35
PSC vs. I+P	-2,55	-2,75
Irinotecan vs. I+P	-2,41	-5,78



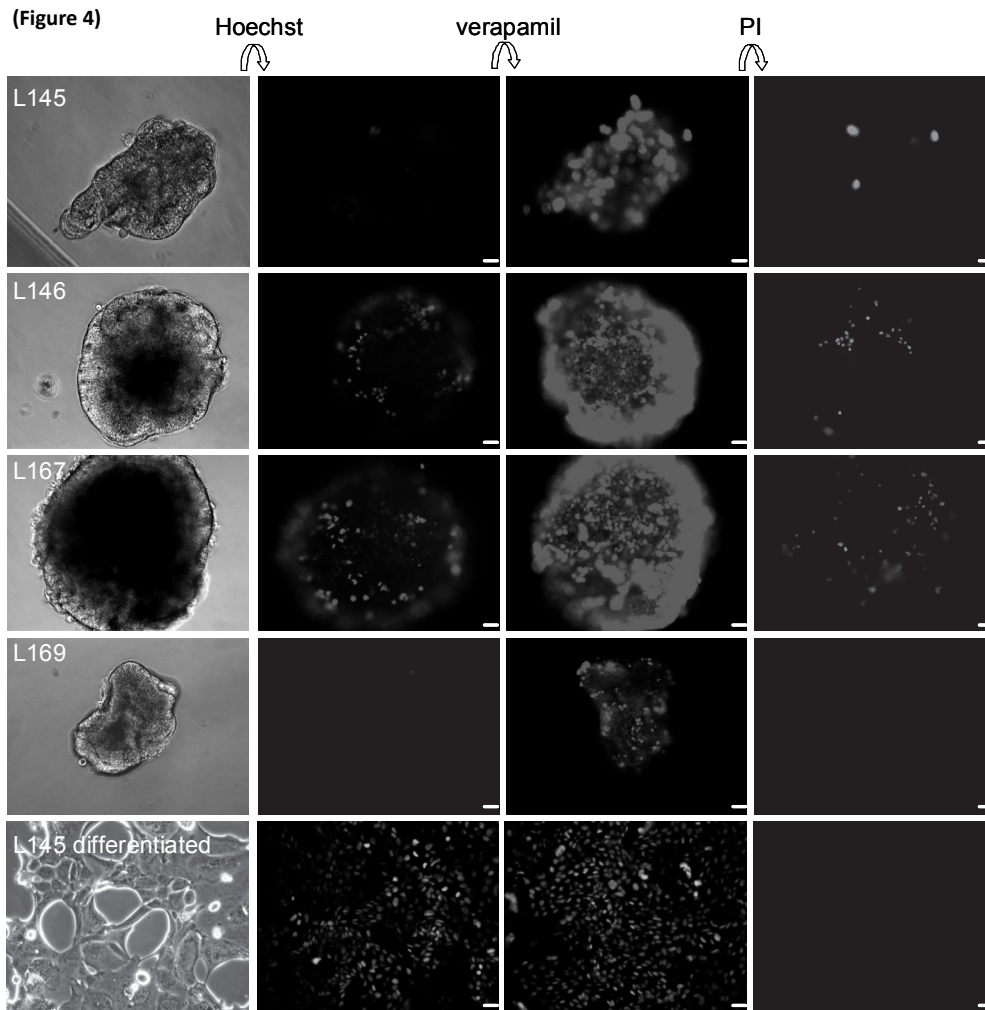
Supplementary Figure 1. Spheroid-initiated tumors display a differentiated phenotype and loose ALDH1 expression. Tumors generated by 200 colonospherederived cells (Table 1) were fixed in formalin and embedded in paraffin. Tissue sections were stained with Haematoxylin and Eosin (H&E) to reveal general tissue architecture. A representative example is shown. Colonosphere-initiated tumors show extensive differentiation and tubule-formation in the xenograft. Western blot analysis shows strongly reduced ALDH1 expression in the xenograft (xeno) when compared to the colonospheres (sph). FACS analysis of these tumors shows that the percentage of ALDH^{high} cells in the tumors is reduced 3-5 fold when compared to colonospheres (Figure 4E). Differentiated tumor cells (diff) are shown for comparison. See page 200 for color figure



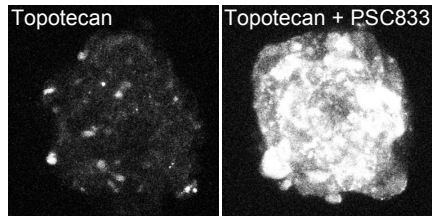
Supplementary Figure 2. The vast majority of Aldefluor[®]-positive cells are also positive for CD44. Colonosphere cells derived of 4 different tumors were analyzed for co-expression of CD44 and high Aldefluor[®] activity. Diethylaminobenzaldehyde (DEAB) was used to identify the negative cell population.



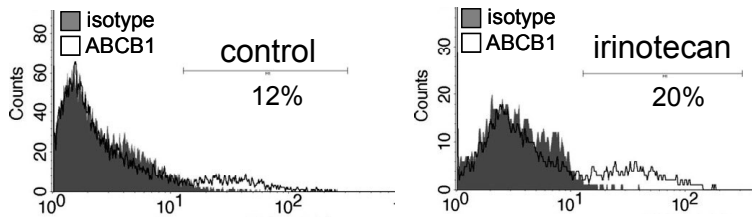
Supplementary Figure 3. ALDH activity marks tumor-initiating cells. Spheroid ALDH activity was assessed by Aldefluor®, using DEAB to identify the negative cell population (upper panel). ALDH^{high} and ALDH^{low} cells were then separated by FACS sorting and injected into nude mice. Only ALDH^{high} cells were capable of forming tumors (Figure 2C). Single cell suspensions of these tumors were generated and evaluated for ALDH activity (lower panel). ALDH^{high}-initiated tumors existed of both ALDH^{high} and ALDH^{low} cells. ALDH^{high} and ALDH^{low} cells were again separated by FACS sorting and evaluated for their tumor-initiating potential (Figure 2C). See page 200 for color figure



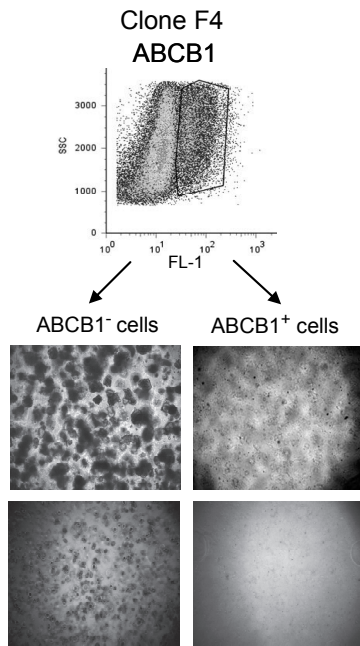
Supplementary Figure 4. Hoechst 33342 retention by colorectal spheroid cultures requires inhibition of ABC transporter activity. Spheroids and differentiated tumor cells were photographed after which Hoechst 33342 (5 $\mu\text{g}/\text{ml}$) was added to the medium. Hoechst uptake was assessed by fluorescence microscopy. Next, verapamil (50 μM) was added to the medium and the same spheroids were analyzed by fluorescence microscopy. To assess cell viability propidium iodide (PI) was added to the culture and PI uptake (dead cells) was assessed by fluorescence microscopy. The figure shows that Hoechst is taken up in spheroids only after verapamil treatment and that this is not due to extensive cell death. Differentiated tumor cells do not require verapamil to take up Hoechst. Bars 40 μm . See page 201 for color figure



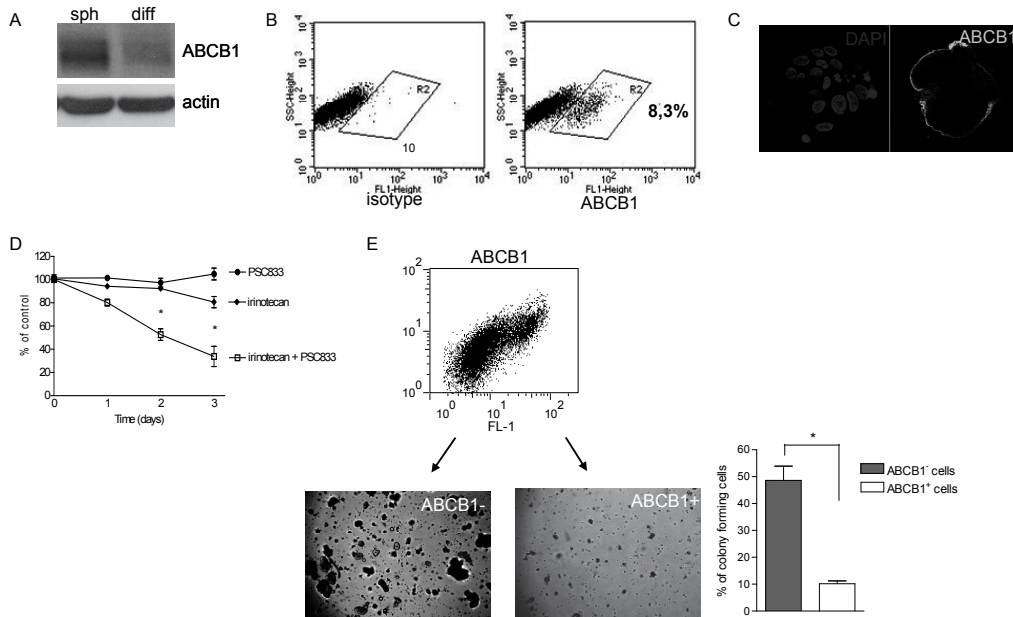
Supplementary Figure 5. PSC-833 allows uptake of topotecan. L145 colonospheres were treated with topotecan (20 μ M) either alone or together with the ABCB1 inhibitor PSC833 (2 μ M). The uptake of fluorescent topotecan was analyzed by confocal microscopy. A z-stack projection of a representative colonosphere is shown. *See page 201 for color figure*



Supplementary Figure 6. Irinotecan exposure increases the percentage of ABCB1-positive cells. L145 colonospheres were treated with vehicle or with irinotecan for 72 hours. Single cell cultures were prepared and analyzed for the presence of cell surface ABCB1 by FACS analysis. An isotype control antibody was used as a negative control.



Supplementary Figure 7. Anti-ABCB1 (clone F4) identifies the non-clonogenic population of colonosphere cells. Single cell populations were generated from colonospheres and were stained with anti-ABCB1 clone F4. After FACS sorting, ABCB1-positive and ABCB1-negative cells were re-suspended in Matrigel and allowed to form clones for three weeks. ABCB1(F4)-negative, but not ABCB1(F4)-positive cells were clonogenic. See page 202 for color figure



Supplementary Figure 8. ABCB1 marks non-clonogenic cells in colonospheres derived from a primary colorectal tumor (CRC26). A. Western blot analysis of ABCB1 in spheroid cultures and isogenic stably differentiated derivatives. B. FACS analysis identifies 8% of the colonosphere cells to be ABCB1 positive. C. Immunofluorescence analysis shows that ABCB1-positive cells represent the single outer cell layer of the colonospheres. D. MTT assays of colonosphere cells exposed to vehicle, irinotecan, PSC-833, or the combination, for 0-3 days. E. Single cell cultures from colonospheres were used to separate the ABCB1-positive from the ABCB1-negative population. Both populations were analyzed for clone-forming potential. A minor population of ABCB1-positive cells also formed colonies but these remained small, were morphologically clearly distinct from true spheroids, and consisted of highly vacuolarized cells that could not be further established. Most likely the latter colonies were initiated by cells with residual proliferative capacity but lacking self-renewal capacity. *See page 202 for color figure*

8

Proteome differences between colon cancer stem cells and differentiated tumor cells identifies BIRC6 as a potential therapeutic target

Winan J. Van Houdt, Benjamin L. Emmink, Thang V. Pham, Sander R. Piersma, André Verheem, Robert G. Vries, Silvana A. Fratantoni, Hans Clevers, Inne H.M. Borel Rinkes, Conny R. Jimenez, Onno Kranenburg

Submitted

Summary

Patients with liver metastases from colon carcinoma show highly variable responses to chemotherapy and tumor recurrence is frequently observed. Therapy-resistant cancer stem cells have been implicated in drug resistance and tumor recurrence. However, the factors determining therapy resistance and tumor recurrence are poorly understood. The aim of this study was to gain insight into these mechanisms by comparing the proteomes of patient-derived cancer stem cell cultures and their differentiated isogenic offspring.

We established colonosphere cultures derived from resection specimens of liver metastases in patients with colon cancer. These colonospheres, enriched for colon cancer stem cells, were used to establish isogenic cultures of stably differentiated non-tumorigenic progeny. Mass spectrometry-based proteomics in conjunction with spectral counting was used to identify proteome differences between three of these paired cultures. The resulting data were analyzed using Ingenuity Pathway software.

Out of a total dataset of 3048 identified proteins, 32 proteins were at least 2 fold upregulated in the colon cancer stem cells when compared to the differentiated cells. Pathway analysis showed that 'cell death' regulation is strikingly different between the two cell types. Interestingly, one of the top-upregulated proteins was BIRC6, which belongs to the class of Inhibitor of Apoptosis Proteins. Knockdown of BIRC6 sensitized colon cancer stem cells against the chemotherapeutic drugs oxaliplatin and cisplatin.

This study reveals that differentiation of colon cancer stem cells is accompanied by altered regulation of cell death pathways. We identified BIRC6 as an important mediator of cancer stem cell resistance against cisplatin and oxaliplatin. Targeting BIRC6, or other Inhibitors of Apoptosis Proteins, may help eradicating colon cancer stem cells.

Introduction

Treatment of colorectal cancer (CRC) patients with chemotherapy is characterized by highly divergent tumor responses, but tumor recurrence is almost always observed. Therefore, chemotherapy is not considered to be a curative modality in the treatment of CRC¹. Tumor recurrence may be due to the presence of therapy-resistant, genetically distinct tumor subclones. These subclones may either be pre-existent or may be generated as a direct result of the chemotherapy itself. More recently, it has been suggested that therapy resistance and subsequent tumor recurrence could be mediated by the 'cancer stem cell' fraction of colorectal tumors. Cancer stem cells make up only a few percent of the total tumor cell mass, but are uniquely endowed with tumor-initiating capacity²⁻⁵.

Interestingly, normal intestinal stem cells have been identified as the cell-of-origin of intestinal tumors^{6,7}. Cancer stem cells may therefore be transformed descendants of normal tissue stem cells. While normal stem cells give rise to differentiated cells lacking tissue-regenerating capacity, cancer stem cells give rise to differentiated tumor cells lacking tumor-regenerating capacity^{8,9}.

Normal colon stem cells are exposed to toxins and drugs for an entire lifetime. To cope with this continuous challenge, stem cells must possess intrinsic resistance mechanisms that protect their DNA from being mutated and that allow prolonged survival. Inheritance of these resistance mechanisms by cancer stem cells may protect them from the cytotoxic action of chemotherapeutic drugs. If cancer stem cells are indeed the major driving force behind tumor recurrence, novel strategies are required to target this subset of cancer cells. Indeed, several studies have shown that residual tumor tissue after chemotherapy is enriched for cancer stem cell-like cells^{10, 11}. However, the relationship between chemo-resistance and tumor-initiating potential and the mechanisms underlying cancer stem cell selective drug resistance are currently poorly understood¹²⁻¹⁵.

Here we set out to address the relationship between colorectal cancer stem cell and drug resistance. To this end, we have generated cancer stem cell enriched human colonosphere cultures from colorectal liver metastases. In addition, we have generated colonosphere-derived stably differentiated progeny. These isogenic cell pairs were then used to identify proteome differences using mass spectrometry. Analysis of the data revealed that proteins governing cell survival are overrepresented in the cancer stem cell cultures. The most prominently overexpressed survival protein, BIRC6/BRUCE/Apollon, was identified as a key mediator of cancer stem cell resistance to cisplatin and oxaliplatin.

Experimental procedures

Colorectal cancer stem cells and differentiated tumor cell cultures

Collection of tumor specimens, isolation and expansion of colorectal cancer stem cell-and differentiated cell cultures was performed as described in Emmink et al¹⁶.

Cell lysis and SDS-PAGE

Paired colonospheres and differentiated tumor cell cultures were seeded in 10 cm² diameter tissue culture plates and cultured for 24 hours in serum free stem cell medium. Cells were subsequently washed twice with PBS, centrifuged and washed with water to get rid of the excess salts. Lysisbuffer (20mM HEPES pH7.4, 1% NP40, 150mM NaCl, 5mM MgCl₂, 10% glycerol) containing proteinase inhibitor was used to lyse cells. Equal amounts of protein (50 µg) were separated on NuPAGE Novex Bis-Tris Mini Gels (Invitrogen). Gels were stained with Coomassie brilliant blue G-250 (Pierce), washed and each lane was sliced into ten bands using a band pattern to guide the slicing. The gel slicing and in-gel digesting was performed in a laminar flow under keratin-free conditions.

In-gel digestion

Before MS analysis, separated proteins were in-gel digested as described¹⁷. Gel lanes corresponding to the different protein samples were sliced into ten bands. The bands were washed/dehydrated three times in 50 mM ammonium bicarbonate pH 7.9 + 50% acetonitrile. Subsequently, cysteine bonds were reduced with 10 mM dithiothreitol for 1 h at 56 °C and alkylated with 50 mM iodoacetamide for 45 min at RT in the dark. After two subsequent wash/dehydration cycles the bands were dried 10 min in a vacuum centrifuge and incubated overnight with 0.06 µg/µl trypsin at 25 °C. Peptides were extracted once in 1% formic acid and subsequently two times in 50% ACN in 5% formic acid. The volume was reduced to 50 µl in a vacuum centrifuge prior to LC-MS/MS analysis¹⁸.

NanoLC-MS/MS analysis

Peptides were separated by an Ultimate 3000 nanoLC system (Dionex LC-Packings, Amsterdam, The Netherlands) equipped with a 20 cm × 75 µm ID fused silica column custom packed with 3 µm 120 Å ReproSil Pur C18 aqua (Dr Maisch GMBH, Ammerbuch-Entringen, Germany). After injection, peptides were trapped at 30 µl/min on a 5 mm × 300 µm ID Pepmap C18 cartridge (Dionex LC-Packings, Amsterdam, The Netherlands) at 2% buffer B (buffer A: 0.05% formic acid in MQ; buffer B: 80% ACN + 0.05% formic acid in MQ) and separated at 300 nl/min in a 10–40% buffer B gradient in 60 min. Eluting peptides were ionized at 1.7 kV in a Nanomate Triversa Chip-based nanospray source using a Triversa LC coupler (Advion, Ithaca, NJ). Intact peptide mass spectra and fragmentation spectra were acquired on a LTQ-FT hybrid mass spectrometer (Thermo Fisher, Bremen, Germany). Intact masses were measured at resolution 50,000 in the ICR cell using a target value of 1 × 10⁶ charges. In parallel, following an FT pre-scan, the top 5 peptide signals (charge-states 2⁺ and higher) were submitted to MS/MS in the linear ion trap (3 amu isolation width, 30 ms activation, 35% normalized activation energy, Q value of 0.25 and a threshold of 5000 counts). Dynamic exclusion was applied with a repeat count of 1 and an exclusion time of 30s.

Database searching, statistics and Ingenuity Pathway Analysis

MS/MS spectra were searched against the human IPI database 3.31 using Sequest (version 27, rev 12), which is part of the BioWorks 3.3 data analysis package (Thermo Fisher, San Jose, CA). MS/MS spectra were searched with a maximum allowed deviation of 10 ppm for the precursor mass

and 1 amu for fragment masses. Methionine oxidation and cysteine carboxamidomethylation were allowed as variable modifications, two missed cleavages were allowed and the minimum number of tryptic termini was 1. After database searching the DTA and OUT files were imported into Scaffold 2.01.01 (Proteome software, Portland, OR). Scaffold was used to organize the gel-band data and to validate peptide identifications using the Peptide Prophet algorithm. Only identifications with a probability > 95% were retained. Proteins that contained similar peptides and could not be differentiated based on MS/MS analysis alone were grouped. For each protein identified, the number of spectra was exported to Excel. The number of spectra per protein per sample was normalized against the total number of measured spectra. The list of differentially expressed proteins, including fold changes was imported in the online software package Ingenuity (Ingenuity IPA, version 7.6) and pathway and network analysis was performed with only direct relationships.

Lentiviral constructs and transduction

The lentiviral short-hairpin RNA (shRNA) constructs targeting BIRC6 were obtained from the TRC-Mm1.0 library (Sigma Aldrich). The target set used for BIRC6 (NM_016252) included TRCN000004157, TRCN000004158, TRCN00000059, TRCN000004160, and TRCN000004161. Of these constructs, transduction of cells with 58 and 59 produced the best knock down. As the control vector, we used the same vector containing a sequence targeting luciferase, TGACCAGGCATTCACAGAAAT.

Western blotting and Antibodies

Lysates of colonospheres and their differentiated offspring were prepared in lysisbuffer (20mM HEPES pH7.4, 1% NP40, 150mM NaCl, 5mM MgCl₂, 10% glycerol). Equal amounts of protein were run out on NuPAGE Novex Tris-Acetate Mini Gel (Invitrogen) and were analyzed by Western blotting using antibodies directed against BIRC6 (Ab 19609). β -Actin (AC-15) was used to control for protein load and the antibodies were obtained from Novus Biologicals, Littleton, CO, USA.

Flow Cytometry and Cell Sorting

Dead cells were excluded using viability marker 7-aminoactinomycin D (7-AAD) and cell doublets and clumps were excluded using doublet discrimination gating. Aldefluor[®]-positive cells were analyzed according to the manufacturer's protocol by using Aldefluor[®] and DEAB (STEMCELL Technologies). The cell sorting experiments were conducted with DAKO-Cytomation MoFlo High Speed Sorter.

Cisplatin and oxaliplatin Sensitivity Assay

Control and BIRC6 knockdown colonospheres and differentiated tumor cells were cultured in the presence of oxaliplatin (Pharmachemie BV, Haarlem) or cisplatin (Pharmachemie BV, Haarlem) at the indicated concentrations for five days. Mitochondrial activity was evaluated using CellTiter 96 Aqueous One Solution Cell Proliferation Assay (MTS) (Promega). All absorbance values are expressed as percentages of vehicle-treated control wells.

Results

Proteome differences between colon cancer stem cells and their differentiated progeny

To compare the proteome of colon cancer stem cells to their differentiated progeny, we analyzed three isogenic pairs of colonospheres and differentiated tumor cells derived from freshly resected liver metastases. All colonosphere cultures were enriched for cancer stem cells based on their high clone- and tumor-forming potential¹⁶

The protein lysates of these cultures were fractionated on an SDS-PAGE gel (Figure 1A), followed by in-gel tryptic digestion. Analysis of the extracted peptides was performed by Nano-LC-MS, followed by database searching. In total, 3048 proteins were identified in all sets of cells together, with an average of 2269 proteins per isogenic couple (Table 1). The number of proteins that were at least 2-fold upregulated in each isogenic pair varied from 377 to 491. Of these >2-fold upregulated proteins, 32 proteins were at least 2-fold upregulated in all isogenic pairs (Figure 1B). The unsupervised heat map of global clustering shows that the similarity between isogenic pairs of colonosphere cells and differentiated tumor cells is greater than the similarity among the different colonospheres cultures (Figure 2A). In contrast, supervised clustering (using all significant upregulated proteins) shows that all colonosphere cultures and differentiated cultures now cluster together (Figure 2B). Ingenuity analysis of all identified proteins for association with cancer, colorectal cancer and metastases revealed 92, 28 and 13 proteins respectively (Table 2).

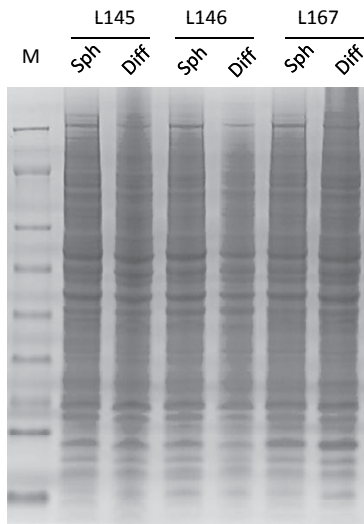
Table 1. Overview of the number of all identified proteins, total upregulated proteins and 2 fold upregulated proteins.

	L145	L146	L167	2/3 pairs	3/3 pairs
all regulated proteins	2242	2290	2376	516	1739
>1 fold upregulated	1078	1001	1093	676	229
>2 fold upregulated	491	377	437	275	32

Table 2. Ingenuity analysis of all identified proteins for association with cancer, colorectal cancer and metastases.

Cancer	N=92	ABAT, ACTB, ADSL, AKR1C1, AKR1C3, ALDH1A1, ALDH1A3, ALDH1B1, ANXA1, ARFGEF1, CALR, CAPG, CAPN2, CAV1, CD59, CD74, CDA, CEACAM7, CENPF, COTL1, COX5A, CTSS, DHCR24, DNAJC15, DPP4, DSG3, DST, EIF2AK2, EIF3H, ENO2, EPPK1, FABP1, FTL, GART, GLUD1, GPX2, GSTP1, HLA-A, HLA-B, HPGD, HSPA4, IFIT3, IFITM1, KIAA0664, KIF11, KRT1, KRT7, KRT8, KRT9, KRT19, KRT6A, LDHA, LGALS4, LGALS3BP, MAPK1, MCM2, MCM3, MCM5, MCM7, MGST2, MTAP (includes EG:4507), MX1, MYO7B, NCAPG, PFKP, PLEC, PPL, PRKDC, PRPF8, PTGR1, RANBP2, RB1, RHOG, RRM2, S100A6, S100A11, S100P, SERPINB5, SFPQ, SLC26A3, SLC27A2, SLC29A1, SNCG, SPTBN1, STAT6, TFRC, TPR, TRAP1, TUBA1A, TUBB3, TUBB2A, UGDH
Colorectal cancer	N=28	ADSL, AKR1C1, AKR1C3, CAPG, CAV1, CEACAM7, CENPF, EIF2AK2, FABP1, GART, GPX2, GSTP1, IFITM1, LDHA, LGALS4, MCM3, MCM5, MYO7B, NCAPG, PLEC, RRM2, SERPINB5, SLC27A2, TFRC, TRAP1, TUBA1A, TUBB3, TUBB2A
Metastases	N=13	ACTB, CAPN2, CAV1, GART, MAPK1, MX1, RB1, RRM2, SNCG, STAT6, TUBA1A, TUBB3, TUBB2A

1A



Sph = spheroid culture enriched for CSC
Diff = isogenic differentiated progeny of spheroid culture

1B

VENN diagram >2-fold upregulated proteins

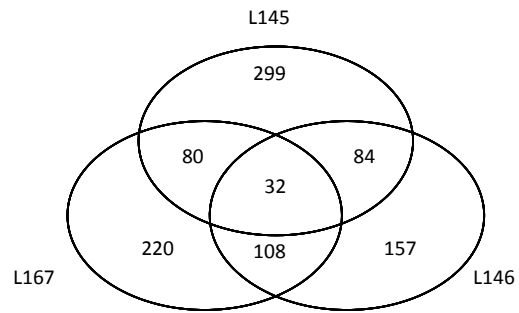
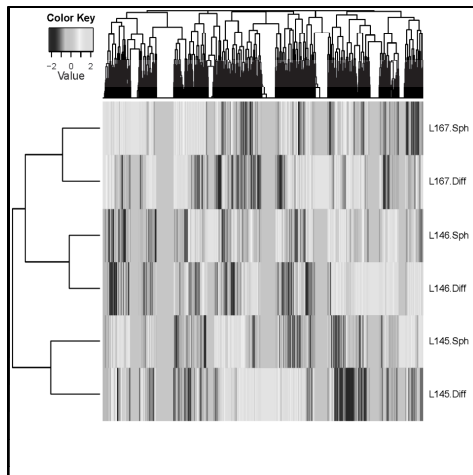


Figure 1. A. Protein gradient gel used for mass-spec analysis. Sph = colonosphere culture enriched for cancer stem cells, Diff = isogenic differentiated progeny of colonosphere culture. B. Venn diagram of all 2 fold upregulated proteins in colonospheres.

2A



2B

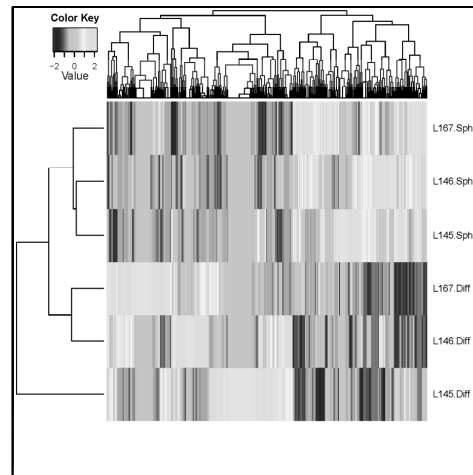


Figure 2. A. Heat map of the unsupervised cluster analysis of all identified proteins. B. Heat map of the supervised cluster analysis, including significant up- and downregulated proteins only. See page 203 for color figure

Table 3. Upregulated proteins in colonospheres categorized according to the criteria mentioned on page 158. Sph = colonosphere culture enriched for cancer stem cells, Diff = isogenic differentiated progeny of colonosphere culture.

>2 fold upregulated proteins in 3/3 combinations											
Protein	Gene	Accession. Number	L145		L146		L167		fold change	location	function
			Diff	Sph	Diff	Sph	Diff	Sph			
glutathione peroxidase 2 (gastrointestinal)	GPX2	IPI00298176	0	13	0	23	0	12	∞	Cytoplasm	enzyme
glutathione peroxidase 1	GPX1	IPI00293975	0	10	0	8	0	12	∞	Cytoplasm	enzyme
ferritin, light polypeptide	FTL	IPI00852596	0	4	0	4	0	7	∞	Cytoplasm	other
neuroblastoma amplified sequence	NBAS	IPI00333913	0	5	0	6	0	3	∞	unknown	other
baculoviral IAP repeat-containing 6	BIRC6	IPI00299635	0	4	0	6	0	3	∞	Cytoplasm	enzyme
microsomal glutathione S-transferase 2	MGST2	IPI00017767	0	3	0	4	0	3	∞	Cytoplasm	enzyme
glutathione peroxidase 4 (phospholipid hydroperoxidase)	GPX4	IPI00304814	0	2	0	5	0	3	∞	Cytoplasm	enzyme
eukaryotic translation initiation factor 3, subunit H	EIF3H	IPI00647650	0	3	0	3	0	3	∞	Cytoplasm	translation regulator
CDGSH iron sulfur domain 3	CISD3	IPI00783359	0	2	0	4	0	3	∞	unknown	other
endosulfine alpha	ENSA	IPI00220797	0	3	0	3	0	2	∞	unknown	transporter
family with sequence similarity 98, member A	FAM98A	IPI00174442	0	2	0	2	0	3	∞	unknown	other
RAN binding protein 3	RANBP3	IPI00456728	0	2	0	2	0	3	∞	Nucleus	other
chromosome 11 open reading frame 31	C11ORF31	IPI00218054	0	2	0	2	0	3	∞	Nucleus	other
mitochondrial ribosomal protein S18B	MRPS18B	IPI00022316	0	2	0	3	0	2	∞	Cytoplasm	other
RRS1 ribosome biogenesis regulator homolog (S. cerevisiae)	RRS1	IPI00014253	0	2	0	3	0	2	∞	Nucleus	other
DEAH (Asp-Glu-Ala-His) box polypeptide 38	DHX38	IPI00294211	0	2	0	2	0	2	∞	Nucleus	enzyme
C-terminal binding protein 1	CTBP1	IPI00012835	0	2	0	2	0	2	∞	Nucleus	enzyme
SIN3 homolog A, transcription regulator (yeast)	SIN3A	IPI00170596	0	2	0	2	0	2	∞	Nucleus	transcription regulator
succinate dehydrogenase complex, subunit B, iron sulfur (Ip)	SDHB	IPI00294911	2	5	0	6	0	8	9,2	Cytoplasm	enzyme
RNA binding motif protein 25	RBM25	IPI00004273	0	6	0	5	2	7	8,7	Nucleus	other
E1A binding protein p400	EP400	IPI00064931	2	5	0	7	0	5	8,2	Nucleus	other
myosin, heavy chain 10, non-muscle	MYH10	IPI00397526	0	3	0	4	4	26	8,1	Cytoplasm	other
leucine rich repeat containing 16A	LRRC16A	IPI00014843	0	17	4	10	0	4	7,4	unknown	enzyme
CDC42 binding protein kinase beta (DMPK-like)	CDC42BPB	IPI00477763	2	6	0	4	0	3	6,2	Cytoplasm	kinase
eukaryotic translation initiation factor 3, subunit J	EIF3J	IPI00290461	2	6	0	2	0	3	5,2	Cytoplasm	translation regulator
TAF15 RNA polymerase II, TATA box binding protein (TBP)-associated factor, 68kDa	TAF15	IPI00020194	0	3	0	2	2	5	4,9	Nucleus	transcription regulator

PTK2 protein tyrosine kinase 2	PTK2	IPI00012885	0	3	0	3	2	4	4,8	Cytoplasm	kinase
protein arginine methyltransferase 5	PRMT5	IPI00441473	0	4	0	2	3	7	4,2	Cytoplasm	enzyme
activating signal cointegrator 1 complex subunit 3	ASCC3	IPI00430472	2	6	0	5	2	6	4,1	Nucleus	enzyme
aldehyde dehydrogenase 1 family, member A1	ALDH1A1	IPI00218914	11	76	26	102	45	113	3,4	Cytoplasm	enzyme
mitochondrial ribosomal protein S27	MRPS27	IPI00022002	0	2	2	6	2	6	3,4	Cytoplasm	other
vacuolar protein sorting 13 homolog C (<i>S. cerevisiae</i>)	VPS13C	IPI00465428	9	19	5	13	5	13	2,3	unknown	other

>1,5 fold upregulated proteins in 3/3 combinations

Protein	Gene	Accession Number	L145		L146		L167		fold change	location	function
			Diff	Sph	Diff	Sph	Diff	Sph			
adenylosuccinate lyase	ADSL	IPI00026904	0	5	3	5	0	5	4,8	Cytoplasm	enzyme
transmembrane protein 205	TMEM205	IPI00063130	0	5	0	3	3	5	4,2	unknown	other
transformation/transcription domain-associated protein	TRRAP	IPI00069084	5	8	0	7	0	6	4,0	Nucleus	transcription regulator
nuclear receptor co-repressor 1	NCOR1	IPI00289344	0	3	0	4	3	5	3,9	Nucleus	transcription regulator
ATP-binding cassette, sub-family B (MDR/TAP), member 1	ABCB1	IPI00027481	0	7	0	11	9	17	3,8	Plasma Membrane	transporter
CDGSH iron sulfur domain 1	CISD1	IPI00020510	0	3	0	8	6	10	3,4	Cytoplasm	other
methionine adenosyltransferase II, beta	MAT2B	IPI00002324	5	8	0	5	0	5	3,4	Cytoplasm	enzyme
NADH dehydrogenase (ubiquinone) 1 alpha subcomplex, 11, 14.7kDa	NDUFA11	IPI00329301	2	5	0	6	4	6	2,7	Cytoplasm	enzyme
succinate dehydrogenase complex, subunit A, flavoprotein (Fp)	SDHA	IPI00305166	5	18	12	21	6	23	2,6	Cytoplasm	enzyme
15 kDa selenoprotein	SEP15	IPI00030877	3	8	5	9	2	7	2,3	Cytoplasm	enzyme
aldehyde dehydrogenase 1 family, member B1	ALDH1B1	IPI00103467	8	17	15	46	14	22	2,2	Cytoplasm	enzyme
acetyl-CoA acyltransferase 1	ACAA1	IPI00012828	2	11	7	11	9	15	2,0	Cytoplasm	enzyme
eukaryotic translation initiation factor 5B	EIF5B	IPI00299254	6	12	6	11	3	8	2,0	Cytoplasm	translation regulator
heterogeneous nuclear ribonucleoprotein A0	HNRNPA0	IPI00011913	3	10	4	6	5	9	2,0	Nucleus	other
UDP-glucose 6-dehydrogenase	UGDH	IPI00031420	4	22	30	45	19	37	1,9	Nucleus	enzyme
valyl-tRNA synthetase	VARS	IPI00000873	9	24	15	22	14	23	1,8	Cytoplasm	enzyme
tubulin tyrosine ligase-like family, member 12	TTLL12	IPI00029048	6	10	12	27	8	12	1,8	unknown	other
interleukin enhancer binding factor 3, 90kDa	ILF3	IPI00298788	20	32	17	28	13	27	1,7	Nucleus	transcription regulator
carbamoyl-phosphate synthetase 2, aspartate transcarbamylase, and dihydroorotase	CAD	IPI00301263	24	36	33	58	19	33	1,6	Cytoplasm	enzyme
RAN binding protein 2	RANBP2	IPI00221325	28	45	22	35	28	42	1,5	Nucleus	enzyme

>1,5 fold upregulated proteins in 2/3 combinations											
Protein	Accession. Number	L145		L146		L167		fold change	location	function	
		Diff	Sph	Diff	Sph	Diff	Sph				
3-hydroxybutyrate dehydrogenase, type 2	BDH2	IPI00607799	0	0	0	4	0	6	∞	Cytoplasm	enzyme
Huntingtin	HTT	IPI00002335	0	0	0	6	0	4	∞	Cytoplasm	transcription regulator
drebrin 1	DBN1	IPI00003406	0	0	0	4	0	5	∞	Cytoplasm	other
leucine zipper transcription factor-like 1	LZTFL1	IPI00299465	0	5	0	0	0	4	∞	unknown	other
DC2 protein	DC2	IPI00183603	0	0	0	4	0	4	∞	Cytoplasm	other
methyltransferase like 7B	METTL7B	IPI00090807	0	6	0	0	0	2	∞	unknown	enzyme
titin	TTN	IPI00023283	0	3	0	5	0	0	∞	Cytoplasm	peptidase
signal recognition particle 54kDa	SRP54	IPI00009822	0	0	0	4	0	3	∞	Cytoplasm	other
COP9 constitutive photomorphogenic homolog subunit 4 (Arabidopsis)	COPS4	IPI00171844	0	4	0	0	0	3	∞	Cytoplasm	other
mannosidase, alpha, class 2A, member 1	MAN2A1	IPI00003802	0	4	0	3	0	0	∞	Cytoplasm	enzyme
YLP motif containing 1	YLPM1	IPI00165434	0	2	0	0	0	5	∞	Nucleus	other
lysophosphatidylcholine acyltransferase 3	LPCAT3	IPI00306419	0	3	0	0	0	3	∞	Plasma Membrane	other
biorientation of chromosomes in cell division 1-like	BOD1L	IPI00386211	0	3	0	0	0	3	∞	unknown	other
NADH dehydrogenase (ubiquinone) 1 beta subcomplex, 11, 17.3kDa	NDUFB11	IPI00472058	0	3	0	3	0	0	∞	Cytoplasm	enzyme
hornerin	HRNR	IPI00398625	0	3	0	3	0	0	∞	Cytoplasm	other
chromobox homolog 1 (HP1 beta homolog Drosophila)	CBX1	IPI00010320	0	0	0	2	0	4	∞	Nucleus	other
thimet oligopeptidase 1	THOP1	IPI00549189	0	0	0	2	0	4	∞	Cytoplasm	peptidase
replication factor C (activator 1) 1, 145kDa	RFC1	IPI00375358	0	0	0	2	0	4	∞	Nucleus	transcription regulator
armadillo repeat containing 10	ARMC10	IPI00217968	0	2	0	4	0	0	∞	Cytoplasm	other
ER lipid raft associated 1	ERLIN1	IPI00007940	0	2	0	4	0	0	∞	Plasma Membrane	other
olfactomedin 4	OLFM4	IPI00022255	6	15	0	38	0	0	8,5	unknown	other
proteasome (prosome, macropain) 26S subunit, non-ATPase, 8	PSMD8	IPI00010201	3	4	0	4	0	7	4,8	Cytoplasm	other
adaptor-related protein complex 1, sigma 1 subunit	AP1S1	IPI00152898	2	2	0	3	0	5	4,8	Cytoplasm	transporter
MDN1, midasin homolog (yeast)	MDN1	IPI00167941	5	5	0	15	2	9	4,0	Nucleus	other
neural precursor cell expressed, developmentally down-regulated 8	NEDD8	IPI00020008	0	4	3	4	0	4	3,9	Nucleus	enzyme
adaptor-related protein complex 3, beta 1 subunit	AP3B1	IPI00021129	3	4	0	3	0	5	3,8	Cytoplasm	transporter
acyl-CoA binding domain containing 3	ACBD3	IPI00009315	3	7	0	5	0	0	3,8	Cytoplasm	other
A kinase (PRKA) anchor protein (yotiao) 9	AKAP9	IPI00019223	6	8	0	7	0	7	3,5	Cytoplasm	other

ATPase type 13A1	ATP13A1	IPI00034277	0	4	0	6	4	4	3,4	Extracellular Space	transporter
acyl-CoA synthetase long-chain family member 1	ACSL1	IPI00012728	2	10	3	3	0	4	3,2	Cytoplasm	enzyme
translocase of inner mitochondrial membrane 50 homolog	TIMM50	IPI00418497	8	8	0	8	0	10	3,1	Cytoplasm	phosphatase
BCL2-associated X protein	BAX	IPI00071059	6	8	0	4	0	7	3,0	Cytoplasm	other
structure specific recognition protein 1	SSRP1	IPI00005154	8	6	2	10	0	15	3,0	Nucleus	other
mediator of DNA-damage checkpoint 1	MDC1	IPI00470805	4	2	2	7	0	9	2,9	Nucleus	other
minichromosome maintenance complex component 5	MCM5	IPI00018350	5	5	3	11	2	12	2,7	Nucleus	enzyme
phosphofructokinase, muscle	PFKM	IPI00465179	0	6	9	11	0	5	2,4	Cytoplasm	kinase
SON DNA binding protein	SON	IPI00000192	9	12	0	6	0	4	2,3	Nucleus	other
UDP glucuronosyltransferase 1 family, polypeptide A6	UGT1A6	IPI00451965	0	7	11	19	0	0	2,3	Cytoplasm	enzyme
LUC7-like 2 (<i>S. cerevisiae</i>)	LUC7L2	IPI00006932	0	8	5	5	4	8	2,3	unknown	other
thiosulfate sulfurtransferase (rhodanese)	TST	IPI00216293	0	12	7	15	10	12	2,2	Cytoplasm	enzyme
cytochrome P450, family 51, subfamily A, polypeptide 1	CYP51A1	IPI00295772	4	4	2	9	4	10	2,2	Cytoplasm	enzyme
aldo-keto reductase family 1, member C3	AKR1C3	IPI00291483	0	15	17	29	4	2	2,1	Cytoplasm	enzyme
aconitase 2, mitochondrial	ACO2	IPI00017855	7	18	18	43	14	17	1,9	Cytoplasm	enzyme
nipsnap homolog 1 (<i>C. elegans</i>)	NIPSNAP1	IPI00304435	2	6	6	16	9	11	1,9	Cytoplasm	enzyme
minichromosome maintenance complex component 3	MCM3	IPI00013214	8	8	8	15	3	14	1,9	Nucleus	enzyme
suppression of tumorigenicity 13 (colon carcinoma) (Hsp70 interacting protein)	ST13	IPI00032826	4	5	7	11	4	13	1,9	Cytoplasm	other
general transcription factor Iii	GTF2I	IPI00054042	12	20	12	16	7	24	1,9	Nucleus	transcription regulator
suppressor of Ty 16 homolog (<i>S. cerevisiae</i>)	SUPT16H	IPI00026970	18	26	12	28	15	32	1,8	Nucleus	transcription regulator
minichromosome maintenance complex component 7	MCM7	IPI00299904	14	7	6	17	2	17	1,8	Nucleus	enzyme
spectrin repeat containing, nuclear envelope 2	SYNE2	IPI00239405	22	43	3	20	22	24	1,8	Nucleus	other
minichromosome maintenance complex component 2	MCM2	IPI00184330	14	10	6	18	6	18	1,7	Nucleus	enzyme
PRP8 pre-mRNA processing factor 8 homolog (<i>S. cerevisiae</i>)	PRPF8	IPI00007928	32	46	26	48	28	50	1,6	Nucleus	other
solute carrier family 12 (sodium/potassium/chloride transporters), member 2	SLC12A2	IPI00022649	22	55	16	41	39	33	1,6	Plasma Membrane	transporter
TNF receptor-associated protein 1	TRAP1	IPI00030275	22	20	17	34	16	35	1,6	Cytoplasm	enzyme
ubiquitin specific peptidase 5 (isopeptidase T)	USP5	IPI00024664	17	32	14	17	7	13	1,6	Cytoplasm	peptidase
phosphoribosylglycinamide formyltransferase,	GART	IPI00025273	33	42	26	42	13	29	1,5	Cytoplasm	enzyme

Proteome differences between colon cancer stem cells and differentiated tumor cells identifies BIRC6

carcinoembryonic antigen-related cell adhesion molecule 5	CEACA	IPI00027486	0	15	15	24	28	27	1,5	Plasma Membrane	other
methylenetetrahydrofolate dehydrogenase (NADP+ dependent) 1,	MTHFD1	IPI00218342	33	42	24	40	18	32	1,5	Cytoplasm	enzyme
protein disulfide isomerase family A, member 4	PDIA4	IPI00009904	50	75	88	119	62	107	1,5	Cytoplasm	enzyme
splicing factor proline/glutamine-rich	SFPQ	IPI00010740	16	32	25	30	16	24	1,5	Nucleus	other
protein kinase, DNA-activated, catalytic polypeptide	PRKDC	IPI00296337	187	198	110	199	178	303	1,4	Nucleus	kinase
splicing factor 3b, subunit 1, 155kDa	SF3B1	IPI00026089	22	36	23	30	19	27	1,4	Nucleus	other
dynein, cytoplasmic 1, heavy chain 1	DYNC1H1	IPI00456969	176	199	129	213	131	210	1,4	Cytoplasm	peptidase
heat shock 70kDa protein 4	HSPA4	IPI00002966	68	70	27	56	20	36	1,3	Cytoplasm	other
epiplakin 1	EPPK1	IPI00010951	35	89	82	43	58	102	1,3	Cytoplasm	other

Proteins associated with survival are upregulated in colon cancer stem cells

Next, we divided the upregulated proteins in three categories:

- Top upregulated, ≥ 2 fold upregulated in 3 out of 3 isogenic pairs
- Sub-top upregulated, $\geq 1,5$ fold upregulated in 3 out of 3 isogenic pairs
- Rest upregulated, $\geq 1,5$ fold upregulated in 2 out of 3 isogenic pairs

The top upregulated category contains 32 proteins. Interestingly, among the top upregulated proteins is ALDH1A1 (aldehyde dehydrogenase 1) which was recently identified by us and others as a bona fide colon cancer stem cell marker¹⁹. The identification of ALDH1 demonstrates the validity of our proteomics approach to identify upregulated factors in cancer stem cells.

Next, we used the Ingenuity Pathway Knowledge Base tool to identify biological functions and canonical pathways that are most different between colonospheres and differentiated cells. As shown in table 4, there are 17 proteins upregulated in colonospheres associated with cell death regulation. Also, this analysis revealed 14 upregulated proteins involved in small molecule degradation. The top canonical pathways as determined by the Ingenuity Pathway Knowledge Base tool were aryl hydrocarbon receptor signaling, estrogen receptor signaling, mitochondrial dysfunction and xenobiotic metabolism signaling.

Given our interest in drug resistance we further focused on proteins regulating cell death and survival. The Ingenuity Pathway Knowledge Base tool shows that proteins promoting cell survival are significantly upregulated in the colonospheres when compared to the differentiated tumor cells (Table 5). Baculoviral IAP repeat-containing 6 (BIRC6; also known as BRUCE or Apollon), an Inhibitor of Apoptosis Protein (IAP), was the most prominently upregulated survival protein.

Table 4. The main biological functions and canonical pathways extracted from table 3, as assessed with Ingenuity Pathway Analysis.

Top Molecular and Cellular Functions	Associated molecules	Focus molecules
Cell Death	ABCB1, ALDH1A1, BAX, BIRC6 , CTBP1, EIF3H, EP400, HSPA4, HTT, MCM2, MDC1, PRKDC, PTK2, SDHA, SDHB, TIMM50, TRAP1	17
Small Molecule biochemistry	ABCB1, ACO2, ADSL, AKR1C3, ALDH1A1, BAX, BDH2, GPX4, HSPA4, HTT, MAT2B, SDHA, TST, UGDH	14
Top Canonical Pathways	Associated molecules	Ratio
Aryl hydrocarbon receptor signaling	ALDH1A1, ALDH1B1, BAX, MCM7, MGST2, NEDD8	6/138
Estrogen receptor signaling	CTBP1, NCOR1, PRKDC, TAF15, TRRAP	5/116
Mitochondrial dysfunction	GPX4, NDUFA11, SDHA, SDHB	4/126
Xenobiotic metabolism signaling	ABCB1, ALDH1A1, ALDH1B1, FTL, MGST2	5/260

Table 5. All upregulated proteins playing a role in cell death signaling. In the last two columns, the sign '+' indicates whether the protein is anti-apoptotic, pro-apoptotic or both.

Protein	Gene	Accession. Number	fold change	anti-apoptotic	pro-apoptotic
baculoviral IAP repeat-containing 6	BIRC6	IPI00299635	∞	+	
eukaryotic translation initiation factor 3, subunit H	EIF3H	IPI00647650	∞	+	
C-terminal binding protein 1	CTBP1	IPI00012835	∞	+	
succinate dehydrogenase complex, subunit B, iron sulfur	SDHB	IPI00294911	9,2	+	+
E1A binding protein p400	EP400	IPI00064931	8,2	+	
PTK2 protein tyrosine kinase 2	PTK2	IPI00012885	4,8	+	
aldehyde dehydrogenase 1 family, member A1	ALDH1A1	IPI00218914	3,4	+	
ATP-binding cassette, sub-family B (MDR), member 1	ABCB1	IPI00027481	3,8	+	
BCL2-associated X protein	BAX	IPI00071059	3,0		+
succinate dehydrogenase complex, subunit A	SDHA	IPI00305166	2,6	+	
Huntingtin	HTT	IPI00002335	∞	+	+
translocase of inner mitochondrial membrane 50	TIMM50	IPI00418497	3,1	+	
mediator of DNA-damage checkpoint 1	MDC1	IPI00470805	2,9	+	+
minichromosome maintenance complex component 2	MCM2	IPI00184330	1,7	+	
TNF receptor-associated protein 1	TRAP1	IPI00030275	1,6	+	
protein kinase, DNA-activated, catalytic polypeptide	PRKDC	IPI00296337	1,4	+	
heat shock 70kDa protein 4	HSPA4	IPI00002966	1,3	+	

BIRC6 mediates resistance of colorectal cancer stem cells to platinum compounds

Given that BIRC6 was the highest upregulated survival protein in colonosphere cells, we hypothesized that it could play a role in chemotherapy resistance. To test this hypothesis, we first validated BIRC6 expression in the three sets of isogenic cell pairs by Western blotting. In line with the proteomics data, BIRC6 was highly upregulated in colonospheres when compared to differentiated cells (Figure 3A). Likewise, we validated the proteomics data for ALDH1¹⁶. Our previous results show that Aldefluor[®] high cells are the tumorigenic and clonogenic cells in colonospheres ¹⁶. Therefore, we separated Aldefluor[®] high and Aldefluor[®] low cells by FACS sorting (Figure 3B). Figure 3C shows that BIRC6 is highly expressed in Aldefluor[®] high cells, but very low in Aldefluor[®] low cells. This result confirms that BIRC6 is mainly expressed in colonogenic/tumorigenic colon cancer stem cells.

Next, we assessed the importance of BIRC6 in mediating colonosphere resistance to oxaliplatin and cisplatin, two frequently used chemotherapeutic drugs. To this end, expression of BIRC6 was suppressed in colonospheres by using a set of lentiviral RNA interference (RNAi) vectors. Two vectors (58 en 59) were found to suppress BIRC6 expression very efficiently (Figure 4A). Control and BIRC6 knockdown colonospheres and differentiated tumor cells were treated with increasing concentrations of oxaliplatin or cisplatin and cell viability was measured by standard MTS assays. Knockdown of BIRC6 resulted in a significantly higher response of colonosphere cells to oxaliplatin and cisplatin (Figure 4B and 4C). The sensitivity of BIRC6 knockdown cells to both drugs was comparable to that of the differentiated tumor cells. These results identify BIRC6 as an important mediator of resistance to oxaliplatin and cisplatin and suggest that high BIRC6 expression may selectively protect the cancer stem cell fraction against these drugs.

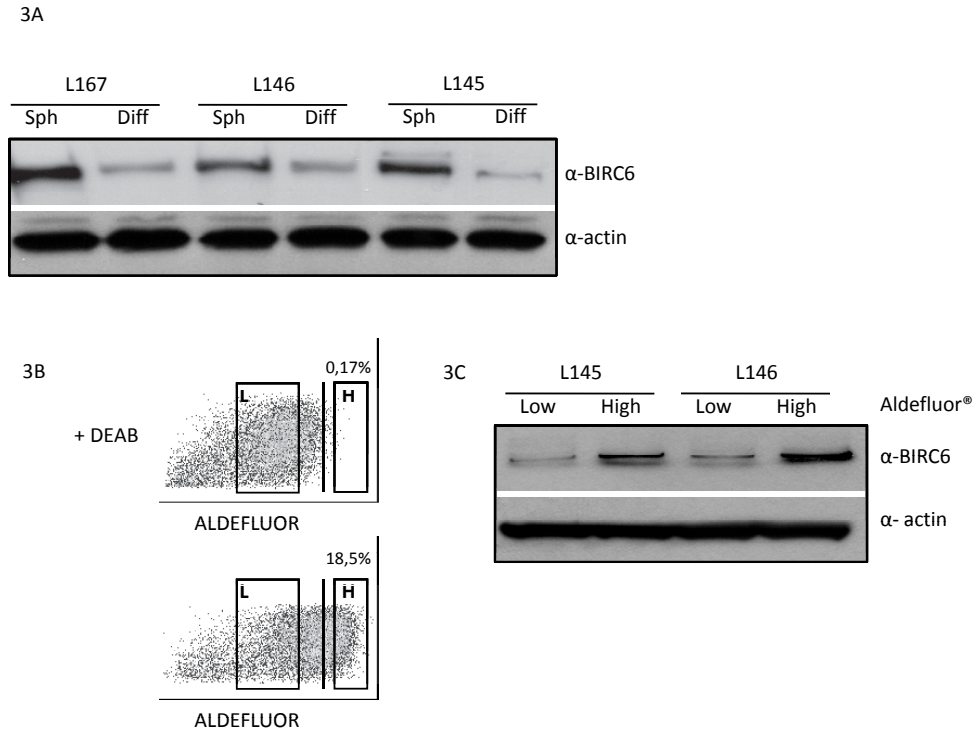


Figure 3. A. Western blotting analysis of BIRC6 levels in colonospheres and differentiated cells in all pairs. B. Aldefluor[®] FACS analysis for L145 colonospheres. C. Western blotting analysis of high and low Aldefluor[®] sorted cell populations of BIRC6. See page 203 for color figure

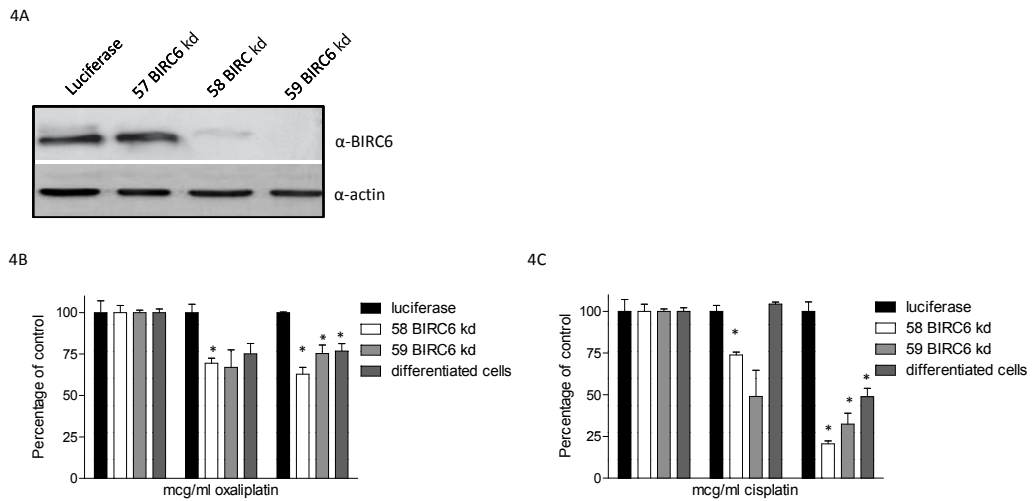


Figure 4. A. Western blotting analysis of efficient knock down of BIRC6 in L145 colonospheres. B. Viability assay of control and BIRC6 deleted L145 cells after treatment with oxaliplatin or cisplatin by MTS assay. * $p < 0,05$.

Discussion

In the present study we have used a proteomics approach to identify potential regulators of drug resistance in colorectal cancer stem cells. We identified known (ALDH1) and novel factors enriched in cancer stem cell cultures (colonospheres) when compared to stably differentiated tumor cells. Importantly, cancer stem cells were characterized by high expression of a set of survival proteins, the most prominent of which was BIRC6. BIRC6 deletion is associated with sensitization to chemotherapy in *in vivo* and *in vitro* studies^{20, 21}. Furthermore, BIRC6 deletion promotes p53 stabilization and caspase 3 activation²².

Our data show that specifically colorectal cancer stem cell cultures display increased resistance to oxaliplatin and to cisplatin and that BIRC6 is an important mediator of resistance. Previously, it was shown by gene expression profiling that BIRC1 and BIRC6 are upregulated in colorectal tumors when compared to normal intestinal issue²³. Our results suggest that it is predominantly the cancer stem cell-fraction in colorectal tumors that expresses this survival protein.

BIRC 6, also known as Apollon or Bruce, belongs to the family of inhibitor of apoptosis (IAP) proteins. IAP's are major regulators of apoptosis due, at least in part, to their ability to inhibit caspase activation^{24, 25}. Human IAP family members include X-chromosome-linked IAP (XIAP, also known as BIRC4), cellular IAP 1 (c-IAP1 also known as BIRC2), c-IAP2 (also known as BIRC3), neuronal apoptosis inhibitory protein (also known as BIRC1) and survivin (also known BIRC5). IAP proteins contain one to three baculovirus IAP repeat (BIR) domains that are required for their antiapoptotic activity²⁴. Our results are in line with previous studies showing that cancer stem cells express high levels of anti-apoptotic proteins and resist apoptotic stimuli^{26, 27}. Recently it was demonstrated that IL4-stimulated expression of survivin (BIRC5) protects colorectal cancer stem cells against apoptosis^{10, 27, 28}. The proteomics approach described here did not identify BIRC5 as a cancer stem cell-enriched protein. Possibly, different tumors resist apoptotic stimuli by increasing the expression of distinct IAP family members.

Since IAP's play an important role in tumor maintenance and therapy resistance they represent attractive targets for targeted therapy. Furthermore, IAP's are highly expressed in several cancer tissues²⁹. Several small molecule IAP inhibitors have been developed, including Smac-based peptides and Smac mimetics targeting a broad spectrum of IAP's^{30, 31}. Pre-clinical studies in mice carrying xenograft tumors have shown promising anti-tumor efficacy in the treatment of malignant glioma, breast cancer, non-small cell lung cancer, and multiple myeloma. However, most of these preclinical studies have focused on XIAP and survivin, rather than on BIRC6^{32, 33}. Several IAP inhibitors are being tested for their safety and anti-tumor efficacy in clinical trials either in combination with irradiation or with chemotherapy.^{34, 35} It is not yet established whether these compounds also target BIRC6. Since SMAC mimetics bind to and inhibit the IAP BIR domains and that SMAC binds BIRC6³⁶, it is not unlikely that SMAC mimetics also inhibit BIRC6 function.

Based on the data presented here we propose that BIRC6 protects the cancer stem cell fraction of colorectal tumors against oxaliplatin and cisplatin. Targeting BIRC6 by SMAC mimetics or by novel BIRC6 inhibitors may therefore be effective in combination with platinum-based anticancer drugs. This may help eradicating the cancer stem cell fraction in colorectal tumors.

References

1. Chau, I. & Cunningham, D. Treatment in advanced colorectal cancer: what, when and how? *Br. J. Cancer* (2009).
2. Ricci-Vitiani, L. et al. Identification and expansion of human colon-cancer-initiating cells. *Nature* 445, 111-115 (2007).
3. O'Brien, C.A., Pollett, A., Gallinger, S., & Dick, J.E. A human colon cancer cell capable of initiating tumour growth in immunodeficient mice. *Nature* 445, 106-110 (2007).
4. Todaro, M., Francipane, M.G., Medema, J.P., & Stassi, G. Colon cancer stem cells: promise of targeted therapy. *Gastroenterology* 138, 2151-2162 (2010).
5. Vermeulen, L. et al. Single-cell cloning of colon cancer stem cells reveals a multi-lineage differentiation capacity. *Proc. Natl. Acad. Sci. U. S. A* 105, 13427-13432 (2008).
6. Barker, N. et al. Crypt stem cells as the cells-of-origin of intestinal cancer. *Nature* 457, 608-611 (2009).
7. Zhu, L. et al. Prominin 1 marks intestinal stem cells that are susceptible to neoplastic transformation. *Nature* 457, 603-607 (2009).
8. Clarke, M.F. et al. Cancer stem cells—perspectives on current status and future directions: AACR Workshop on cancer stem cells. *Cancer Res.* 66, 9339-9344 (2006).
9. Hamburger, A.W. & Salmon, S.E. Primary bioassay of human tumor stem cells. *Science* 197, 461-463 (1977).
10. Todaro, M. et al. Colon cancer stem cells dictate tumor growth and resist cell death by production of interleukin-4. *Cell Stem Cell* 1, 389-402 (2007).
11. Dylla, S.J. et al. Colorectal cancer stem cells are enriched in xenogeneic tumors following chemotherapy. *PLoS ONE* 3, e2428 (2008).
12. Dean, M., Fojo, T., & Bates, S. Tumour stem cells and drug resistance. *Nat. Rev. Cancer* 5, 275-284 (2005).
13. Dean, M. ABC transporters, drug resistance, and cancer stem cells. *J. Mammary. Gland. Biol. Neoplasia* 14, 3-9 (2009).
14. Liu, G. et al. Analysis of gene expression and chemoresistance of CD133+ cancer stem cells in glioblastoma. *Mol. Cancer* 5, 67 (2006).
15. Hermann, P.C. et al. Distinct populations of cancer stem cells determine tumor growth and metastatic activity in human pancreatic cancer. *Cell Stem Cell* 1, 313-323 (2007).
16. Emmink, B.L. et al. Differentiated colorectal cancer cells protect tumor-initiating cells from irinotecan. *Gastroenterology* in press. 2011. Ref Type: Generic
17. Shevchenko, A., Wilm, M., Vorm, O., & Mann, M. Mass spectrometric sequencing of proteins silver-stained polyacrylamide gels. *Anal. Chem.* 68, 850-858 (1996).
18. Shevchenko, A., Wilm, M., Vorm, O., & Mann, M. Mass spectrometric sequencing of proteins silver-stained polyacrylamide gels. *Anal. Chem.* 68, 850-858 (1996).
19. Huang, E.H. et al. Aldehyde dehydrogenase 1 is a marker for normal and malignant human colonic stem cells (SC) and tracks SC overpopulation during colon tumorigenesis. *Cancer Res.* 69, 3382-3389 (2009).
20. Chu, L. et al. Oncolytic adenovirus-mediated shRNA against Apollon inhibits tumor cell growth and enhances antitumor effect of 5-fluorouracil. *Gene Ther.* 15, 484-494 (2008).
21. Chen, Z. et al. A human IAP-family gene, apollon, expressed in human brain cancer cells. *Biochem. Biophys. Res. Commun.* 264, 847-854 (1999).
22. Lopergolo, A. et al. Apollon gene silencing induces apoptosis in breast cancer cells through p53 stabilisation and caspase-3 activation. *Br. J. Cancer* 100, 739-746 (2009).
23. Bianchini, M. et al. Comparative study of gene expression by cDNA microarray in human colorectal cancer tissues and normal mucosa. *Int. J. Oncol.* 29, 83-94 (2006).
24. Salvesen, G.S. & Duckett, C.S. IAP proteins: blocking the road to death's door. *Nat. Rev. Mol. Cell Biol.* 3, 401-410 (2002).
25. Deveraux, Q.L., Stennicke, H.R., Salvesen, G.S., & Reed, J.C. Endogenous inhibitors of caspases. *J. Clin. Immunol.* 19, 388-398 (1999).
26. Eramo, A. et al. Chemotherapy resistance of glioblastoma stem cells. *Cell Death. Differ.* 13, 1238-1241 (2006).

27. Signore,M., Ricci-Vitiani,L., & De,M.R. Targeting apoptosis pathways in cancer stem cells. *Cancer Lett.* (2011).
28. Di Stefano,A.B. et al. Survivin is regulated by interleukin-4 in colon cancer stem cells. *J. Cell Physiol* 225, 555-561 (2010).
29. Yang,L., Cao,Z., Yan,H., & Wood,W.C. Coexistence of high levels of apoptotic signaling and inhibitor of apoptosis proteins in human tumor cells: implication for cancer specific therapy. *Cancer Res.* 63, 6815-6824 (2003).
30. Chen,D.J. & Huerta,S. Smac mimetics as new cancer therapeutics. *Anticancer Drugs* 20, 646-658 (2009).
31. Flygare,J.A. & Fairbrother,W.J. Small-molecule pan-IAP antagonists: a patent review. *Expert. Opin. Ther. Pat* 20, 251-267 (2010).
32. Oost,T.K. et al. Discovery of potent antagonists of the antiapoptotic protein XIAP for the treatment of cancer. *J. Med. Chem.* 47, 4417-4426 (2004).
33. Fulda,S., Wick,W., Weller,M., & Debatin,K.M. Smac agonists sensitize for Apo2L/T. *Nat. Med.* 8, 808-815 (2002).
34. Gyrd-Hansen,M. & Meier,P. IAPs: from caspase inhibitors to modulators of NF-kappaB, inflammation and cancer. *Nat. Rev. Cancer* 10, 561-574 (2010).
35. Fulda,S. Targeting inhibitor of apoptosis proteins (IAPs) for cancer therapy. *Anticancer Agents Med. Chem.* 8, 533-539 (2008).
36. Chen,D.J. & Huerta,S. Smac mimetics as new cancer therapeutics. *Anticancer Drugs* 20, 646-658 (2009).

— |

— |



9

General Discussion

Viral gene therapy for solid tumors

Genetic manipulation of oncolytic viral vectors in order to enhance infectivity and improve selectivity has resulted in the generation of dozens of vectors available for evaluation in specific settings. In this thesis, we evaluated the efficacy of a series of oncolytic viral vectors for the treatment of glioma and colorectal tumors. In **chapter 2**, we showed successful infection of glioma cells *in vitro* by capsid-modified adenoviral vectors, but disappointing enhancement of infectivity in *in vivo* experiments. This may be explained by the limited ability of viral vectors to infiltrate the tissue due to dense tumor structure and extra cellular matrix proteins¹. Also, since the viral vectors were replication incompetent, infection is likely to be restricted to tumor cells up to 5 layers away from the needle tract². Furthermore, viral particles may bind to matrix proteins which can act as virus scavengers³. Also the host immune response might play a role in resistance⁴. Despite all these potential hurdles towards effective oncolysis, capsid modification strategies were very efficient in *in vitro* and *in vivo* studies on ovarian carcinoma⁵. One way to increase infectivity is to apply the capsid modifications to conditionally replicating adenoviral vectors^{6,7}

In **chapter 3**, we presented a very selective, conditionally replicating adenovirus for the treatment of glioma. Since the survivin promoter is highly active in glioma cells, this virus selectively kills glioma cells while sparing astrocytes and human brain cells. Interestingly, viral vectors based on selective activation of the survivin promoter have been successfully tested both *in vitro* and *in vivo* in the treatment of several other cancer types, like oral cancer, cholangiocarcinoma and ovarium cancer⁸⁻¹¹. Remarkably, these viral vectors combined transcriptional targeting with selective capsid modification, underscoring the potential of transductional targeting strategies. In ongoing clinical trials, most adenoviral vectors are combining conditional replication strategies with selective capsid modification. Future research will probably have to combine both selective replication and capsid modification techniques, wherein the application of targeting strategies depend on specific tumor or patient bound molecular factors. This concept of personalized medicine is already accepted in several new targeting strategies like herceptin or cetuximab treatment, but might also play a role in oncolysis therapy.

Several clinical trials with different viral vector types have been reported on oncolytic therapy for glioma.¹² Although the safety of these vectors has been confirmed, viral therapy for glioma has so far failed to improve patient survival. One of the major limitations in systemic treatment for glioma is the difficult delivery to the tumor, due to the blood brain barrier. Therefore, the novel technique of convection-enhanced delivery (CED) has been developed. The CED technique involves intracranial therapeutic drug delivery via a subcutaneous port access system connected to an external pump. This allows highly efficient, homogeneous, and targeted administration of the drug, bypassing the blood–brain barrier¹³. This technique has revealed promising results for oncolysis therapy as well.¹⁴

Since reovirus oncolysis is facilitated in cells with an activated RAS pathway^{15, 16}, we evaluated the Reovirus type 3 Dearing (T3D) strain in the context of colorectal cancer (**chapter 4**). We demonstrated that in freshly isolated colorectal cancer samples, efficient infection of reovirus T3D is hindered unless viral particles are proteolytically transformed into infectious subviral particles (ISVPs). Furthermore, even after successful infection, the cells rapidly shut down viral protein synthesis. These major limitations for infectivity in human biopsies suggest that systemic mono-treatment of colorectal cancer with reovirus is expected to fall short. However, combination treatment using reovirus T3D in combination with chemotherapy or radiation may yield synergistic anti-tumor effects¹⁷. Therefore, current clinical trials combine reovirus treatment with conventional chemotherapy or radiotherapy.¹⁸⁻²⁰ Another limitation of reovirus as an oncolytic agent is that genetic manipulation of reovirus is challenging due to its double stranded RNA genome and the tight packaging constraints imposed on progeny virus. Nevertheless, several novel experimental techniques allowing genetic modification of reovirus genomes have recently been developed²¹. This may result in more promising reovirus based treatment strategies in the future.

Targeting the EGFR-RAS-ERK pathway in colorectal cancer

In **chapter 5 and 6**, we analyzed how activating mutations in the *KRAS* oncogene influence targeting strategies in colorectal cancer. The *KRAS* oncogene is known to be a strong negative predictor of response to EGFR targeted therapy. In **chapter 5**, we focused on the effects of *KRAS* mutations on EGFR signaling and inhibition. In line with the growing evidence in large clinical studies²²⁻²⁴, we found that both extracellular and intracellular EGFR targeting agents are ineffective in colorectal cancer cells with an activating mutation in *KRAS*. In search for explanations for this striking resistance, we found that mutant *KRAS* causes intracellular retention of the EGFR which diminishes the tumor cell response to both EGF induced activation and EGFR inhibition. Our results are in line with and extend the current dogma that resistance is due to the constitutive activation of downstream *KRAS* signaling pathways^{25, 26}. This reduces tumor cell dependency on activation of those pathways by upstream growth factor receptors like EGFR. However, our results indicate that endogenous *KRAS* mutations are not only associated with complete EGFR independence, but also with aberrant EGFR localization. Interestingly, we found that inhibition of BRAF, MEK, p38 or PI3K or combined inhibition of these pathways did not lead to renewed sensitivity of the cells to EGFR inhibition nor restoration of EGFR localization. Taken together, these results confirm the strong association between the oncogene *KRAS* en resistance to EGFR targeted therapy. Furthermore, endogenous *KRAS* mutations are strongly associated with aberrant EGFR localization, which adds an alternative explanation for resistance to EGFR targeted therapy. Future work is needed to expose the mechanism underlying these findings.

Of all colorectal cancer patients treated with EGFR inhibitors, about 10% respond to therapy.²⁷ This implies that mutations in the *KRAS* oncogene cannot be the only negative predictor for response, since only 30-40% of all colorectal cancer patients harbor a *KRAS* mutation. Several negative predictors have been suggested, including mutations in the PI3K/PTEN pathway,

mutations in PIK3CA or loss of PTEN^{27, 28}. High levels of the EGFR protein as determined by immunohistochemistry fail to correlate with response to EGFR targeted therapy²⁹, in contrast to the strong correlation between Her-2-Neu expression and response to trastuzumab in breast cancer.³⁰ Of note, we observed a striking pattern of aberrant EGFR localization in about 80 % of all tumors in clinical samples of colorectal tumors. The normal, basolateral-membranous staining was only observed in a small minority of the tumors. Therefore, it is possible that localization of EGFR, rather than total protein levels, may predict therapy response in wild type KRAS tumors. This hypothesis should be further explored in samples of cetuximab-treated cohorts of colorectal cancer patients.

The classical RAS/RAF/MEK/ERK pathway, one of the 4 MAPKinase pathways, is a logical target for therapeutic intervention. It is known to play a role in cell transformation and oncogenesis in cancer types driven by KRAS, NRAS or BRAF mutations³¹. In the case of tumors with BRAF mutations, for example melanoma, direct inhibition of BRAF or inhibition of downstream MEK is very effective and suppresses growth of tumors in *in vivo* models.³² However, KRAS-induced oncogenesis may not depend on MEK/ERK signaling. In **chapter 6**, we further explored the hypothesis that tumor cells with endogenous KRAS mutations are less sensitive to MEK inhibition. This is in line with recent literature reporting resistance of KRAS mutated cells to MEK inhibition.^{33, 34} We demonstrated that mutant KRAS allows cells to bypass MEK/ERK inhibition by activating the p38 MAPKinase pathway³⁵. This allows activation of transcriptional targets that are shared by the MEK/ERK and the p38 MAPK pathway.

MAPK signaling cascades are intensively studied in the context of human cancer. In cells with oncogenic mutations such as those in KRAS or BRAF, constitutive downstream signaling results in several pathological cross talk mechanisms between the different MAPK pathways.³⁶ This is in line with reports proving that activation of p38 and JNK can result in activation of MEK 1/2 via activating kinases downstream p38 and JNK^{37, 38}. These findings combined with our results raises the question whether targeting a single MAPK pathway such as the MEK/ERK pathway in cells harboring a KRAS mutation will lead to efficient tumor cell eradication. Combination regimens targeting two or more MAPK pathways are perhaps more likely to be successful.

The strong correlation between KRAS mutations and resistance to both EGFR and MEK directed therapy can have important consequences. Response predictors including KRAS mutations can prevent potential harmful side effects of unnecessary treatment and increase their cost-effectiveness³⁹. The average costs per patient for medical treatment of tumors have raised significantly since the introduction of targeted therapy. Therefore, the cost-effectiveness profile of new targeted therapy agents has become more important. Recently, the National Institute for Health and Clinical Excellence (NICE) in Great Britain has decided, based on cost-effectiveness profiles, not to recommend treatment of metastatic squamous cell carcinoma of the head and neck with cetuximab combined with platinum-based regimens.⁴⁰ These developments underline the importance of patient selection for targeted therapy, based on predictors for response to treatment.

Targeting colon cancer stem cells

Drug resistance in colon cancer stem cells

Colon cancer stem cells may be inert to toxic environmental agents due to several intrinsic resistance mechanisms. These resistance mechanisms may include high expression levels of ABC transporters, active DNA repair capacity and high expression of anti-apoptotic factors^{41, 42}. Interestingly, by using a cancer stem cell tissue culture model (**chapter 7**) we showed that one of the ABC transporters, ABCB1, plays an important role in resistance to irinotecan treatment. However, our results indicate that colorectal cancer stem cells do not display intrinsic resistance to irinotecan. Instead, the drug-sensitive cancer stem cells appear to be protected by a drug resistant, differentiated cell population originating from the cancer stem cells. The concept of functional cooperation between differentiated (non-tumorigenic) and undifferentiated tumorigenic colon cancer stem cells in mediating drug resistance provides a novel paradigm for drug resistance. So far, several reversal trials with ABC transporter inhibitors in combination with chemotherapeutics have been performed in colorectal cancer patients, but none of these involved irinotecan. Also, these results are generally disappointing.^{43, 44} The contribution of ABC transporters to resistance to irinotecan treatment in colorectal cancer patients is currently unknown, but future studies should focus on analyzing patients samples of irinotecan treated tumors for correlations between ABC transporter expression, localization and response to therapy. Furthermore, combined treatment of human colorectal cancer tissue with ABCB1 inhibitors and irinotecan should be performed to determine the killing potential on cancer stem cells.

In **chapter 8**, we have defined a different resistance mechanism that operates in the cancer stem cells themselves. Altered expression of apoptosis regulators has been related to chemoresistance in several tumor types⁴⁵ Remarkably, the results of the unbiased proteomics study also suggests that cancer stem cells are characterized by altered cell death signaling, when compared to differentiated tumor cells. BIRC6 was identified as a key player in apoptosis resistance to platinum containing anti-cancer drugs. BIRC6 is a member of the inhibitors of apoptosis proteins (IAPs), proteins known to play an important role in preventing apoptosis in cancer cells.⁴⁶ The BIRC6-related protein survivin (BIRC5) also plays an important role in therapy resistance in colorectal cancer stem cells.^{47, 48} So far, no specific BIRC6 inhibitors have been developed, but our results indicate that efforts to target BIRC6 are recommended for the treatment of colon cancer stem cells. In addition, other inhibitors of apoptosis proteins have been successfully targeted in pre-clinical and clinical studies by SMAC mimetics.⁴⁹⁻⁵¹ These SMAC mimetics target several IAP members, but were not specifically tested for their ability to inhibit BIRC6. Nevertheless, since we showed that the cell death machinery in colon cancer stem cells is altered, new studies with SMAC inhibitors targeting several BIRC proteins combined with platinum based chemotherapy are logical next steps for further exploration.

Taken together we have demonstrated in **chapter 7 and 8** that the relationship between cancer stemness and tumor initiating potential can be radically different when studying different anti-cancer drugs. Resistance to oxaliplatin follows the dogma that colon cancer stem cells are intrinsically resistant to anticancer drugs. In addition, we have identified BIRC6 as a novel key player mediating this resistance.

By contrast, the relationship between irinotecan resistance and tumor initiating potential is radically different. In this case the colon cancer stem cells are intrinsically drug-sensitive and are protected by a shield of drug resistant and drug-expelling differentiated tumor cells. In this case we propose that differentiated cells keep the intratumor drug concentration low by actively expelling irinotecan into the tumor lumen, thereby providing *in trans* protection of colon cancer stem cells against the drug.

References

1. Sauthoff, H. et al. Intratumoral spread of wild-type adenovirus is limited after local injection of human xenograft tumors: virus persists and spreads systemically at late time points. *Hum. Gene Ther.* 14, 425-433 (2003).
2. Jia, W. & Zhou, Q. Viral vectors for cancer gene therapy: viral dissemination and tumor targeting. *Curr. Gene Ther.* 5, 133-142 (2005).
3. Haviv, Y.S. & Curiel, D.T. Conditional gene targeting for cancer gene therapy. *Adv. Drug Deliv. Rev.* 53, 135-154 (2001).
4. Liu, Q. & Muruve, D.A. Molecular basis of the inflammatory response to adenovirus vectors. *Gene Ther.* 10, 935-940 (2003).
5. Wu, H. et al. Preclinical evaluation of a class of infectivity-enhanced adenoviral vectors in ovarian cancer gene therapy. *Gene Ther.* 11, 874-878 (2004).
6. Ulasov, I.V. et al. Survivin-driven and fiber-modified oncolytic adenovirus exhibits potent antitumor activity in established intracranial glioma. *Hum. Gene Ther.* 18, 589-602 (2007).
7. Zhu, Z.B. et al. Incorporating the survivin promoter in an infectivity enhanced CRAAd-analysis of oncolysis and anti-tumor effects in vitro and in vivo. *Int. J. Oncol.* 27, 237-246 (2005).
8. van Zeeburg, H.J. et al. Comparison of oncolytic adenoviruses for selective eradication of oral cancer and pre-cancerous lesions. *Gene Ther.* 17, 1517-1524 (2010).
9. Kimball, K.J. et al. Novel infectivity-enhanced oncolytic adenovirus with a capsid-incorporated dual-imaging moiety for monitoring virotherapy in ovarian cancer. *Mol. Imaging* 8, 264-277 (2009).
10. Zhu, Z.B. et al. Survivin promoter-based conditionally replicative adenoviruses target cholangiocarcinoma. *Int. J. Oncol.* 29, 1319-1329 (2006).
11. Zhu, Z.B. et al. Development of an optimized conditionally replicative adenoviral agent for ovarian cancer. *Int. J. Oncol.* 32, 1179-1188 (2008).
12. Dent, P. et al. Searching for a cure: gene therapy for glioblastoma. *Cancer Biol. Ther.* 7, 1335-1340 (2008).
13. Bogdahn, U. et al. Targeted therapy for high-grade glioma with the TGF-beta2 inhibitor trabedersen: results of a randomized and controlled phase IIb study. *Neuro. Oncol.* 13, 132-142 (2011).
14. Debinski, W. & Tatter, S.B. Convection-enhanced delivery to achieve widespread distribution of viral vectors: Predicting clinical implementation. *Curr. Opin. Mol. Ther.* 12, 647-653 (2010).
15. Smakman, N. et al. KRAS(D13) Promotes apoptosis of human colorectal tumor cells by ReovirusT3D and oxaliplatin but not by tumor necrosis factor-related apoptosis-inducing ligand. *Cancer Res.* 66, 5403-5408 (2006).
16. Coffey, M.C., Strong, J.E., Forsyth, P.A., & Lee, P.W. Reovirus therapy of tumors with activated Ras pathway. *Science* 282, 1332-1334 (1998).
17. Thirukkumar, C. & Morris, D.G. Oncolytic viral therapy using reovirus. *Methods Mol. Biol.* 542, 607-634 (2009).
18. Harrington, K.J. et al. Two-stage phase I dose-escalation study of intratumoral reovirus type 3 dearing and palliative radiotherapy in patients with advanced cancers. *Clin. Cancer Res.* 16, 3067-3077 (2010).
19. Comins, C. et al. REO-10: a phase I study of intravenous reovirus and docetaxel in patients with advanced cancer. *Clin. Cancer Res.* 16, 5564-5572 (2010).
20. Lolkema, M.P. et al. A phase I study of the combination of intravenous reovirus type 3 dearing and gemcitabine in patients with advanced cancer. *Clin. Cancer Res.* 17, 581-588 (2011).
21. Van Den Wollenberg, D.J., Van Den Hengel, S.K., Dautzenberg, I.J., Kranenburg, O., & Hoeben, R.C. Modification of mammalian reoviruses for use as oncolytic agents. *Expert. Opin. Biol. Ther.* 9, 1509-1520 (2009).
22. Allegra, C.J. et al. American Society of Clinical Oncology provisional clinical opinion: testing for KRAS gene mutations in patients with metastatic colorectal carcinoma to predict response to anti-epidermal growth factor receptor monoclonal antibody therapy. *J. Clin. Oncol.* 27, 2091-2096 (2009).
23. Linardou, H. et al. Assessment of somatic k-RAS mutations as a mechanism associated with resistance to EGFR-targeted agents: a systematic review and meta-analysis of studies in advanced non-small-cell lung cancer and metastatic colorectal cancer. *Lancet Oncol.* 9, 962-972 (2008).
24. Amado, R.G. et al. Wild-type KRAS is required for panitumumab efficacy in patients with metastatic colorectal cancer. *J. Clin. Oncol.* 26, 1626-1634 (2008).

25. Normanno,N. et al. Implications for KRAS status and EGFR-targeted therapies in metastatic CRC. *Nat. Rev. Clin. Oncol.* 6, 519-527 (2009).
26. Benvenuti,S. et al. Oncogenic activation of the RAS/RAF signaling pathway impairs the response of metastatic colorectal cancers to anti-epidermal growth factor receptor antibody therapies. *Cancer Res.* 67, 2643-2648 (2007).
27. Siena,S., Sartore-Bianchi,A., Di,N.F., Balfour,J., & Bardelli,A. Biomarkers predicting clinical outcome of epidermal growth factor receptor-targeted therapy in metastatic colorectal cancer. *J. Natl. Cancer Inst.* 101, 1308-1324 (2009).
28. De,R.W. et al. Effects of KRAS, BRAF, NRAS, and PIK3CA mutations on the efficacy of cetuximab plus chemotherapy in chemotherapy-refractory metastatic colorectal cancer: a retrospective consortium analysis. *Lancet Oncol.* 11, 753-762 (2010).
29. Parra,H.S. et al. Analysis of epidermal growth factor receptor expression as a predictive factor for response to gefitinib ('Iressa', ZD1839) in non-small-cell lung cancer. *Br. J. Cancer* 91, 208-212 (2004).
30. Banerjee,S. & Smith,I.E. Management of small HER2-positive breast cancers. *Lancet Oncol.* 11, 1193-1199 (2010).
31. Weinstein,I.B. & Joe,A. Oncogene addiction. *Cancer Res.* 68, 3077-3080 (2008).
32. Solit,D.B. et al. BRAF mutation predicts sensitivity to MEK inhibition. *Nature* 439, 358-362 (2006).
33. Wee,S. et al. PI3K Pathway Activation Mediates Resistance to MEK Inhibitors in KRAS Mutant Cancers. *Cancer Res.*(2009).
34. Haigis,K.M. et al. Differential effects of oncogenic K-Ras and N-Ras on proliferation, differentiation and tumor progression in the colon. *Nat. Genet.* 40, 600-608 (2008).
35. McDermott,E.P. & O'Neill,L.A. Ras participates in the activation of p38 MAPK by interleukin-1 by associating with IRAK, IRAK2, TRAF6, and TAK-1. *J. Biol. Chem.* 277, 7808-7815 (2002).
36. Noselli,S. & Perrimon,N. Signal transduction. Are there close encounters between signaling pathways? *Science* 290, 68-69 (2000).
37. Blank,J.L., Gerwins,P., Elliott,E.M., Sather,S., & Johnson,G.L. Molecular cloning of mitogen-activated protein/ERK kinase kinases (MEKK) 2 and 3. Regulation of sequential phosphorylation pathways involving mitogen-activated protein kinase and c-Jun kinase. *J. Biol. Chem.* 271, 5361-5368 (1996).
38. Karandikar,M., Xu,S., & Cobb,M.H. MEKK1 binds raf-1 and the ERK2 cascade components. *J. Biol. Chem.* 275, 40120-40127 (2000).
39. Shirowa,T., Motoo,Y., & Tsutani,K. Cost-Effectiveness Analysis of KRAS Testing and Cetuximab as Last-Line Therapy for Colorectal Cancer. *Mol. Diagn. Ther.* 14, 375-384 (2010).
40. Bagust,A. et al. Cetuximab for recurrent and/or metastatic squamous cell carcinoma of the head and neck: a NICE single technology appraisal. *Pharmacoeconomics.* 28, 439-448 (2010).
41. Dean,M., Fojo,T., & Bates,S. Tumour stem cells and drug resistance. *Nat. Rev. Cancer* 5, 275-284 (2005).
42. Donnenberg,V.S. & Donnenberg,A.D. Multiple drug resistance in cancer revisited: the cancer stem cell hypothesis. *J. Clin. Pharmacol.* 45, 872-877 (2005).
43. Bradshaw,D.M. & Arceci,R.J. Clinical relevance of transmembrane drug efflux as a mechanism of multidrug resistance. *J. Clin. Oncol.* 16, 3674-3690 (1998).
44. Linn,S.C. & Giaccone,G. MDR1/P-glycoprotein expression in colorectal cancer. *Eur. J. Cancer* 31A, 1291-1294 (1995).
45. Johnstone,R.W., Ruefli,A.A., & Lowe,S.W. Apoptosis: a link between cancer genetics and chemotherapy. *Cell* 108, 153-164 (2002).
46. Salvesen,G.S. & Duckett,C.S. IAP proteins: blocking the road to death's door. *Nat. Rev. Mol. Cell Biol.* 3, 401-410 (2002).
47. Signore,M., Ricci-Vitiani,L., & De,M.R. Targeting apoptosis pathways in cancer stem cells. *Cancer Lett.* (2011).
48. Di Stefano,A.B. et al. Survivin is regulated by interleukin-4 in colon cancer stem cells. *J. Cell Physiol* 225, 555-561 (2010).
49. Oost,T.K. et al. Discovery of potent antagonists of the antiapoptotic protein XIAP for the treatment of cancer. *J. Med. Chem.* 47, 4417-4426 (2004).
50. Fulda,S. Targeting inhibitor of apoptosis proteins (IAPs) for cancer therapy. *Anticancer Agents Med. Chem.* 8, 533-539 (2008).
51. Gyrd-Hansen,M. & Meier,P. IAPs: from caspase inhibitors to modulators of NF-kappaB, inflammation and cancer. *Nat. Rev. Cancer* 10, 561-574 (2010).

— |

— |



10

Summary in Dutch
Nederlandse Samenvatting

Dit proefschrift heeft als titel 'Targeting solid tumors; advances in treatment strategies for glioma and colorectal cancer', hetgeen betekent 'Het gericht behandelen van tumoren; nieuwe ontwikkelingen in behandelstrategieën voor het glioom en het colon carcinoom.

Gliomen en colon carcinomen zijn solide tumoren. Een glioom is een kwaadaardige hersentumor, colon carcinoom is een andere benaming voor dikke darm kanker. Curatieve behandeling, dus genezing van de meeste solide tumoren kan niet zonder chirurgische resectie van de tumor. Echter, het optreden van locale recidieven of metastasen op afstand is significant lager als patiënten behandeld worden met systemische of lokaal toegediende chemotherapie of met één van de nieuwe 'targeted therapies'. In de laatste tien jaar zijn veel nieuwe targeting strategies ontwikkeld voor diverse soorten tumoren. Het verschil tussen de ouderwetse chemotherapie en deze nieuwe therapieën is vergelijkbaar met het verschil tussen ouderwetse massale bombardementen en moderne precisie bombardementen met raketten. Chemotherapie beschadigt alle snel delende cellen, waarbij kankercellen wel doodgaan maar ook heel veel gezonde delende cellen leiden hier zeer onder. De nieuwe vormen van gerichte therapie, 'targeted therapy' of 'therapie op maat', zijn heel nauwkeurig gericht op specifieke moleculen of eigenschappen van kankercellen, zodat selectief kankercellen worden geraakt en gezonde cellen worden gespaard.

In dit proefschrift wordt onderzocht welke van deze nieuwe behandelstrategieën succesvol zouden kunnen zijn voor de behandeling van gliomen en colon carcinomen, maar ook op welke manier kankercellen kunnen ontsnappen aan dergelijke gerichte therapie. Dit is allereerst belangrijk om te weten, omdat hiermee de basis kan worden gelegd voor het ontwikkelen van nieuwe therapieën die de resistentie mechanismen kunnen omzeilen. Daarnaast is het belangrijk om te kunnen voorspellen welke patiënten wel of niet zullen reageren op bepaalde vormen van therapie en zo te komen tot een betere patiënten selectie.

In dit proefschrift komen drie verschillende vormen van moderne, vaak experimentele behandelstrategieën aan de orde.

1. In **hoofdstuk 2**, **hoofdstuk 3** en **hoofdstuk 4** gaat het over de behandeling van tumoren met virussen, ook wel virale genterapie genoemd. In **hoofdstuk 2** en **hoofdstuk 3** is dit toegespitst op de behandeling van gliomen, kwaadaardige hersentumoren, in **hoofdstuk 4** op de behandeling van dikke darm kanker (coloncarcinoom).
2. In **hoofdstuk 5** en **hoofdstuk 6** gaat het over het remmen van specifieke moleculen in kankercellen, met name de moleculen EGFR en MEK in het colon carcinoom.
3. In **hoofdstuk 7** en **hoofdstuk 8** wordt gekeken naar manieren om therapie op maat te ontwikkelen voor zogenaamde kanker stamcellen in het colon carcinoom.

In het hele proefschrift worden de verschillende behandelmethoden getest en geanalyseerd in het laboratorium, zowel op cel niveau in kankercellen die in het laboratorium groeien (*in vitro*) als in diermodellen (*in vivo*). In de meeste hoofdstukken wordt ook gebruik gemaakt van tumorbipten die gelijk uit de patiënt naar het laboratorium gehaald zijn, om daar experimenten mee te doen.

In de komende twee paragrafen wordt enige achtergrond informatie gegeven over gliomen en colon carcinomen, daarna volgen er drie paragrafen waarin de drie thema's verder worden besproken.

Glioom

Bij volwassenen zijn gliomen de meest voorkomende maligne (kwaadaardige) hersentumoren. Deze tumoren ontstaan uit steuncellen van het zenuwweefsel, de zogenaamde glia cellen. Er bestaand diverse soorten gliomen, waarvan de glioblastoma multiforme de meest agressieve vorm is. Helaas heeft ongeveer 50% van alle patiënten op het moment van diagnose deze agressieve vorm. Gliomen metastaseren zelden, maar infiltreren wel lokaal. Patiënten met glioblastoma multiforme hebben derhalve een zeer slechte 5-jaars overleving van ongeveer 2%. De behandeling van gliomen bestaat normaal gesproken uit chirurgie, gecombineerd met radiotherapie. Aanvullende (adjuvante) chemotherapie haalt weinig uit bij deze ziekte, alhoewel recente studies met het middel temozolomide een lichte verbetering van de overleving gaf van 12,1 naar 14,6 maanden. Omdat de prognose van deze tumoren zo slecht is zijn alternatieve behandelmethoden, zoals met virale gentherapie, meer dan welkom.

Colon carcinoom

Het colon carcinoom is één van de belangrijkste oorzaken voor kanker gerelateerde sterfte. Wereldwijd krijgen bijna 1 miljoen mensen per jaar krijgen de diagnose colon carcinoom. Behandeling van coloncarcinomen bestaat vrijwel altijd uit een operatie, al dan niet gecombineerd met chemotherapie en radiotherapie. Ongeveer de helft van alle patiënten met een colon carcinoom krijgt levermetastasen. De doodsoorzaak bij mensen met een colon carcinoom is meestal gelegen in de gevolgen van deze levermetastasen. De behandeling van levermetastasen beperkte zich tot voor kort voor de grote meerderheid van de patiënten tot palliatieve chemotherapie, wat resulteerde in een mediane survival van 6-12 maanden. Curatieve chirurgische resecties waren slechts heel beperkt mogelijk als behandeling. Echter, recent zijn er veel hoopvolle ontwikkelingen in de behandeling van het colon carcinoom. Het percentage patiënten dat in aanmerking komt voor een curatieve resectie wordt aanmerkelijk hoger dankzij verbeterde operatietechnieken en neo-adjuvante chemotherapie. Daarnaast is er tegenwoordig ook de mogelijkheid om metastasen te behandelen met radio frequente ablatie technieken (RFA). Desalniettemin blijft de 5-jaars overleving van patiënten met colorectale levermetastasen beperkt tot ongeveer 20 %.

In ongeveer 35-40% van alle colorectaal tumoren wordt een mutatie gevonden in het KRAS oncogen. Deze mutatie wordt waarschijnlijk al verworven in de vroege ontwikkeling van de tumor. Het KRAS oncogen codeert voor het kleine eiwit KRAS. Dit eiwit speelt een cruciale rol in signalering cascades van groeifactor receptoren als EGFR. Als er een mutatie optreedt in dit oncogen, signaleert de activeringscascade vanaf KRAS via BRAF, MEK en ERK continu, resulterend in ongeremde groei, invasie en resistentie tegen apoptose (geprogrammeerde zelfdood).

Virale gentherapie

Gentherapie bestaat sinds ongeveer 20 jaar. Het principe van gentherapie is het bezorgen van een gezond gen in cellen met een beschadigd, slecht werkend of afwezig gen om zo de 'zieke cel' weer beter te maken. Het is oorspronkelijk ontwikkeld voor diverse genetische ziekten, met name als de oorzaak gelegen is in één specifiek gen. Voor de toepassing bij de behandeling van kanker werd eerst getracht een gen tot expressie te laten komen in kankercellen die de cellen aanzet tot apoptose, gereguleerde zelfdood. Als middel om deze genen in een cel te brengen wordt doorgaans gebruik gemaakt van bestaande virussen, die worden aangepast om gebruikt te worden in de mens.

In de moderne gentherapie voor kanker wordt meestal geen gebruik meer gemaakt van zo'n apoptose gen, maar wel van de virussen. Bepaalde virussen blijken namelijk in staat kankercellen te kunnen doden, waarbij ze dusdanig genetisch gemanipuleerd kunnen worden dat ze vrij specifiek alleen kanker cellen kunnen doden. De virussen doen dit door de cellen te infecteren, in de cel zichzelf te vermenigvuldigen en dan de cel aanzetten tot een proces van cel lysis, waarbij de cel kapot gaat en er nieuwe virussen vrij komen. Deze nieuwe virussen zijn dan in staat om in naburige cellen hetzelfde proces te doorlopen, resulterend in tumorafname. De meest gebruikte virussen voor dit doeleinde zijn het adenovirus en het retrovirus. Daarnaast wordt onder andere voor het colon carcinoom gebruik gemaakt van het reovirus.

Voor de experimentele behandeling van gliomen wordt veel gebruik gemaakt van het adenovirus. Deze virussen worden genetisch gemanipuleerd op twee manieren: 1. *transductional targeting* en 2. *transcriptional targeting*. Bij *transductional targeting* worden de bindingseigenschappen van het virus dusdanig aangepast dat het zo goed mogelijk specifiek kan binden aan tumorcellen. Bij *transcriptional targeting* wordt het virus zo aangepast dat het zich alleen gaat vermenigvuldigen als het zich bevindt in een kanker cel of in een cel van een bepaalde oorsprong (bijvoorbeeld een darmcel). In **hoofdstuk 2** laten we zien dat diverse *transductional targeted* virussen goed in staat zijn glioomcellen in het laboratorium te infecteren, maar dat deze niet in staat zijn geïnduceerde tumoren in muizen binnen te komen. In **hoofdstuk 3** laten we zien dat een *transcriptional targeted* virus niet alleen succesvol is in de behandeling van glioom cellen, maar ook in de behandeling van tumoren in muizen en behandeling van vers tumormateriaal. Aan het begin van het DNA van dit virus bevindt zich de survivin promoter. Een promoter is een soort schakelaar die het aflezen van het DNA wat na de promoter komt aan of uit zet. In glioom cellen is de survivin promoter zeer actief, in tegenstelling tot de gezonde hersencellen rondom. Als het virus in glioom cellen binnenkomt zal de promoter in het virus ook zeer actief worden, waardoor het virus goed in staat is zijn werk te doen. Dit virus is potentieel zeer interessant om te ontwikkelen tot een klinisch toepasbare therapie, al dan niet in combinatie met een modificatie van de bindingcapaciteit.

Het is al meerdere keren bewezen dat reovirus behandeling van colon carcinoom cellen resulteert in efficiënte celdood van colon carcinoom, als deze cellen een KRAS mutatie hebben. Om een stap verder te gaan hebben we in **hoofdstuk 4** gekeken naar het effect van behandeling met reovirus op verse bipten van humane colon carcinomen. Dit zijn bipten genomen van tumoren die bij patiënten op de operatie kamer worden weggehaald, en vervolgens gelijk worden overgebracht naar het laboratorium. In dit hoofdstuk laten we zien dat het reovirus niet in staat

is om de kankercellen in deze biopten binnen te dringen. Dit heeft waarschijnlijk te maken met de relatief lage expressie van de natuurlijke receptor JAM1 op de colon carcinoom cellen, maar ook met de extracelulaire matrix-eiwitten tussen alle cellen die goede verspreiding van het virus tegen gaan. Door het virus eerst te incuberen met het enzym chemotrypsine veranderen de bindingseigenschappen van het virus dusdanig dat het wel in staat is de cellen binnen te dringen, maar zelfs dan blijkt dat de virussen maar kort in leven kunnen blijven in de cellen. Alhoewel in de darm een geringe hoeveelheid chemotrypsine aanwezig is, is op basis van deze experimenten te voorspellen dat mono-therapie van colon carcinoomen met reovirus waarschijnlijk niet succesvol zal zijn.

EGFR en MEK remmers bij het colon carcinoom

Bij de (adjuvante) behandeling van colorectale levermetastasen of lokaal uitgebreide colon carcinoomen zijn diverse 'targeted therapeutics' getest in zowel laboratorium modellen als in klinische trials. In **hoofdstuk 5 en hoofdstuk 6** laten wij zien hoe de aanwezigheid van een activerende KRAS mutatie de gevoeligheid van colorectale kankercellen voor 'targeted therapy' kan veranderen. Eén van deze moderne geneesmiddelen is cetuximab, een antilichaam wat de groeifactor receptor EGFR blokkeert en zo tumorgroei remt. Nu blijkt in klinische studies dat slechts ongeveer 10 procent van de patiënten reageert op deze behandeling, waarna een zoektocht is begonnen naar redenen waarom 90 procent van de patiënten niet reageert. De belangrijkste voorspeller van therapie resistentie blijkt de aanwezigheid van een KRAS mutatie te zijn. In **hoofdstuk 5** gebruiken we een model van cellijnen met en zonder KRAS mutatie om aan te tonen dat de aanwezigheid van een KRAS mutatie inderdaad leidt tot resistentie van deze cellen voor EGFR remmers. In dit model tonen we aan dat een verklaring voor deze resistentie een afwijkende lokalisatie van de EGF receptor kan zijn. In de cellen met een KRAS mutatie is de EGF receptor niet meer gelegen op de celmembraan maar meer intracellulair in het cytoplasma. De EGF receptor activeert diverse signaleringsroutes in de cel die kunnen leiden tot celdelingen. Een van deze signaleringsroutes is de EGFR-(K)RAS-(B)RAF-MEK-ERK signaleringsroute. Omdat colorectale kankercellen vaak een KRAS mutatie hebben, zijn er diverse remmers van MEK ontwikkeld om zo te proberen de activatie van deze route in cellen met een KRAS mutatie te remmen. Echter, wanneer wij in **hoofdstuk 6** MEK remmen of zelfs weghalen uit een cel blijkt dat dit in onze cellijnen maar een tijdelijk effect heeft. De eerste dagen hebben de cellen hier veel last van, maar daarna zijn ze in staat weer heel hard te delen. Wij laten zien dat dit komt doordat KRAS in staat is een alternatieve route te activeren na MEK inhibitie, namelijk de p38 route. Wij laten in ons model zien dat KRAS mutaties in colorectale kanker cellen dus niet gevoelig zijn voor MEK remming, maar juist resistent zijn tegen MEK gerichte therapie. KRAS mutaties kunnen dus potentieel gebruikt worden als voorspellers van therapie resistentie bij deze vormen van targeted therapie, wat kan leiden tot een betere patiënten selectie.

Het behandelen van kanker stamcellen van het colon carcinoom

De laatste jaren is meer en meer bewijs verkregen dat tumoren niet bestaan uit een verzameling identieke cellen, maar dat er binnen de tumor grote verschillen bestaan tussen de verschillende cellen en dat er zelfs een soort hiërarchie bestaat. Het grootste deel van de cellen in de tumor is meestal redelijk tot goed gedifferentieerd en niet of nauwelijks in staat tumoren te vormen, maar

een klein deel (enkele procenten van het totale tumorweefsel) van de cellen in een tumor zijn weinig gedifferentieerd en zeer tumorigeen, dus zeer goed in staat om tumoren te vormen. Deze laatste groep cellen worden ook wel kanker stamcellen genoemd, of ook wel tumorinitiërende cellen. In normaal colon bevinden zich ook stamcellen, welke voortdurend delen en zodoende zorgen voor een continue verversing van de gedifferentieerde oppervlakkige epitheel cellen in de darm. Deze normale darm stamcellen moeten een leven lang mee. Om te voorkomen dat er door de tijd teveel DNA-mutaties ontstaan, hebben stamcellen doorgaans een hoge DNA-reparatie activiteit. Daarnaast wordt de normale stamcel ook gekenmerkt door resistentie tegen schadelijke stoffen. Er zijn aanwijzingen dat darmtumoren alleen kunnen ontstaan vanuit een gemuteerde normale stamcel, en niet vanuit een gedifferentieerde cel. Kanker stamcellen die rechtsreeks afstammen van normale stamcellen zouden daarmee ook de resistentiemechanismen geërfd kunnen hebben die hun normale voorgangers kenmerken. Hieruit is het huidige dogma ontstaan dat kanker stamcellen, door de geërfd resistentiemechanismen en hoge DNA-reparatie activiteit, resistent zijn tegen chemotherapeutica.

In **hoofdstuk 7** en **hoofdstuk 8** beschrijven wij de resultaten verkregen met een model van colorectale kanker stamcellen die wij zelf ontwikkeld hebben uit vers tumor materiaal na de resectie van tumoren bij patiënten met een colon carcinoom. De kanker stamcellen groeien uit tot 3D-tumorbolletjes of sferoïden, welke bestaan uit kanker stamcellen en daaromheen meer gedifferentieerde cellen. In **hoofdstuk 7** onderzoeken we de resistentie van kanker stamcellen voor het bekende chemotherapeutikum irinotecan. We laten zien dat kanker stamcellen zelf wel gevoelig zijn voor irinotecan behandeling, maar dat meer gedifferentieerde cellen rondom de kanker stamcellen in staat zijn om irinotecan weg te houden van de kanker stamcellen door middel van het actief uitpompen van irinotecan door de ABCB1 pomp. Vervolgens laten we zien dat het behandelen van sferoïden en tumoren in muizen met zowel irinotecan als een remmer van de ABCB1 eiwit pomp resulteert in tumorreductie en celdood van kanker stamcellen. Concluderend laten wij in dit hoofdstuk zien dat kanker stamcellen zelf niet resistent zijn tegen irinotecan, maar beschermd worden door omliggende meer gedifferentieerd cellen. In **hoofdstuk 8** beschrijven we de resultaten van een proteomic screen (een overzicht van expressie van alle eiwitten in de cel) waarin sferoïden met kanker stamcellen vergeleken worden met daaruit voortkomende gedifferentieerde cellen. Wat ons opviel in de resultaten van de screen is dat in de kanker stamcellen vooral veel eiwitten zijn opgereguleerd die te maken hebben met geprogrammeerde celdood, apoptose. Het apoptose gerelateerde eiwit wat het hoogst tot expressie kwam in de sferoïden was BIRC6, een anti-apoptose eiwit. Vervolgens hebben we dit eiwit weggehaald uit deze cellen, waarna de cellen veel gevoeliger bleken voor apoptose inducerende chemotherapie. We laten in dit hoofdstuk dus zien dat over-expressie van BIRC6 een middel van therapie resistentie is in kanker stamcellen. We suggereren in dit hoofdstuk dat BIRC 6 een goede 'target' kan zijn om specifieke remmers voor te ontwikkelen, zodat kanker stamcellen niet meer resistent zijn tegen apoptose. Kortom, we laten in **hoofdstuk 7** en **hoofdstuk 8** zien dat het mechanisme van therapie resistentie in colon kanker stamcellen heel divers kan zijn, afhankelijk van het type therapie wat gegeven wordt.

Conclusie

Dit proefschrift geeft ons meer inzicht in de mogelijkheden en beperkingen van nieuwe gerichte behandelstrategieën voor gliomen en colon carcinomen. Virale genterapie in gliomen kan zeer veelbelovend zijn maar kent ook zijn beperkingen. Het reovirus als behandelmethode voor het coloncarcinoom lijkt minder veelbelovend. Colon carcinomen met een KRAS mutatie blijken niet gevoelig voor EGFR en MEK remming, wat kan leiden tot een betere patiëntselectie voor deze vormen van therapie en dus het voorkomen van het geven van onnodige therapie. Daarnaast laten we zien dat colon kanker stamcellen verschillende mechanismen van therapie resistentie kennen, maar dat de combinatie behandeling van irinotecan met een ABCB1 remmer, of remming van BIRC6 zou kunnen leiden tot het uitschakelen van de stamcellen. Dit proefschrift wil hiermee een bijdrage leveren aan het verder ontwikkelen, verfijnen of persoonlijk afstemmen van deze moderne vormen van therapie voor patiënten met een glioom of een colon carcinoom.

11

Acknowledgements - Dankwoord
Curriculum vitae auctoris
List of publications

Prof. dr. I.H.M. Borel Rinkes, beste Inne,

Eerste indrukken schijnen voor altijd doorslaggevend te zijn voor de mate waarin je vertrouwen hebt in de ander. Dat geldt zeker voor onze eerste ontmoeting begin 2005. Jij besloot na een paar minuten dat we samen een AGIKO subsidie gingen aanvragen, ik besloot dat mijn toekomst in de chirurgische en wetenschappelijke wereld onder jouw leiding vorm zou moeten krijgen. De rest is geschiedenis. Inne, jouw positieve, betrokken en joviale stijl van leiding geven waren erg stimulerend. Het was goed te merken dat alles met jou bespreekbaar was en dat je veel ruimte gaf om mijn eigen pad te volgen. Ik heb veel van je geleerd en hoop dat in de toekomst te kunnen blijven doen. Ik waardeer zeer het vertrouwen dat je me vanaf het begin hebt gegeven en nog steeds geeft; DANK!

Dr. O. Kranenburg, beste Onno,

Het doel van promoveren is niet alleen het produceren van een proefschrift, maar ook om opgeleid te worden tot een zelfstandig onderzoeker en wetenschapper. Voor beide doelen was jouw inbreng, geduld en opleidingstalent onontbeerlijk. Het was niet gelukt zonder jouw grote inhoudelijke kennis en jouw gedrevenheid om pas afgestudeerde artsen in korte tijd op te leiden tot onderzoekers op het lab. Je discipline en werklust in rustige maar soms ook in drukke of zware tijden bewonder ik zeer. Dank voor al de mooie momenten (Los Angelos), je hulp en je inzet om dit proefschrift tot een goed einde te brengen.

Prof. dr. R.H. Medema, beste Rene,

Het was me een buitengewoon genoegen om onderzoek te doen in jouw directe nabijheid en die van jouw groep. Jouw inbreng - op het scherpst van de snede – tijdens werkbesprekingen en daarbuiten, maar ook jouw humor en vrolijk cynisme waren een zeer waardevolle aanvulling op mijn onderzoek. Jouw positieve houding ten opzichte van artsen op het lab is geen vanzelfsprekendheid, maar heeft me wel gemotiveerd om dit werk met heel veel plezier te doen. Dank dat je voor mijn verdediging zeer bewust tijd hebt willen vrijmaken.

Prof. dr. C.M.F. Dirven, beste Clemens,

Al in 2002 zette ik bij jou en Martine Lamfers de eerste stappen in mijn wetenschappelijke carrière. Zonder jullie was ik nooit bij professor Curiel terecht gekomen om daar een tweetal artikelen te publiceren die aan de basis staan van dit proefschrift. De samenwerking met jou en Martine was bijzonder prettig en stimulerend. De mogelijkheid die je me later gaf om bij jou te komen werken heeft me voor misschien wel de moeilijkste keuze in mijn leven geplaatst. Als chirurg, als arts en als mens heb ik je zeer hoog en ik ben dan ook zeer vereerd dat je deel wilt nemen in de promotie commissie.

Dr. Y.S. Haviv, dear Yosef,

When I came to Birmingham as a medical student you were the one to coach and teach me the basics of gene therapy science at the Gene therapy center of professor David Curiel. My two glioma papers would not have been published if it wasn't for you. We keep warm memories of celebrating the Purim party in Birmingham with you and also to our visit to Jerusalem. It was very special to get to know you and to share the interest in science and medicine but also in philosophy, culture and religion. Thanks for all your support and friendship.

Prof. dr. E. Voest, beste Emile,

Ik heb je leren kennen als een zeer gedreven en ambitieuze man die nauw betrokken is bij het onderzoek. Je onderkoelde humor gecombineerd met scherp commentaar vond ik prachtig. Veel plezier met je sabbatical in La Jolla en ik vind het erg jammer dat je niet in de oppositie kan plaatsnemen.

Overige leden van de beoordelingscommissie,

Prof. dr. P.J. van Diest, beste Paul, dank voor je hulp met de immunohistochemie en het EGFR project, en dank voor je werk als voorzitter van mijn beoordelingscommissie.

Prof. dr. R. van Hillegersberg, beste Richard, dank voor je betrokkenheid en support tijdens mijn onderzoek, dank voor je bijdrage aan de beoordelingscommissie.

Prof. dr. R.C. Hoeben, beste Rob, dank voor je bijdrage aan het reovirusproject en kritisch doornemen van mijn manuscript.

Prof. dr. P.D. Siersema, dank voor uw bijdrage aan de beoordelingscommissie.

Dr. G. J. Clevers, dr. A. Pronk en alle chirurgen en arts-assistenten van het Diaconessenhuis in Utrecht, hartelijk dank voor jullie hulp en betrokkenheid bij het afronden van het proefschrift. Apollo, dank voor je belangstelling tijdens mijn onderzoek en je deelname aan de promotiecommissie!

Alle collega's van het lab en samenwerkende groepen wil ik bedanken voor alle hulp, feed-back en mooie lab-borrels:

Het lab van de experimentele oncologie:

Met de Medema groep was de verstandhouding altijd prima, wij lieten samen zien dat artsen en wetenschappers goed kunnen samenwerken in een uitstekende sfeer. **Marvin Tanenbaum, Gerben Vader, Monica Alvarez, Arne Lindqvist, Geert Kops, Anniek Janssen, Martijn Vromans, Rob Klompmaker, Livio Kleij,** en alle anderen: dank daarvoor.

De dr. **P.W.D. Derksengroep: Patrick,** je bent een mooie kerel. We hebben mooie tijden beleefd op Long Island en onze etentjes met Frederik waren fantastisch. Je directheid had niet misstaan in de chirurgische wereld. **Ron Schackmann en Miranda van Amersfoort,** bedankt.

De Medische Oncologie crew: de dames van de Voest groep - en Joost – waren een welkome aanvulling van arts-onderzoekers op het lab. **Marlies Langenberg, Jeanine Roodhart, Laura Daenen en Joost Vermaat,** dank voor de plezierige samenwerking, feedback en gezelligheid. Ook **Rachel Giles, Sander Basten en Dorus Mans** van de Giles groep en **Judith Jans en Stephanie Kroezen** van de urologie: dank voor jullie support.

Rob Vries van het Clevers lab, dank voor je hulp met het stamcelproject, ik vond en vind het erg leuk om met je samen te werken.

Conny Jimenez van het OncoProteomics Lab van de VU, dank voor je samenwerking met de proteomics studie.

Diana van den Wollenberg van het Hoeben lab in Leiden, dank voor je hulp met het reovirus artikel.

Alle (oud) mede onderzoekers van de Heelkunde,

Onze tegenspelers van Isengard, **Bobby Bloemendaal, Falco Hietbrink en Stein van Esser**, vanuit de tower of Sin hielden we jullie goed in gaten. Het waren mooie tijden, ik hoop dat we elkaar nog vaak mee mogen maken, in de kliniek of daarbuiten. **Eline van Hattum, Judith Boone en Tjaakje Visser, Charlotte van Kessel, Roy Verhage, Wouter Peeters, Erik Tournoy, Claire Pennekamp, Daphe de Groot, Janesh Pillay, Olaf Bakker, Ralf Sprengers, Willem Hellings, Wouter Derksen, Anne den Hartog**: dank voor de gezelligheid

Onze voorgangers, **Niels Smakman, Jarmila van der Bilt en Liesbeth Veenendaal**, dank voor het bereiden van de weg voor een nieuwe generatie onderzoekers.

Onze analisten, **Danielle Raats en Andre Verheem**, onze post-doc **Jamilla Laoukili**, dank voor jullie hulp en inzet.

Klaas Govaert en Ernst Steller, twee van de opvolgers van onze generatie onderzoekers, jullie zijn mooie kerels en gaan het helemaal maken, mooi jullie te leren kennen.

Vrienden van het Borel Rinkes/Kranenburg lab van de Chirurgische Oncologie, **Nikol Snoeren, Menno de Bruijn en Maarten Nijkamp**. Veel tijd hebben we samen doorgebracht en ik vind het bijzonder dat we het zo goed met elkaar kunnen vinden.

Nikol, als enige dame in ons gezelschap heb je een speciaal plekje in mijn hart veroverd. Wat ben jij een topvrouw. Je bent ongelofelijk sociaal, werkte samenbindend en verzoenend en bent onvermoeibaar in het organiseren van sociale activiteiten. Maar je bent vooral jezelf, je kiest je eigen pad op een manier die bij JOU past. Ik respecteer dat zeer. Heel veel succes in de toekomst, waar die ook maar zal liggen.

Menno, onze gesprekken ging over veel meer dan het onderzoek en de lab perikelen. Samen hebben we discussies gevoerd die in de tweede kamer niet zouden misstaan, maar ik denk dat wij samen sneller oplossingen kunnen verzinnen dan de 'hoge heeren in Den Haag'. In de drukke tijden van promotie onderzoek en later kliniek vond ik het een verademing om over andere onderwerpen van gedachten te wisselen.

Maarten, vent, wat heb ik genoten van je humor, je onbezonnenheid, directheid en relaxte houding. Samen konden we prima relativeren, dank voor je steun in mooie en zware tijden. Het was prachtig om samen een solide financiële basis te leggen onder het voorjaarssymposium, maar minstens zo mooi was het samen 'van Lauwerszee tot Dollard tou' aanheffen in de Euroborg. Ik ben ontzettend blij dat we weer samenwerken in de kliniek, het is een voorrecht om met vrienden te werken.

Mijn paranimfen, **Frederik Hoogwater en Benjamin Emmink**,

Frederik, ouwe, wat ben jij een prachtkerel. We hebben samen hard gewerkt, soms back-to-back tot diep in de nacht op het lab wat vervolgens naadloos overging in back-to-back vazen Paulaner drinken in de Poort. Onze reis met z'n tweeën naar Cold Spring Harbour en Princeton zal ik nooit vergeten, wat hebben we daar genoten van onze residentie met privé vervoer. Je humor, relativiseringsvermogen, je aanwezigheid, het heeft me geholpen om mooie momenten te delen, de saaiheid te doorbreken, en op zware tijden er doorheen te worden gesleept. Dank voor alles. Fantastisch dat we ook in de kliniek nog een half jaartje samen hebben mogen werken. Onze vriendschap is in de jaren nadat ik vertrokken was alleen maar hechter geworden, en ik weet zeker dit in de toekomst niet anders zal zijn.

Benjamin, trouwe springbok, we kenden elkaar vaag van ons bijbaantje in 'de Wijngaard' toen je als student bij mij begon. Wat volgde was een fantastische periode van een zeer prettige, stimulerende en vruchtbare samenwerking tot op de dag van vandaag. Dank voor al het werk wat je verzet hebt, wat geleid heeft tot twee prachtige cancer stem cells artikelen in dit proefschrift. Wat hebben we veel gespard, besproken, gesquasht en gediscussieerd en veel van elkaar geleerd. Je bent enorm trouw en doortastend, en altijd bereid om te helpen of adviseren waar nodig. Onze vanzelfsprekende vriendschap en altijd goede verstandhouding die weinig woorden nodig heeft waardeert ik zeer.

Marijke, mijn lieve vrouw,

Je hebt me altijd gesteund en gestimuleerd om af te maken wat ik begonnen was, ook na de geboorte van Charlotte en Hugo, en hebt me daarmee een zeer stabiel fundament gegeven om dit proefschrift te kunnen afmaken. Nooit heb ik je horen klagen over lange werkdagen, werken in avond- en weekenduren of buitenlandse reizen. Dank je wel voor al je steun, support en het liefdevol aanhoren van de (saaie?) verhalen over het lab en het spuien van frustratie na tegenvallende resultaten. Ik hou van je.

Curriculum vitae auctoris

Winan van Houdt graduated from the VWO at the Greydanus college in Zwolle in 1995, after which he started medical school at Ghent University in Belgium. After one year, he went to Utrecht University in the Netherlands, to study Pharmaceutical Sciences. In 2003, he received his master of science degree (MSc) in pharmacy. In 1998, he was admitted to medical school at Utrecht University. From 2002 until 2003 he has been doing research at the Gene Therapy Center, University of Alabama at Birmingham (UAB), Birmingham AL, USA. He worked on the improvement of viral vectors for gene therapy applications for glioma, under supervision of professor D.T. Curiel and dr. Y.H. Haviv. In 2005 he received his medical degree (MD), after which he worked for half a year as a surgical resident at the cardio-thoracic surgical department at the University Medical Center in Utrecht. In 2005 he received an AGIKO grant from The Netherlands Organisation for Scientific Research (ZonMw by NWO). With this financial support he started working in 2006 on his thesis at the laboratory of Surgical Oncology at the University Medical Center Utrecht, under supervision of Professor I.H.M. Borel Rinkes and dr. O. Kranenburg. In 2008 he received the award for best presentation at the Symposium on Experimental Research for Surgical Specialities in the Netherlands. In 2009 he started his residency program in general surgery under supervision of dr. G.J. Clevers and dr. A. Pronk at the Diakonessenhuis hospital in Utrecht. He is expected to finish his surgical residency program in 2014 at the University Medical Center Utrecht under supervision of professor I.H.M. Borel Rinkes.

Winan van Houdt is married and a proud father of two children.

List of Publications

Van Houdt WJ, Emmink BL, Pham T, Piersma S, Verheem A, Fratantoni S, Borel Rinkes IHM, Jimenez CR, Kranenburg O.

Proteome differences between colon cancer stem cells and differentiated tumor cells identifies BIRC6 as a potential therapeutic target

Submitted

Van Houdt WJ, Emmink BE, Vries RG, Hoogwater FJH, Govaert KM, Verheem A, Nijkamp MW, Steller EJA, Jimenez CR, Clevers H, Borel Rinkes IHM, Kranenburg O.

Differentiated tumor cells protect human colorectal tumor-initiating cells from irinotecan

Gastroenterology, 2011 March 31 (epub ahead of print)

van Houdt WJ, Hoogwater FJH, de Bruijn MT, Emmink BL, Nijkamp MW, Raats DA, van der Groep P, van Diest P, Borel Rinkes IHM, Kranenburg O.

Oncogenic KRAS desensitizes colorectal tumor cells to epidermal growth factor receptor inhibition and activation.

Neoplasia, 2010 Jun;12(6):443-52.

van Houdt WJ, de Bruijn MT, Emmink BL, Raats D, Hoogwater FJH, Borel Rinkes IHM, Kranenburg O.

Oncogenic K-ras activates p38 to maintain colorectal cancer cell proliferation during MEK inhibition.

Cellular Oncology, 2010 Jan 1;32(4):245-57.

de Bruijn MT, Raats DA, Hoogwater FJ, van Houdt WJ, Cameron K, Medema JP, Borel Rinkes IH, Kranenburg O.

Oncogenic KRAS sensitises colorectal tumour cells to chemotherapy by p53-dependent induction of Noxa.

British Journal of Cancer, 2010 Apr 13;102(8):1254-64.

Hoogwater FJ, Nijkamp MW, Smakman N, Steller EJ, Emmink BL, Westendorp BF, Raats DA, Sprick MR, Schaefer U, Van Houdt WJ, De Bruijn MT, Schackmann RC, Derksen PW, Medema JP, Walczak H, Borel Rinkes IH, Kranenburg O.

Oncogenic K-Ras turns death receptors into metastasis-promoting receptors in human and mouse colorectal cancer cells.

Gastroenterology, 2010 Jun;138(7):2357-67.

Nijkamp MW, van der Bilt JD, Snoeren N, Hoogwater FJ, van Houdt WJ, Molenaar IQ, Kranenburg O, van Hillegersberg R, Borel Rinkes IH.

Prolonged portal triad clamping during liver surgery for colorectal liver metastases is associated with decreased time to hepatic tumour recurrence.

European Journal of Surgical Oncology, 2010 Feb;36(2):182-8.

van Houdt WJ, Smakman N, van den Wollenberg DJ, Emmink BL, Veenendaal LM, van Diest PJ, Hoeben RC, Borel Rinkes IH, Kranenburg O.

Transient infection of freshly isolated human colorectal tumor cells by reovirus T3D intermediate subviral particles.

Cancer Gene Therapy, 2008 May;15(5):284-92.

Van Houdt WJ, Wu H, Glasgow JN, Lamfers ML, Dirven CM, Gillespie GY, Curiel DT, Haviv YS.

Gene delivery into malignant glioma by infectivity-enhanced adenovirus: in vivo versus in vitro models.

Neuro Oncology, 2007 Jul;9(3):280-90.

Van Houdt WJ, Haviv YS, Lu B, Wang M, Rivera AA, Ulasov IV, Lamfers ML, Rein D, Lesniak MS, Siegal GP, Dirven CM, Curiel DT, Zhu ZB.

The human survivin promoter: a novel transcriptional targeting strategy for treatment of glioma.

Journal of Neurosurgery, 2006 Apr;104(4):583-92.

Haviv YS, van Houdt WJ, Lu B, Curiel DT, Zhu ZB.

Transcriptional targeting in renal cancer cell lines via the human CXCR4 promoter.

Molecular Cancer Therapy, 2004 Jun;3(6):687-91.

— |

— |



12

Color figures

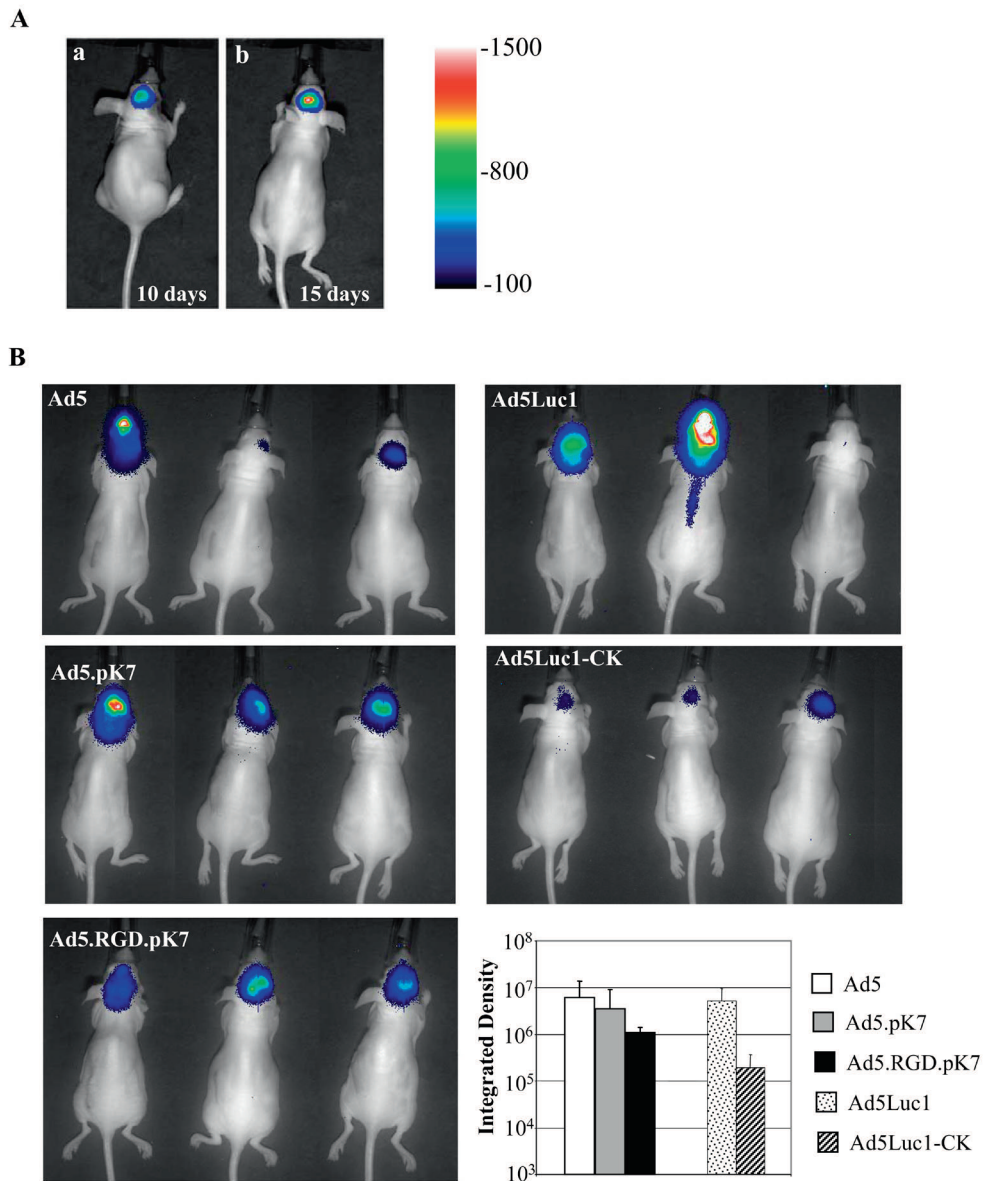


Figure 6ab page 34

B

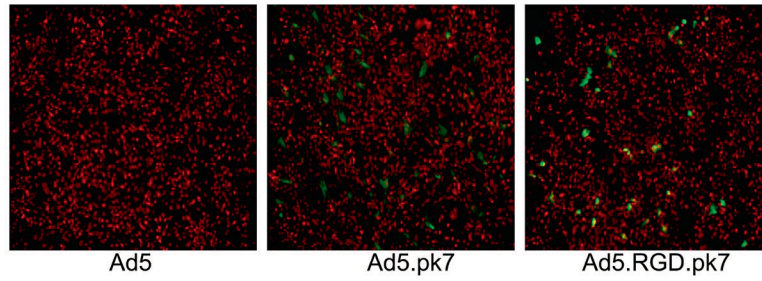


Figure 3b page 29

C

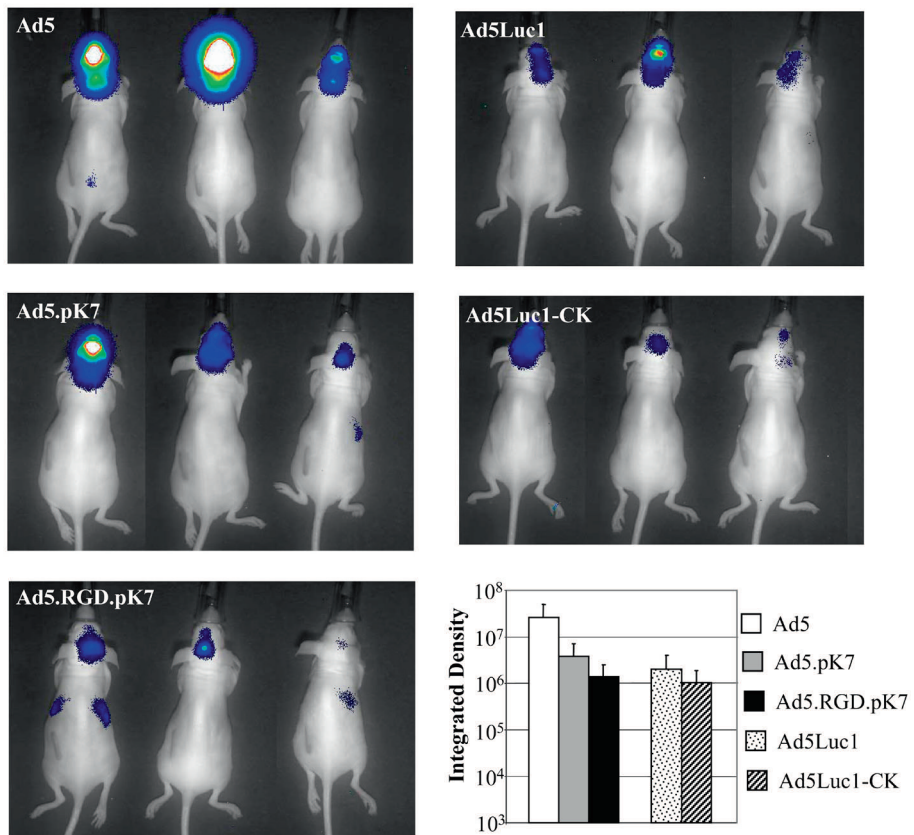


Figure 6c page 35

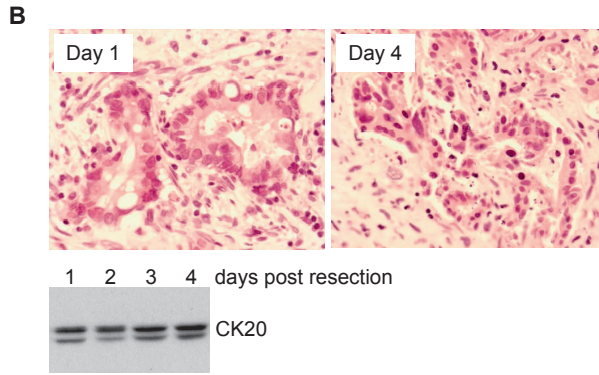


Figure 1b page 64

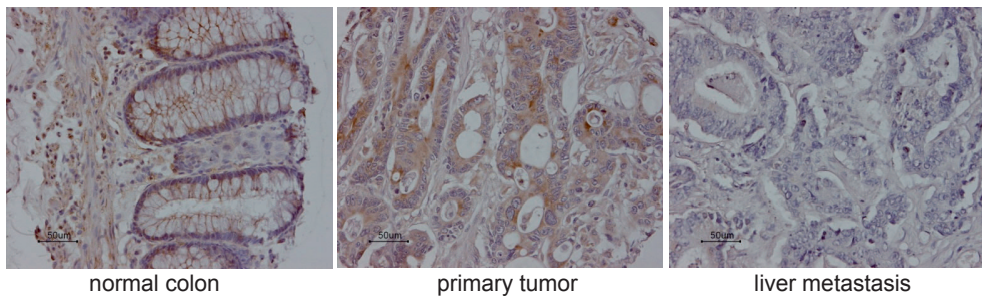


Figure 5 page 70

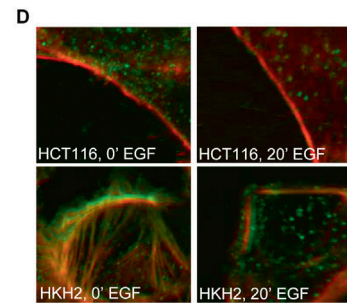
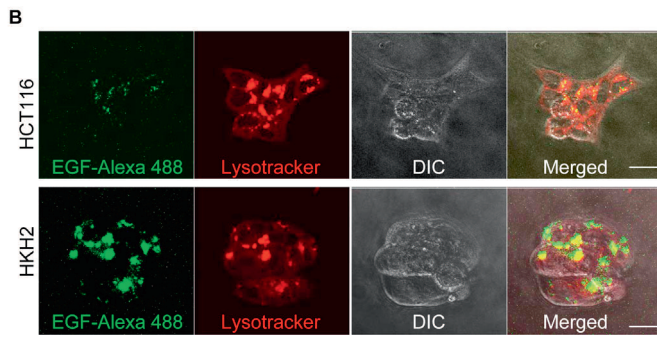


Figure 6b and d page 86

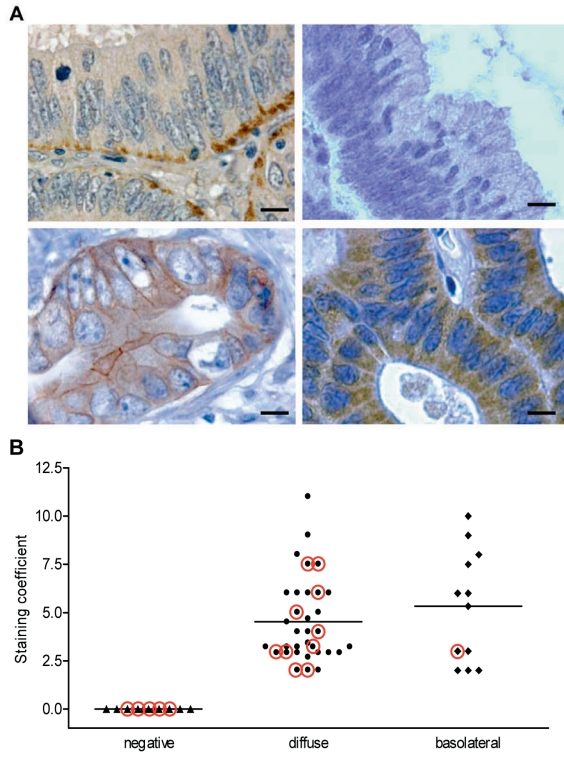
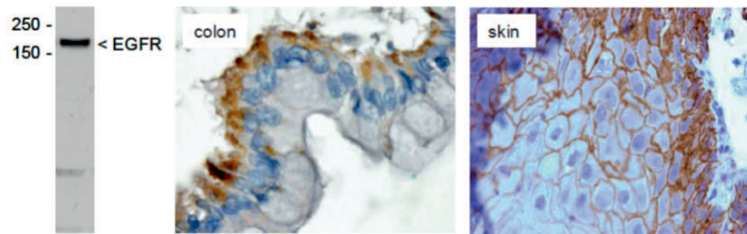


Figure 6 page 88



Supplemental Figure 3 page 96

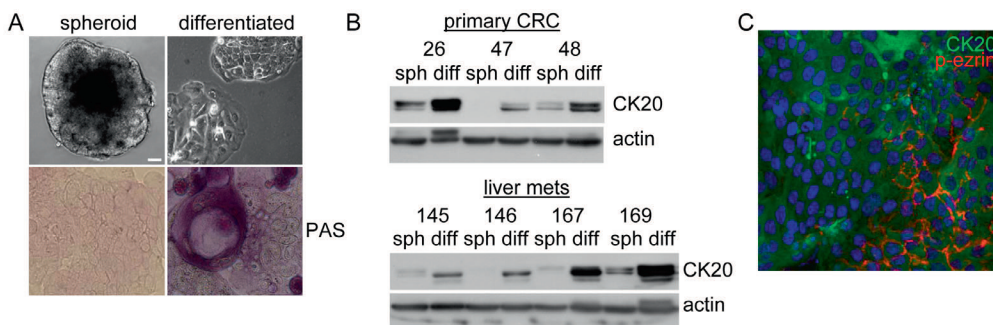


Figure 1 page 119

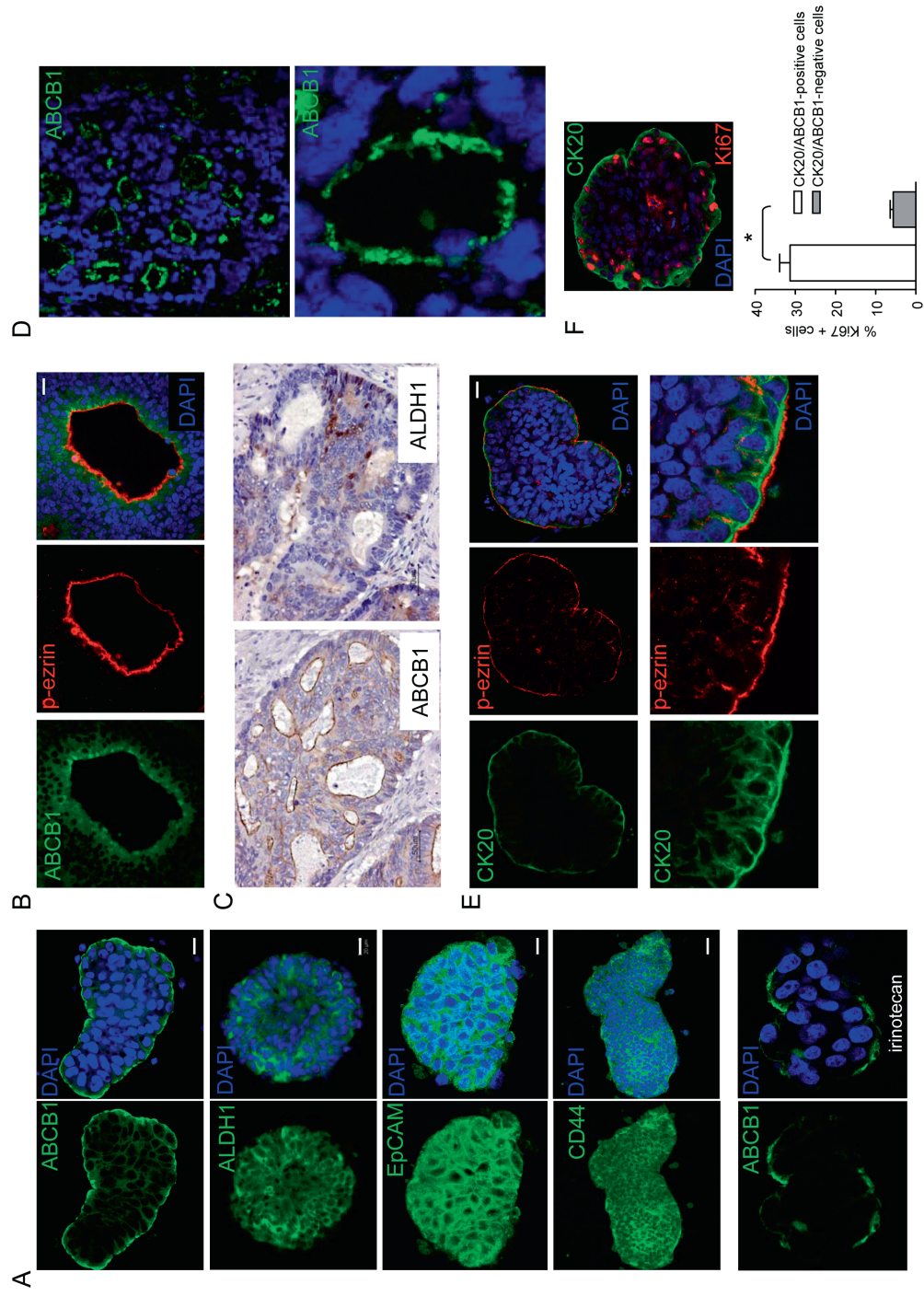


Figure 5 page 125

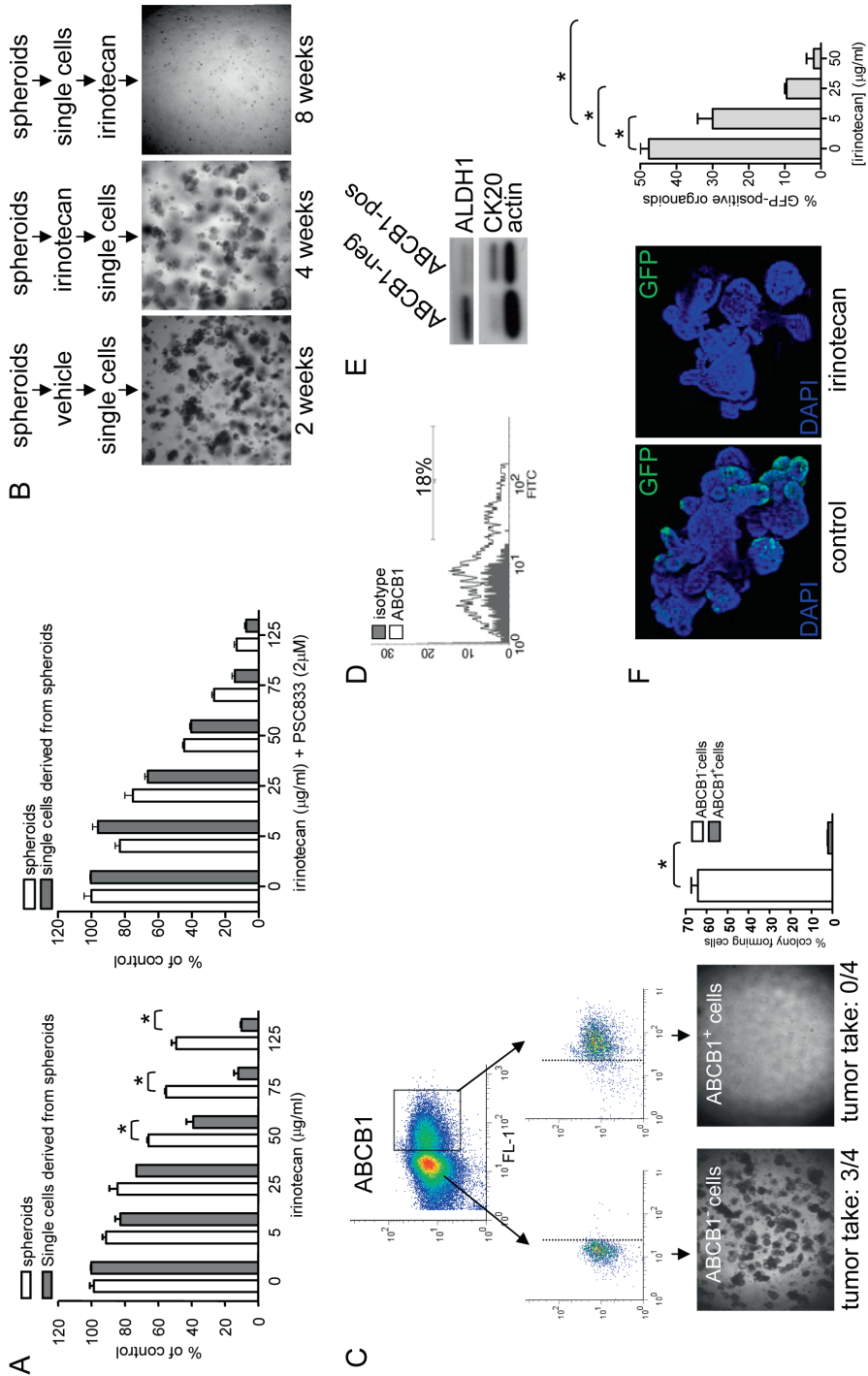
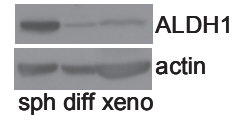
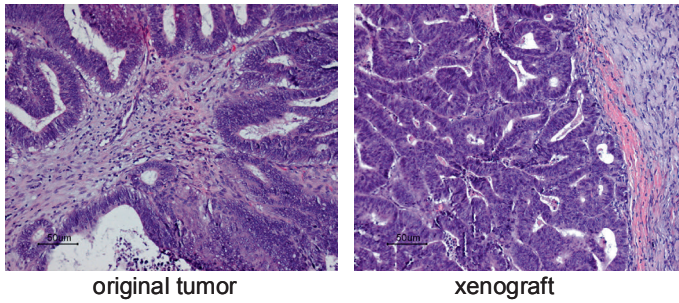
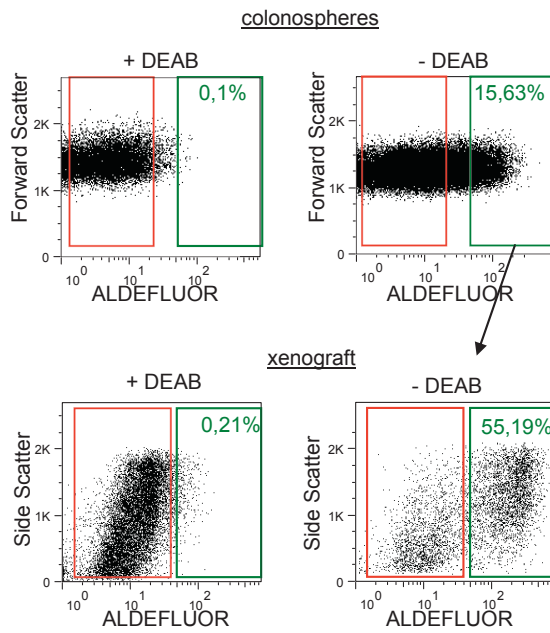


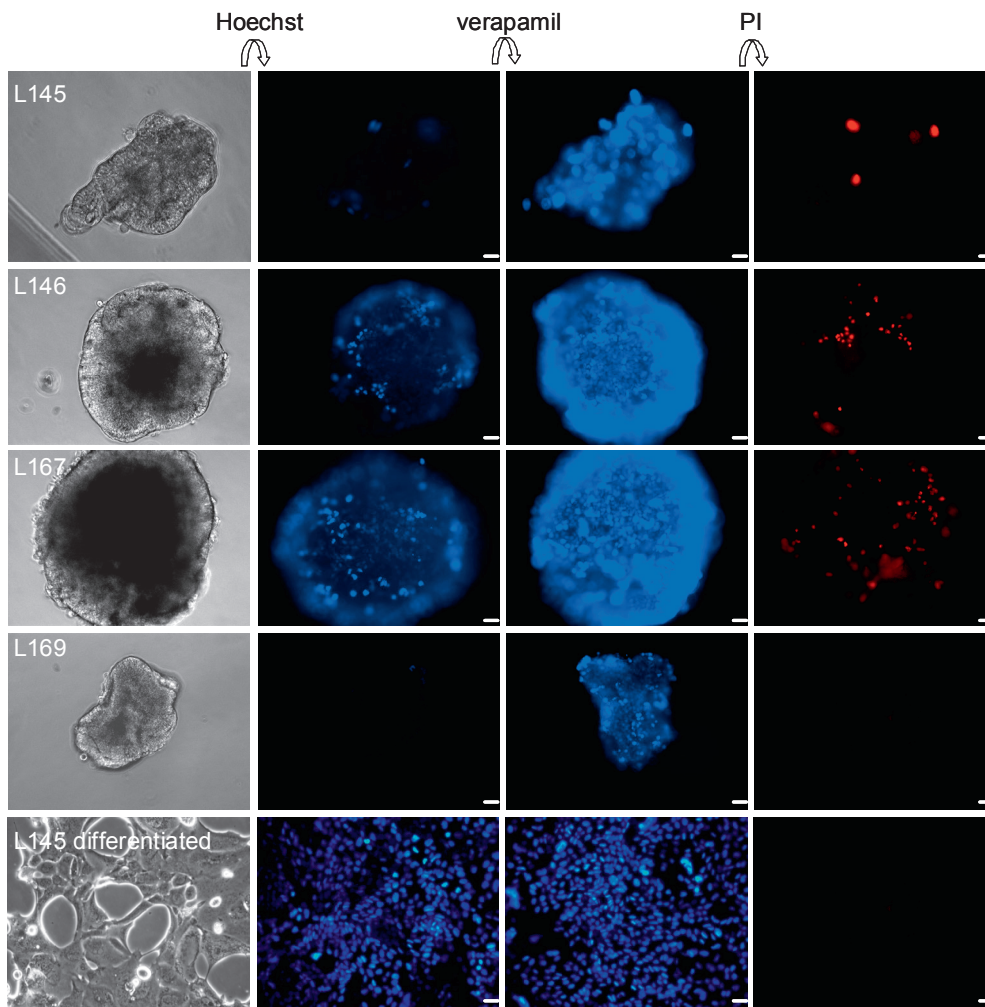
Figure 6 page 126



Supplemental Figure 1 page 139



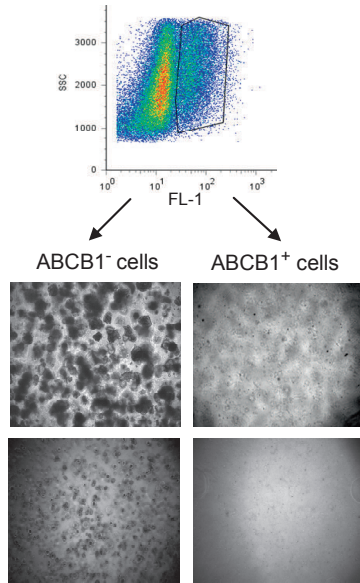
Supplemental Figure 3 page 140



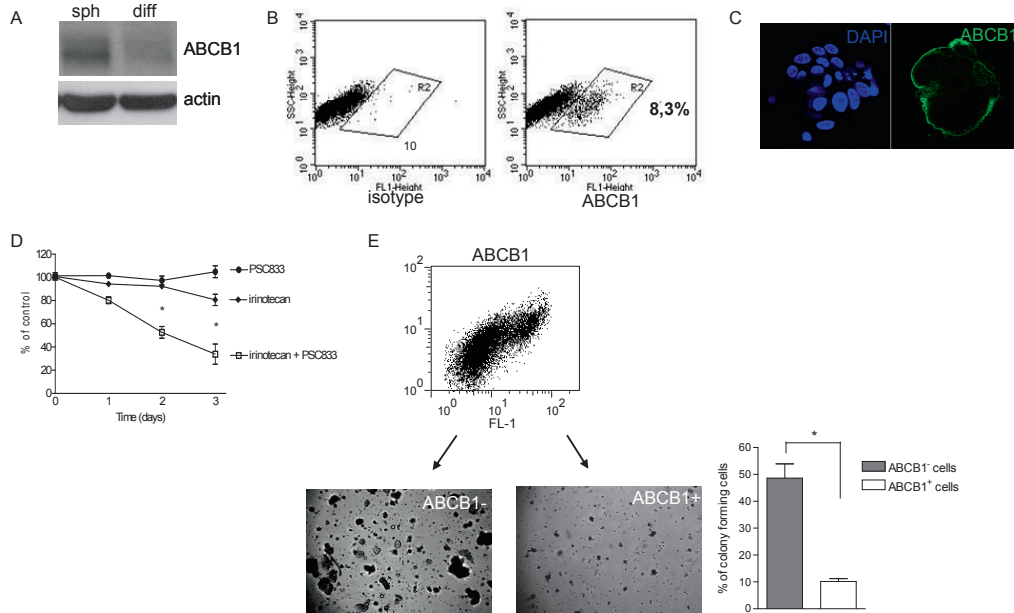
Supplemental Figure 5 page 141



Clone F4
ABCB1

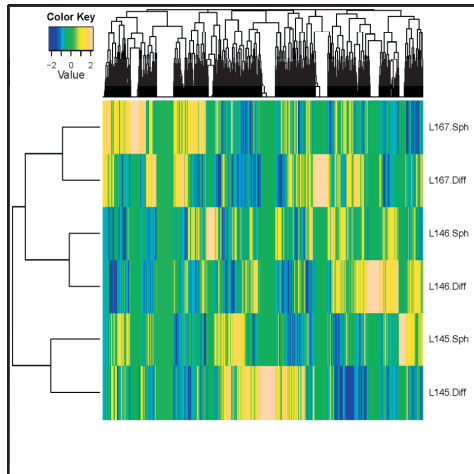


Supplemental Figure 7 page 143



Supplemental Figure 8 page 144

2A



2B

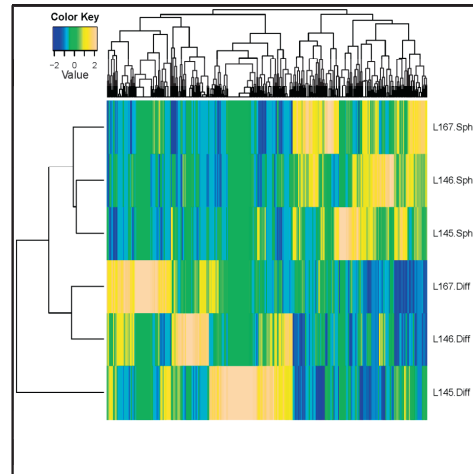
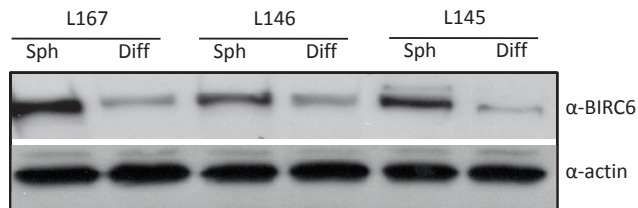
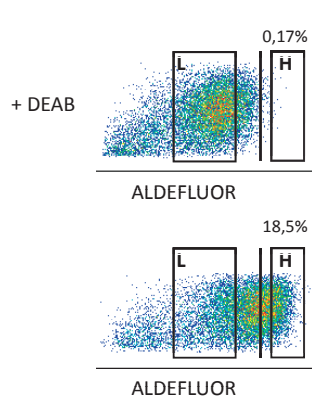


Figure 2 page 151

3A



3B



3C

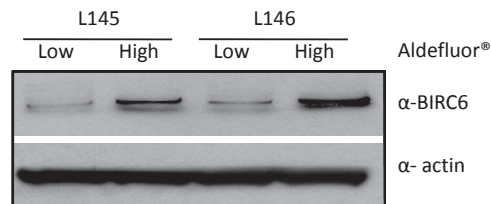


Figure 3 page 159

